CHARACTERISTICS AND MANAGEMENT IMPLICATIONS OF MOLLIC SOILS IN FOREST VERSUS GRASSLAND SETTINGS IN CENTRAL CALIFORNIA

A Thesis
presented to
the Faculty of California Polytechnic State University,
San Luis Obispo

In Partial Fulfillment
of the Requirements for the Degree
Master of Science in Agriculture with specialization in Soil Science

by
Brian Clark
March 2021

COMMITTEE MEMBERSHIP

TITLE:	Characteristics and Management Implications of Mollic Soils in Forest Versus Grassland Settings in Central California
AUTHOR:	Brian Charles Clark
DATE SUBMITTED:	March 2021
COMMITTEE CHAIR:	Gordon Rees, Ph.D. Professor of Forest and Range Soils
COMMITTEE MEMBER:	Chip Appel, Ph.D. Professor of Soil and Water Chemistry
COMMITTEE MEMBER:	Yamina Pressler, Ph.D. Assistant Professor of Soil Science and Restoration Ecology

ABSTRACT
Characteristics and Management Implications of Mollic Soils
in Forest Versus Grassland Settings in Central California
Brian Charles Clark

Efforts to sequester soil carbon (C) should consider soils intrinsically capable at C retention. Of the mineral soil orders, Mollisols have minimum requirements for soil organic C (SOC; over 0.06 %) and basic saturation (over 50 %). In the U.S., grasslands comprise 93% of the vegetation mapped above Mollisols. Soils beneath the southern extent of *Sequoia sempervirens* (redwood) forests in central California are mapped as Molliols. It widely accepted that redwood forests harbor considerable biomass C, but the extent to which aboveground C is retained in the soil is not well understood. This study aimed to: (i) to gather baseline soils data (bulk density, pH, basic saturation, cation exchange capacity, SOC, total nitrogen, structure, depth) for an iconic and understudied ecosystem, the southern extent of coast redwood forests and to compare said properties to those in adjacent grasslands, (ii) to identify taxonomic classifications of said soils, (iii) to investigate the influence of vegetative gradation on soil properties between these ecosystems using auger sampling, (iv) to compare levels of basic cations between the forest floor and mineral horizons and, (v) to characterize the total C and active C pools within these ecosystems and to explore interpretations of these pools.

In sites randomly selected across two regions, Swanton Pacific Ranch (SPR) and Landels-Hill Big Creek Reserve (LHBCR), soil was collected and described in 24 profiles beneath redwoods and compared to 19 profiles in nearby grasslands. Auger samples at fixed depths were collected in a complimentary study from 5 randomized transects that transitioned through mixed-evergreen forest (and across ecotones) between redwoods and coastal grasslands at SPR. Mineral soil samples were analyzed for SOC, permanganate oxidizable C (POXC), C/N ratio, pH, extractable basic cations, and cation exchange capacity. Samples of forest litter were analyzed for basic cation composition.

Multivariate regression models of profile data found higher values of pH, C/N, and CEC in redwoods than in grasslands, and lower values of bulk density in redwoods than in grasslands. Redwood soils were conducive to mollic epipedon formation (21 of 24 profiles in the redwoods as Mollisols) and generally had high base levels, for which extractable calcium from the forest floor was the main driver. Along the transects, multivariate regression returned generally consistent and graded patterns for C/N ratios, POXC/SOC ratios, and pH; these variables were generally highest in the redwood forest and decreased sequentially across mixed-evergreen forest and into the grassland

Our look at soil C pools focused on the fraction of SOC that was POXC. Observed higher ratios of POXC/SOC in redwoods than in the grasslands at SPR was corroborated by the transect study; at LHBCR, the regression model provided no evidence for a significant difference in POXC/SOC ratios between communities. Differences in POXC fractions across plant communities and localities were postulated as the result (and combination) of contrasting ecologies, and different management strategies and disturbance histories. The data collected in this study does not provide clear mechanisms to explain these discrepancies, and further research is needed;

disharmonious interpretations of POXC across the literature suggested that the replacement of operationally defined C fractions with pools tied to a particular stabilization mechanism would provide clearer insights across ecosystems to land managers.

Our estimates of SOC in the top 1 m of soil showed redwood soils stored as much or more C than soils in the neighboring grasslands, at SPR, 144 (± 21) and 123 (± 25) tons SOC per ha in the top 1 m of redwoods and grasslands, respectively, and at LHBCR, 221 (± 23) and 126 (± 24) tons SOC per ha in the top 1 m of redwoods and grasslands, respectively. The carbon densities provided in this study can be used as a baseline to measure changes to SOC and POXC pools in response to future activities to sequester C in our study regions and/or to assess losses from recent 2020 wildfires.

We are curious to see how the breadth of information gathered in this study can provide refinement for following questions that will hopefully one day, direct considerate and conscientious management in response to the environmental challenges ahead.

Keywords: Mollisols, *Sequoia sempervirens*, California grasslands, soil organic carbon, permanganate oxidizable carbon, Swanton Pacific Ranch, Landels-Hill Big Creek Reserve

ACKNOWLEDGMENTS

I'd like to thank Brian Dietterick at Swanton Pacific ranch, had it not been for our relationship- I don't think I would have had the opportunity to jump in on this project.
I'd like to thank Grant Williams and Becca Pulcrano for greeting me atop Nacimiento Ridge in the Santa Lucia Mountains, and convincing me to apply for an internship at Swanton Pacific Ranch.
Integral members (and relics) of the Swanton community that led me to pursue a graduate degree in soil science include: John Hardy, Cody Morse, Devin Patrick Peterson, and Adrian Broz.
I'd like to thank Gordon Rees, the key collaborator on this project with me who conceived these questions and wrote the grants, for blessing me with financial support for two years and supporting me in this project through its depths and entirety.
Much gratitude goes towards a swath of hired undergraduate research assistants and friends of mine (in order of involvement): Zoe Phaler, Zachary Barber, Braden Povah, Jordan Gosse, Emma Minnnahan, Rio Turrini-Smith, and Olivia Tarrin
I'd like to thank Craig Stubler for essential contributions of time and energy toward laboratory efforts associated with this project amidst an incomprehensible to-do list.
Connie Wong and Kamille Garcia were always eager to help me in the lab, be it on a homework problem or trying to find the nearest pipette tips.
Andrew Schaffner, Heather Smith and Matthew Hui contributed valuable statistical guidance in these efforts.
Thanks to Bwalya Malama for introducing me to soil science, for welcoming all my questions and for lots of shared laughter.
Thanks to Charlotte Decock and Richard Cobb and your enthusiasm to help me out.
Appreciation towards Daniel Johnston and his fervent passion to be in the field and share knowledge of soil morphology.
Jenn Yost and Matt Ritter, thank you for teaching me about plants.
Lisa Coffman, thank you for helping me establish a literary voice away from science.
I'm grateful for the support of Yamina Pressler and her eagerness to dive into conversations about this complicated thing we call soil carbon.
I'm grateful for the friendship of Chip Appel, his technical expertise and shared time in the ocean.
Special homage towards Eric Greening, and his personal sacrifice to improve the lives of others, his devotion to attend every public meeting accessible by bus in SLO county, and his relentless instillment of curiosity.
Last, the sincerest of gratitude to the friends and family that have supported me throughout my development as human, your impact on my life is more than you know.

TABLE OF CONTENTS

LIST OF TABLES

LIST OF FIGURES

Figure Page

ABBREVIATIONS

BS Basic saturation
C Carbon
C/N Soil organic carbon to nitrogen ratio
CO_2 eq Carbon dioxide equivalent
G Grassland
GWP Global warming potential
LHBCR Landels-Hill Big Creek Reserve
LSM Least squares mean
MAOC Mineral associated organic carbon
ME Mixed-evergreen forest
POC Particulate organic carbon
POM Particulate organic matter
POXC Permanganate oxidizable carbon
RW Redwood forest
SE Standard error
SOC Soil organic carbon
SOM Soil organic matter
SPR Swanton Pacific Ranch
USDA United States Department of Agriculture

CHAPTER 1

Introduction

Soil carbon (C) sequestration is a technique used to mitigate atmospheric C and has the potential to displace global fossil-fuel emissions by 5-15% (Lal, 2004a; Srivastava et al., 2012). Of the different mineral soil classifications, mollic soils are taxonomically distinguished as having captured large amounts of C (Bockheim, 2014; Soil Survey Staff, 2014). It is necessary to investigate mollic soils to inform land management with the goal of sequestering C belowground.

Mollic soils contain mollic epipedons, though the term mollic is not synonymous with the Mollisol order (Soil Survey Staff, 2014). General requirements of a mollic epipedon include a basic cation saturation greater than 50%, organic C content greater than 0.6%, Munsell color value and chroma less than 3 when moist (or value less than 5 when dry), and a minimum thickness that depends on development and depth to bed rock (Soil Survey Staff, 2014). While the requirements of the mollic epipedon are morphological and not tailored to any soil genesis properties, grasslands and steppe ecosystems comprise 93% of Mollisol native vegetation in the United States (U.S.) where fine root turnover is the main source of C (Bockheim, 2014). In contrast, soil mapping suggests that Mollisols dominate soils beneath the redwood forests of the Central California coast (UC Davis California Soil Resource Lab, 2018).

The coast redwood forest ecosystem consists of primarily second and third growth stands of *Sequoia sempervirens* that extend the Coast Ranges from southwestern Oregon to southern Monterey County, California. The redwood range is broadly divided into three sections (northern, central, and southern) based on differences in climate and

ecology (Noss, 2000a). Apart from soil map units that indicate Mollisols in a Xeric moisture regime (UC Davis California Soil Resource Lab, 2018), there is limited information available on soils beneath the southern redwood forests (Noss, 2000b; UC Davis California Soil Resource Lab, 2018). Soils beneath the northern and central extent of the redwood range have been broadly characterized by intense leaching and a pH between 5.0-6.5 where the principal soil orders mapped are Ultisols and Inceptisols (Noss, 2000b; UC Davis California Soil Resource Lab, 2018). In the northern and central extent of the redwood range, there is no shortage of efforts to study the soil (Popenoe et al., 1992; Pillers and Stuart, 1993; Burgess and Dawson, 2004; Enloe et al., 2006, 2010; Sanderman et al., 2008; Sanderman and Amundson, 2008, 2010; Johnstone and Dawson, 2010; Ewing et al., 2012). In southern redwoods where Mollic distribution occurs, we found one study of soil respiration rates (Potter, 2012) and one study of impacts to topsoil nutrients from fire-disease interactions (Cobb et al., 2016). Outside of one large-scale and poorly constrained effort to estimate C stocks for each forest type in California (Christensen et al., 2018; Forest Climate Action Team, 2018), a review of the literature returned no studies that have tried to quantify the amount of C stored below redwood forests in stocks.

It is clear that the motivations for land managers to sequester soil C have reached importance on an international level (Lal, 2004a; b, 2005). While the U.S. involvement in the Paris Agreement of 2015 (the most recent installment of the United Nations Framework Convention on Climate Change) has been erratic and subject to the executive leadership of the federal government- California, among other states, has its own international C cap and trade program. Under this program, covered entities (including

primary electricity providers, fuel distributors and industrial facilities) pay a per price unit for every ton of CO_2 emitted over the annual limit (Climate Policy Initiative, 2019). This money ($1.5 billion appropriated in 2019 fiscal year) goes to state projects under the California Climate Investments program including but not limited to programs that compensate land managers for implementation of soil C sequestration projects (State of California, 2019).

Agency programs do not consider unique pools of soil organic C (SOC) when budgeting for C sequestration, and instead focus on the total mass of SOC per unit area (Pearson et al., 2007; Jandl et al., 2014; Domke et al., 2017; P. Alvarez of California Carbon Cycle Institute, personal communication, 6 April 2020). SOC is separated into active and stabilized pools, and in order for the soil to act as an effective C sink, C needs not only to be inputted, but stabilized for the long term (Gulde et al., 2008). An emergent view has been to separate SOM with respect to different "stabilization mechanisms" that serve to preserve C within the soil ecosystem and make it less susceptible to further decomposition (e.g. aggregation, organo-mineral associations, environmental conditions, etc.; Schmidt et al., 2011; Srivastava et al., 2012; Cotrufo et al., 2013). New research has suggested that organic matter traditionally coined as "stable" for chemical recalcitrance actually has less mass retained in the soil overtime than labile organic matter-this phenomena can be explained by microbial efficiency-matrix stabilization framework (Cotrufo et al., 2013).

The presence of mollic epipedons in the southern redwoods provided an opportunity to compare soil C pools in contrasting adjacent communities, one community generally understood as conducive to mollic formation (grasslands) and one being a

novelty (the redwood forest). Given strong association of grassland vegetation on mollic distribution and given base saturation requirements on soil exchange sites (over 50% basic saturation), it can be asserted that grasslands systems can play a role in cycling bases in the soil. Suggested base inputs for mollic genesis include root exudation of calcium, weathering parent material, and mineralization of soil organic matter (Bockheim, 2014). Mollic formation under the canopy of redwoods allowed for investigation towards the role of redwood litter in providing basic cations for mollic classification.

Furthermore, there is limited research on gradation of soil properties across plant communities on a local landscape-level (Marfo et al., 2019a; b). Amiotti et al. (2000) found that individual trees played enough of a role in influencing soil pedologic composition that distinctions at highest level of taxonomy (soil order) could be made at the border of one tree's influence. In order to improve the understanding of vegetation as a player in localized soil formation, efforts to compare soils of close yet disjointed ecosystems should consider soil properties across the gradient of plant communities in between.

In this work, we investigated soils in a region of forest and rangeland along the Central California coast that are mapped to be rich in SOC but have not been extensively studied. Understanding the soil C pools and morphological properties of mollic soils formed under two contrasting ecosystems will inform forest and range managers on the Central California coast with management objectives of soil C sequestration. The objectives of this study were fivefold: (i) to gather baseline soils data (bulk density, pH, basic saturation, cation exchange capacity, SOC, total nitrogen, structure, depth) for an

iconic and understudied ecosystem, the southern extent of coast redwood forests and to compare said properties to those in adjacent grasslands, (ii) to identify taxonomic classifications of said soils, (iii) to investigate the influence of vegetative gradation on soil properties between these ecosystems using auger sampling, (iv) to compare levels of basic cations between the forest floor and mineral horizons and, (v) to characterize the total C and active C pools within these ecosystems and to explore interpretations of these pools.

CHAPTER 2

Literature Review

2.1 Introduction

Atmospheric carbon (C) is of increasing concern to scientists across the globe (Srivastava et al., 2012). Of the many approaches to atmospheric C mitigation, soil C sequestration is a promising, untapped technique (Lal, 2004a; Srivastava et al., 2012). In order to effectively manage C in soils, an understanding of C fractionation is critical because the components of C in the soil impact the response of C to disturbances (Culman et al., 2012). Of the different mineral soil classifications, mollic soils are taxonomically distinguished as having captured large amounts of C (Bockheim, 2014; Soil Survey Staff, 2014). In managed ecosystems, the ability of mollic epipedons to store organic C is important in the context of atmospheric C mitigation, ecological health, livestock forage, plant productivity, water purification and storage, and economic incentives (Huston and Marland, 2003; Mooney et al., 2004; Lal, 2004a, 2008; Lal et al., 2007; DiPerna, 2018). This literature review will summarize the body of knowledge that relates to soil carbon sequestration in the context of global climate concerns. Next an overview of mollic epipedons and the methods to measure mollic properties will be provided. Last, this review will summarize what is known about soils of the coast redwood forest and California's coastal grasslands.

2.2 The relevance of soil C in the context of global climate

2.2.1 Overview

There is a gap in the literature between the science of capturing soil C and the underlying motivations. The words, “climate change”, “soil C sequestration”, “sustainable”, and “management” amongst others, are used frequently together in scientific papers without a concrete fastening of each to each other (Huston and Marland, 2003; Lal, 2004a and b, 2005; Parolari and Porporato, 2016; Srivastava et al., 2012). In this review section I construct a holistic narrative between soil C sequestration and its relation to the C cycle, greenhouse gas mitigation, soil C fractionation, land management, and C trading.

2.2.2 Global C cycle

In order of C abundance, the five distinct C pools include the oceanic pool, the geologic pool, the pedosphere, atmosphere and biosphere (Fig. 2.1) (Srivastava et al., 2012) . The behavior and storage of C in these pools comes in many forms and the cycle can be characterized by a system of fluxes in and out of each pool. Whereas the biotic and soil pools contain mostly organic C, the geologic, oceanic, and atmospheric pools hold primarily inorganic C (e.g carbonates.) (Fig. 2.1). The oceanic and geologic pools contain the largest depositories of C, however, the flux of C in and out of these pools occurs at large geologic time scales and is not practical for management (Riebeek, 2011).

2.2.3 Atmospheric CO_2 in the near and distant past

There is growing concern that levels of greenhouse gases in the atmospheric C pool have accumulated at an unprecedented rate (Intergovernmental Panel on Climate Change, 2014; Prescott, 2010; Srivastava et al., 2012). The term greenhouse gas refers to

an atmospheric constituent that absorbs terrestrial infrared radiation, and in the process, converts the light energy to heat (Intergovernmental Panel on Climate Change, 2013). Carbon dioxide (CO_2), methane, nitrous oxide, ozone and water vapor are all important greenhouse gases (Intergovernmental Panel on Climate Change, 2013).

An overwhelming body of empirical data has established the positive correlation between greenhouse gas concentrations and globally averaged temperatures (Intergovernmental Panel on Climate Change, 2014). Likewise, an abundance of scientific literature sheds light on the negative implications of a world with continued acceleration of globally-averaged temperatures, including but not limited to threats to past, present, and future biodiversity, food security, and public health. (Intergovernmental Panel on Climate Change, 2014).

Global Warming Potential (GWP) is a standardized metric to compare the relative impact of one greenhouse gas to another, and uses the intrinsic tendency of a gas molecule to absorb radiation over a period of time (United States E.P.A., 2020). In the GWP concept, CO_2 is used as the reference gas and emissions of other gases are turned into a CO_2 equivalent using their GWP value. Methane has a relatively short residence time in contrast to CO2, which resides in the atmosphere for thousands of years, but its radiative forcing is much greater than CO_2 and over a 20-year timespan the GWP of methane is 84 (compared to 1 for CO_2; Intergovernmental Panel on Climate Change, 2014; United States E.P.A., 2020). Nitrous oxide and flourocarbons have longer residence times than methane and their 20-year GWPs are 264 and 4,880 respectively (Intergovernmental Panel on Climate Change, 2014). Despite the potency of other

greenhouse gases, CO_2 remains the primary constituent in today's greenhouse gas budget and accounts for over 60% of annual anthropogenic emissions (see Figure 2.2).

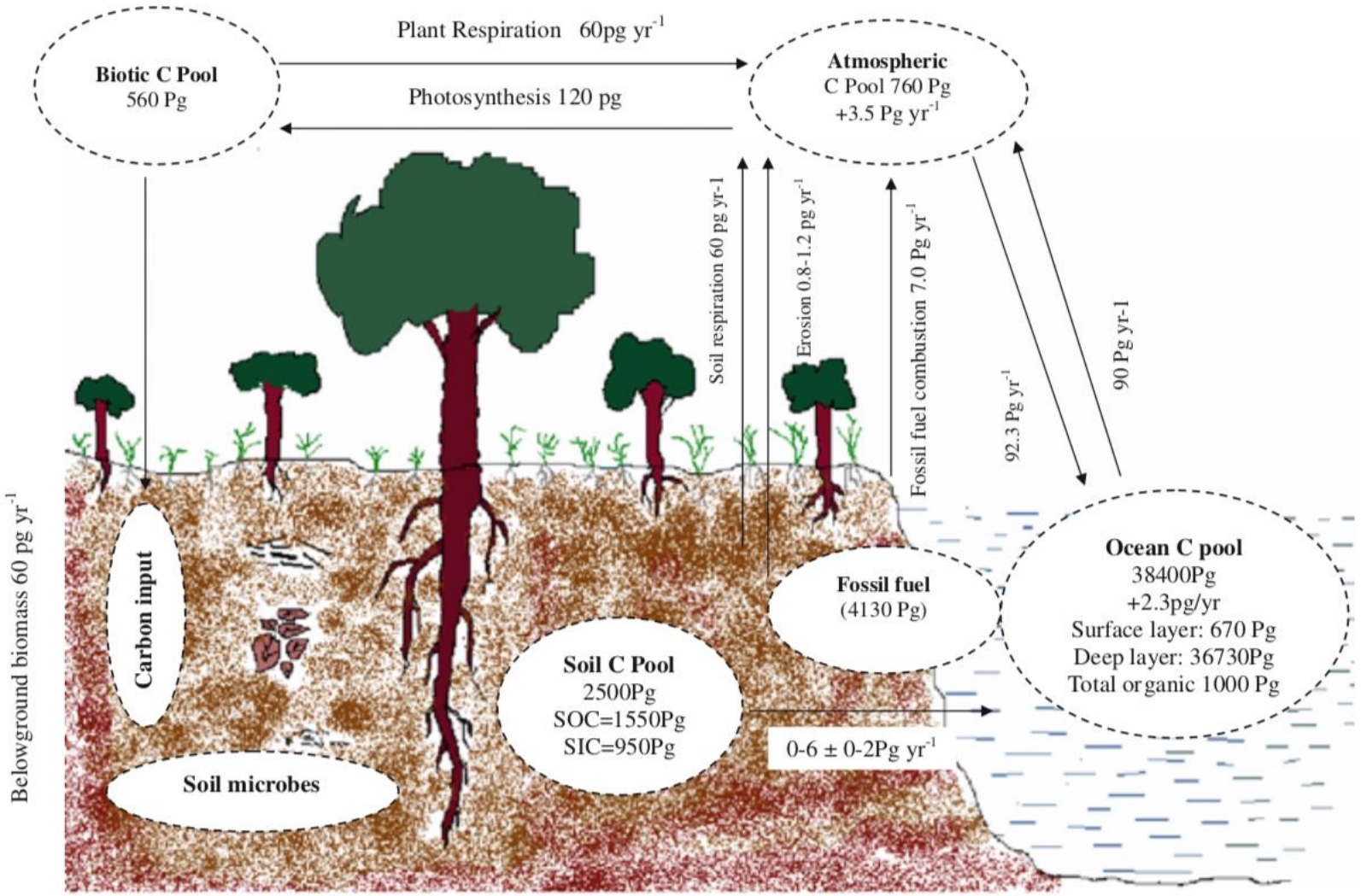

Figure 2.1. An overview of the C cycle (excerpted from Srivastava et al., 2012). Carbon stocks in units of petagrams (Pg).

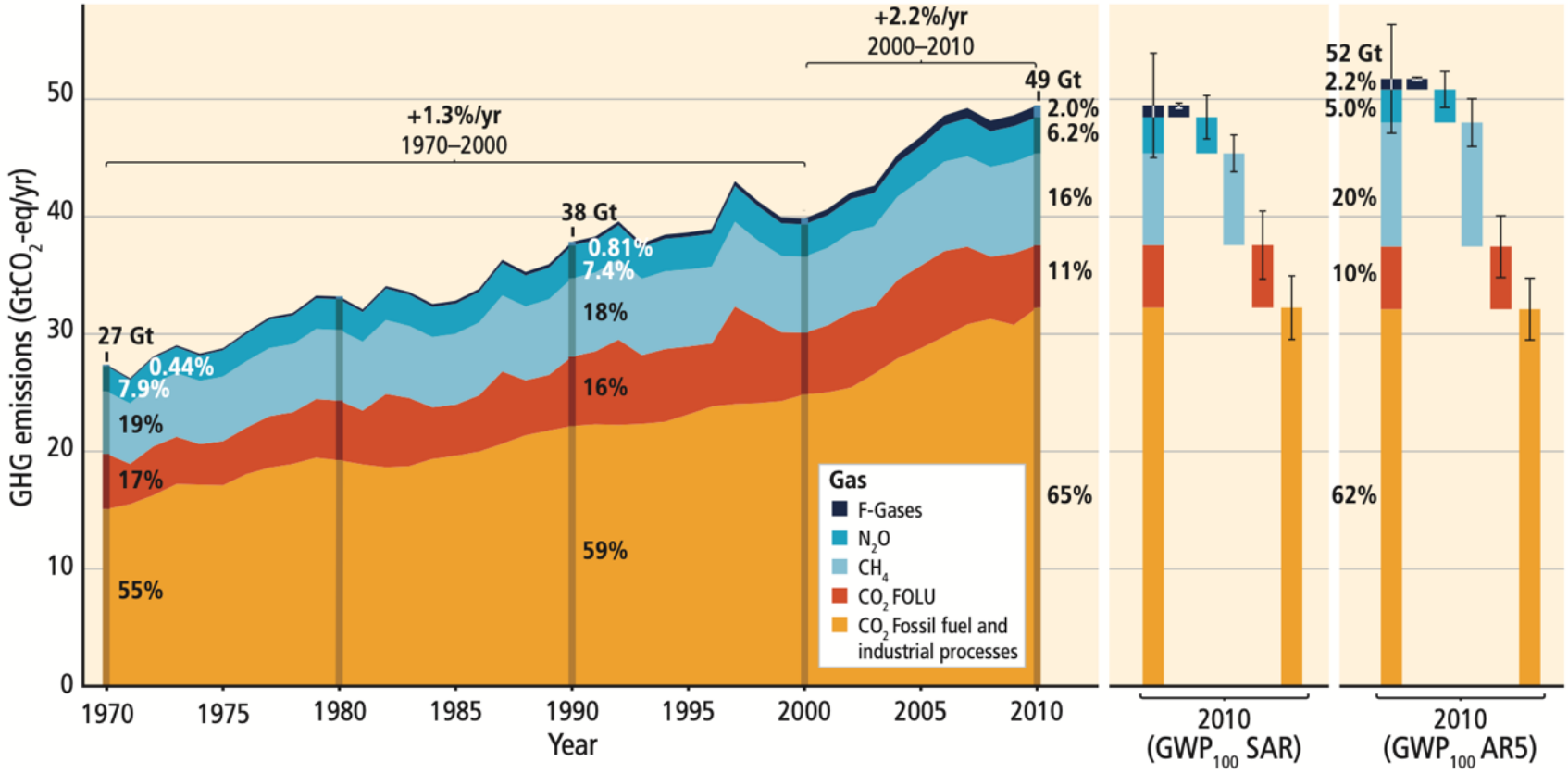

Figure 2.2. Total annual anthropogenic emissions by greenhouse gasses from 1970-2010, excerpted from Intergovernmental Panel on Climate Change (2014) .

Polar ice sheets contain a record of CO_2 concentrations (gas trapped in ice) that can be traced over hundreds of millennia within 10% accuracy (see Fig. 2.3; Raynaud et al., 1993). Methods to measure historic gas levels are based upon ice-core dating in conjunction with gas chromatography to measure concentration of gas. Ice-cores are dated using one (or a combination of) the following techniques: (1) counting annual seasonal-variations in ice strata, (2) correlating to known reference layers, (3) ice-flow modeling, (4) radioactive isotope dating (Raynaud et al., 1993).

Evidence from ice-core greenhouse gas studies suggests that the current global CO_2 levels are the highest recorded in records that extend to 800,000 years ago (see Fig. 2.3; Earth Systems Research Lab, 2019). Furthermore, anthropogenic causation for the post-industrial spike in CO_2 levels has been corroborated by isotopic carbon tracing techniques. The uptake of atmospheric C into the terrestrial biosphere is distinct from that of the oceans, as plants exhibit preference for lighter CO_2 (less ^{13}C isotope compared to ^{12}C isotope) during photosynthesis at a discrimination rate markedly higher than oceanic uptake (Prentice et al., 2001; NOAA: ESRL-Global Monitoring Division Laboratory, 2020).

Research in C isotopic trends suggested that levels of δ^{13} C (deviation of ^{13}C /^{12}C from standard reference material) in the atmosphere immediately began to decrease in the post-industrial era and have steadily decreased thereafter (Figure 2.4 (b); Graven et al., 2017). This decrease of globally averaged $\delta^{13}C$ levels coincided with: (1) a rise into to the highest levels of CO_2 in 800,000 years of ice core data (Figure 2.3), (2) the addition of a new C flux into the global C cycle, the burning of fossil fuels (i.e. decomposed plants)

made of isotopically light C, and (3) the decline of $\Delta^{14}C$ (deviation of ^{14}C /C ratio from standard reference material levels) until the mid-twentieth century (1955-1963) when nuclear weapons testing increased $\Delta^{14}C$ levels by 836 % (Figure 2.4 (a); Graven et al., 2017). Elevated $\Delta^{14}C$ levels have declined since then and are near pre-war levels (Figure 2.4). While plants and animals contain trace amounts of ^{14}C (the heaviest and only radioactive isotope of C), fossil-fuel reservoirs do not because any initial ^{14}C present decayed over millions of years (NOAA: ESRL-Global Monitoring Division Laboratory, 2020); a decline in atmospheric $\Delta^{14}C$ levels is further evidence of atmosphere saturation with fossil-fuel associated greenhouse gases.

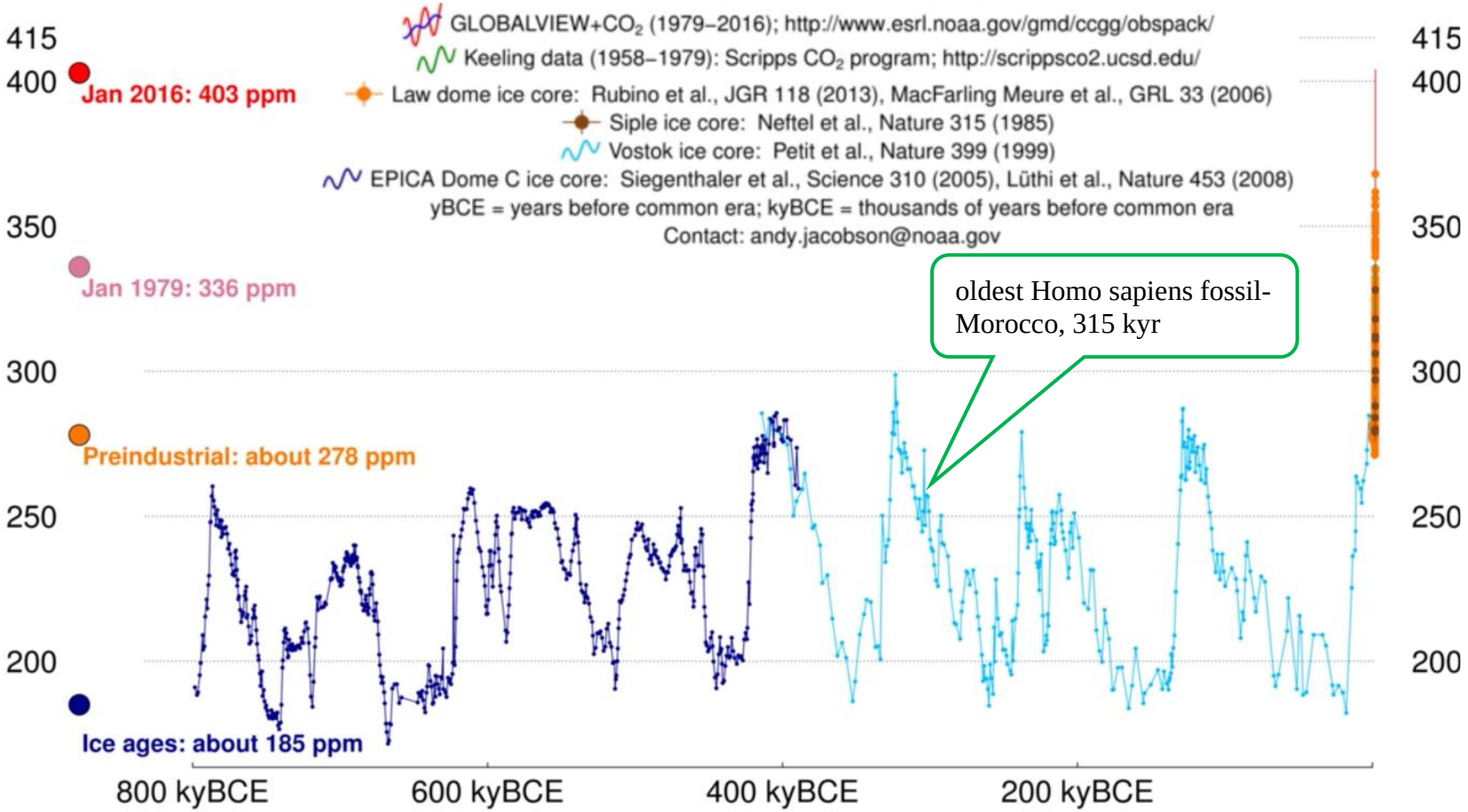

Figure 2.3. Globally averaged atmospheric CO_2 levels (ppm) from 800,00 years ago to 2016 (excerpted from Earth Systems Research Lab, 2019) fossil from (Hublin et al., 2017).

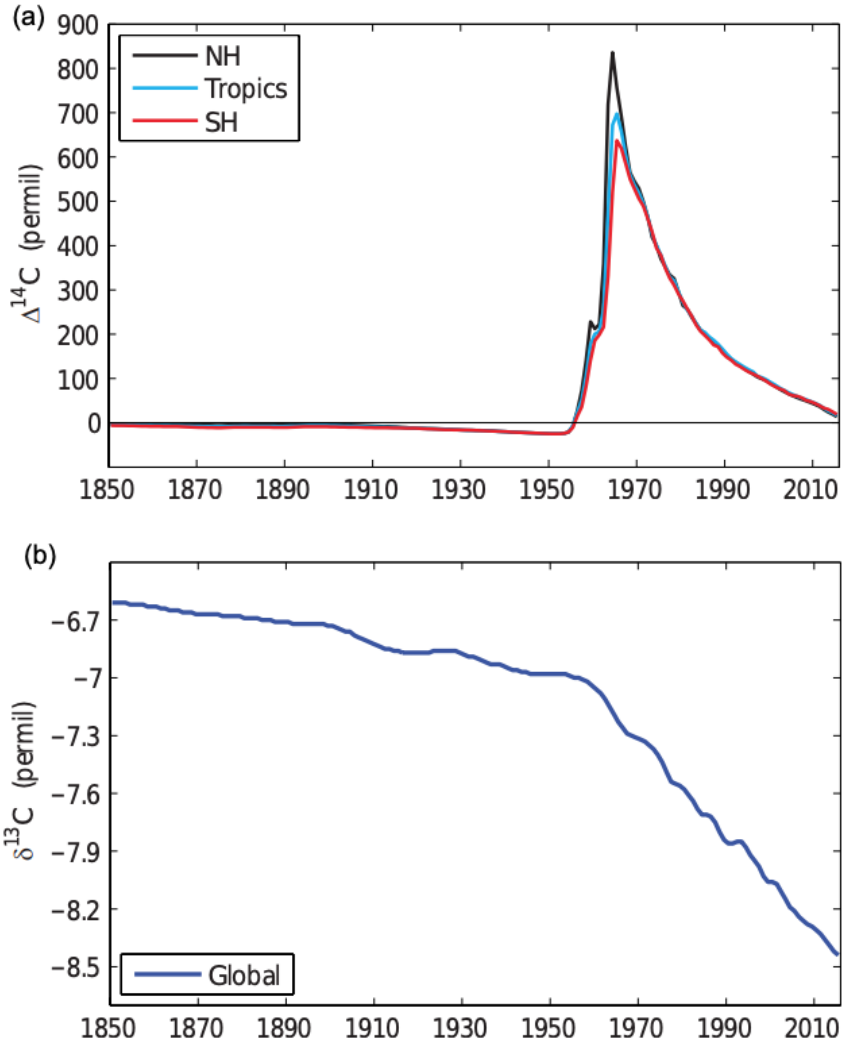

Figure 2.4. Globally averaged $\Delta^{14}C$ (a; deviation of ^{14}C /C ratio from standard reference material) and δ^{13} C (b; deviation of ^{13}C /^{12}C from standard reference material) levels from 1850-2010, excerpted from (Graven et al., 2017).

2.2.4 Atmospheric C in deep geologic time

One question becomes- if the earth is 4.5 billion years old (Patterson, 1956), is the rise in CO_2 concentrations over 800,000 years and fall of δ^{13} C concentrations since the industrial revolution unprecedented in the history of the earth? Research suggested that current CO_2 levels are not the highest that have ever been recorded in earth's history (see Figure 2.5; Retallack, 2009) and such insights are disguised in presentations of resolute climate data focused in relation to the industrial revolution, as in the case of a "hockey-stick" graph (see Figure 2.4; Retallack, 2013).

Evidence from the deeper geologic record indicated the earth has witnessed CO_2 levels of up 7200 ppm, which is about 17 times higher than our levels today of 420 ppm CO_2 (compare Figure 2.3 to Figure 2.5; Retallack, 2009). This insight is gained from a CO_2-stomatal index relationship and paleobotanic records of Gingko leaves, a plant taxon with fossils extending into the Permian era, around 300 mya (Retallack, 2009).

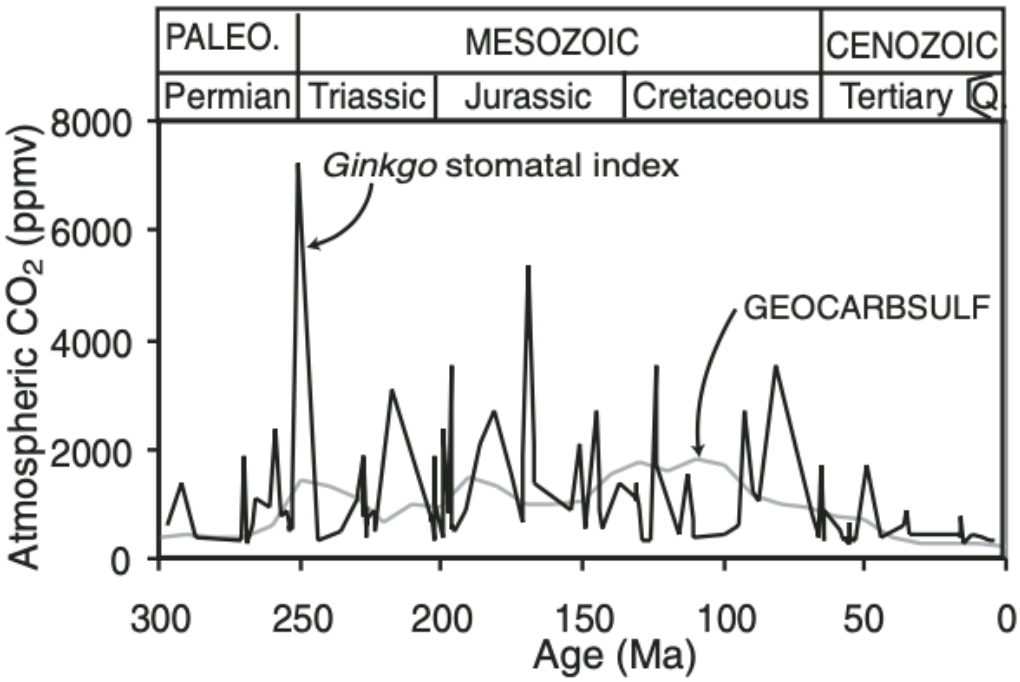

Figure 2.5: Atmospheric CO_2 levels over the last 300 million years from Ginko-stomatal index relationship data excerpted from (Retallack, 2009).

To put geologic records into human context, current CO_2 levels are the highest that have been recorded in the ice-core observations that date to before the oldest known Homo sapiens fossil, 315 kya (Hublin et al., 2017; Figure 2.3). Each time these levels exceed 2000 ppm, a mass extinction was associated (Retallack, 2009). Furthermore, the rise in atmospheric CO_2 concentration between 1990-2010 was 100 times greater than the highest observed rate of change in a well-resolved record that covers the last glacial termination (approximately 150 kya; Waters et al., 2016). Given these phenomena, societies are looking for ways to reduce carbon emissions.

2.2.5 Soils for greenhouse gas mitigation

Three overarching approaches to greenhouse gas mitigation are (1) to reduce the amount of fossil fuel used (i.e. more efficient technologies, modified lifestyles), (2) to expand the use of energy that does not consume fossil fuels and (3) to sequester carbon in other pools (Schrag, 2007; Srivastava et al., 2012).

Because (1) the global soil carbon reserve in terrestrial ecosystems is 4.5 times that stored in above ground biomass (Lal, 2004a; 2,500 Gt C in the pedosphere as opposed to 560 Gt in the biosphere), and (2) the below ground carbon is highly interconnected to the aboveground carbon (Cotrufo et al., 2015), and (3) the belowground terrestrial carbon pool is more protected from disturbance (fire, deforestation, etc.) when compared to the aboveground pool (Follett et al., 2001), strategies to mitigate greenhouse gasses are centered on expanding the pool of C in the soil and efforts to increase the plant biomass (biosphere carbon) can be considered one of the tactics to achieve said strategy (Lal, 2004a).

The onset of settled agriculture 10,000 years ago marked the beginning of soil disruption and it is estimated that many cultivated soils have lost 50-75% of antecedent soil C (Lal, 2007; Lorenz and Lal, 2018). Industrialization in the 19th century dramatically compounded these impacts the release of fossil fuels. In 2010, agriculture, forestry and other land use (AFOLU) contributed to about 25% of total anthropogenic greenhouse gas emissions when compared to other economic sectors (See Figure 2.6). Today, “sustainable”, recommended management practices (RMP) for agriculture can help reclaim the C that has been lost in the soil (Lal, 2007).

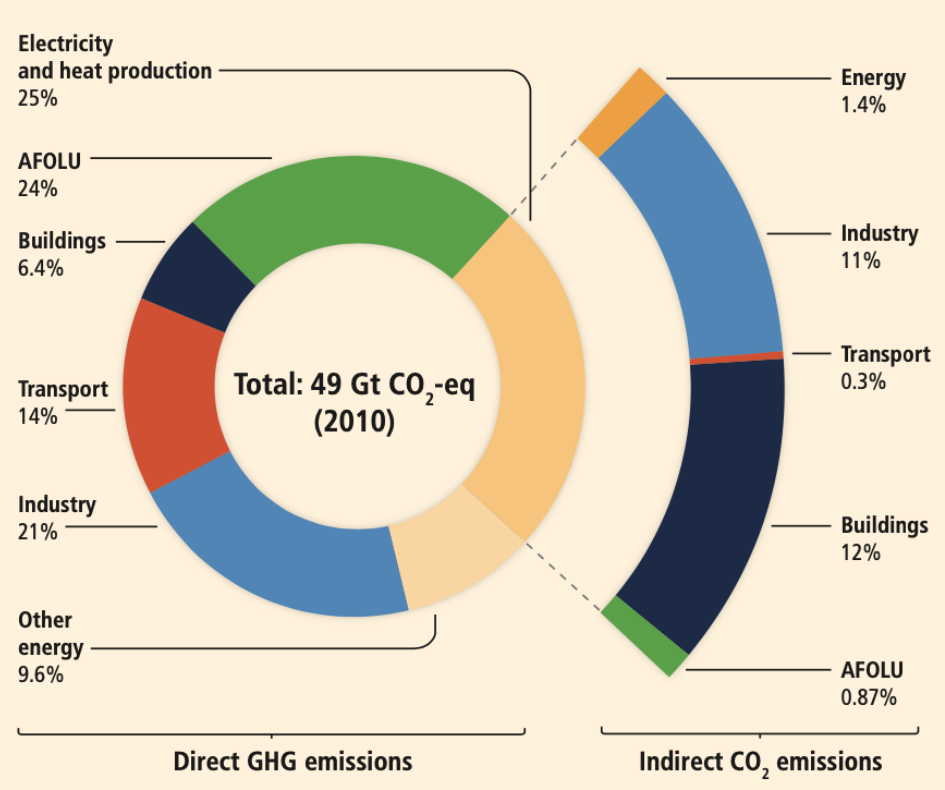

Figure 2.6. Total anthropogenic greenhouse gas emissions by economic sector in 2010, excerpted from Intergovernmental Panel on Climate Change (2014).

2.2.6 Fractions of soil C

Inorganic and organic components of soil C depend on climate, with inorganic C being more common in arid ecosystems (Lal, 2004b). In natural ecosystems, organic soil C is accumulated from plant, microbial, and faunal substrates and residues, and balanced by losses to decomposition, leaching, erosion, and fire (Lorenz and Lal, 2018). Inorganic soil C is primarily composed of mineral carbonates and bicarbonates, but also includes CO_2, carbonates, and bicarbonates found in the soil pore space (Lorenz and Lal, 2018).

Soil organic C is broken further broken down into unique pools: microbial biomass C, particulate organic C (POC), mineral associated C, mineralizable C, dissolved organic

C, Permanganate oxidizable C (POXC), etc. For the purposes of management, it is important to fractionate soil C into the stable and active pools (Gulde et al., 2008; Srivastava et al., 2012). In order for the soil to act as an effective C sink, C inputs must be retained over the long term. Preservation of C in the soil is called stabilization.

2.2.7 Mechanisms of soil C stabilization

One challenge in interpreting pools of SOC, is understanding what those pools represent from a management and ecological perspective. Traditionally, SOM "stability" was viewed and modeled from the perspective of residence time in the soil (Hurisso et al., 2016). Furthermore, SOM that is more complex in carbon chemistry was labeled "stable", because complex carbon molecules take more time to decompose than simpler carbon molecules (Tirol-Padre and Ladha, 2004; Schmidt et al., 2011; Cotrufo et al., 2013).

Recent studies have suggested that the division of SOM into operationally defined pools of chemical stability (e.g. "humin, humic acids, and fluvic acids") are an outdated, management-irrelevant practice (Lehmann and Kleber, 2015). Such historic fractionation (dated to 1786) was premised on formation of "humic substances" with varying stabilities that have not observed by modern techniques and were separated via solubility in alkaline solutions (not relevant to the natural environment; Lehmann and Kleber, 2015). Nowadays, advanced techniques are able to characterize soil organic matter at a finer scales (e.g. aromatic C, phenolic C, lignin, etc.; Kelleher and Simpson, 2006; Lehmann et al., 2008) and these compounds are not products of an extraction (e.g. "humic substances"). More recently, a shift of focus has been to separate SOM in respect to different stabilization mechanisms that serve to preserve carbon within the soil ecosystem

and make it less-susceptible to further decomposition (e.g. protection in soil aggregates, bonds via organo-mineral associations, inhibited loss because of environmental conditions, bonds to polyvalent cations, etc.; Schmidt et al., 2011; Srivastava et al., 2012; Cotrufo et al., 2013, see Figure 2.7).

New research has suggested that plant litter traditionally understood as "stable" for chemical recalcitrance, has less mass retained in the soil overtime and less mass converted into microbial products than "labile" plant litter composed of lower weight molecular compounds-this phenomena can be explained by the microbial efficiency-matrix stabilization framework. Microbial substrate use efficiency is the proportion of assimilated substrates used for microbial growth and enzyme production versus that which is respired. A higher substrate use efficiency indicates that microbes are more efficient at decomposing the C and therefore a higher proportion of the C remains in the soil instead of going to CO_2.

Despite lower substrate use efficiency and lower assimilation into organo-mineral associations that serve to stabilize SOM in the long-term, recalcitrant materials are protected from decomposition via other mechanisms that operate over shorter time scales (Lützow et al., 2006; Cotrufo et al., 2013). For example, as a function of molecular properties, recalcitrant materials in early stages of decomposition (e.g. days to months to years) exhibit initial resistance to degradation when compared to labile inputs because of selective preservation of the less-easily degraded materials (Lützow et al., 2006; Cotrufo et al., 2013). Additionally, physical inaccessibility from decomposition via occlusion in soil aggregates can stabilize recalcitrant materials, however protection from this mechanism is vulnerable to disturbance and subject to faster turnover times (e.g. decades)

when compared to stabilization with mineral surfaces (e.g. centuries; Lützow et al., 2006; Cotrufo et al., 2013, 2019).

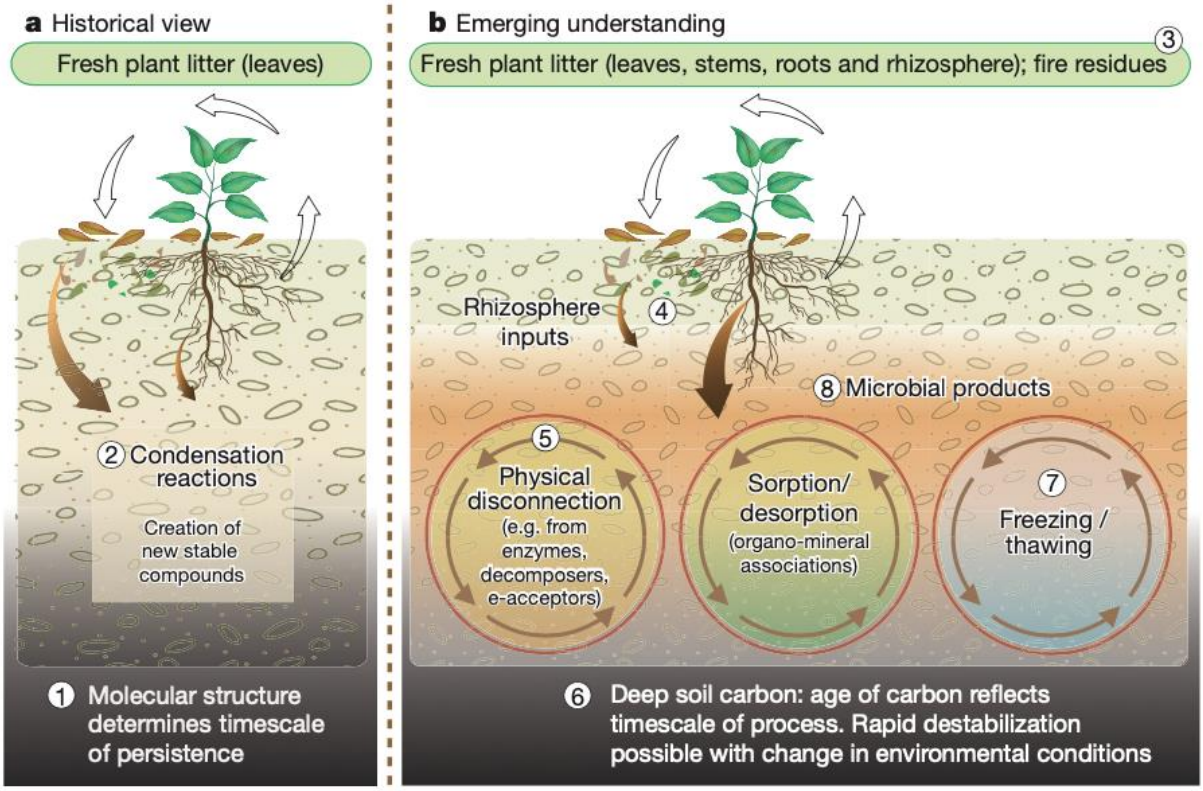

Figure 2.7 Recent paradigm shift in SOM conceptualization, excerpted from (Schmidt et al., 2011).

It is important to realize soil C is the result of fluxes co-occurring at different temporal scales and the strategy to sequester C in the soil is to maximize inputs and minimize outputs. If soils were a limitless avenue to C drawdown, continued inputs of C to the soil would be a no-brainer, however, insights from the behaviors of active and stabilized pools indicate that things are not so simple (Gulde et al., 2008; Cotrufo et al., 2019). Additionally, despite opportunity for soil management to attenuate acceleration of atmospheric greenhouse gas levels, it is important to consider the other ecosystem services that soils can provide including but not limited to: food security, pest and disease

suppression, conservation of biodiversity, protection of cultural resources, and purification of water and contaminants, to name a few.

Long-duration experiments in Canada suggested soil aggregates exhibited a limit in their ability to act as C sinks, and after a certain threshold, any additional C inputs from manure only contributed to saturation of the active pool (Gulde et al., 2008). Similarly, Cotrufo et al. (2019) found that while particulate associated organic matter (POM) is directly proportional to SOC across a wide range of SOC values, the mineral associated organic matter pool of SOC plateaued at around 50 g C kg^{-1} of soil in of European forests and rangelands (Figure 2.8); which suggested saturation of an active pool.

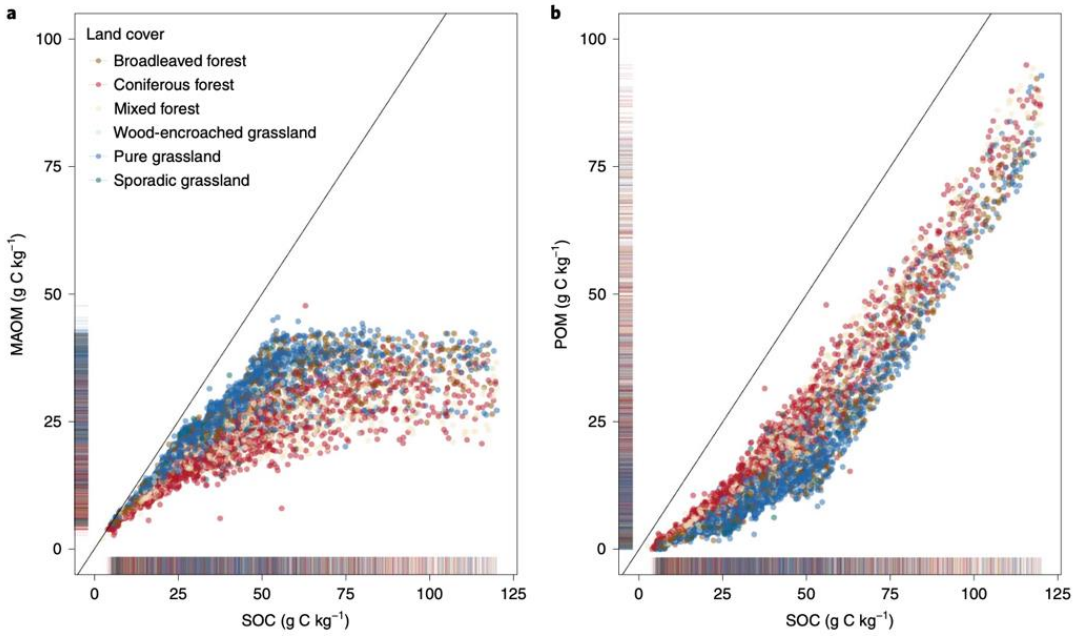

Figure 2.8. Mineral associated organic matter (MAOM) in g C kg^{-1} (a) and particulate associated organic matter in g C kg^{-1} (b) as a function of SOC, g C kg^{-1} in grassland (blue) and forest soils (red) (excerpted from Cotrufo et al., 2019).

Soil C undergoes flux and inputs and outputs of SOM are facilitated by interactions with the biosphere and atmosphere. Insightful management of soil C should not only address the total SOC but consider pools of SOC and the respective residence times and stabilization mechanisms.

2.2.8 Permanganate oxidizable C as a fraction of soil C

Permanganate Oxidizable C (POXC) is a fraction of SOC that represents an active pool, and has been recommended (Culman et al., 2012; USDA-NRCS, 2014; Hurisso et al., 2016) as a useful indicator of soil quality for its ease of measurement and affordability. Permanganate oxidizable C is not attached to mechanistic-based C pool (e.g. separation at 53 μm), instead, it is an operationally defined fraction of SOC that is reactive in the presence of potassium permanganate (Culman et al., 2014) .

Across the literature, interpretations of POXC are disharmonious. Some studies state POXC is a useful measure of SOC that is "labile" or "sensitive to management" (Culman et al., 2012; Hurisso et al., 2016) while other studies have critiqued it for its inability to discriminate between SOC fractions (Tirol-Padre and Ladha, 2004b; Romero et al., 2018). One trend that remained ubiquitous across studies was that POXC increased with SOC (Tirol-Padre and Ladha, 2004a; Skjemstad et al., 2006a; USDA-NRCS, 2014; Romero et al., 2018).

If POXC is indicative of a SOC pool sensitive to management (Culman et al., 2012; Hurisso et al., 2016), from a mechanistic framework, POXC would be active. The use of "labile" to describe POXC is misleading (Culman et al., 2012), given studies that show POXC is a strong indicator of lignin (Tirol-Padre and Ladha, 2004a; Skjemstad et al., 2006b) and paritculate organic C (POC; Culman et al., 2012). Lignin is a compound

that is traditionally understood as more resistant to microbial decomposition (Schmidt et al., 2011; Cotrufo et al., 2013) when compared to compounds with lower C/N ratios and molecular weights (e.g. soluble sugars, amino acids, etc.). “Labile” typically implies simple molecular structure (Cotrufo et al., 2013; Romero et al., 2018) but the term “labile” has also been used describe the residence time of soil C (Hurisso et al., 2016). Given recent “paradigm shift” in SOM investigation, misinterpretations from ambiguous jargon have become an unavoidable challenge, and clarity in future communications about SOM pools is necessary in discussions that look to inform management.

Nonetheless, positive relationships between POXC and POC (Culman et al., 2012; Hurisso et al., 2016), mixed relationships between POXC and microbial biomass C (Tirol-Padre and Ladha, 2004a; Culman et al., 2012) and non-directionally informative relationships about POXC and other fractions (Hurisso et al., 2016) suggest that if there is one fraction of soil C that POXC most consistently represents, it is POC. This assertion would further invalidate the use of “labile” when describing POXC, as POC is generally indicative of higher SOM stoichiometry (C/N) and biochemical recalcitrance (Cotrufo et al., 2019).

2.2.9 Land management and soil C

No-till or conservation-till farming, implementation of cover crops, and application of organic manures and compost are examples of recommended management practices (or “sustainable” strategies) growers can use to minimize SOM depletion (Lal, 2004b). Tillage and crop rotation in agricultural fields degrades soil aggregates and increases the loss of SOM (Gulde et al., 2008). Once tilled, soil temperatures are not buffered to the same extent as natural soil, moisture retention is decreased, and soil

structure is weakened causing losses of soil C due to mineralization (oxidation) and erosion (Lal, 2004b).

The overall potential for improved management of grazed lands to mitigate greenhouse gas emissions is less than that in croplands (Lorenz and Lal, 2018). Studies generally point towards increased soil C sequestration potential from application of organic matter to rangelands (Ryals and Silver, 2013; DeLonge et al., 2013; Ryals et al., 2016), however some conflict (Owen et al., 2015).

Cotrufo et al. (2019) found that grasslands had higher ratios of mineral associated organic matter (MAOM) to SOC and lower ratios of particulate organic matter (POM) to SOC when compared with coniferous forests in Europe. This finding conforms to the general understanding of organic matter accumulation in forests and grassland ecosystems, which can be summarized by: (i) considerably higher belowground biomass per plant in grasslands when compared to forests (ii) secretions and exudates of fine roots being the primary organic inputs in grasslands as compared to litterfall and large woody root decay in forests, and (3) bacterial dominance in the grassland soil community as compared to fungal dominance in in forests soil community (Bockheim, 2014; Orgiazzi et al., 2016a) .

In U.S. forest ecosystems, 59% of C contribution is from the soil (Birdsey, 1992). Studies of forest harvest impacts to soil C provide mixed results (Lal, 2005; Parolari and Porporato, 2016). Certainly, the extent of forest harvested (clear-cut vs. selective) has some impact. Compaction is a major disturbance associated with forest operations (Orgiazzi et al., 2016b). Main impacts from logging include depletion of soil moisture, oxygen limitation, loss of biotic activity, disruptive mixing of the litter layer, and erosion;

however, if forest operations are carefully managed some studies show little impact on soil C (Lal, 2005). In general, fungi are less resilient to forest disturbance from logging than bacteria (Orgiazzi et al., 2016a) .

2.2.10 Grasslands as global drivers of cooling

Researchers that have traced global CO_2 levels over the last 300 million years (Retallack, 2009) also suggested that over the last 40 million years, the spread of mollic epipedons in association with displacement of woodlands was a driver for global climate cooling (Retallack, 2013). Evidence for Cenozoic grassland expansion into the 400-1000 mm isohyet (precipitation regime) is found in the paleosol record across three continents and coincides with decreased CO_2 levels from pedogenic carbonate and *Ginko* stomatal-index records (ee figure 2.9; Retallack, 2013). Two global hothouse events with spiked CO_2 levels (attributed to basalt and craters) occurred in the late Eocene (35mya) and middle Miocene (16 mya; see figure 2.9; Retallack, 2013). It was suggested grasslands expanded into wetter areas with newly evolved mollic epipedons, C4s after the first spike and C3s after the second spike, and thereafter served to cool climate (Retallack, 2013). The cause for global cooling after these events was attributed to the way in which grasslands promote higher soil C retention, higher soil moisture (lower atmospheric humidity), higher surface albedo (lower solar radiative absorbance), and faster nutrient exploitation (increased plant and oceanic productivity) as compared to woodlands (Retallack, 2013). This research served to highlight the importance of grasslands in global climate system over deep time and in no way suggested type conversion of ecosystems into grasslands for the purpose of global cooling.

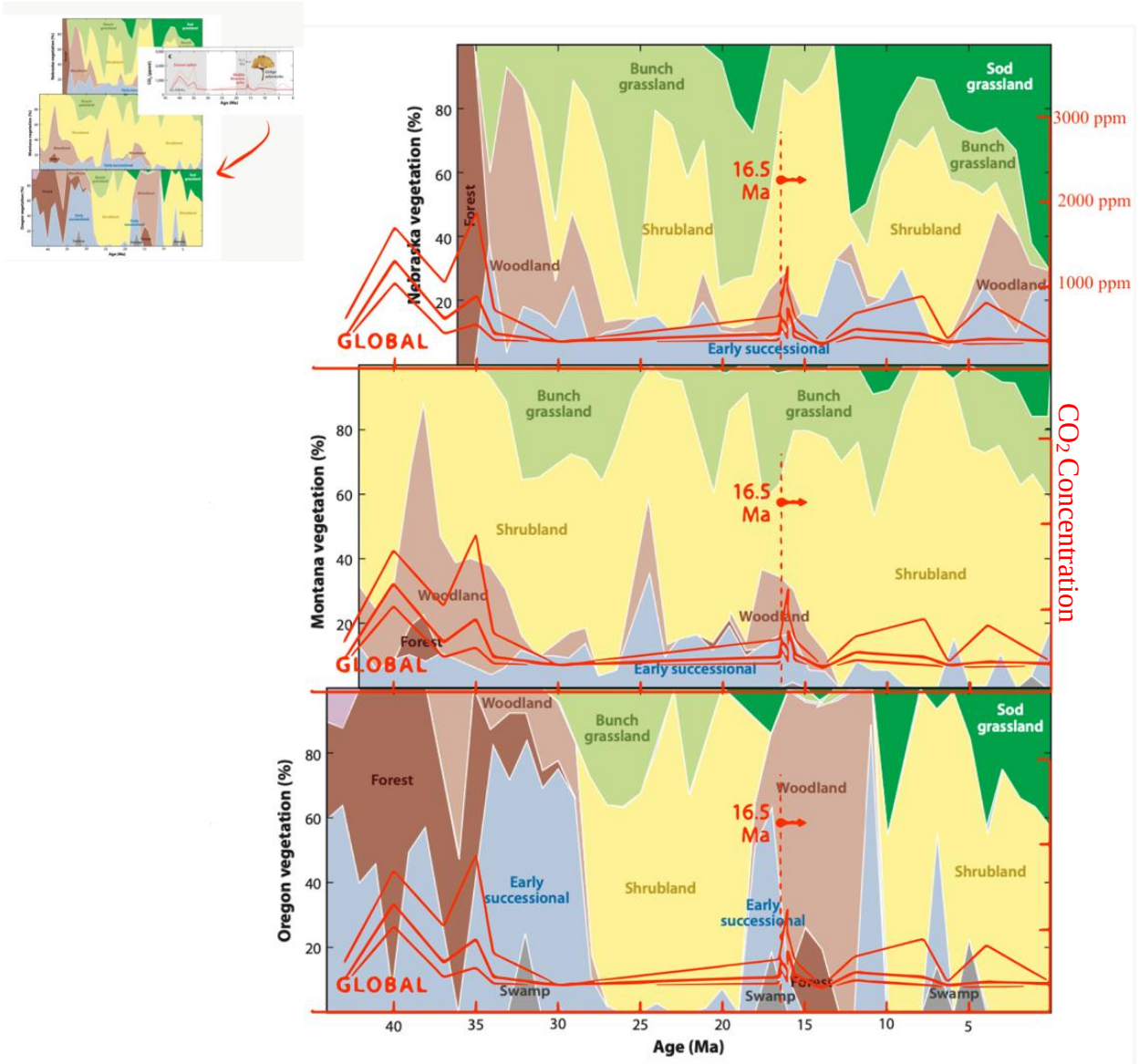

Figure 2.9. Superimposed schematic of plant composition (% cover) mapped in three North American paleosols and carbon dioxide concentrations (ppm) from Gingko tree stomatal index data over the last 40 million years. Both excerpted from Retallack (2013).

2.2.11 Global and local C incentives

In 1997, the United Nations Framework Convention on Climate Change facilitated the formation of the Kyoto Protocol where signatory nations agreed to reduce carbon emissions relative to that of 1990 emissions by 2012. Initially under the Kyoto Protocol, countries were to trade C credits from accumulation of C stocks in forests for greenhouse

gas emissions that exceeded national limits, eventually the trading of C credits via soil C sequestration was included (Huston and Marland, 2003; Mooney et al., 2004; Srivastava et al., 2012).

The Kyoto Agreement is one example of international bodies working together to set limits on carbon emissions. Most recently, the 2015 Paris Agreement aimed to make participatory nations accountable towards the goal of limiting increased globally averaged temperature to below 1.5 ^{o}C from pre-industrial levels via a complex network of emission reduction strategies (Schleussner et al., 2016).

While the U.S. is no longer involved the Paris Agreement of 2015, California, among other states, has its own international carbon emissions program. Under the California cap and trade program, covered entities (including primary electricity providers, fuel distributors and industrial facilities) pay a per price unit for every ton of CO_2 emitted over the annual limit (Climate Policy Initiative, 2019). This money ($1.5 billion appropriated in the 2019 fiscal year) goes to state environmental projects under the California Climate Investments program (State of California, 2019). Some of the projects (e.g. Healthy Soils Program) compensate voluntary land managers for implementation of C sequestration strategies (State of California, 2019). At a federal level, the NRCS also provides compensation to voluntary land managers under the Conservation Stewardship Projects program.

2.2.12 Summary of soil carbon sequestration in light of climate

This review chapter summarized the influence of the Anthropocene as manifested in the atmospheric CO_2 record and established context for the pressing and promising mitigation strategy soil C sequestration. In order for the C to be retained effectively, an

understanding of SOM accumulation and SOM stabilization is necessary, however interpretation of past research is a challenge given a recent paradigm shift in SOM conceptualization. Whereas the influence of forest and range management is less understood, agriculture and urbanization has degraded SOM stabilization mechanisms in natural ecosystems. Finding ways to promote C stabilization in land management is important for the sustainability of the world's societies and grasslands offer a promising niche.

2.3 Mollic epipedons

2.3.1 Soil taxonomy

Soil taxonomy is the way in which differences and similarities in soil properties are communicated between scientists across ecosystems and societies. While the classification of a soil (in it of itself) may not provide the information necessary to initiate management actions, the classification enables an otherwise undescribed soil to enter the discussion for management actions and can guide future exploratory questions.

While general conclusions about soil properties can be translated and expressed universally, the procedures to classify soils vary internationally. The classification of soils in the United States is determined according to the *Keys to Soil Taxonomy* (Soil Survey Staff, 2014). In keeping with the scope of the project, the classifications systems in other countries will not be addressed in this literature review, and instead it will focus on how a mollic soil is defined in the Unites States.

The categorization of a soil using according to the *Keys to Soil Taxonomy* is based upon the identification of diagnostic features and horizons (requiring field and laboratory information). The *Keys to Soil Taxonomy* assumes familiarity with procedures,

nomenclature, and conventions for describing detailed in the *Soil Survey Manual* (Soil Science Division Staff, 2017) and the *Field Book for Describing and Sampling Soils* (Schoeneberger et al., 2012; Soil Survey Staff, 2014). The *Kellogg Soil Survey Laboratory Methods Manual* (Rebecca Burt and Soil Survey Staff, 2014) is a compilation of procedures that enables standardized protocols to collect laboratory data on soils for the purpose of classification.

To collect the field information necessary to classify a soil, establishment of a profile is superior to other sampling methods (e.g. auguring), which may be less resource intensive. Interpretation of soil properties across space can be hindered when soils are sampled at a defined uniform depth-intervals, or when only the top-soil (e.g. 0-20 cm) is sampled for sake of convenience and feasibility (Schoeneberger et al., 2012). In contrast, when an entire soil profile is investigated (e.g. 0-1.5 m), a greater understanding of the soil and its subsurface variability is provided. The *Field book for Describing and Sampling Soils* (Schoeneberger et al., 2012) identifies sampling by horizon (as opposed to fixed depths), as the superior sampling method.

An epipedon is "a soil horizon that forms at or near the surface and in which most of the rock structure has been destroyed" (Soil Survey Staff, 2014). An endopedon, or subsurface horizon, is a horizon that forms lower in the soil. Identification of epipedons, endopedons and other diagnostic features form the framework for soil classification.

2.3.2 Mollic taxonomic requirements

A mollic epipedon is identified based on soil structure, color, basic cation saturation, soil organic C content, thickness, and climate. The following bullet points are an abbreviated summary of the "*Mollic Epipedon"* section found under *"Horizons and*

Characteristics Diagnostic for the Higher Categories" in the *Keys to Soil Taxonomy* (Soil Survey Staff, 2014)*:*

- Structural requirements: rock structure in less than one-half of the epipedon volume.
- Color requirements: value of 3 or less (moist) or 5 or less (dry), and chroma of 3 or less (moist).
- Basic cation saturation: must exceed 50 percent throughout the epipedon
- Carbon content: higher than 0.6 percent (if epipedon has a moist color value of 4 or 5, carbon content of 2.5 percent or greater will override disqualification)
- For thickness:
    - At least 25 cm thick if the texture is (1) fine loamy sand or coarser, (2) if there is no diagnostic horizon below, or (3) if the nearest underlying diagnostic feature is at least 75 cm below the surface, or
    - At least 10 cm thick if the epipedon (1) sits directly above weathered or unweather bedrock and (2) the soil texture is finer then loamy fine sand, or
    - At least 18-25 cm thick and one-third or more of the total depth to an underlying diagnostic feature if the former don't apply, or
    - At least 18 cm thick if none apply
- Climate: some part of the epipedon must be moist for a cumulative total of at least 90 days with a temperature of 5 degrees Celsius or more at 50 cm depth during normal years

While the Mollisol order is the most common order for soils containing a mollic epipedon, mollic epipedons can occur also in other orders including Vertisols, Andisols, and Ultisols, which key out before Mollisols based on another diagnostic feature

(Bockheim, 2014). Alfisols, Entisols, and Inceptisols may have mollic epipedons or exhibit mollic-like features such as dark coloring over a certain thickness, which may be recognized with a "humi-" or mollic modifier in the taxonomic name, but for at least one reason these soils fail to meet the full definition of a Mollisol (e.g. one horizon below the epipedon may have a base cation saturation less than 50 %, etc.) (Bockheim, 2014).

2.3.3 Distribution of Mollisols

In the United States, grasslands make up 93% of the native vegetation in Mollisol distribution (Bockheim, 2014). There are four large assemblages of Mollisols on the global scale: (i) the Central Plains of North America, (ii) the Sub-humid steppes of southeastern Europe, (iii) Northeastern China, and (iv) central-eastern Argentina and most of Uruguay (Liu et al., 2012). Across these regions, Mollisols are extensively managed for grain and legume crops as well as for grass production in support of livestock (Liu et al., 2012).

2.3.4 Genesis of Mollisols

Because the SOC requirements for epipedons are not based on unique C pools, mechanisms for stabilization are heterogenous. Dominant processes associated with mollic epipedon development include Melanization (darkening of the soil from organic matter), Cumulization (buildup of materials in a toeslope position on the landscape), Calcium-humate formation and Bioturbation (movement of organic matter through soil depth via roots and microorganisms) (Bockheim, 2014).

Grasslands and prairies are the archetypal ecosystem associated with mollic epipedons and the way in which soil organic matter accumulates in mollic soils can be broadly conceptualized as the way in which grasslands input and stabilize organic matter

in the soil. Thus, exudates and residues from fine root systems that have low C/N when compared to woody debris (Cotrufo et al., 2019), and the incorporation of said inputs by typical grassland soil fauna and microbial communities, is a suitable model of mollic formation (given proper climate, topography, and parent material). A parent material that is rich in bases (e.g. limestone), a slope and site position that is conducive to accumulation, and a climate that supports grasslands are other plausible soil-forming factors to promote mollic formation (Bockheim, 2014).

In the U.S., 93% of Mollisol native vegetation is mapped as grasslands (Bockheim, 2014); thus, mollic formation that occurs outside of the grassland-steppe setting is more common for non-Mollisol soil orders. Examples of this include mixed and broad leaved forests (which collectively account for 86% of the native vegetation associated with Inceptisols containing a mollic epipedon in the U.S.; Bockheim, 2014). One study in Montana details the formation of Mollisols under Douglas fir forest, a coniferous forest ecosystem (Bakeman, 1983).

2.3.5 Lab determination of mollic properties

For USDA classification, SOC is determined via dry combustion (Soil Survey Staff, 2014). This method measures total C released as gas during combustion of organics, and for soils with carbonates (inorganic C), contributions to total C from carbonates are subtracted to determine the soil organic C content.

Basic saturation (BS) is the sum of extractable basic cations (Ca^{2+}, Mg^{2+}, K+, Na^{+}) over the total exchangeable cations in the soil (CEC; Ca^{2+}, Mg^{2+}, K+, Na^{+}, Al^{3+}, H^{+}) multiplied by 100. In USDA soil classification, sum of exchangeable bases are extracted in ammonium acetate at pH 7 (Soil Survey Staff, 2014).

Cation exchange capacity is total charge per kilogram of soil and determined by extraction of the total exchangeable cations ($Al^{3+,}$ H^{+}, Ca^{2+}, Mg^{2+}, K+, Na^{+}). In USDA classification, CEC can be determined using three methods. One method measures net negative charge by displacement of ammonium by potassium chloride after extraction of bases by ammonium acetate at pH 7. Another method is the by sum of exchangeable bases (in ammonium acetate at pH 7) plus sum of extractable acidity (in barium chloride at pH 8.2). The last method, effective CEC, is by sum of exchangeable bases plus sum extractable Al (in 1N KCL; Soil Survey Staff, 2014).

For USDA classification of Mollisols, the CEC for BS is determined with ammonium acetate at pH 7. When salts or carbonates are present, BS often exceeds 100% and is reported as 100% (Soil Survey Staff, 2014).

Information from particle size is a common criterion used in USDA soil taxonomy and particle size analysis is determined via one of two methods, pipette or hydrometer, with corrections for organic matter and gypsum (Soil Survey Staff, 2014).

2.4 The redwood forests and California grasslands

2.4.1 Ecosystem characteristics

The distribution of *Sequoia Sempervirens* (coast redwood, hereafter redwood*)* ranges from the Salmon Creek watershed at the bottom of the Big Sur coastline northward along the California coast into southern Oregon and closely reflects the summer “fog belt” of California (Noss, 2000a; Burgess and Dawson, 2004; Johnstone and Dawson, 2010). One study observed the ability of redwood leaves to directly absorb moisture from fog (Burgess and Dawson, 2004), however, the role of fog was more so to suppress losses from evapotranspiration than to supply water to foliage, in addition, 30%

of annual hydrologic inputs to redwood forests have been traced to fog-drip from leaf interception (Burgess and Dawson, 2004; Johnstone and Dawson, 2010).

Beginning in the 1800s, almost all old growth forest was logged for timber and forests became second and third growth. The remaining original forests (4%) are protected in Humboldt St Park, Big Basin St. Park, and Redwood National Park (Noss, 2000c; Save the Redwoods League, 2020). In addition to being the tallest species on the planet, stands of old growth coast redwood forest hold the world record for total above ground carbon per hectare (Van Pelt et ai)., 2016).

Substantial regional variations in environmental conditions, forest structure, and ecology has warranted a broad categorization of the redwood range into northern, central and southern sections (Noss, 2000a). The southern redwood forests are distinct from the northern forests in that 1) they collect less annual rainfall, 2) the extent and position on the landscape position is more limited, and 3) they support a different shrub layer beneath the canopy when compared to the northern forests (Noss, 2000a).

Rangelands cover approximately 50% of land area in the state of California (Silver et al., 2010). Following Spanish colonization, most native perennial California grasslands were outcompeted by introduction of exotic annual Euro-Asian species (Keeley, 2002; Ryals and Silver, 2013; Scaramozzino, 2015; Ryals et al., 2016). It was estimated that less 1% of native perennial bunchgrasses remain in the grasslands of central and southern California (Keeley, 2002). Despite non-native invasion, the potential for California grasslands to serve as a C sink is promising (Silver et al., 2010).

2.4.2 Soils of the Redwoods

Soils beneath the northern and central extent of redwoods have been generally characterized by intense leaching and a pH between 5.0-6.5 (Noss, 2000b). Principal soil orders mapped in these forests are Ultisols and Inceptisols (Noss, 2000b; UC Davis California Soil Resource Lab, 2018). Efforts to investigate soils in the northern and central redwood regions of the redwood included studies of epipedon-vegetation relationships (Popenoe et al., 1992), leaf litter decomposition rates (Pillers and Stuart, 1993), dynamics of dissolved organic carbon (Sanderman et al., 2008; Sanderman and Amundson, 2008), carbon dioxide production (Sanderman and Amundson, 2010), soil organic matter accumulation in arboreal Histosols (Enloe et al., 2006, 2010), the role of fog in redwood nutrient and water relations (Burgess and Dawson, 2004; Johnstone and Dawson, 2010; Ewing et al., 2012). Popenoe et al. (1992) provided basic soil properties (SOC, C/N, pH, bulk density, pH, cation levels) across vegetation types, epipedons, and drainage classes in northwestern California; redwood sites were included, but insights about mollic epipedons beneath them was hidden in a mollic-umbric-forest category (Popenoe et al., 1992).

In the southern redwoods, soil mapping indicates a dominance of Mollisols in a Xeric soil moisture regime (Noss, 2000b; UC Davis California Soil Resource Lab, 2018). There has been limited soils research in the southern redwoods (Noss, 2000b); we found a study on soil respiration rates (Potter, 2012) and a study of impacts to topsoil nutrients from fire-disease interactions (Cobb et al., 2016).

2.4.3 Soils of California grasslands

Due to the wide distribution and diveristy of mixed annual and perrenial medterranian grasslands, a review of soils across these ecosytems would be a unfit compairson to the redwood forest, an ecosytem endemic to one coastline. Thus, California grasssland soils can be considred intiriscally more varibale than redwood soils given their land areas. Furthermore, the influence of management on soil properties across grasslands is presumably more variable when compared to redwoods.

Overarching properties in grassland soil ecosytems when compared to coniferous forests include dominant inputs of SOM via root decay, secretions and exudates (less POM on the surface), lower C/N ratios in SOM, and dominance of arbuscular mycorrhizal fiungi when compared to ectomycorrhizal fungi (Orgiazzi et al., 2016a; Cotrufo et al., 2019). When compared to the life-cycle of perennial grasslands, the strategy of annual grasses (which are now dominant in California) incurs temporal variability in SOM inputs, shallower roots, and lower root-to-shoot allocaitions (Silver et al., 2010).

2.4.4 Importance of California's grasslands and redwood forests

Redwood forests are a unique resource to California that support the tourism and forest management industries, they also offer rich habitat capable of supporting wildlife at unparalleled heights (e.g. the iconic and federally threatened Northern Spotted Owl). Similarly, rangelands of California protect habitats in approximately 24 million hectares (Silver et al., 2010) of non-ununrbanized lands, support the livestock industry, and promote floristic diversity (Ryals et al., 2016).

2.5 Summary

Given concerns with atmospheric CO_2 levels across historical timescales, finding ways to promote C stabilization in land management is important for the sustainability of the world's societies. Recently there was paradigm shift in the way which SOM stabilization was understood which discouraged the association of chemical complexity with stability, and instead shifted focus to a more holistic approach that encouraged consideration of different mechanisms (and associated pools) which govern SOM residence times and mass incorporation. Mollic soils are taxonomically distinguished as having captured C and they offer a promising niche in soil C sequestration. Mollic soils are generally associated with grasslands but have been mapped in the southern redwood forest of central California. This review introduced those ecosystems and compared what is known about soils in those settings.

CHAPTER 3

Description of Study Areas

3.1 Swanton Pacific Ranch

3.1.1 Overview

Swanton Pacific Ranch (SPR) is a 3,200-acre property located in Davenport, California of northern Santa Cruz County. It is owned by the Cal Poly Corporation and operated by the College of Agriculture, Food, and Environmental Sciences at California Polytechnic State University of San Luis Obispo (Swanton Pacific Ranch, 2020a). The Ranch hosts more than 1,400 acres of forestland, 1,500 of acres of rangelands and 100 acres of cropland (Brian C. Dietterck et al., 2020). The property contains multiple sub-basins within the Scott Creek Watershed, which is approximately 30 square miles and contains at least 10-12% of California's flora (West, 2016).

3.1.2 Landuse and history

The descendants of the native peoples to inhabit the Scotts Creek Watershed refer to themselves as the Amah Mutsun, but scholars decide to use the larger label, Ohlone, to describe these people (Scaramozzino, 2015). Ohlone people represented approximately 40 tribelets who lived peacefully and non-nomadically in the resource-abundant lands that surrounded the San Francisco Bay and Monterey Bay; the first Ohlone settlement may have been 4,5000 to 5,000 years ago (Margolin, 1978). Each tribelet (250 people, on average) was autonomous in nature yet shared similar cultural traditions and world views (Margolin, 1978). There were approximately 12 languages spoken amongst the Ohlone people; not all tribelets shared common language (Margolin, 1978). For each tribelet, the resources utilized changed with the surrounding ecologies; in general, basket weaving,

shellfish gathering, acorn harvesting, and hunting for deer, salmon, and grizzly bears were integral practices of the Ohlone (Margolin, 1978). The indigenous peoples of California participated in the trading of resources and the Ohlone were no exception (Margolin, 1978; Scaramozzino, 2015). The indigenous populations established extensive trial networks used for trading throughout the state, and these routes continued into the Pacific Northwest and across the Sierra Nevada into the Great Basin (Margolin, 1978).

The earliest land management that would have occurred in the Coast Ranges before written times is the native peoples' use of fire to encourage herbaceous replacement of woody chaparral to improve access to harvestable plant, animal, and water resources; a phenomenon recorded during European contact (Scaramozzino, 2015). Fire was also used by the Ohlone to reduce fuel loading for prevention of catastrophic fire (Margolin, 1978). The native peoples were hunter gatherers and agriculture did not exist in California until 18th century Spanish colonization (Scaramozzino, 2015). The depletion and assimilation of native populations into the Spanish mission system resulted in irreversible ecological changes on the coastal Californian landscape as fire management was altered, and the introduction of exotics species with extensive grazing disrupted the native flora and fauna of grassland communities (Keeley, 2002; Owen et al., 2015; Scaramozzino, 2015; Ryals et al., 2016).

Recorded history of the Scotts Creek Watershed begins with a Spanish-Mexican land grant established in 1839 and titled "Agua Puerca y las Trancas", translated as "hog water and the bars" (Scaramozzino, 2015). Claims to property rights under this grant incurred several ownerships before 1867, after which the property was sold to James Archibald who established a dairy with Ambrogio Gianone.

Legacies of land acquisitions in the Scotts Creek Watershed thereafter have persevered through geographic nomenclature (e.g. Archibald Creek, Stuab House, Swanton Valley, Queseria Creek, etc.), standing historic structures (e.g. barn made from the Portuguese-shipwreck, the Queseria, the school house), and multi-generational family inhabitance (e.g.Mcracrys of Big Creek Lumber). Fred Swanton, Mayor of Santa Cruz, built a hydroelectric dam on Big Creek (a basin within Scotts Creek) that supplied power to Santa Cruz from 1899- 1948. Clear-cut logging by the San Vicente Lumber Company and construction of the Ocean Shore Railroad began in the Watershed during the early 1900s and was closely followed by the establishment of row crop agriculture and cattle operations that included encampments in the upper coastal terraces (Smith, 1990) .

In 1978, Al Smith (Orchard Supply Hardware founder and Cal Poly alumnus) bought the 3,200 acres of land that is SPR; in 1993, he donated the land to the College of Agriculture Food and Environmental Science at the California Polytechnic University of San Luis Obispo (Swanton Pacific Ranch, 2020a).

There are 701 acres of forest land in SPR that are managed under a non-industrial timber management plan that was approved by the State of California in 2008(Brian C. Dietterck et al., 2020). The goals of the plan are to ensure a healthy forest ecosystem and to generate revenue from lumber (under the Forest Stewardship Council certification) in a commercial second-growth redwood forest. In the management plan, provision of research and educational opportunities in forest management in an upmost priority (Brian C. Dietterck et al., 2020).

The University manages roughly 1,600 acres of rangeland (grassland, chaparral, prairie) on the coastal marine terraces that drain directly into the Pacific Ocean or down

the foothills to Scotts Creek. The ranch maintains a grass-fed beef operation with 75-125 head of resident cattle, additionally the ranch brings on 250-450 stocker cattle each spring. The rangeland management program includes collaboration with student enterprise and research projects to achieve holistic management objectives that include the support of: biodiversity, water quality, soil health and student learning (Swanton Pacific Ranch, 2020b).

3.1.3 Environmental setting

3.1.3.1 Climate

The climate on the Central Coast of California is generally classified as Mediterranean. Globally, Mediterranean climatic regions are located at latitudes 32-40° north or south of the equator on the western coasts of continents; in these locations, proximity to ocean water, and dry summers with westerly air flow are the dominant weather influences (Henson and Usner, 1993). Seasonality on the California Central Coast can be characterized by moderate diurnal variations in winter air surface-temperatures when compared to the summer, several extreme rainfall events each year (>50 mm rain per day), and high sustained wind speeds (>40 miles per hour; Potter, 2012). The topography of the California Central Coast represents the steepest coastal gradient in North America, and thus, the advection of Pacific marine stratus over the mountainous terrain functions to reduce insulation and temperatures, raise humidity, and supply water directly to the landscape (Potter, 2012).

At Swanton, precipitation measurements from a tip-bucket gauge (located approximately 300 m above sea level) indicate that from 2000 to 2014, average annual rainfall was 84 cm, with 74 days of measurable rainfall per year, on average (Kenny,

2020). The Natural Resource Conversation Service has maintained six weather stations located inside the Ranch boundary since 2011. Data from these weather stations indicate soil temperature regimes at 50 cm (depth used for U.S. soil classification) are thermic (15-22°C mean annual temperature with at least 6 °C difference in mean winter and summer temperatures; Soil Survey Staff, 2014) in the lower coastal stations and isomesic (8-15°C with less than 6°C difference in mean winter and summer temperatures; Soil Survey Staff, 2014) in the higher inland stations (Natural Resource Conservation Service, 2020). Air temperatures at these stations indicate an average of approximately of 13°C, with minimum temperatures reaching -6°C and maximum temperatures reaching 40°C across the weather stations (Natural Resource Conservation Service, 2020).

3.1.3.2 Geology

The dominant parent material beneath Swanton Pacific Ranch is Santa Cruz Mudstone, an upper Miocene medium to thick bedded siliceous mudstone (this map unit is contiguous across the west side of the northern foothills of Santa Cruz County; U.S. Geological Survey, 1989). In thin veins that surround the creeks, parent material is mapped as undifferentiated Holocene alluvial deposits (Brabb, 1989). On the coastal terraces where cattle graze, there are disjointed units of Pleistocene coastal terrace deposits that are composed of marine sand and irregular gravels (Brabb, 1989).

3.1.3.3 Flora

A recent floristic study by Kenny (2020) documented 634 total plant taxa within the Ranch boundary. Of the many taxa, Kenny (2020) reported 2 endemic taxa, 18 taxa at the end of the species range extent, and 16 taxa with California Native Plant Society rare plant rankings (i.e. listed or in consideration of being listed species). In approximate

ascending order of elevation, examples of plant communities that occur in SPR include salt march, coastal bluff, coastal prairie, riparian forest, mixed conifer forest, and chaparral- to name a few (Kenny, 2020).

3.1.3.4 Fire history

Before August 2020, the only record of fire in Swanton Valley was the 2009 Lockheed fire which burned approximately 7,800 acres, including 90% of the Little Creek Watershed (John Hardy, 2017; Capital Public Radio, 2019). Following the Lockheed fire, there were several efforts to study the impacts (Niebrugge, 2012; Auten, 2012; Loganbill, 2013; Theobald, 2014)-to name a few. Information on the 2020 CZU Lightning Complex fire is found in a later section of this document (6.5.5).

3.2 Landels-Hill Big Creek Reserve

3.2.1 Overview

Landels-Hill Big Creek Reserve (LHBR) is 4,328-acre property located on the Big Sur coastline of southern Monterey County with an additional 5,228 acres accessible by use-agreement (University of California at Santa Cruz, 2020). It is owned by the University of California and managed by the University of California at Santa Cruz.

Drastic topography and small-scale climatic variations in the Reserve have provided a diversity of flora that includes 11 distinct plant communities and roughly 350 species (Bickford and Rich, 1984). If there has been an effort to map the categorized plant communities or habitat types that make up LHBR, such information is not easily accessible.

3.2.2 Landuse and history

The oldest known archeological site in proximity to the Big Sur Coastline is 8,430 years old and located near Cambria, in San Luis Obispo County, California (Henson and Usner, 1993). In Big Sur, there are two archeological sites (near Church Creek and Esselen Institute) that dated back to about 4,500 years ago (Henson and Usner, 1993). The Esselen people inhabited "the heart" of Big Sur coastline sharing a boundary with the Costanoan-Ohlone people near Point Sur to the north, and to the south the inhabitance changed to that of the Salinan peoples near the Big Creek watershed (Henson and Usner, 1993). The Esselen people may have spoken the most complex indigenous language in North America (Georgette, 1981).

The Esselen people where hunter-gatherers and traveled seasonally up the slopes of the Big Sur coast for terrestrial resources (e.g. deer and acorns) and down the slopes for mussels and abalone (Henson and Usner, 1993). While there is evidence that native peoples on the California coast used fire to manage the ecology, it is not clear whether or not the Esselen used this strategy (Georgette, 1981; Henson and Usner, 1993).

When the Portola expedition left Mexico for Monterey and reached the Big Sur Coastline, the travelers were discouraged by the treacherous topography and moved inland to establish the route that would later guide the Missions away from the coast and into the Salinas Valley. The construction of the Monterey Mission in 1770 was the beginning of the end of Esselen culture as most of the native peoples were brought there and exposed to disease and forced labor (Georgette, 1981).

It wasn't until the 1860s that pioneer families began to inhabit the isolated canyons and ridgelines of Big Sur (Henson and Usner, 1993). Due to the coastlines' steep

slopes, the land was not suitable to agriculture however families raised livestock, planted orchards, and grew food for themselves (subsistence farming; Henson and Usner, 1993). While the rangelands of the Reserve property were historically used by local ranchers for decades, grazing hasn't has occurred on the Reserve since 1984 (Bickford and Rich, 1984).

Because of its rugged terrain and restrictive access, the cost of logging the Big Sur Coastline protected the Santa Lucia Mountain from the wide-spread impacts of industrial logging that swept the redwood coastline (including the Santa Cruz mountains) during the late 19th century (Henson and Usner, 1993). Despite this geographic disadvantage to logging activities, in 1924, the California State Board of Forestry reported half of the virgin timber in Big Sur remained (Henson and Usner, 1993). Aside from small-scale logging activities associated with current and historic homesteads, and road and trail maintenance, it is reported that no major logging operations have occurred within the Reserve (Bickford and Rich, 1984).

The construction of highway one through the Big Sur coastline marked the ending of the coastline's restricted physical access. Tourism is now the main industry along the approximately 80 mile stretch of coastline. With increased traffic, invasive species such as the Pampas grass (*Cortaderia selloana*) have established populations along the roadside. Despite ruderal disturbance most of the land area is protected by California State Parks (e.g. Pfeiffer St. Park), the United States Forest Service (Los Padres National Forest) and the Department of Defense (Fort-Hunter Liggett).

3.2.3 Environmental setting

3.2.3.1 Climate

A description of the regional climate and seasonality for the Central Coast of California (as applicable to LHBCR) was provided for SPR, in an earlier section of this chapter (3.1.3.1).

For Big Sur particularly, the coastal influence and wall-like topography of the Santa Lucia range can create vastly contrasting temperatures and moistures across the landscape (Henson and Usner, 1993). In higher elevations and on east side of the Santa Lucia crest, hot and dry summer conditions can exist concurrently with cool fog at lower elevations on the coast (Henson and Usner, 1993). The distribution of the coast redwood forests have been strongly associated with (and confined to) the geographical influence of fog on the California coast, this, due to the role of fog in suppression of atmospheric water vapor pressure deficits and contribution to canopy drip during the summer months (Johnstone and Dawson, 2010).

There is no easily accessible weather data (precipitation, stream stage, soil moisture, soil temperature, air temperature) in the Reserve akin to the data available at SPR. The Reserve website reports average precipitation is 62 cm on the coastline and 102 cm on the ridgelines (University of California at Santa Cruz, 2020).

3.2.3.2 Geology

The geologic formations of the Big Creek Reserve are a product of the Sur Fault Zone, which cuts across the property in a northwest-southeast diagonal. The major geologic units are: (i) the Franciscan Complex (a slurry of conglomerate, sandstone, shale, volcanic rocks, chert, serpentinite, and blueschist) on the coast, (ii) the Coast Ridge

Belt (intrusive igneous and metamorphic rock) to the east, and (iii) an unnamed upper Cretaceous sedimentary formation that rests unconformably over the ridge belt (named the “Big Creek Conglomerate”). In some parts of the reserve, landslide and marine terrace deposits overlay underlain parent material (Norris, 1985).

3.2.3.3 Flora

Plant communities are highly aspect-driven and can be sharply contrasting, as in the case of moist redwood canyons (at the southern extent of the taxa) that mingle with dry yucca hillslopes (at the northern extent of the taxa). Other communities within the reserve include mixed-oak woodlands, coastal grasslands, pine forests, and a diversity of “hard” and “soft” chaparral communities. (Bickford and Rich, 1984)(Bickford and Rich, 1984)The Santa Lucia fir (*Abies bracteata*) is the rarest fir in North America and can be found in the upper elevations of the Devil’s Canyon. Floristic studies that occurred in the reserve between 1978-1979 documented 342 plant species (Bickford and Rich, 1984).

3.2.3.4 Fire history

Historical fire maps suggest that over the last 150 years, there has been infrequent massive burns along the Big Sur Coastline (Capital Public Radio, 2019). Major fires to impact the Big Creek watershed were the 1985 Rat Creek-Gorda fire (60,000 acres; Henson and Usner, 1993), the 1999 Kirk Complex Fire (86,700 total acres burned; National Interagency Fire Center, 2020) as well as two smaller unnamed fires in 1941 and 1917 (Capital Public Radio, 2019). Information on the 2020 Dolan fire is found in a later section of this document (6.5.5).

CHAPTER 4

Materials and Methods

The Materials and Methods chapter is first organized by study objective, under which the materials, study design, field work, and a list of laboratory analysis, and statistical analyses (if pertinent) are described. Procedures for laboratory analyses are presented in an individual subsequent section of the Materials and Methods chapter, as details for each procedure were applicable to multiple study objectives. A summary of quality control measures implemented for laboratory procedures and data analysis is found in Appendix G.

4.1 Objective 1: gather baseline soils data for the Coast Redwood forest and compare said properties to those in adjacent grasslands

4.1.1 Materials

We investigated 43 soil profiles at two properties on the central cost of California We hand-dug pits and described 28 soil profiles at Swanton Pacific Ranch (SPR) and 15 soil profiles at the Landels-Hill Big Creek Reserve (LHBC; Figure 4.1). Both properties are university-owned lands that contain redwood forest and grassland ecosystems underlaid by soil map units with mollic epipedons.

Within the property boundaries of SPR, we set up three sub-populations or "zones" to increase the diversity of profile sites on the ranch while providing stream-lined access points (Figure 4.2). Zone 1 was near the Boy Scout Camp and Deer-Hunter Trail ridgeline (10 soil profiles), Zone 2 was inside the Little Creek watershed and ascended towards the Lions Flat ridgeline (9 soil profiles), and Zone 3 was in the upper rangeland

and adjacent forest above Scotts Creek (9 soil profiles). A map of all the soil profiles we instigated SPR is found in Figure 4.3.

The profiles we investigated at the Landels-Hill Big Creek Reserve were confined to the southern extent of the property in a single zone that captured a tributary of redwoods that drained into the Vicente Creek Watershed, as well as the southwest-facing grassy slopes above (Figure 4.4).

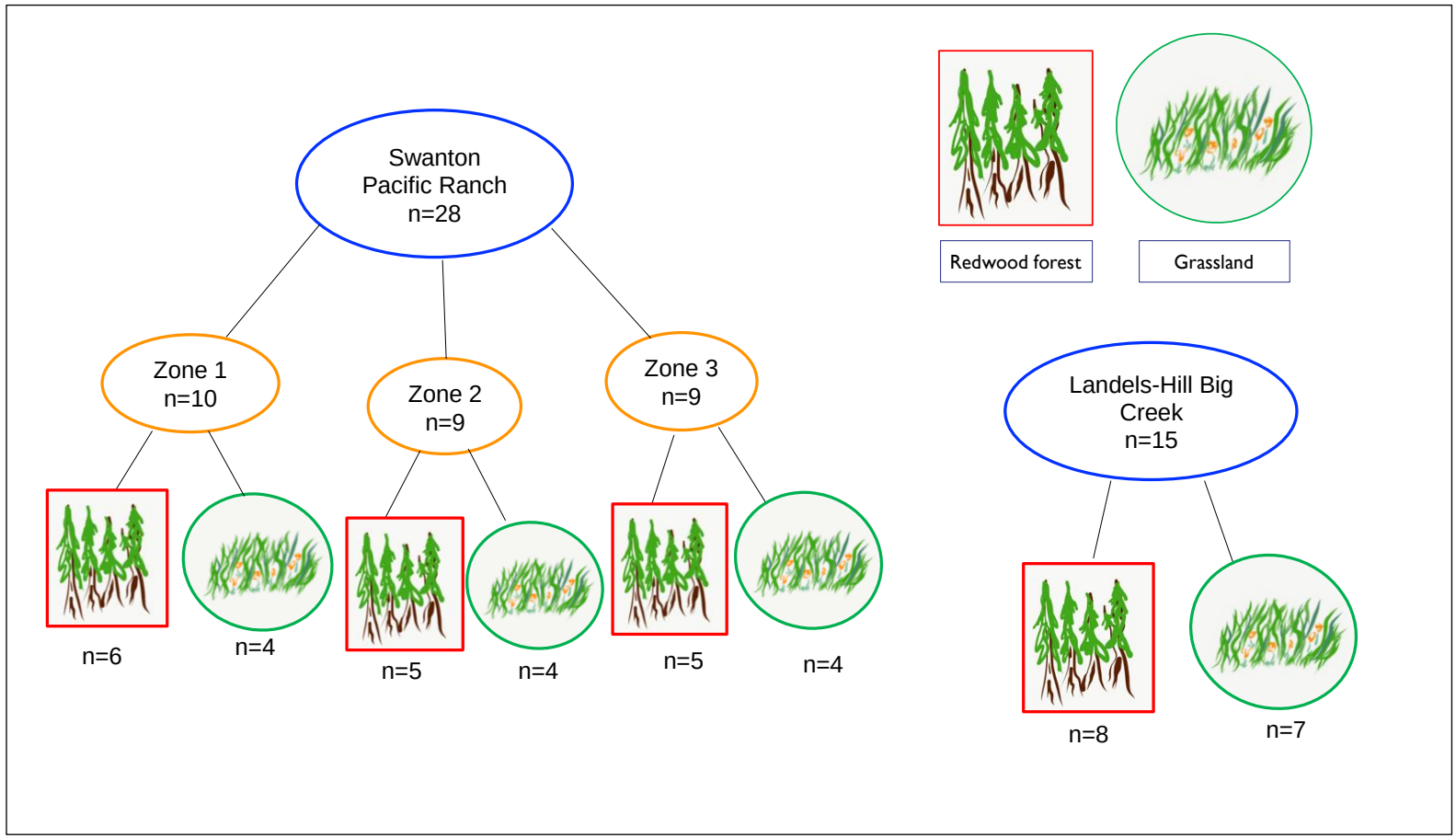

Figure 4.1. Schematic of study design for soil profiles. The "n" refers to number of pits in respective category. Redwood forest (red, left) and grassland (green, right) plant communities are displayed as drawings.

Figure 4.2. Zones 1, 2, and 3 for profile site-selections at Swanton Pacific Ranch, Santa Cruz County, CA. Soil pits were dug in spring of 2018.

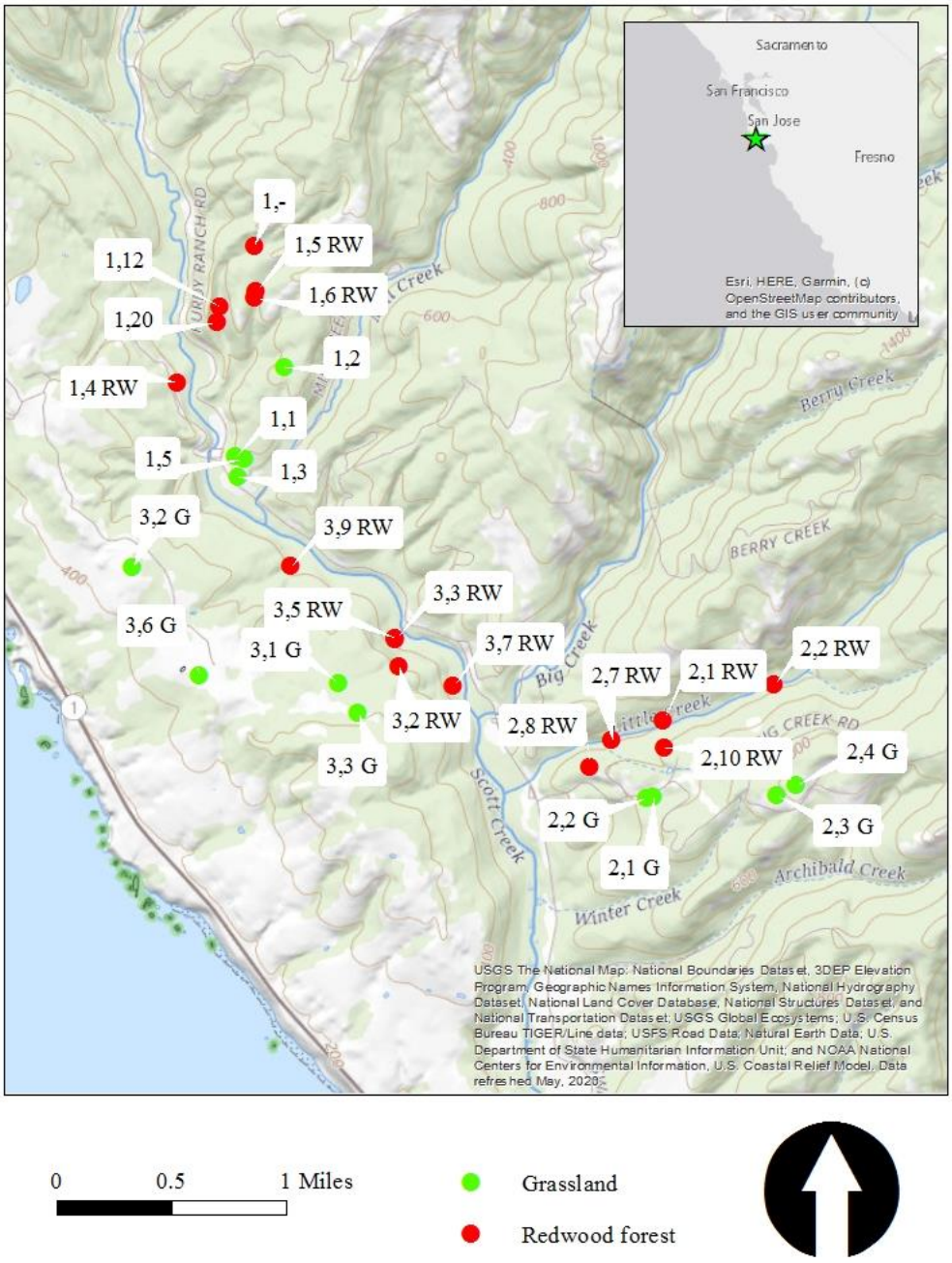

Figure 4.4 Soil profile sites in 2018 at Swanton Pacific Ranch, Santa Cruz County, CA. Profiles are labeled by unique identification numbers, the first number in the label indicates the zone. Coordinates of each profile are found in Appendix O.

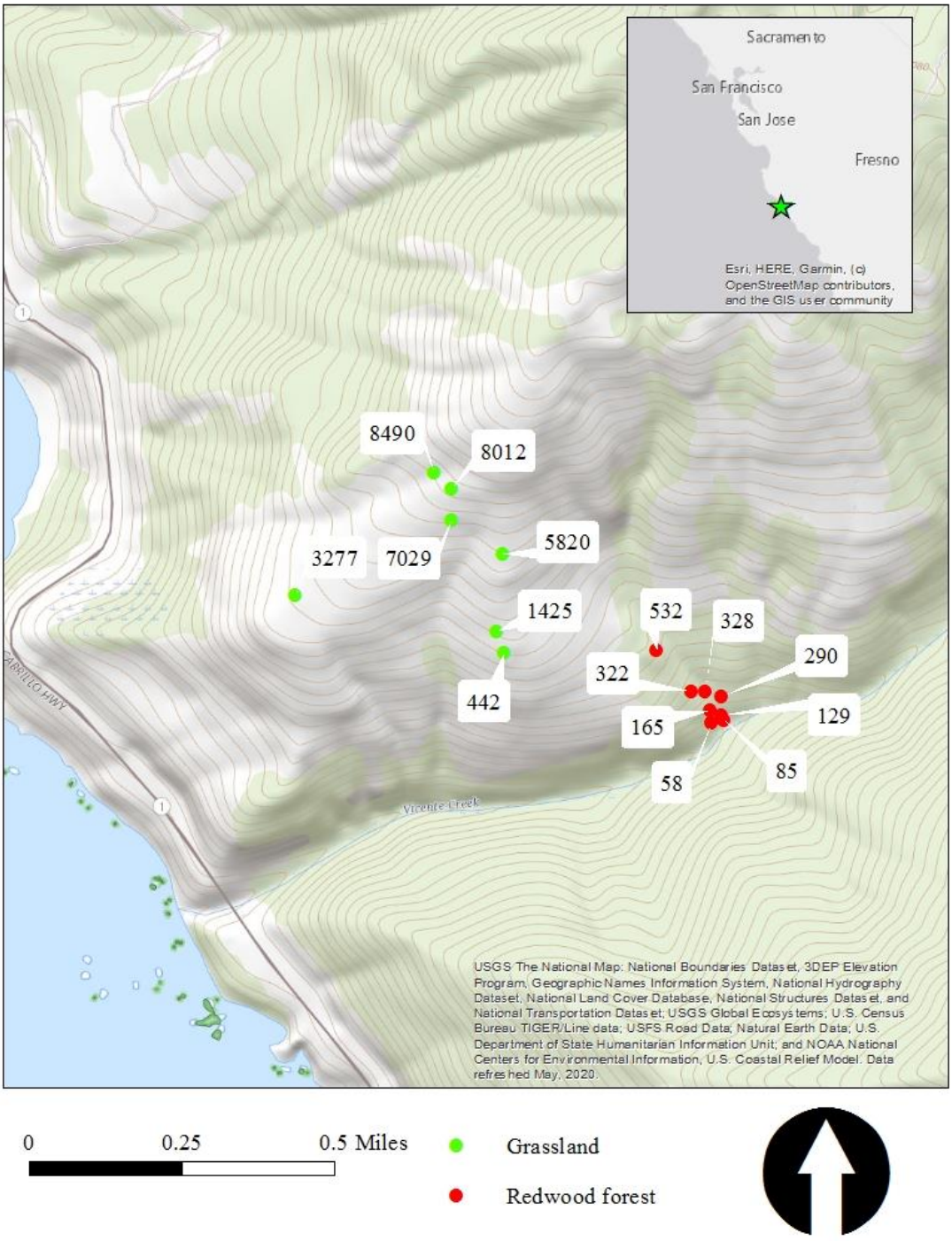

Figure 4.4 Soil profile sites in 2019 at Landels-Hill Big Creek Reserve, Monterey County, CA. Coordinates of each profile are found in Appendix O.

4.1.1.1 Soils Series Mapped

Dominant soil series in each study site mapped by *Soil Web Survey* (UC Davis California Soil Resource Lab, 2018) are listed in Table. 4.1. Mollisols were the dominant soil order.

Table 4.1. Dominant soils mapped by *Soil Web Survey* (UC Davis California Soil Resource Lab, 2018) within study areas at Swanton Pacific Ranch and Landels-Hill Big Creek Reserve. Soil series separated by plant community (redwood forest and grassland). Soils are labeled by series name (and family name in parentheses).

Location		---------- mapped series----------	
Plant community		Redwood forest	Grasslands
Swanton Pacific Ranch	Zone 1	• Santa Lucia (Clayey-skeletal, mixed, superactive, thermic Pachic Ultic Haploxerolls)	• Aptos (Fine-loamy, mixed, superactive, mesic Pachic Ultic Argixerolls) • Bonny Doon (Loamy, mixed, superactive, thermic, shallow Entic Haploxerolls)
	Zone 2	• Ben Lomond (Coarse-loamy, mixed, superactive, mesic Pachic Ultic Haploxerolls) • Catelli (Coarse-loamy, mixed, superactive, mesic Ultic Haploxerolls) • Sur (Loamy-skeletal, mixed, superactive, mesic Entic Haploxerolls)	• Tierra (Fine, smectitic, thermic Mollic Palexeralfs) • Watsonville (Fine, smectitic, thermic Xeric Argialbolls) • Bonny Doon (Loamy, mixed, superactive, thermic, shallow Entic Haploxerolls)
	Zone 3	• Ben Lomond (Coarse-loamy, mixed, superactive, mesic Pachic Ultic Haploxerolls) • Catelli (Coarse-loamy, mixed, superactive, mesic Ultic Haploxerolls) • Sur (Loamy-skeletal, mixed, superactive, mesic Entic Haploxerolls) • Santa Lucia (Clayey-skeletal, mixed, superactive, thermic Pachic Ultic Haploxerolls)	• Bonny Doon (Loamy, mixed, superactive, thermic, shallow Entic Haploxerolls) • Elkhorn (Fine-loamy, mixed, superactive, thermic Pachic Argixerolls) • Los Osos (Fine, smectitic, thermic Typic Argixerolls)
Landels-Hill Big Creek Reserve		• Gazos (Fine-loamy, mixed, superactive, thermic Pachic Haploxerolls) • Gamboa (Loamy-skeletal, mixed, superactive, mesic Pachic Haploxerolls) • Sur (Loamy-skeletal, mixed, superactive, mesic Entic Haploxerolls).	• McCoy (Fine-loamy, mixed, superactive, thermic Pachic Argixerolls) • Gaviota (Loamy, mixed, superactive, nonacid, thermic Lithic Xerorthents)

4.1.1.2 Plant communities

A description of the plant communities at SPR and LHBCR can be found in Appendix A.

4.1.2 Study Design

The design for the soil pit study was implemented in ArcMap 10.5 (ESRI, Redlands, CA) and Google Earth. All soil pit locations were generated by random selection within areas of redwood forest and grassland determined via aerial imagery. Random selection within areas was facilitated by the Excel (Microsoft, Redman WA) *random number generator function* to generate a number that corresponded with a grid point. Grid points were evenly spaced (every 25 feet at SPR and every 5 meters at LHBCR) and established using the *fishnet tool* in ArcMap. Each grid point had unique latitudinal and longitudinal values for a hand-held GPS unit or cell phone. Areas for grid-point establishment conformed to zones if applicable (i.e. at SPR) and were within property lines. Areas were designed to exclude any adjacent, non-redwood or non-grassland ecosystems (mixed evergreen forest, chaparral or coastal scrub) and to allow reasonable access. The study design was created in consultation with a statistical consultant before implementation in the field.

At SPR, all soil profile sites were controlled for geology and slope. Sites were exclusively selected on Santa Cruz Mudstone, which was the dominant parent material beneath study area (Brabb, 1989); additionally, we excluded sites with over 30% slope. Initial screening for slope and geology was done in GIS with a georeferenced geological map (Brabb, 1989) and DEM layer provided in a University mapping database.

At LHBCR, there were multiple geologic formations beneath the study area of interest; the map units identified within this area were landslide deposits (Holocene), Franciscan Greywacke and mélange (Jurassic), and Franciscan metavolcanics (Jurassic; Rosenberg and Wills, 2016). For feasibility, because of mixed parent materials in our desired study area and surrounding environs, and in the interest of capturing the true characteristics of the plant communities (i.e. since redwoods are found in steep-sloping canyons, we decided not to establish a slope threshold), we chose not to control for geology and slope at LHBCR.

Because there is less existing research on redwood soils, we designed the study so that there would be slightly more redwood soil profiles than grassland soil. In Zone 1 at SPR, we established 6 redwood pits and 4 grassland pits, for Zones 2 and 3, we established 5 redwood pits and 4 grassland pits (Figure 4.1). At LHBCR there were 8 redwood pits and 7 grassland pits (Figure 4.1).

For instances in which we arrived at a soil pit location but considered the site to be unsuitable (e.g. dense poison oak, slope too steep for SPR, etc.), discretion was used to either, 1) relocate to the next random site in chronological order, or 2) to stay in place and implement an alternative protocol. This protocol was to move 1 meter north, if site still not suitable then, 1 meter east, 2 meters south, 2 meters west, 3 meters north, and so on as to move outward around the GPS coordinate in a non-biased pattern until a suitable site was reached.

4.1.3 Field work

With the exception of access to an off-highway vehicle for two days at SPR, all soil pits were accessed via foot, and the coordinates for each pit were located in the field using a handheld GPS unit or cellphone with downloaded Google Earth KMZ layers.

Each pit was hand-dug using a round-tipped standard spade shovel and drain-spade sharp-shooter shovel. The soil profile was dug to 1.5 meters depth or until weathered bedrock was reached.

Soil pits were described according to the conventions and procedures identified in the *Soil Survey Manual* (Soil Science Division Staff, 2017) and the *Field Book for Describing and Sampling Soils* (Schoeneberger et al., 2012). Once soil horizons were designated, the following soil (and site) attributes were described on a field-description sheet:

- Clay percentage and USDA texture class (estimated by feel)
- Moist color using Munsell color book
- Soil structure (grade, size, and shape)
- Percent rock fragments
- Root distribution (size and abundance)
- Soil pedogenic horizon designation
- Horizon depth
- Slope
- Aspect
- Landform and position

For every mineral soil horizon designated, 2 samples were collected in labeled quart-sized plastic bags: (1) the main soil sample for all lab analyses that are described below, and (2) a bulk density core-sample when possible (i.e. when the percent of soil covered by rock fragments was low enough to allow coring).

In 2018, a brass Soil Moisture Equipment Corp soil bulk density corer (153.11 cm^3) was used to collect bulk density samples. In 2019, a stainless steel AMS soil bulk-density corer (90.59 cm^3) was used. For redwood soils, a representative sample of the forest floor was collected for every organic horizon identified.

Samples were packed out from the field and brought to the laboratory. Soil bags were opened and left outside to air dry before preparation for analysis.

4.1.4 Laboratory analysis

The following analyses were performed on all mineral horizons collected from soil profiles at SPR and LHBC, and the details of each method can be found below in a subsequent section of this chapter titled "Description of laboratory procedures" (4.6):

- Air-dry gravimetric water content
- Soil pH (1:1 deionized water, 1:2 0.01 *M* $CaCl_2$)
- Soil organic carbon
- Permanganate oxidizable carbon
- NH_4OAc extractable Ca, Mg, K, and Na
- Cation exchange capacity
- Basic cation saturation
- Particle size analysis (for SPR soils only)
- Bulk density

4.1.5 Statistical analysis

All data was organized in Excel (Microsoft, Redman, WA) and saved on the cloud in One-Drive (Microsoft, Redman, WA). Statistical analysis was done in JMP (SAS Institute, Carey, NC).

4.1.5.1 Multivariate regression for soil pits

A multivariate regression model was created to analyze response variables with controls for site slope, vegetation, pedogenic horizon, and horizon depth as explanatory variables. At SPR, we included the zone variable (1, 2, or 3) in the model, as said variable were nested into the study design (this was not applicable to LHBCR). We looked for pairs of interactions between vegetation, slope, and horizon depth for each response variable of interest.

This model was created in consultation with a statistical consultant in the Statistics Department at the California State Polytechnic University of San Luis Obispo. The general regression expression for soil profile analyses is found in Eq. 16 (Appendix F).

For any horizon with a BS greater than 1.0, (7 of 102 horizons at SPR and 33 of 56 horizons at LHBCR) we assumed there was dissolution of pedogenic carbonates and for the purpose of analysis, we changed these horizons to be 1.0 as per USDA soil classification guidelines (Soil Survey Staff, 2014).

Because there were more observations at shallower depths, we log-transformed horizon center-depth. Furthermore, in an effort to achieve normality and equality of

spread in the residuals across the predicted values of the model, we preformed transformations to response variables as fit. Transformations are identified in Table 5.1.

Last, all horizon designations in the field (e.g. Bt1, Bt2, Ap, Bw) were simplified into 4 broader horizon designation categories A, AB, B, and C for the purpose of including enough samples for each category.

4.1.5.2 Least squares mean

We were interested in the average value for redwood and grassland plant communities when other factors included in the regression model were considered. In consultation with a statistician, we decided to report the "least squares mean" for each plant community. The least squares mean is a value used in regression modeling that is the mean of a categorical effect when other continuous effects included the model are set to their mean values (SAS Institute Inc., 2018). Nominal effects included in the model do not influence the least squares mean (SAS Institute Inc., 2018).

In instances where the response variable was transformed to fit the model, we created 95% confidence intervals from the LSM (and standard error) values. These confidence intervals were then back-transformed into original units, this all to preserve the uncertainty associated with the asymmetric distribution of the data, as per consultation with a statistician (Eq. 23 Appendix F).

4.2 Objective 2: identify taxonomic classifications of said redwood forest and grassland soils

We used information collected in the field described above (section 4.1.3; texture by feel, clay films, horizon designations, etc.) in conjunction with the data analyzed in the laboratory (SOC, BS, etc.; section 4.1.4) to classify 43 soil profiles to the family name in adherence to *The Keys to Soil Taxonomy* (Soil Survey Staff, 2014). Excel (Microsoft, Redman, WA) was used to run descriptive analyses on the soil orders.

4.3 Objective 3: investigate the influence of vegetative gradation on soil properties between the redwood forest and adjacent grasslands

4.3.1 Materials

At SPR, we investigated soil properties at several points along five transects (designated as 114, 6092, 2156, 3339, 5849) at three depths (0-10 cm, 10-25 cm, and 25-50 cm; X, Y, and Z respectively; Figure 4.5). Each transect captured a gradient of plant communities that began in the redwood forest and transitioned (rising in elevation) into mixed evergreen forest, coastal scrub (only in 1 of 5 cases), and finally into coastal grassland (Figure 4.6). Soil was collected (at each of the three depths) for in every plant community and "ecotone" (transitional area between plant communities) along the transect.

All five transects were located within the Zone 3 (upper rangelands and adjacent forest above Scotts Creek) of the previously described soil pit study at SPR. A description of soils mapped in this area can be found above in the summary of soils mapped in Zone 3 for the profile study (section 4.1.1.1).

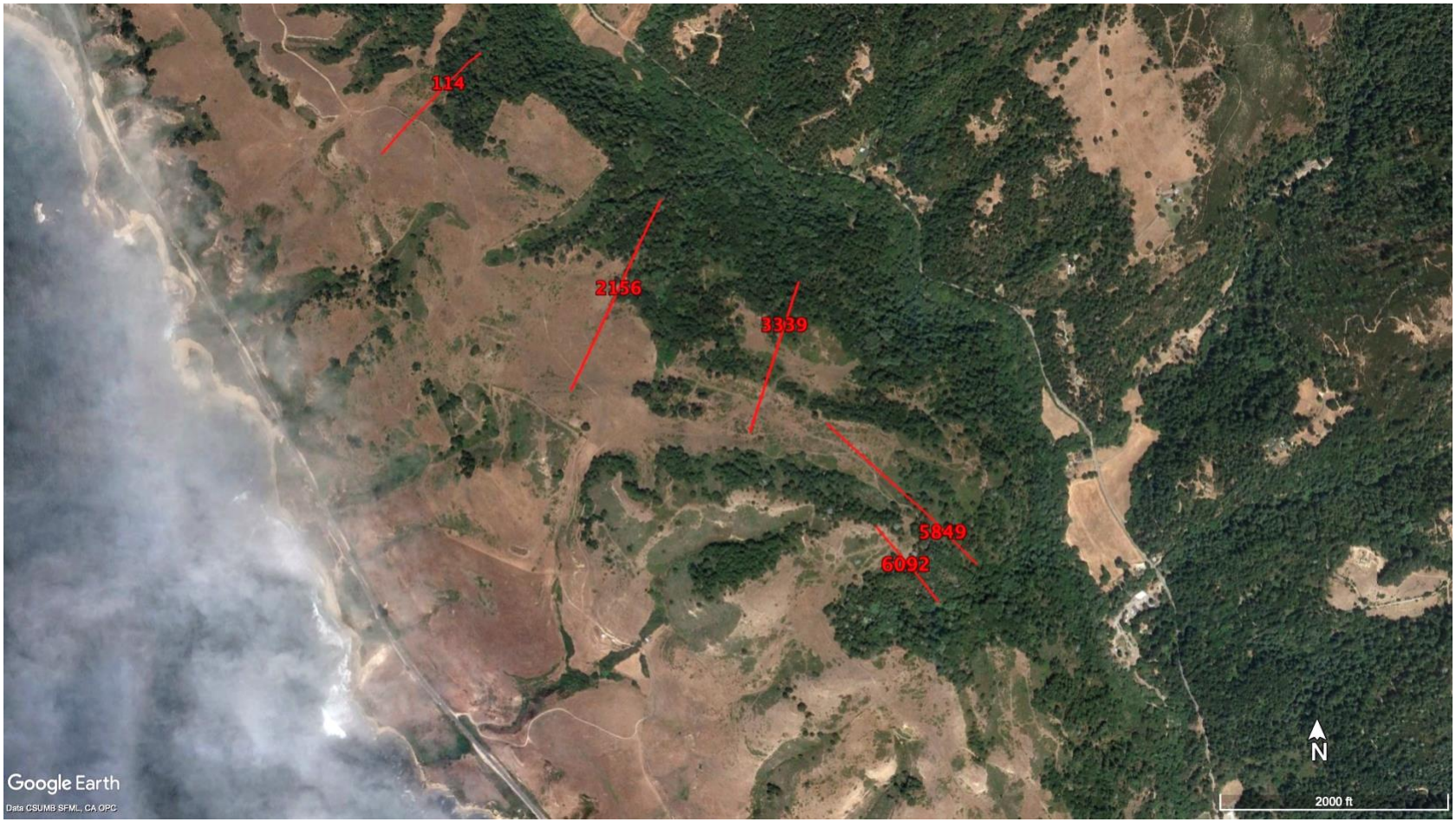

Figure 4.5. Overview of 2019 transects (designated as 114, 2156, 3339, 5849, and 6092) from north to south at Swanton Pacific Ranch, Santa Cruz County, CA.

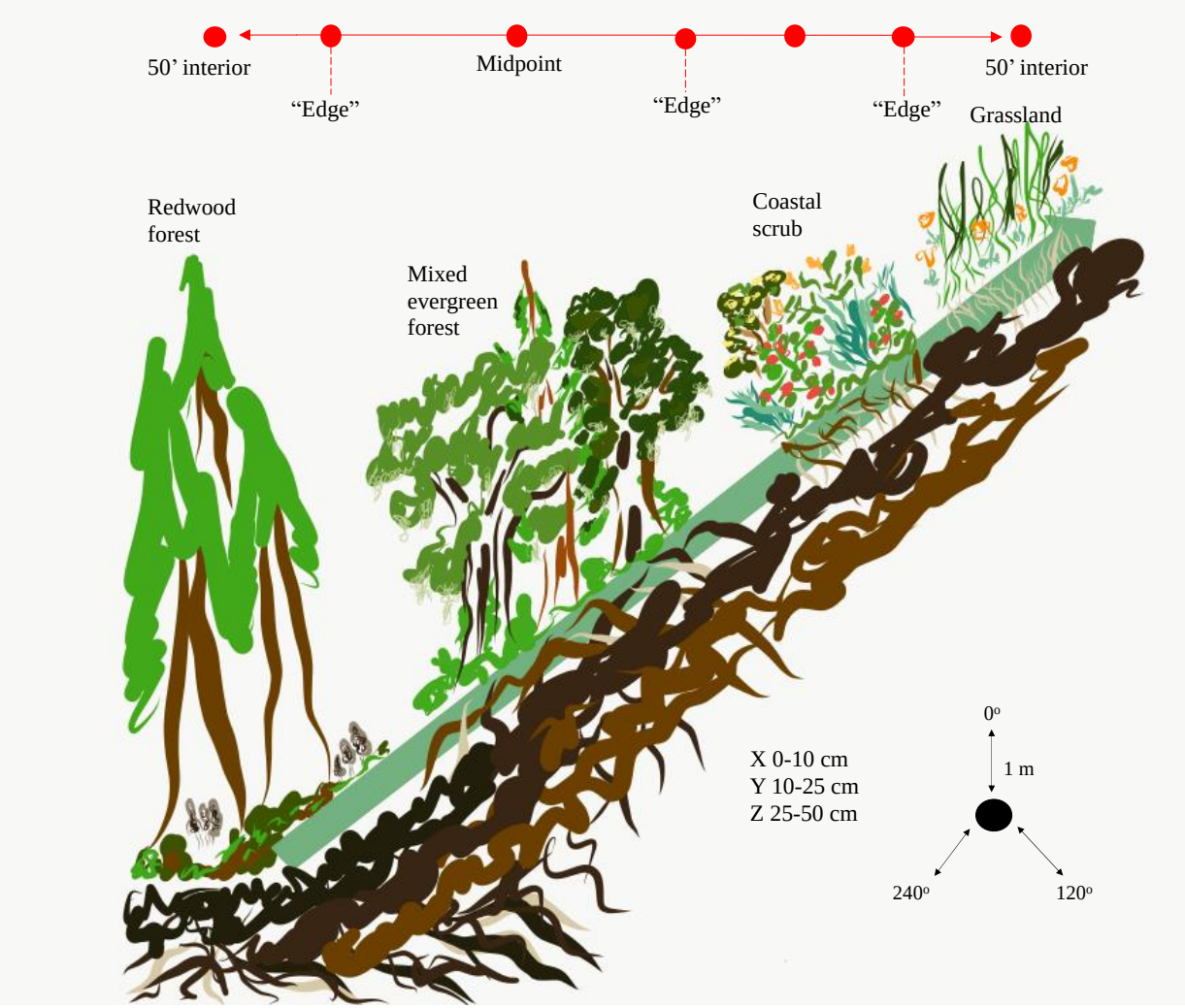

Figure 4.6 Schematic of an example transect where soil samples were collected at Swanton Pacific Ranch, Santa Cruz County, CA in July 2019. “Edge” represents the ecotone between plant communities.

4.3.2 Study-Design

The general concept behind the transect study was to pick a random location along a forest edge in SPR, and to move inwards and outwards along a randomized bearing to measure soil properties as plant communities transitioned from redwood forest into grasslands.

Using aerial imagery and ArcMap 10.5 (ESRI, Redlands, CA), a rough forest-rangeland boundary line was digitized as a single shapefile in the upper rangeland of SPR. The total distance of this boundary line was determined in feet, and in Excel, the *random number generator function* was used to generate a random distance in feet (between 0 and the total length of the line in feet) to travel from South to North along the boundary. A point was digitized at the random distance, and the azimuth for the approximate perpendicular line to the forest edge at that point (Figure 4.7). Using the *random number generator function* again in Excel, a final random azimuth (in-between 45^{o} greater than the azimuth of the perpendicular line and 45^{o} less than azimuth of the perpendicular line) was generated. This random azimuth was the transect line. This was repeated 10 times as to have 5 secondary (back-up) transect lines to the primary 5 transects.

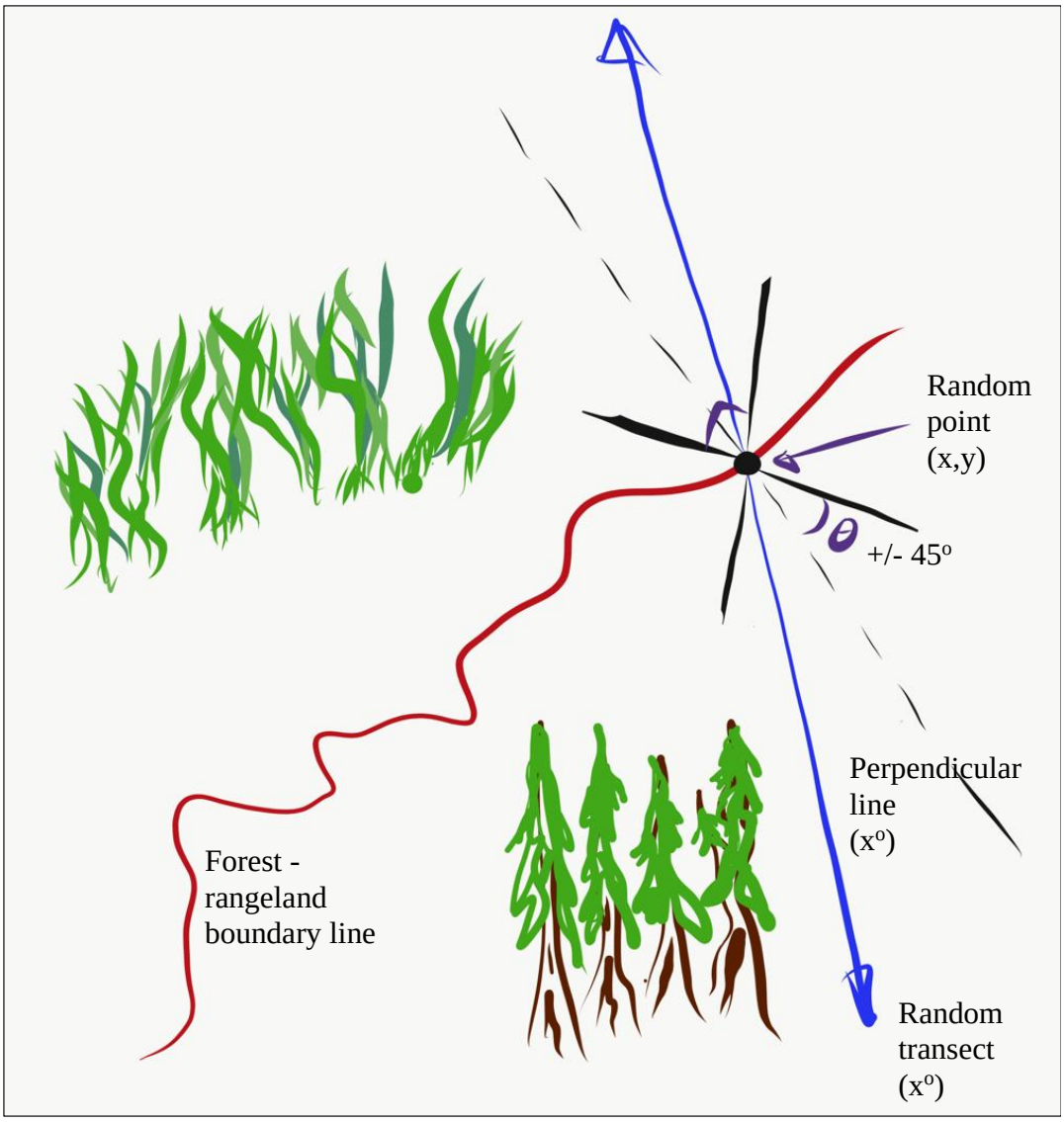

Figure 4.7. Schematic of random transect design for soil exploration at Swanton Pacific Ranch, Santa Cruz County, CA. Red line indicates approximate boundary between grassland and forest.

4.3.3 Field work:

At SPR, we hiked to the predetermined points along the forest edge and used cell phone GPS positioning in conjunction with downloaded map layers on the Google Earth

app. Once we arrived the point, we used the downloaded map and cell phone GPS to stay on the approximate azimuth of the transect line.

The goal thereafter was to find the nearest stand of contiguous redwood trees along the transect line. For some of the transects, there was considerable distance of mixed evergreen forest to travel through before the nearest redwoods. If fuels and topography made access to the nearest redwood stand along the transect line too challenging, we added (or subtracted) 5^{o} from the original azimuth.

Once a stand of contiguous redwood trees was located, we positioned ourselves along the transect line at the ecotone between redwood forest and mixed evergreen forest. We determined the ecotone to be where both the canopy and leaf litter was influenced by approximately 50% redwood forest and 50 % mixed-evergreen forest. From this point of shared canopies, we walked into the redwood canopy approximately 50 horizontal feet (distance measured on google earth) and established a redwood point for soil collection.

From here, we used the same standardized protocol at each site for every transect. Using a compass, we created a triangle around the point with three vertices approximately 1 m away from the central point in the 0^{o}, 120^{o}, and 240^{o} directions (Figure 4.6) These vertices served as the soil collection points that were combined together to create a composite sample at 0-10 cm, 10-25 cm, and 25-50 cm depths. Soil was collected using an augur with marked depths along the tool to distinguish the depth intervals. If a rock layer or bedrock was reached before 50 cm at any of the points, said sample was not collected, and this was noted in a field notebook.

Samples of each depth class were mixed together on a tarp and homogenized and then placed into labeled plastic bags. Remaining soil was placed back into the augur holes as to minimize disturbance,

At each point along the transect, plant community structure and composition was described in a field notebook according to the techniques instilled in the California Polytechnic State University of San Luis Obispo field botany course, BOT 433: CA Native Plants.

After soil was collected at the redwood site, we moved back in the direction we came from (along the transect line) to the ecotone between the redwood forest and the next plant community (i.e. redwood forest and mixed-evergreen forest ecotone) and performed the same protocol (Figure 4.6)

Thereafter, we moved into the approximate center of the next plant community (i.e. mixed-evergreen forest). Center was determined as the mid-point along the transect line in-between the redwood ecotone and the next respective ecotone (coastal scrub or grassland) using the Google Earth app. At the midpoint, we preformed the same protocol, and so on.

A comprehensive list of the plant communities and ecotones observed is presented below:

- Redwood forest
- Redwood forest/mixed-evergreen forest
- Mixed-evergreen forest
- Mixed-evergreen forest/coastal scrub
- Coastal scrub

- Coastal scrub/mixed annual and perennial grassland
- Mixed evergreen coniferous forest/ mixed annual and prerenal grassland
- Mixed annual and perennial grassland

4.3.4 Laboratory analysis:

The following lab analyses were performed on all mineral horizons collected from soil profiles at SPR and LHBC, and the details of each method can be found below in a subsequent section of this chapter, "Laboratory Procedures":

- Air-dry gravimetric water content
- Soil pH (1:1 deionized water, 1:2 0.01 *M* $CaCl_2$)
- Soil organic carbon
- Permanganate oxidizable carbon
- NH_4OAc extractable Ca, Mg, K, and Na
- Cation exchange capacity
- Basic cation saturation

4.3.5 Statistical analysis

All data was organized in Excel (Microsoft, Redman, WA) and saved on the cloud in One-Drive (Microsoft, Redman, WA). Statistical analysis was done in JMP (SAS Institute, Carey, NC).

4.3.5.1 Multivariate regression design for transects

To analyze soil properties from samples collected at depths along the transects, we used a regression model and controlled for site slope, vegetation category (plant community or ecotone), and depth category (0-10 cm, 10-25 cm, 25-50 cm)-we also controlled for interactions between pairs of these variables. Additionally, we controlled

for the transect number, which was a categorical variable and part of the study design. We used the *multiple comparison* feature in JMP (SAS Institute, Carey, NC) to generate values for each response variable by vegetation category and depth class. The general regression expression for transect analyses is found in Eq. 17 (Appendix F).

In an effort to achieve normality and equality of spread in the residuals across the predicted values of the model, we preformed transformations to response variables as fit. Transformations are identified in Table 5.2.

We were interested in the average value for each vegetation category and depth interval when other factors included in the regression model were considered. In consultation with a statistician, we decided to report the least squares mean; a definition of the "least squares mean" is found in an earlier section of this chapter for Objective 1.

In instances where the response variable was transformed to fit the model, we created 95% confidence intervals from the LSM (and standard error) values. These confidence intervals were then back-transformed into original units, this all to preserve the uncertainty associated with the asymmetric distribution of the data, as per consultation with a statistician (Eq. 23 Appendix F).

4.4 Objective 4: compare levels of basic cations between the forest floor and mineral surface

Samples of organic materials were collected from forested sites in the profile study (Objective 1) and transect study (Objective 3). While there were samples of forest floor collected in the transect study (Objective 3) that were beneath a mixed-evergreen forest as well as the ecotone of the mixed-evergreen and redwood forest, for the purposes of this analysis, they were ignored, and only organic materials from the redwood forest

were investigated. This made for 28 organic samples collected in the redwood forest (16 from profiles at SPR in 2018, 7 from profiles at LHBCR in 2019, and 5 from transect study at SPR in 2019).

Samples of redwood materials were incinerated into ash and an acid digestion was performed for analysis of total Ca, Mg, K, Na in the forest litter. The procedure for this method is found in a subsequent section of this chapter titled “Description of laboratory procedures” under “Forest floor analysis”. For each base (Ca, Mg, K, Na), the relationship between the total cation level in the redwood forest litter and the extractable cation level (of the matching base) in the mineral soil surface was investigated using univariate regression modeling in JMP (SAS Institute, Carey, NC).

In these regression models, we included redwood organic horizons collected in both the profile study (Objective 1) and transect study (Objective 3). For the mineral surface horizons, we included the uppermost A-horizons collected at redwood sites from the profile study (Objective 1) as well as samples collected at the 0-10 cm depth interval from redwood sites in the transect study (Objective 3). Thus, in these models, the data representing the mineral surface included soil from samples designated to pedogenic horizon in the field (e.g. A horizons in the profiles), as well as from samples that were collected at a standardized depth interval (0-10 cm) from the surface, in the transects.

In addition to the comparisons for each individual base (e.g. sodium in the forest floor versus sodium in the mineral surface, etc.), we also ran a univariate regression model using JMP (SAS Institute, Carey, NC) for the sum of bases in the organic material and the sum of extractable bases in the mineral surface.

Last, because calcium contributed to at least 58% (on average) to total basic charge in redwood and grassland mineral horizons at both locations in the profile study, the relationship between calcium levels and soil depth (in redwood and grassland soils) was investigated using all mineral horizons (as opposed to just the surface). Again, a univariate regression model was used in JMP (SAS Institute, Carey, NC), and in this model, no data from the transect study (Objective 3) was included.

4.5 Objective 5: characterize total C and active C pools within these ecosystems and explore interpretations of these pools

4.5.1 Stock calculations for SOC and POXC

Note- the method described for determination of SOC density and SOC stocks was the same method used to determine POXC density and POXC stock. For sake of brevity, the following outline only mentions only "SOC" in the steps described, but the same was applied to measurements of POXC as well.

For each horizon in the profile study, we multiplied: bulk density values, horizon thickness, and SOC content to generate horizon "densities" (in units of mass SOC per area). For each profile, SOC density values for each horizon were summed to 1 m in depth to generate a total mass SOC in the top 1 m of soil per profile; this was performed in Excel (Microsoft, Redman WA). If a soil profile had horizon depths that extended beyond 100 cm, thickness of the horizons after 100 cm were not included. Summary tables of summed density values for profiles at each location are found in Appendix B.

A regression model created in JMP (SAS Institute, Carey, NC) was used generate LSM SOC density values in the top 1 m of soil by plant community for each location. In addition to plant community, the regression incorporated slope of each profile, interaction

of slope and plant community, as well as zone category for SPR (see Eq. 18 in Appendix F). Note- unlike the previous regression models (Eq. 16 and 17, Appendix F) where a soil horizon, or sample from known depth interval were examined, in this regression, the soil profiles were the observational unit because total SOC (across horizons) in each profile was summed to 1 meter in depth, thus, there were less observations in the model.

To determine SOC "stocks" (in units of total mass SOC), the LSM SOC densities determined in the model were multiplied by land areas of the respective plant communities for each location (Table 4.2). For SPR, land areas for redwood and grassland plant communities were obtained from a GIS layer that is stored in a database at the California Polytechnic State University of San Luis Obispo.

Because there was no mapped vegetation data available for the LHBCR property, C stocks for this area were extrapolated to the entire Big Sur eco-region with data from Meentemeyer et al. (2008) who provided redwood acreage and acreage of a non-discrete, shrub-grassland category. To generate a grassland-only land area value, we used percentage values from the mix of dominant vegtation types in the Monterey coast landscape (northern Santa Luica range) as provided by Stephenson and Calcarone (1999) to break up the shrub and grassland combined values provided by Meentemeyer et al. (2008). In effect, using the information from Stephenson and Calcarone (1999), it was generalized that in a shrub-grassland category for the Big Sur ecoregion, approximately 80% would be shrubland (including coastal sage scrub and chaparral shrubland) and approximately 20% would be grassland.

Table 4.2 Land areas used for SOC and POXC stock calculations.

Location		Area (ha)
Big Sur Ecoregion†	Redwood forest	13,386
	Grassland	8,542
Swanton Pacific Ranch‡	Redwood forest	372
	Grassland	508

†Areas calculated using data from Stephenson and Calcarone (1999) and Meentemeyer et al. (2008); details in text above.
‡ Areas obtained using GIS layers of Swanton Pacific Ranch and stored in a database at the California Polytechnic State University of San Luis Obispo

4.5.2 Missing bulk density values

When rock fragments or coarse roots made collection of bulk density cores infeasible in the field, we did not collect cores (this is the case for 24 of the 102 soil horizons described at SPR, and 21 of the 56 horizons described at LHBCR).

We determined a standardized protocol to generate hypothetical bulk density values for missing horizons (see below). Note- these values were used exclusively for C density calculations. Horizons without bulk density measurements were excluded from the regression analysis (in objective 1) that was used to determine bulk density values reported in Table 5.1.

Protocol for missing bulk density values:

1. When adjacent overlaying and underlaying horizons (with known bulk densities) from the same pit were available (Appendix B), we used these to generate an interpolated bulk density value for the unknown
2. If either an above or below bulk density value was not available, we used whichever one was available, in conjunction to an average bulk density for the unknown sample horizon-type (A,AB,B, or BC) and plant community (redwood or grassland) per location (SPR or LHBCR; Appendix J)
3. When no known adjacent horizon bulk density data was available, we used the average bulk density for the unknown sample horizon-type and plant community per location (Appendix J)

The use of available adjacent underlain or overlaying horizon data to predict unknown values in incomplete bulk density datasets was in accordance with the findings of Sequeira et al. (2014). A table of the average bulk density values separated by horizon designation, and location is found in Appendix J.

4.5.3 Interpretations of soil C pools

To investigate interpretations of POXC levels within the context of our study, and to provide a discussion of POXC (that to our knowledge) has not been described in existent literature, we used JMP (SAS Institute, Carey, NC) to build graphs and test for significant interactions. In *Graph Builder*, horizon data was separated by location (LHBCR or SPR) and the following relationships were explored: POXC vs SOC,

POXC/SOC v. SOC, POXC/SOC v. depth, C/N ratio v. depth, and C/N ratio v. SOC. In these regressions, F-tests were used to determine if there were significant associations from plant community (redwood or grassland horizons) on the way in which the explanatory variable (e.g. depth) effected the response.

4.5.4 Depth Weighted Averages in Top 20 cm

Many studies to measure SOC have sampled soil from shallow, uniform depth intervals (<20 cm; Harrison et al., 2011; Jandl et al., 2014). In contrast, the samples collected (for objective 1) were from horizons described at various depths in the field.

One advantage of sampling at uniform depth intervals is standardized comparisons across similar depths, however, the natural development of distinct soil horizons (that do not conform to fixed depths) is lost, and can result in erroneous in interpretations (Schoeneberger et al., 2012; Rebecca Burt and Soil Survey Staff, 2014). Furthermore, while sampling at the surface can be more feasible, it results in underestimations of SOC stocks (Harrison et al., 2011).

We wanted to compare POXC/SOC values and C/N ratios from our study to the data provided by Cotrufo et al. (2019); this study measured pools of soil organic matter (mineral associated organic matter and particulate organic matter) from a large database of samples collected in the topsoil (upper 20 cm) of European forests and rangelands.

In an effort to compare our data to this study (Cotrufo et al., 2019), we used the arithmetic means from our horizon data in each profile (weighted by horizon thickness) to create depth-weighted averages in the top 20 cm of soil (Eq. 22, Appendix F). This represented a hybrid approach, as we used data that originated from horizons while standardizing the analysis between profiles at a fixed depth (upper 20 cm). In a review of

the literature, we did not find any studies that have explicitly communicated use of this hybrid approach.

4.6 Description of laboratory procedures

4.6.1 General statements about laboratory equipment and dishwashing procedures

- For large volume allocations of solutions, 0-25 mL and 5-50 mL bottle-top dispensers were used (e.g. Dispensette brand). When aliquots were smaller in volume (10 uL- 5 mL) and variable in quantity, an assortment of Eppendorf Research Plus adjustable single-channel pipettes were utilized.
- For mass readings to the nearest 1.00 g, the Mittler Toledo XS2002S Balance was used. For mass reading to the nearest 1.00 mg, the Mittler Toledo XS205 Dual Range Balance was used.
- All labware used for chemical analyses received triple-rinsing with deionized water before use. Falcon tubes for re-use were washed with Liquonox prior to DI rinse.

4.6.2 Lab Schedule and batches

The way in which the data associated with this project was analyzed in the lab was the result of a number of factors including but not limited to the time at which the samples were collected from the field, the time availability of the graduate student, the time at which there was additional undergraduate student assistance, and the time at which certain instruments, materials, and reagents were available for use in the laboratory. All lab extractions and analyses were attached to a date.

Because samples were collected in the field over two years, most laboratory procedures were organized by what we will call “batches”. These batches formed a

structure and organization in the data processing for which notes, and experimental errors could be traced to. The data was not structurally separated from the batch hierarchy until it was ready for statistical analysis.

Mineral soils from SPR soil pits were collectively analyzed in one batch, "Mineral Batch 1" (n= 102). Mineral soils from LHBC (n=56) and soil form SPR Transects (n=76) were collectively analyzed in another batch, "Mineral Batch 2" (n=131). All organic horizons (n=41) were analyzed together.

4.6.3 Sample preparation

All mineral soil samples, organic samples, and bulk density samples were left to air dry before lab analyses. In order to standardize the air-drying procedure, any visible water-moisture collected on the inside of the plastic bag was used as an indication that a sample was not yet dry.

Once air-dry, mineral horizons from the pit study were given a dry color using the Munsell color book (these were taken from peds in the main horizon sample)

All air-dry mineral samples were ground with mortar and pestle and sieved through a 2000 μm sieve (USA Standard ASTM Specification E11) in order to separate the fine earth fraction in accordance with the *Kellogg Soil Survey Laboratory Methods Manual* (Chapter 1B1b; Rebecca Burt and Soil Survey Staff, 2014).

After processing, these samples remained in plastic bags and were stored in lab room cabinets.

For organic horizons, a coffee grinder was used to pulverize the litter.

For C/N analysis, a sub sample (<10 g) of each sieved mineral soil was ground with mortar and pestle for a second time, this time, to a fine powder, and placed in separate labeled vial.

4.6.4 Air-dry gravimetric water content

At least 10.00 g (+/- .05) of every soil sample collected in the field was weighed and placed in the drying oven (at 105 ^{o}C for at least 18 hours) to calculate and correct for the air-dry gravimetric water content. Air-dry gravimetric water content was calculated as amount of water lost from oven drying over the air-dry mass (Eq. 1 of Appendix F). The air-dry gravimetric water content was then used to calculate an oven-dry mass for each soil sample (Eq. 2 Appendix F), and this value was applied to all laboratory methods that required a concentration of analyte per mass of air-dry soil conversion.

4.6.5 Bulk density

Using the air-dry gravimetric water content, an oven-dry mass was determined for each bulk density sample collected in the field and this mass was divided by the volume of the core to generate a bulk density value (Eq. 3 in Appendix F).

As to not lose any soil mass from the bulk-density samples, bulk-density cores were weighed inside of the plastic bag. We determined the average weight (of a least 3) plastic bags for each brand used (Ziploc and First Street) and subtracted this mass from the sample mass.

4.6.6 Soil pH

Soil pH was measured on the prepared soil samples using the Accumet AB 150 Potentiometer (Fisher Scientific, Waltham, MA) and the Accumet Combination Glass

Electrode (Fisher Scientific, Waltham, MA; Serial No. VXX1-4116-16). Procedure for pH determination followed outlined in the *Kellogg Manual* (Chapter 4C1a2; Rebecca Burt and Soil Survey Staff, 2014) and was measured in two matrices: (a) 1:1 soil to solution ratio in deionized water and (b) 1:2 soil to solution in 0.01 *M* $CaCl_2$.

The method involved the measurement of 20.00 g (+/- 0.05) of soil for each sample and the addition 20.00 mL of deionized water into a beaker. The soil solution was left alone for one hour (timed) and stirred occasionally (every 15 min.) The method was implemented in batches of approximately 20 samples. After one hour, each sample was stirred continuously for 30 sec. and then let to rest for one minute. Immediately after one minute had passed, an electrode was placed into the soil solution and pH was recorded to the nearest one-hundreds place (once the value was stabilized for at least 10 sec.).

Immediately after this observation was recorded in 1:1 soil to water, 20.00 mL of 0.02 *M* $CaCl_2$ were dispensed into the same sample (diluted to 0.01 *M* $CaCl_2$). Again, the sample was stirred for 30 sec. continuously, and left to rest for 1 minute. The pH in 1:2 soil to 0.01 *M* $CaCl_2$was then recorded in same manner as described above.

4.6.7 Particle Size Analysis

Particle size analysis (to determine percent sand, silt, and clay, as well as USDA textural class) was performed on samples from the Swanton profiles only. The purpose of this method was to support field estimates of clay percentage and soil texture by feel. Due to time and budgetary constraints, and because the information gained from particle size analysis was used for descriptive purposes (e.g. presence of an argillic horizon to determine soil order) and not for published values (e.g. mean clay % of study

population)- we opted not to perform the method on soils collected in the Big Creek Reserve.

For particle size analysis, we followed the hydrometer method described in the *Soil, Plant and Water Reference Methods for the Western Region* (S-14.10; Miller et al., 2013). Due to logistical constraints there was no correction for organic matter. We measured 40.00 g +/- (0.05) of air-dry soil into a dispersal cup and added 100 mL of Sodium Hexametaphosphate. We let the soil sit in dispersal solution overnight as to chemically agitate and break apart the soil microaggregates. After about 12 hours, we added roughly 500 mL of deionized water into the dispersal cup and mixed the suspension using an electric mixer (Hamilton Beach Scovill Model 936- Drink mixer) on medium speed for at least 7 minutes.

After 7 minutes, the soil solution was quantitively transferred into sedimentation cylinders and brought to 1 L in volume using deionized water.

A method blank sedimentation cylinder was prepared with without soil to correct for temperature and solution viscosity.

To determine the percent sand (the first particle size class determination), a plunger was inserted into the suspension until the soil-solution was evenly distributed. Once the plunger was removed from the sedimentation cylinder, a timer began. To determine % sand, the hydrometer reading was recorded 40 sec following removal of the plunger. This was repeated twice again, and an average of three readings was used. A hydrometer reading for the blank was recorded in the same manner as to correct for solution viscosity at 40 seconds following removal of the plunger.

To determine the percent clay, temperature in the blank was taken 6 hours after removal of the last plunger, and a temperature-corrected time for clay particle settling was determined. For 20^{o}C, the time for clay particle settling is 7 hours and 45 min following removal of the plunger (see Appendix K). A hydrometer reading was taken at the temperature-corrected time for each soil sample and the method blank.

4.6.8 Cation exchange capacity (CEC) and extraction of soil basic cations

4.6.8.1 Extraction

Extraction of basic cations (Ca, Mg, Na, K) and determination of CEC for each sample were determined via a two-step extraction method for each sample. All samples were run in analytical triplicates. Basic cations on soil exchange sites were extracted via pH 7 1 *M* Ammonium Acetate (NH_4OAc) and cation exchange capacity (CEC) was determined using ammonium replacement with 2 *M* Potassium Chloride (KCl) extraction.

The method used was adapted and assembled from techniques found in the *Kellogg Manual* (Chapter 4B1a; Rebecca Burt and Soil Survey Staff, 2014), the *Soil, Plant, and Water Reference Methods for the Western Region* Methods (S-5.10 and S-10.10; Miller et al., 2013), and the *Fall 2018 Soil and Water Chemistry Laboratory Manua*l for the California State Polytechnic University of San Luis Obispo (Appel and Stubler, 2018) to fit laboratory and budgetary constraints.

The ammonium acetate and potassium chloride extractions were a laborious process. The number of samples analyzed with each extraction event varied, but generally ranged from 25-75 samples (depending on laboratory logistics). Often times the extraction was spread over two days, but the time it took to complete an extraction event

never exceeded two days. Method blanks and standard reference soils were used for every extraction event.

For extraction of soil basic cations, 35 mL of 7 1 *M* Ammonium Acetate (NH_4OAc) was dispensed into a centrifuge tube with 2.5 g of air-dry soil sample. Each sample was shaken on an oscillating shaker (New Brunswick Scientific Innova 2100 Open-Air Platform Shaker) for 30 min at 180 cycles per min, and then centrifuged (Eppendorf 5810R Centrifuge, serial no. 0034398) at 2000 rotations per minute. After centrifugation, the soil in solution was flocculated in a pellet at the bottom of the tube. The supernatant (the basic cation extract) was filtered (via syringe filter or through filter paper) and poured into a labeled 20 mL scintillation vial. Unless extracts were to be analyzed on the ICP within 2 weeks of the extraction (for which the refrigerator was an appropriate storage space), all scintillation vials were placed in the freezer until analysis on the ICP. Immediately in advance of analysis on the ICP, samples were thawed to room temperature.

To determine CEC, we used the same falcon tube (with recently centrifuged soil pellet saturated with pH 7 1 *M* NH_4OAc), and we made sure to discard all remaining supernatant that was not poured into scintillation vial (see earlier step). Then an additional 25 mL of NH_4OAc was added to each falcon tube and the samples were placed on the shaker, and subsequently, inside the centrifuge (at the previously mentioned settings above). The purpose of this step was to further saturate soil exchange sites with Ammonium from the NH_4OAc.

Next we rinsed off any excess Ammonium that was not bound to exchange sites during ammonium replacement as per methodologies in the *Kellogg Soil Survey*

Laboratory Methods Manual (Chapter 4B1a; Rebecca Burt and Soil Survey Staff, 2014) and the *Soil, Plant, and Water Reference Methods for the Western Region* (S-10.10; Miller et al., 2013). We used 91% isopropyl alcohol as the cleansing solution and preformed three consecutive rounds of "washing", one round of washing included: 25 mL of alcohol dispensed into falcon tube, then falcon tube placed on shaker (for 5 min only this time) at 180 cycles per min, then placed in centrifuge at 180 rpm for 5 min, and then the supernatant was discarded into hazardous waste container. Following 3 rounds of washing, we made sure there was no remaining supernatant, and then dispensed 35 mL of 2 *M* KCl into the falcon tube. There was a final round of shaking (30 min at 180 cycles per minute) and centrifugation (5 min at 2000 rpm) and then the supernatant was poured into a new labeled scintillation vial, this was the final extract for CEC via ammonium replacement. As with the base cation extracts, all CEC vials were placed in the freezer until analysis on the photo spectrometer and thawed before measurement.

4.6.8.2 Analysis

Basic cation extracts were analyzed for Ca, Mg, K, Na on the HORIBA Scientific-Ultima 2 ICP-OES (Inductively Coupled Plasma Optimal Emission Spectrometer; HORIBA FRANCE SAS, Longjumeau, France) housed in the NRES Instrumentation Room. Each event on the ICP analyzed 120-180 samples. ICP was run using PEAK Scientific gas generation partner and CEATA Ultrasonic Nebulizer U5000AT.

Using standard-stock Ca, Mg, K, and Na, a 5-point curve was prepared in NH_4OAc to fit the expected range of concentrations for each ion of interest. Concentrations of each ion were given in mg/L. Once the data was exported into Excel

(Microsoft, Redman WA), we used the equations 4-8 (found in Appendix F) to calculate the amount of charge per kg of soil.

CEC was determined via ammonium colorimetric analysis on a Thermo-Scientific 201 UV-visible spectrometer (Thermo-Scientific, Waltham, MA; serial# 5A3R169011) at 650 nm. CEC extracts were diluted 45 times less than the original concentration in 2 *M* KCl in an effort to keep absorbance readings at detectable levels for the instrument (i.e. absorbance value under 1.0).

For the colorimetric reaction, two reagents (A and B) were necessary.

- Reagent A (protected from light in aluminum foil) contained the following chemical components:
    - 0.05g sodium nitroprusside
    - 13g sodium salicylate
    - 10g sodium citrate
    - 10g sodium tartrate
    - 100 mL DI water
- Reagent B included:
    - 6g sodium hydroxide dissolved in 100 mL DI water
    - 2 mL sodium hypochloride

Each sample for soil CEC analysis received the following aliquots via pipette, (pipette tips were changed in between soil samples and ammonium standards but not during solution or reagent allocations):

- 1090 uL of 2 *M* KCl

- 10 uL of soil sample CEC extract (used Sartorius Proline Plus 10 uL Single-Channel Pipette)
- 450 uL of reagent A
- 450 uL of reagent B

For every 100 cuvette samples, approximately 4 sets of 5-point Ammonium standard sequences (0, 1, 2.5, 5 and 10 ppm) were prepared with the following aliquots (i.e. in every 100 cuvettes used for analysis, 80 of those cuvettes were soil extracts and 20 of those cuvettes were for the standard curve), :

- 650 uL of 2 *M* KCl
- 450 uL of Ammonium standard
- 450 uL of reagent A
- 450 uL of reagent B

Ammonium standards were prepared using Ammonium standard stock solution and 2 *M* KCl. For each ammonium analysis event, a standard curve was created using the average absorbance at each standard concentration. There were approximately 75-150 samples (including standards) for each analysis event. After every all aliquots had been pipetted into cuvettes, cuvette trays were immediately covered with parafilm and shaken 5 times with mixing apparatus. Absorbance readings were collected from Ocean Optics UV-VIS at 650 nm no earlier than 1 hour before, and no later than 4 hours after the cuvettes were mixed. Spectrophotometer was warmed up (turned on) for approximately 30 minutes before most recording events began.

Each sample received considerable dilution in order to be at a detectable level on the spectrophotometer (45 times less than original concentration) and some sample

replicates had ammonium readings that were more separated across the group than expected (see Quality Control, Appendix G). Because of aforementioned reasons, a trial run, with an alternate analysis strategy on select samples (including replicates) was explored. Using an ion selective electrode to measure ammonium, the method of ammonium measurement via colorimetric analysis was validated. The procedure used for measurement of exchanged ammonium via ammonia gas electrode is found in the Appendix L.

We used Eq. 9-10 (Appendix F) to calculate ppm Ammonium, and subsequently to convert ppm Ammonium into CEC with units of cmolc per kg soil. Basic saturation was calculated with Eq. 11 (Appendix F).

4.6.9 Soil Organic Carbon and Total Nitrogen

Total soil C and N contents were determined via combustion. Batch 1 samples were analyzed on Elemetar Vario (Elemetar, Langenselbold, Germany; contact NRES department for serial number of old instrument) and later, Batch 2 sample were analyzed on the Elemantar Vario MAX Cube (Elemetar, Langenselbold, Germany; serial no. 29191038). 10% of the samples were duplicated for method-level quality control.

To determine soil organic C content (SOC), we applied an inorganic C correction to total C values determined via combustion. Calculation of organic C via subtraction of inorganic C contributed by carbonates is in conformance with the protocol outlined in the Organic Analyses section of the Laboratory Methods chapter of the *Keys to Soil Taxonomy* (Soil Survey Staff, 2014).

For soil samples with base saturation (BS) that exceeded 120% (in theory 100% BS, but in practice above 120% BS due to 20% error associated with method)-we

assumed that any contribution to basic charge that exceeded the exchangeable charge of the soil was the result of calcium from calcium carbonate dissolution. Furthermore, we assumed that any inorganic C in the soil was the result of calcium carbonate. Under these assumptions (for soils above 120% BS) we used the extracted basic charge that exceed exchangeable charge to approximate the C content associated with assumed calcium carbonate. We then subtracted this value from our total C content to determine SOC. The expressions used to approximate C associated with assumed dissolution of calcium carbonate are found in Appendix F (Eq. 12-14).

The soil organic C values determined using this method were applied to C/N ratios and POXC/SOC ratios in the analysis. 1 of 102 soil horizons at SPR was corrected for carbonates. 17 of 56 horizons at LHBCR were corrected for carbonates. 1 of 75 transect samples from SPR was corrected for carbonates.

4.6.10 Labile Carbon

Samples were analyzed for labile C using the Permanganate Oxidizable C method described by Culman et al. (2014). The method involves measuring the amount of 0.2 *M* Potassium Permanganate (KMnO4) reduced as a proxy of "active" C in the soil.

For each extraction event there was subsequent analysis on the same day. All samples were run in analytical triplicates. Method blanks were performed for each extraction event, no standard reference materials were used because there were no available reference soils with POXC data.

4.6.10.1 Extraction

The extraction method for POXC was time-sensitive, as any C will continue to reduce KMnO4 as function of time, thus precautions were taken to create a standardized

work flow in the laboratory with no more than 10 samples being extracted during one time sequence (up to 7 sequences per day, approximately 70 samples per day).

For each sample, 18.0 mL of deionized water was dispensed into falcon tube containing 2.5 g (+/ 0.05) of air-dry soil. Next, 2.0 mL of 0.2 *M* KMnO4 was quickly dispensed into each centrifuge tube with soil and water and a timer began. Samples (no more than 10) were immediately transferred onto a reciprocating shaker (New Brunswick Scientific Innova 2100 Open-Air Platform Shaker) and shook at 240 oscillations for 2 minutes (before each sample was placed on the shaker it was shaken vigorously by hand for approximately 2 seconds to ensure dispersion). After 2 minutes on the shaker, samples were taken off the shaker and placed in a dark cabinet for 10 minutes exactly. Meanwhile, corresponding dilution tubes were prepared with 49.5 mL of deionized water. Once 10 minutes of settling time had passed, samples were taken out of the cabinet and a 0.5 mL aliquot of supernatant from each sample was quickly dispensed into the corresponding dilution tube. Diluted samples were placed in a dark cabinet until ready for analysis (approximately 1 hour after the last sequence was extracted).

The process described above was repeated until approximately 70 samples were extracted and diluted. To standardize the procedure, we waited one hour before we began to analyze the first samples. Analysis of samples followed the same sample-order as the extraction.

4.6.10.2 Analysis

Samples were analyzed at 550 nm on the Milton Roy Co. 20D Spectronic (serial no. 3322216030). Before analysis, the spectrophotometer was warmed up for approximately 30 min. A 4-point curve of KMnO4 was established each day with “working” (i.e.

diluted) standards from prepared stock solutions at concentrations of 0.05, 0.01, 0.015, and 0.02 *M* KMnO4. These standard stock solutions (0.05, 0.01, 0.015, and 0.02 *M)* were prepared from 0.2 *M* KMnO4 and had a shelf life of three days (i.e. one set of standards was used for three sequential days of extractions and analysis before another set was prepared). The R^2 of the curve was checked in Excel (Microsoft, Redman WA; at least 0.99) before sample were run for absorbance readings.

For every 10 samples we performed an instrument quality control check by running the 10^{th} sample again, and rotating analysis on one of the KMnO4 standards. To convert absorbance readings to mg of POXC per g of soil, we used Eq. 15 (Appendix F).

4.6.11 Forest floor analysis

4.6.11.1 Extraction

An adapted method of dry ash acid-digestion from Soil, Plant, and Water Reference Methods for the Western Region (B-4.10; Miller et al., 2013) was used for this procedure. All forest floor samples were analyzed in triplicates, each extraction event was one complete replication round (3 events). For each extraction event we prepared a method blank and standard reference material (pine needles).

Forest litter was pulverized to a fine powder in a coffee grinder, except toward the end of our grinding efforts, the coffee grinder broke, and we used a Micro Mill II Grinder (Bel-Art-SP Scienceware) instead.

Crucibles (for ashing in the furnace) were washed with Liquinox, then triple-rinsed with deionized water, and lastly washed in 10%, 1.0 N Hydrochloric Acid (HCl).

1.00 mg of each sample was weighed on a balance and placed into a labeled crucible (weight was recorded).

Samples (43 per round) were placed into a Fisher Scientific Isotemp Programmable Muffle Furnace (serial no. 307N0035) and brought to 480^{o}C at 2^{o}C per minute (approximately 2 hours). The positioning of labeled samples in the furnace was drawn on a map, as our sharpie labels wore off the ceramic in the heat. Once 480^{o}C was reached, samples were left in the furnace to burn for 18 hours. Afterwards, we let the samples sit and cool in the furnace for an additional day before we digested them in acid.

On the day of acid-digestion, we carefully removed samples out of the furnace (as to not spill any light ash) and relabeled them in accordance with our map. Then we dispensed 10 mL of 1 N HCl into each crucible and placed crucibles on a warming plate (9 per plate) beneath a fume hood at 80^{o}C for 10 min as to standardize the procedure and to ensure complete dissolution of ash material.

We set up an array of funnel racks and funnels containing acid-washed funnel paper to collect the digested ash. We labeled and placed self-standing centrifuge tubes beneath each funnel.

Once each sample had been heated for 10 min, we let them cool for 10 min, and then quantitatively transferred the entire contents of each crucible down a funnel with filter paper into the corresponding centrifuge tube and rinsed the filter 3 times with reagent grade deionized water (filter rinses occurred over the time-span of approximately 30 min).

After each sample had been transferred and received 3 filter-rinses, we brought all the samples to 50 mL in volume with reagent grade deionized water. Final volume allocation was performed at eye-level with a dropper.

Some fine particulates passed through the filters, but we left the samples to sit and settle, and we made sure to pour carefully, only allowing top of the sample (free of particulates) into ICP tubes for analysis.

4.6.11.2 Analysis

Acid solutions were analyzed for extractable Ca, Mg, K, Na on the HORIBA Scientific-Ultima 2 ICP-OES (Inductively Coupled Plasma Optimal Emission Spectrometer; HORIBA FRANCE SAS, Longjumeau, France) housed in the NRES Instrumentation Room. Using standard-stock solutions of Ca, Mg, K, and Na-a 5-point curve was prepared in a matrix of HCl and reagent grade deionized water to fit the expected range of concentrations for each ion of interest. After the standard received the appropriate aliquot of standard stock solution, 10 mL of HCl was added and the rest of the sample was brought to volume with reagent grade deionized water (50mL).

4.7 Quality control

Quality control measures were implemented for all soil chemical analyses (pH, CEC, extraction of base cations, digestion of organic material, POXC, soil organic C and soil organic N). Presentations and commentary on instrument and method level quality control are found in Appendix G.

CHAPTER 5

Results

5.1 Objective 1: gather baseline soils data for the Coast Redwood forest and compare said properties to those in adjacent grasslands

5.1.1 Swanton Pacific Ranch

In horizon data from SPR, the regression model provided no evidence for an association ($P>0.05$) of vegetation on square roots of SOC ($R^2=0.71$) and N ($R^2=0.69$; Table 5.1). This suggested there was no difference, on average, in redwood and grassland SOC and N values in horizons at SPR. We observed a significant association ($P<0.05$) of vegetation on C/N ratios ($R^2=0.48$), with LSM values of 14.3 and 11.4 in redwood and grassland horizons respectively (Table 5.1). The model predicted significantly higher POXC values in the redwood when compared to the grasslands with 95% confidence intervals of (0.490, 0.607) and (0.245, 0.368) mg POXC per g soil, respectively ($R^2=0.83$; Table 5.1). Similarly, the model found the fraction of SOC that was POXC (POXC divided by SOC; $R^2=0.60$) was higher in redwood horizons when compared to grasslands horizons, with LSM values of 2.5% and 1.5%, respectively ($P<0.05$; Table 5.1). Redwood horizons at SPR had higher LSM pH values than grassland horizons in both matrices ($R^2=0.62$ and 0.68, in 1:1 H_2O and 1:2 in $CaCl_2$ respectively; $P<0.05$; Table 5.1). Similarly, our model found redwood horizons had higher BS ($R^2=0.66$) than in grasslands horizons, with LSM predictions of 79% and 50%, respectively ($P <0.05$; Table 5.1). The model found evidence for higher cation exchange capacity ($R^2=0.66$) in the redwoods when compared to the grasslands ($P <0.05$; Table 5.1).

5.1.2 Landels-Hill Big Creek Reserve

At LHBCR, the model predicted higher values of SOC, N, C/N, and POXC in redwood horizons, on average, than grassland horizons (R^2=0.80, 0.84, 0.68, and 0.87 respectively; P<0.05; Table 5.1). With 95% confidence, the LSM for SOC was between 2.07 and 3.02% in the redwoods and between 0.84 and 1.39% in the grasslands (Table 5.1). With 95% confidence, LSM for C/N was between 14.6 and 17.1 in the redwood horizons and between 8.5 and 10.6 in grassland horizons (Table 5.1). Least-square means for POXC were 0.762 and 0.352 mg POXC per g of soil in redwood and grassland horizons, respectively (Table 5.1). There was no evidence of association with plant community on POXC/SOC ratios (R^2=0.65; P>0.05; Table 5.1). In both pH methods (R^2=0.72 and 0.78, in 1:1 in H_2O and 1:2 in $CaCl_2$ respectively) the model predicted higher values in redwood horizons than in grassland horizons (P<0.05; Table 5.1). The model found that cation exchange capacity (R^2=0.77) was higher in redwood horizons than in grassland horizons (P<0.05; Table 5.1). There was no evidence of an association from vegetation on BS (R^2=0.42) in the model (P>0.05; Table 5.1)

Table 5.1 Summary of soil properties from 102 horizons collected at Swanton Pacific Ranch, Santa Cruz Co., CA in 2018 and 56 horizons collected at Landels-Hill Big Creek Reserve, Monterrey Co., CA in 2019. Values reported as least square's means (LSM) plus or minus the standard error (SE) of the regression model in JMP (SAS Institute, Carey, North Carolina) and presented as a function of vegetation type (redwood forest versus mixed annual-perennial grassland). If a transformation was performed, it is noted and the 95% confidence interval is reported in parentheses with back-calculated units.

	---Swanton Pacific Ranch---				---Landels-Hill Big Creek Reserve---			
			Plant Community				Plant Community	
Soil Property	**Transformation**	**R^2**	**Redwood forest (n=57)**	**Grassland (n=45)**	**Transformation**	**R^2**	**Redwood forest (n=28)**	**Grassland (n=28)**
SOC†	Square root	0.71	(2.05, 2.69)	(1.57, 2.40)	Natural log	0.80	(2.07, 3.02)*	(0.84, 1.39)
N‡	Square root	0.69	(0.147, 0.19)	(0.147, 0.209)	Natural log	0.84	(0.138, 0.181)*	(0.095, 0.136)
C/N§		0.48	14.3* ± 0.4	11.4 ±0.6	Natural log	0.68	(14.6, 17.1)*	(8.5, 10.6)
POXC¶	Square root	0.83	(0.490, 0.607)*	(0.245, 0.368)		0.87	0.762* ± 0.034	0.352 ± 0.045
POXC/SOC#		0.60	0.025* ± 0.001	0.015 ± 0.001		0.65	0.024 ± 0.001	0.024 ± 0.001
BD††		0.58	0.881* ± 0.032	0.986 ± 0.031		0.78	1.21* ± 0.05	1.34 ± 0.04
pH 1:1 H_2O		0.62	6.62* ± 0.07	5.84 ± 0.10		0.72	6.95* ± 0.05	6.57 ± 0.07
pH 1:2 $CaCl_2$		0.68	6.01* ± 0.07	4.98 ± 0.10		0.78	6.37* ± 0.05	5.74 ± 0.07
CEC‡‡	Square root	0.66	(22.4, 26.3)**	(18.6, 23.8)	Natural log	0.77	(19.1, 23.3)*	(13.9, 18.1)
BS§§		0.66	0.79* ± 0.02	0.50 ± 0.03		0.42	0.90 ± 0.02	0.95 ± 0.03

*Significant model association of plant community and response, P <0.05

** Despite overlapping confidence intervals in mean comparison, the t-test for the difference in means between grassland and redwood was significant

† Soil organic carbon (%)

‡ Soil total nitrogen (%)

§Soil organic carbon to nitrogen ratio

¶ Permanganate oxidizable carbon (mg POXC g $soil^{-1}$)

Fraction of soil carbon that is permanganate oxidizable carbon

††Soil bulk density (g soil cm^3 $soil^{-1}$)

‡‡ Cation exchange capacity (cmol charge kg $soil^{-1}$)

§§ Basic saturation of soil cations, calculated as sum of total extractable basic charge over cation exchange capacity

5.2 Objective 2: identify taxonomic classifications of redwood forest and grassland soils

We used laboratory and field data to classify 43 soil pits according to the *Keys to Soil Taxonomy* (2014). Of the 28 pits dug at SPR, 18 were classified as Molliols, 8 as Inceptisols and 2 as Alfisols (Figure 5.1). Of the 8 Inceptisols at SPR, 3 were Humixerepts that contained a mollic epipedon (Appendix I). Of the 15 pits at the Landels-Hill Big Creek Reserve, 13 were classified as Mollisols, in addition to 1 Inceptisol and 1 Alfisol (Figure 5.1). A list of all soil profiles classified to family name is found in Appendix I.

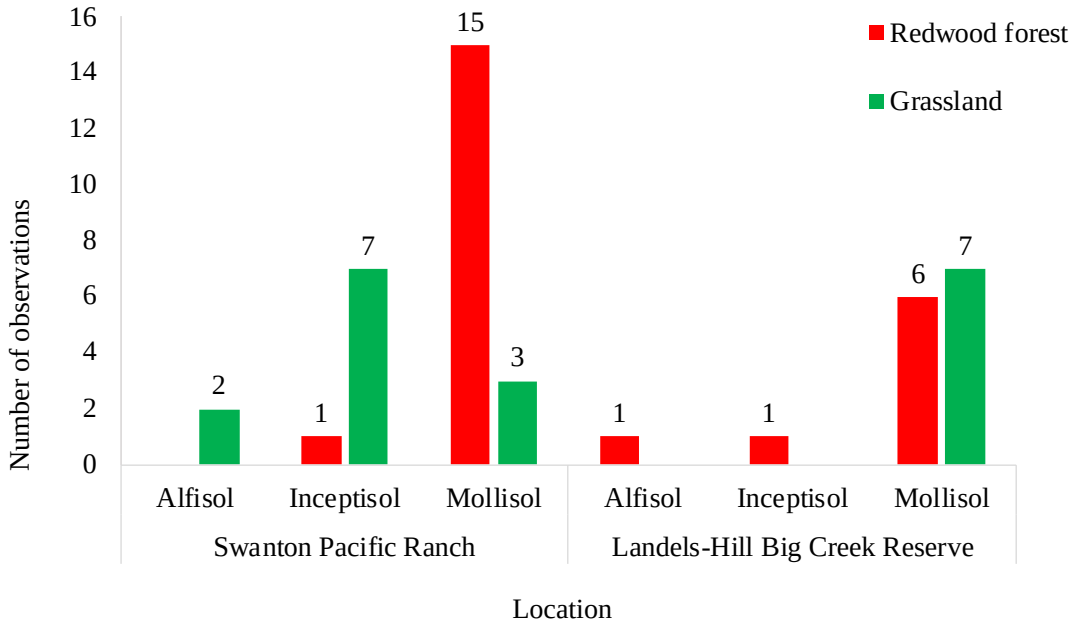

Figure 5.1 Histogram of soil pits classified by soil order according to the *Keys to Soil Taxonomy* (2014) using lab and field data from samples collected at Landels-Hill Big Creek Reserve in 2019 (right) and Swanton Pacific Ranch in 2018 (left).

5.3 Objective 3: investigate the influence of vegetative gradation on soil properties between these ecosystems

Note- a description of the plant community physiognomies that were encountered is found in Appendix A.

With consideration of all explanatory variables in the regression model for transect data (Eq. 17, Appendix F), there was evidence for a significant association ($P<0.05$) between vegetation (plant community or ecotone) and C/N ratios ($R2=0.75$), POXC ($R2=0.83$), POXC/SOC ($R2=0.82$), and pH in both matrices (0.81 and 0.88 for 1:1 H2O and 1:2 CaCl2 respectively; Table 5.2). The model found no evidence for a significant association ($P>0.05$) between vegetation and SOC in the model ($R2=0.80$; Table 5.2). In the regression model for BS, there was no evidence for a significant association ($P>0.05$) with any of the explanatory variables ($R2= 0.47$; Table 5.2)

Table 5.2 presents model least-squares means and standard error values by vegetation category and depth interval. Using the Tukey HSD test to compare LSM values for POXC/SOC fractions by vegetation, alone (i.e. not in a multiple comparison with depth), there were significantly higher values in the redwoods and in the redwood mixed-evergreen forest ecotone when compared to the grasslands and grassland mixed-evergreen ecotone ($P <0.05$; Figure 5.2); this is with consideration of all explanatory variables included in the model.

Table 5.2a Summary of regression analysis on soil properties from 60 samples collected along 5 transects in 2019 at Swanton Pacific Ranch, Santa Cruz Co., CA. Values reported as the least square's means (LSM) and standard error (SE) of *multiple comparisons* between depth interval and vegetation in the regression model made in JMP (SAS Institute, Carey, North Carolina). Significant associations and interactions of explanatory variables ($P<0.05$) are reported for each response variable. If a transformation was preformed, the 95% confidence interval is back-transformed in parentheses. Note, the total number of observations (n=) for each plant community or ecotone, includes observations collected over three depth intervals.

					Plant community or ecotone									
Response variable	**Transformation**	**R^2**	**Sig. association**	**Depth Interval (cm)**	**Grassland (G) n=10**		**ME/G Ecotone n=9**		**Mixed-evergreen forest (ME) n=15**		**ME/RW Ecotone n=11**		**Redwood forest (RW) n=15**	
					LSM	**SE**	**LSM**	**SE**	**LSM**	**SE**	**LSM**	**SE**	**LSM**	**SE**
SOC†	Natural log	0.80	Depth Slope Transect No..	0-10	(2.83, 7.92)		(4.41, 42.5)		(3.64, 6.16)		(4.32, 7.92)		(2.99, 10.22)	
				10-25	(2.18, 6.09)		(3.41, 32.86)		(2.28, 3.86)		(2.6, 4.77)		(1.9, 6.47)	
				25-50	(1.43, 6.02)		(2.42, 23.29)		(1.46, 2.47)		(1.29, 2.6)		(1.17, 4)	
N‡	Square root	0.78	Depth Slope Transect No	0-10	(0.27, 0.56)		(0.33, 1.18)		(0.25, 0.39)		(0.29, 0.46)		(0.14, 0.43)	
				10-25	(0.18, 0.44)		(0.27, 1.07)		(0.17, 0.28)		(0.18, 0.32)		(0.09, 0.33)	
				25-50	(0.1, 0.42)		(0.21, 0.94)		(0.11, 0.21)		(0.09, 0.2)		(0.03, 0.21)	
C/N§		0.75	Vegetation Depth Ecotone*Slope Transect No.	0-10	11.4	1.3	15.0	2.9	15.8	0.7	16.1	0.8	20.4	1.6
				10-25	11.7	1.3	14.2	2.9	14.2	0.7	14.5	0.8	18.3	1.6
				25-50	11.7	1.9	13.8	2.9	12.5	0.7	13.6	0.9	18.9	1.6
POXC¶	Square root	0.83	Vegetation Depth Transect No.	0-10	(0.45, 1.18)		(0.55, 2.72)		(0.81, 1.24)		(1.12, 1.7)		(0.93, 2.12)	
				10-25	(0.29, 0.9)		(0.39, 2.35)		(0.55, 0.91)		(0.75, 1.23)		(0.67, 1.72)	
				25-50	(0.13, 0.87)		(0.24, 1.96)		(0.33, 0.62)		(0.36, 0.77)		(0.36, 1.2)	
POXC/C#		0.82	Vegetation Slope	0-10	0.016	0.002	0.012	0.005	0.021	0.001	0.024	0.001	0.027	0.003
				10-25	0.015	0.002	0.011	0.005	0.023	0.001	0.027	0.001	0.032	0.003
				25-50	0.014	0.003	0.009	0.005	0.023	0.001	0.029	0.002	0.031	0.003

† Soil organic carbon (%)
‡ Total nitrogen (%)
§ SOC to N ratio
¶ Permanganate oxidizable carbon (mg POXC g $soil^{-1}$)
# Fraction of SOC that is permanganate oxidizable

Table 5.2b Continued summary of regression analysis on soil properties from 60 samples collected along 5 transects in 2019 at Swanton Pacific Ranch, Santa Cruz Co., CA. Values reported as the least square's means (LSM) and standard error (SE) of *multiple comparisons* between depth interval and plant community in the regression model made in JMP (SAS Institute, Carey, North Carolina). Significant associations and interactions of explanatory variables ($P<0.05$) are reported for each response variable. If a transformation was preformed, the 95% confidence interval is back-transformed in parentheses. Note, the total number of observations (n=) for each plant community or ecotone, includes observations collected over three depth intervals.

Response variable	Transformation	R^2	Sig. association	Depth Interval (cm)	Plant community or ecotone: Grassland (G) n=10		ME/G Ecotone n=9		Mixed-evergreen forest (ME) n=15		ME/RW Ecotone n=11		Redwood forest (RW) n=15	
					LSM	SE	LSM	SE	LSM	SE	LSM	SE	LSM	SE
pH 1:1 H_2O		0.81	Vegetation Transect No.	0-10	6.15	0.24	5.39	0.53	5.87	0.12	6.14	0.14	6.93	0.29
				10-25	6.19	0.24	5.41	0.53	5.84	0.12	6.22	0.14	7.17	0.29
				25-50	6.40	0.34	5.28	0.53	5.61	0.12	5.90	0.17	7.09	0.29
pH 1:2 $CaCl_2$		0.88	Vegetation Depth Transect No.	0-10	5.33	0.24	4.64	0.52	5.07	0.12	5.47	0.14	6.29	0.28
				10-25	5.19	0.24	4.56	0.52	4.98	0.12	5.36	0.14	6.33	0.28
				25-50	5.18	0.33	4.20	0.52	4.68	0.12	5.01	0.16	6.15	0.28
CEC††	Square root	0.63	Depth Transect No.	0-10	(20.39, 62.25)		(0, 54.98)		(26.4, 47.13)		(39.99, 69.08)		(39.69, 106.6)	
				10-25	(20.45, 62.36)		(0.1, 59.91)		(24.33, 44.35)		(27.97, 52.94)		(25.14, 81.7)	
				25-50	(8.9, 59.33)		(0, 54.22)		(22.19, 41.45)		(21.05, 47.49)		(22.77, 77.3)	
BS‡‡		0.47		0-10	0.68	0.10	1.11	0.23	0.79	0.05	0.65	0.06	0.57	0.12
				10-25	0.61	0.10	1.07	0.23	0.65	0.05	0.82	0.06	0.77	0.12
				25-50	0.73	0.15	1.01	0.23	0.66	0.05	0.70	0.07	0.75	0.12

†† Cation exchange capacity (cmol charge kg $soil^{-1}$)

‡‡ Basic saturation of soil cations

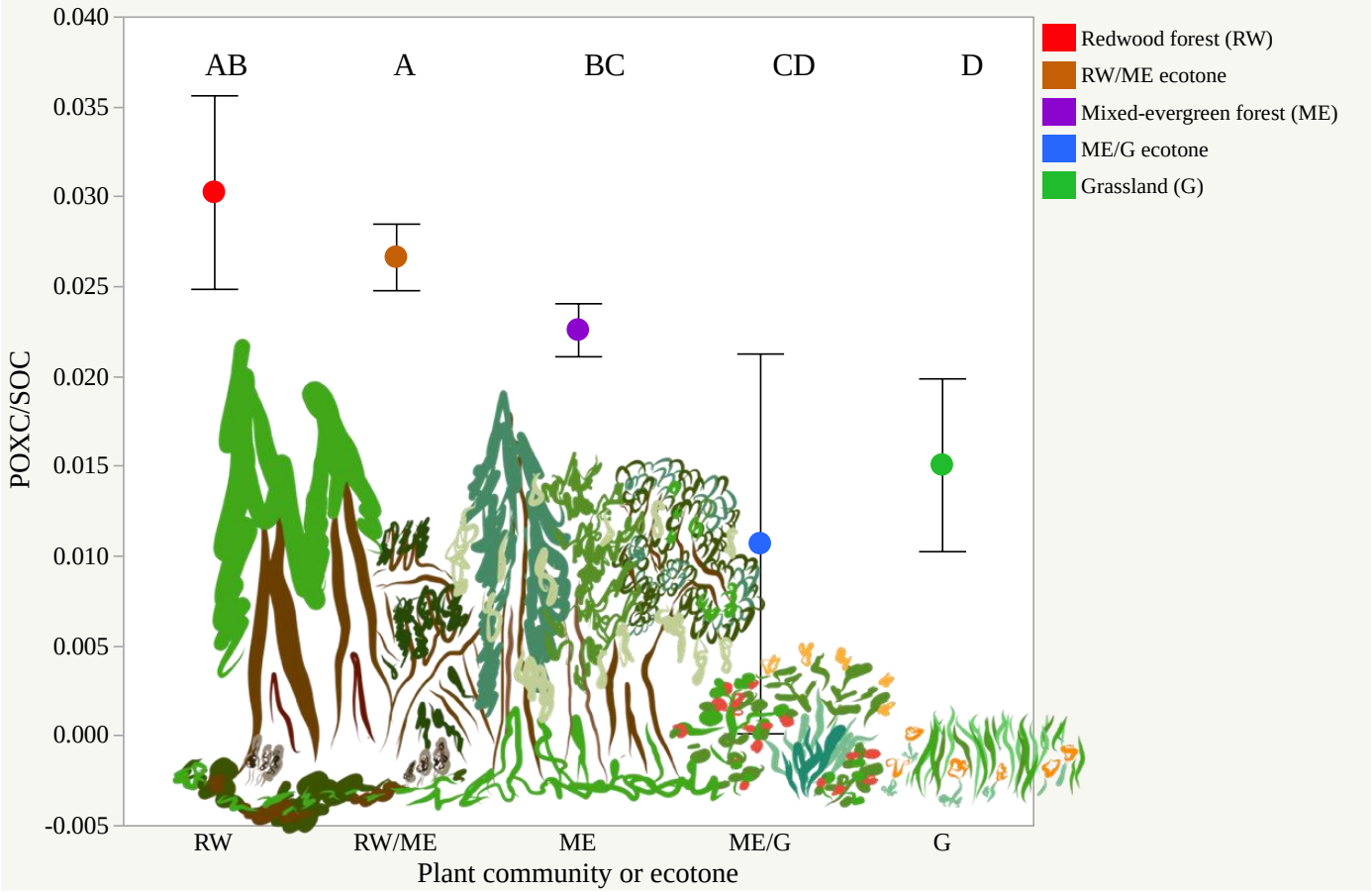

Figure 5.2. Least squares means (LSM) by plant community or ecotone in the regression analysis for the fraction of SOC that is POXC from 60 soil samples collected along 5 transects at Swanton Pacific Ranch, Santa Cruz Co., CA, in 2019. Ecotone is the transitional area between plant communities. Error bars represent 95% confidence intervals of the predicted values in Tukey HSD (honestly significant difference) test. Plant communities and ecotones not connected by the same capital letter indicate a significant difference in LSM ($P<0.05$). The displayed values represent the LSM of the plant community or ecotone, when all three depth intervals and other explanatory variables are included (held constant) in the model.

5.4 Objective 4: compare levels of basic cations between the forest floor and mineral horizons

The relationship between basic cation composition of organic material (acid-ash digestion) and extractable basic cation levels in the underlying mineral surface (ammonium acetate extraction) was analyzed in samples collected from 28 redwood forest sites (16 from profiles at SPR in 2018, 7 from profiles at LHBCR in 2019, and 5 from transect study at SPR in 2019).

We ran univariate regression models between the surface sample (A horizon or 0-10 cm depth interval; details in Chapter 4 under Objective 4) and organic sample for each basic cation of interest (Ca, K, Mg, and Na) and found that the only cation with no evidence for a significant ($P<0.05$) relationship between materials was K (Figure 5.3). This indicated an increase in extractable Ca, Mg, and Na in the mineral surface as Ca, Mg, and Na in the forest floor increased (Figure 5.3)

We also investigated the sum of extractable bases in the mineral surface as a function of the sum of extractable bases in the O horizon; the model provided evidence for a significantly positive relationship ($P<0.05$; Figure 5.4).

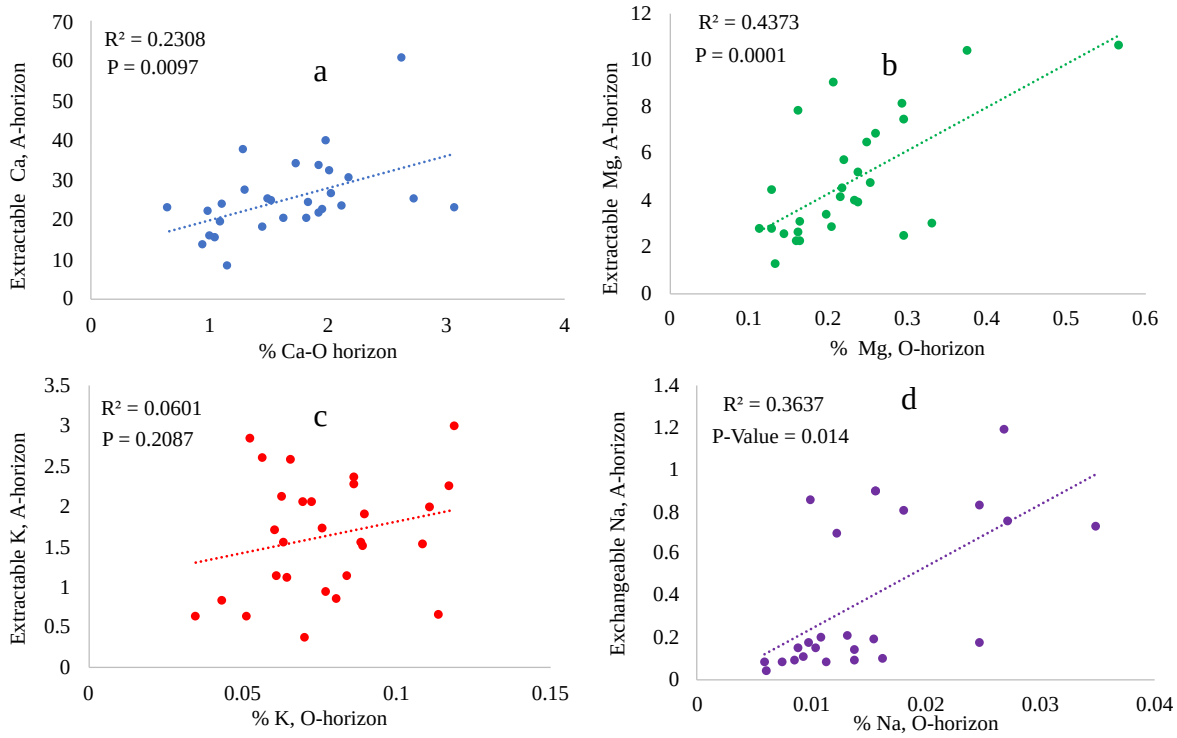

Figure 5.3. Plots of mineral surface extractable bases, Calcium (a), Magnesium (b), Potassium (c), and Sodium (d) in units of cmolc per kg soil on the y-axis, versus overlaying forest floor base composition of respective cation in units of percent, on the x-axis. Mineral surface (A horizons for profiles; 0-10 cm depth interval for transects) and litter layer (O horizons) collected from 28 coast redwood forest locations on the California Central Coast. Coefficients of determination and p-values from univariate ANOVA are displayed for each plot.

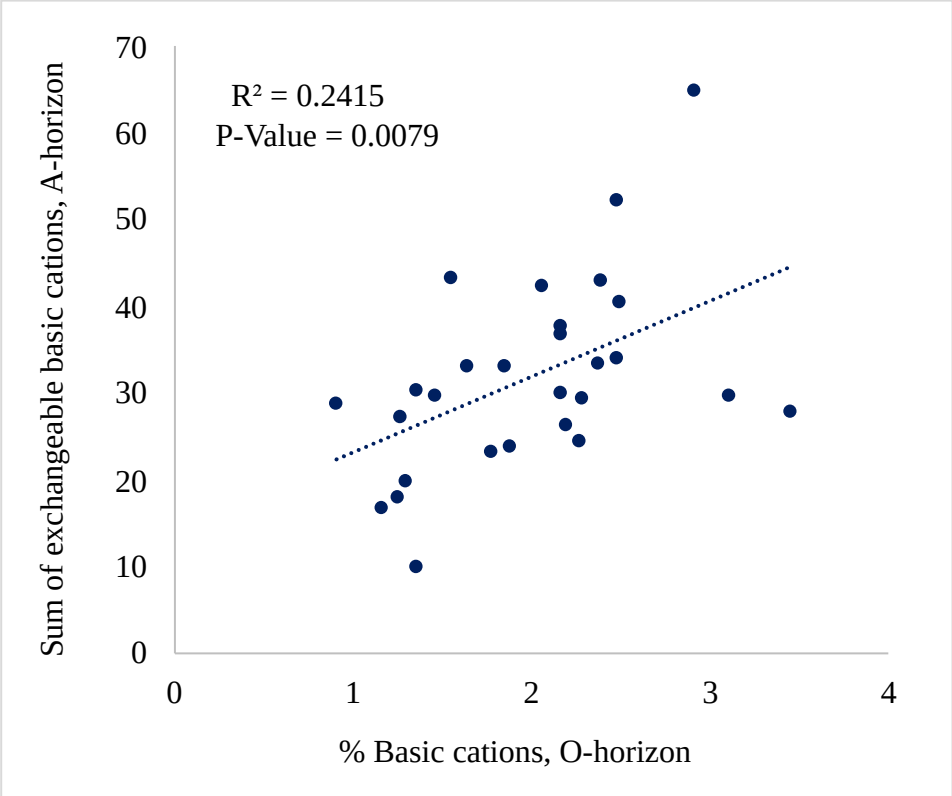

Figure 5.4. Plot of surface-horizon total extractable bases (Ca, Mg, K, and Na) displayed in units of cmolc per kg soil on the y-axis, versus the total basic cation composition of overlaying forest floor (sum of Ca, Mg, K, and Na) displayed in units of percent on the x-axis. Mineral surface (A horizons for profiles; 0-10 cm depth interval for transects) and litter layer (O horizons) collected from 28 coast redwood forest locations on the California Central Coast. Coefficient of determination and p-value from univariate ANOVA is displayed.

Being that we were interested in the relationship of cation levels in organic materials and the mineral soil of the same site, we decided to investigate cation levels through the entire depth of the profile (Figure 5.5). In this inquiry, we removed samples collected in transect study and included soil horizons collected in the grasslands. We decided to focus on calcium exclusively, as calcium was the main contributor to total extractable basic charge (in redwood and grassland horizons alike). In horizons collected at SPR, average contribution of extractable calcium to total extractable basic charge was 67% (±% SE) and 78 % (±1 SE) in grasslands and redwoods, respectively. In horizons

from LHBCR, average contribution of calcium to total basic charge was 58% (±1 % SE) and 76 % (±1 SE) in grassland and redwoods, respectively.

We found evidence for significant negative relationships between calcium levels and soil depth for redwood horizons at both locations, and in grassland horizons at SPR ($P<0.05$; Figure 5.5). This suggested that extractable calcium was higher at shallower depths and decreased as depth increased. There was no evidence for a relationship between calcium levels and depth in grassland horizons at LHBCR ($P<0.05$; Figure 5.5).

Figure 5.5. Extractable calcium levels (cmolc per kg soil) in the soil horizons as a function of horizon center depth (cm) from profiles at two locations in central California, Swanton Pacific Ranch (n=102) and Landels Hill Big Creek reserve (n=56). Data is displayed by plant community, redwood forest (red) and grassland (green). Note- the y-axis is reverse order.

5.5 Objective 5: characterize the total C and active C pools within these ecosystems and to explore interpretations of these pools

5.5.1 C stocks

For each location and plant community, densities and stocks were calculated for SOC and POXC in the top 1 m of soil. At SPR, we found SOC densities of 123 (±25) and 144 (±21) tons of SOC per hectare in the top meter of soil, on average, in redwood and

grassland profiles respectively (Table 5.3). At SPR, the model provided no evidence for a significant difference in SOC densities between plant communities ($P<0.05$). At LHBCR, the model predicted SOC densities were higher in the redwoods, with 221 (±23) tons of SOC per hectare in the top meter of soil, when compared to the grasslands, 126 (±24) tons of SOC per hectare in the top meter of soil, on average ($P<0.05$; Table 5.3).

Because, there was no vegetation mapping available for the land area of LHBCR, the greater area of Big Sur (with mapped vegetation data available) was applied to the LHBCR density to calculate stocks.

Table 5.3 Summary of soil carbon pools from horizon data in the top 1 m of soil profiles in redwood forest and grassland sites along the California Central Coast. Soils collected and analyzed between 2018-2019. Carbon pools were calculated using regression analysis in JMP (SAS Institute, Carey, NC). Values are reported as least square's means plus or minus the standard error for each plant community (redwood forest and mixed annual perennial grassland) at two locations (Landels-Hill Big Creek Reserve and Swanton Pacific Ranch).

Location	Plant Community	Area (ha)	R^2	SOC density‡	C stock§	R^2	POXC density¶	POXC stock#
Big Sur Ecoregion	Grassland (n=7)	8,542†	0.45	*126.3 ±24.2	1,078.6 ± 207.0	0.33	2.9 ± 0.5	25.1 ± 4.3
	Redwood forest (n=8)	13,386†		220.7 ±22.7	2,954.3 ± 303.5		4.4 ± 0.5	58.5 ± 6.4
Swanton Pacific Ranch	Grassland (n=12)	508	0.18	122.9 ± 24.5	62.4 ±12.5	0.26	2.1 ± 0.5	1.1 ± 0.2
	Redwood forest (n=16)	372		143.7 ± 20.9	53.5 ±7.8		3.3 ± 0.4	1.2 ± 0.2

*In the model used to generate soil organic carbon densities applied to the Big Sur Ecoregion, there was a significant association with plant community on the response variable ($P<0.05$)

† Area calculated using data from Stephenson and Calcarone (1999) and Meentemeyer et al. (2008)

‡ Soil organic carbon density, tons soil organic carbon per hectare in top 1 m of soil

§ Soil organic carbon stock, thousand tons soil organic carbon in top 1 m of soil

¶ Permanganate oxidizable carbon density, tons permanganate oxidizable carbon per hectare in top 1 m of soil

Permanganate oxidizable carbon stock, thousand tons permanganate oxidizable carbon in top 1 m of soil

5.5.2 Characterization of C in the soil

There was a significant positive relationship between the natural log of POXC values (mg POXC per g soil) and the natural log of SOC values (%) for soil horizons in each plant community and across both locations ($P<0.05$; Figure 5.6). This suggested that in both locations, POXC content increased with SOC content in redwood and grassland horizons alike.

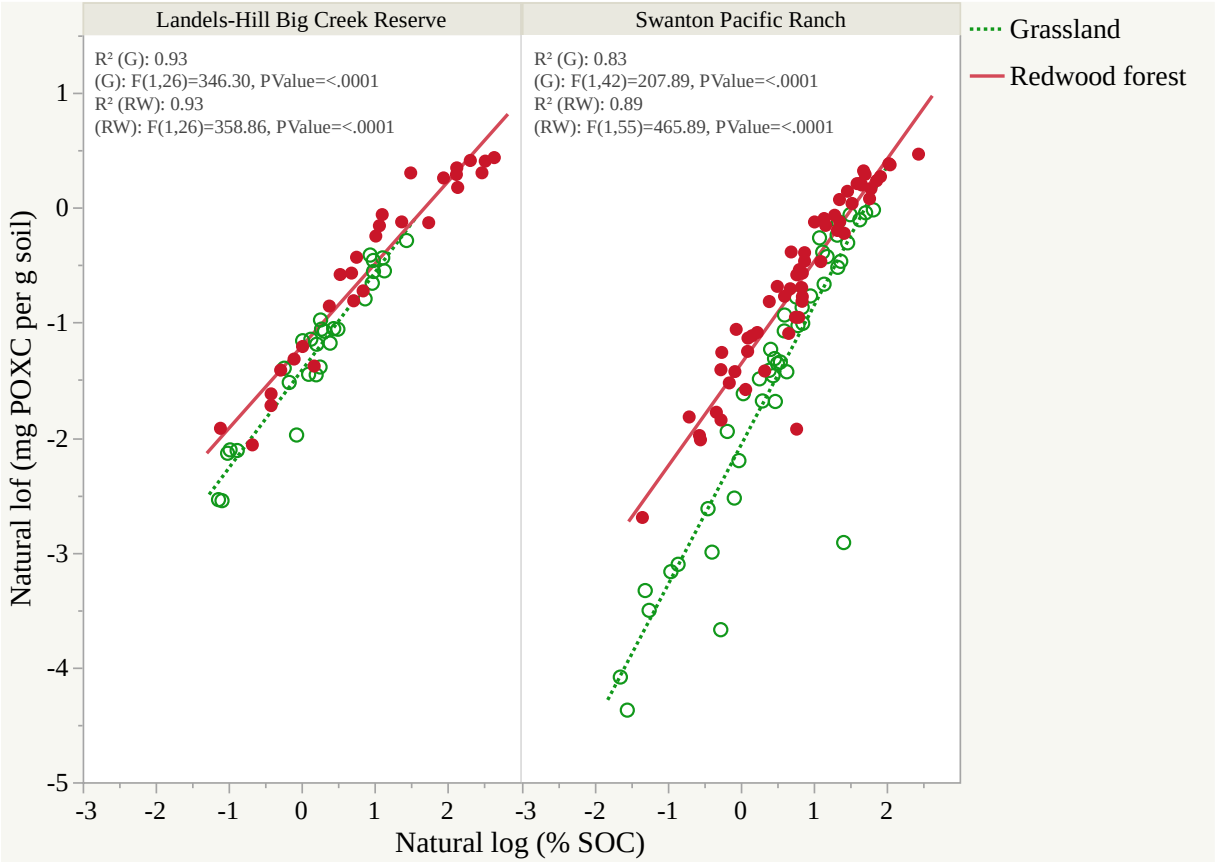

Figure 5.6. Plot of soil horizon permanganate oxidizable carbon (POXC, mg POXC per g soil) versus natural log of soil organic carbon (SOC, %) by location (Landels-Hill Big Creek Reserve, n=56, and Swanton Pacific Ranch, n=102) and plant community (redwood forest and grassland).

Focusing now on the fraction of SOC that was POXC, and when data was restricted to the 20 cm, alone- significant negative relationships were observed between

POXC/SOC fractions and SOC content in redwood profiles at both locations, and in the grasslands of LHBCR ($P < 0.05$, Figure 5.7). This suggested that in the top 20 cm of soil, the fraction of SOC that was POXC (POXC/SOC) decreased as SOC content increased in redwood profiles (at both locations) and in grasslands profiles of LHBCR. There was no evidence for a significant relationship between POXC/SOC fractions and SOC content in the top 20 cm of grassland profiles at SPR ($P < 0.05$, Figure 5.7). Across locations and plant communities, there were no evidence for significant relationships between stoichiometries (C/N) and SOC in the top 20 cm of soil ($P < 0.05$, Figure 5.7).

Figure 5.7 Soil profile depth-weighted averaged values (from horizons) for fraction of soil carbon that is permanganate oxidizable carbon (POXC) and for carbon to nitrogen ratio (C/N) in the top 20 cm as a function of SOC (%). Soil pits are displayed by location (Swanton Pacific Ranch or Landels-Hill Big Creek Reserve) and vegetation (redwood forest or grassland). At SPR, n=16 for redwood profiles, and n=12 for grassland profiles. At LHBCR, n=8 for redwood profiles and n=7 for grassland profiles.

Next, we examined the relationship of POXC/SOC percentage and SOC content for all horizon depths (in contrast to the top 20 cm alone) and interpretations remained the same for redwood populations (at both locations) and grassland horizons at LHBCR; evidence for significant negative relationships ($P<0.05$; Figure 5.8a). Interestingly, evidence for a significant positive relationship was observed for grassland horizons at SPR ($P <0.05$; Figure 5.8a). This suggested that in contrast to the other groups (of plant

community and location), the fraction of SOC that was POXC in the grassland horizons of SPR increased with SOC content.

When the influence of depth was investigated, POXC/SOC fractions increased (significantly) across the natural log of horizon center depth for redwood horizons at LHBCR, and decreased (significantly) across natural log of horizon center depth for grassland horizons at SPR ($P < 0.05$; Figure 5.8b). This suggested higher POXC/SOC composition through depth in redwoods at LHBCR and lower POXC/SOC composition through depth in grasslands at SPR. There was no evidence for a significant relationship between POXC/SOC and natural log of horizon center depth in grasslands at LHBCR, and likewise no evidence for a significant relationship between POXC/SOC and depth in redwoods at SPR ($P<0.05$; Figure 5.8b).

Overall, redwood horizons at SPR had higher POXC/SOC values across depths than in grassland horizons (Figure 5.8b). At LHBCR, there was no clear difference in POXC/SOC values between vegetation types (Figure 5.8b).

(a) (b)

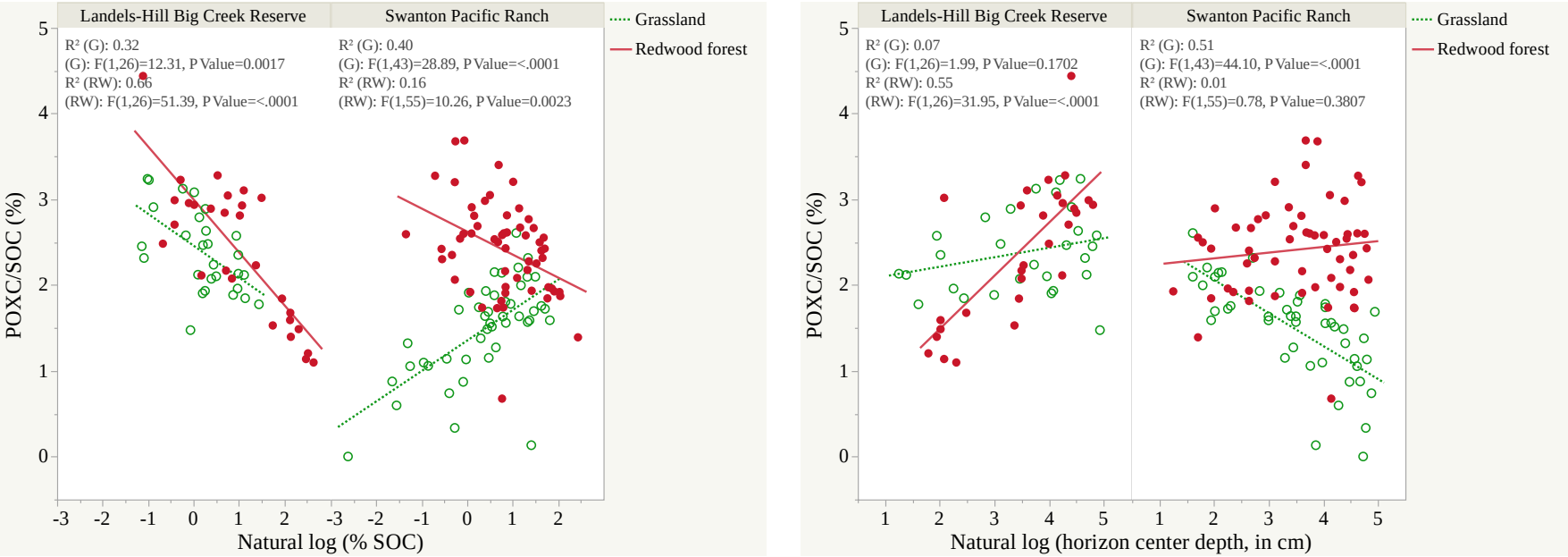

Figure 5.8. Plots for the percent of horizon SOC that is POXC (POXC/C) as function of the natural log of horizon SOC (a) and the natural log of horizon center depth (b). Plots are separated by location and colored by plant communities. Soils were collected from Swanton Pacific Ranch (n=102) in 2018 and the Landels-Hill Reserve (n=56) in 2019.

Evidence for significant negative relationships (P<0.05) were observed between C/N ratios and the natural log of horizon center depth across locations for redwood horizons, and in the grassland horizons of LHBCR (Figure 5.9). This suggested C/N decreased with depth for all groups except the grasslands of SPR, where no evidence for a significant relationship was observed (P<0.05; Figure 5.9).

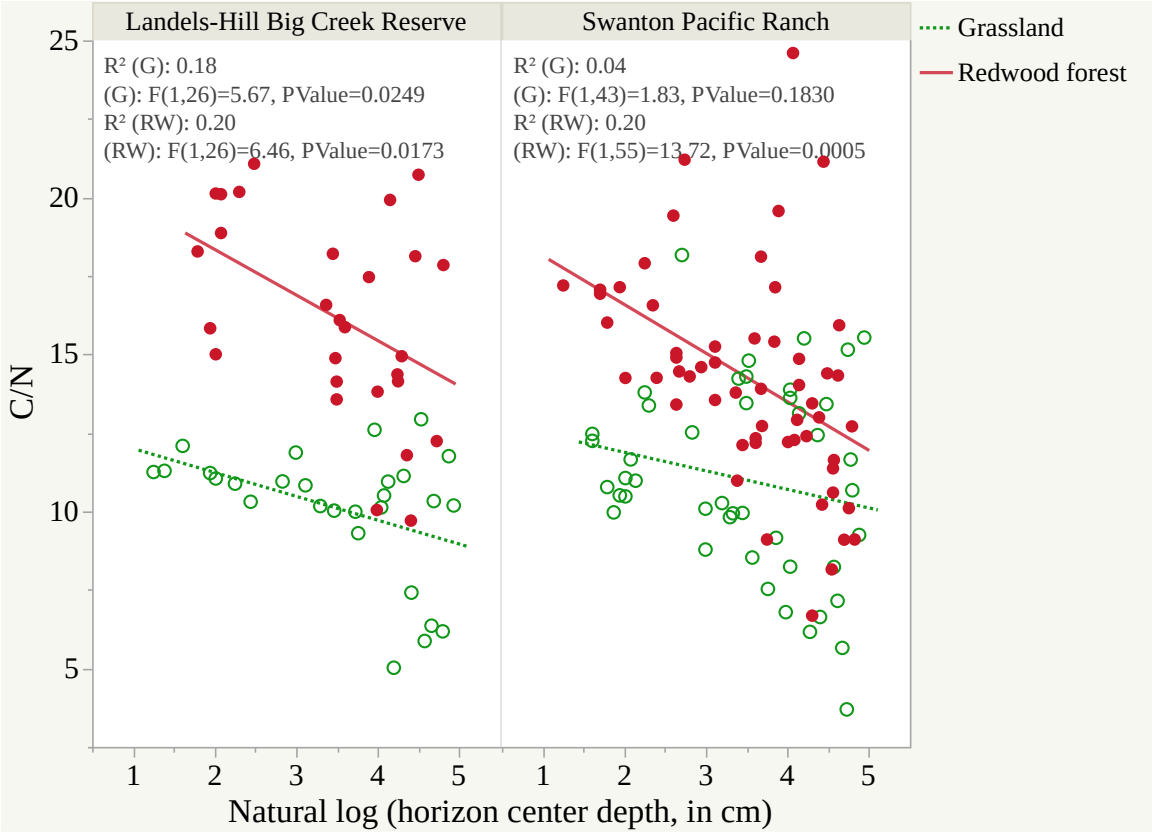

Figure 5.9. SOM stoichiometry (C/N ratio) as a function of natural log of horizon center depth. Plots are separated by location and colored by plant communities. Soils were collected from Swanton Pacific Ranch (n=102) in 2018 and the Landels-Hill Reserve (n=56) in 2019.

CHAPTER 6

Discussion

6.1 Objectives 1-2: gather baseline soils data for the Coast Redwood forest and compare said properties to those in adjacent grasslands; identify their taxonomic classifications

When we compared soils beneath redwood forests to nearby coastal grasslands, we found Mollisols in both ecosystems (Figure 5.1). Mollisols are the type-order for soils with mollic epipedons; mollic epipedons are thick, dark, surface horizons that meet a minimum carbon and basic saturation requirement (Bockheim, 2014; Soil Survey Staff, 2014). Soils of other orders can be distinguished as containing a mollic epipedon at lower taxonomic levels (Soil Survey Staff, 2014).

In the United States, most soils mapped as Mollisols are found below grassland or savanna plant communities; the same can be said for soils that contain a mollic epipedon but are of Vertisol, Andisol, and Alfisol orders (Bockheim, 2014). Presence of mollic epipedons in Inceptisols of the Unites States tends to be below mixed or broad-leaved forests. While there is work that describes mollic epipedons in coniferous forest settings (Bakeman, 1983; Popenoe et al., 1992), such observations are limited, and our findings of mollic formation in coast redwood forests add to this collection.

At LHBCR there was no striking difference in order classification between plant communities (6 of 8 pits as Mollisols in the redwoods and 7 of 7 pits as Mollisols in the grasslands; Figure 5.1). At SPR, redwood forests were more dominated by mollic epipedons than in grasslands (15 of 16 pits as Mollisols in the redwoods and 3 of 12 pits as Mollisols in the grasslands; Figure 5.1).

Mollisols maintain high BS (over 50%) throughout the soil profile (Soil Survey Staff, 2014). If a soil does not maintain high BS through the entire profile, it may still contain a mollic epipedon if all other mollic requirements are met-so long as the BS is above 50% throughout the depth of the identified epipedon.

The reason that many grassland soils at SPR (7 of 12 profiles) did not contain mollic epipedons was due to horizons with low BS (under 50%; Appendix B). Of the 7 grassland profiles at SPR that keyed out as Inceptisols (Figure 5.1), 6 of them were Humiexerpts (Appendix I), which meant they had either a mollic or umbric epipedon. Two of the 6 Humiexerpts in the grasslands contained mollic epipedons (Appendix I), which indicated that BS was above 50% in the surface of these profiles but dropped through depth. In the 4 grassland Humiexerpts profiles that did not contain mollic epipedons, horizon BS was lower than 50% at the surface.

Apart from taxonomy, we were interested in how soil properties varied across plant communities and what were the controlling variables in these differences. When we included potential influences of soil formation (depth, vegetation, slope, and horizon) and associated interactions (depth*slope, veg*slope, veg*depth) in a regression model, we found higher values of pH, C/N stoichiometry, and CEC in redwood soils than in grasslands, and lower predicted values of bulk density in redwoods than in grasslands-these trends were ubiquitous across both locations (Table 5.1).

Least square mean values for SOC were above the minimum mollic requirement (0.6% SOC) in each population (Table 5.1) and none of the soils we classified failed to meet mollic requirements because of individual horizon SOC values (Appendix B). Our model found that redwood horizons had higher SOC concentrations than the grasslands at

LHBCR, and at SPR, there was no difference between plant communities (Table 5.1). When looking at the POXC pool, redwoods had higher POXC concentrations than in the grasslands at both locations (Table 5.1). Thus, while redwoods had a higher ratio of POXC to SOC than the grasslands at SPR, there was no difference in this ratio between plant communities at LHBCR. A continued discussion on POXC/SOC ratios and SOC is found in a subsequent section of this discussion chapter.

Consistent significant associations from horizon depth and site slope (and the interactions of each of with vegetation) throughout response variables in the models (Appendix D and E) served to highlight the importance of soil forming factors that vary with position on the landscape and are not purely associated with vegetation.

6.2 Objective 3: investigate the influence of vegetative gradation on soil properties between these ecosystems

As was the composition of the flora across transects transitional in nature from grassland to redwood forest (Appendix A), so too were several soil properties beneath the forest floor (Table 5.2). A generally consistent and graded pattern was observed for C/N ratios, POXC/SOC ratios, and pH (in both matrices); these variables were generally highest in the redwood forest and decreased sequentially across the vegetative gradients through mixed-evergreen forest and into the grassland; this was consistent across the three depth-intervals (Table 5.2; Figure 5.2). This graded behavior for select soil properties across plant communities (and depths) served to contrast to the assertion that ecotones (and the soil beneath) tend to exhibit unique ecological properties that stand out as different in respect to adjoining plant communities (Marfo et al., 2019a). Instead, our study showed changes belowground can be reflected in a similar pattern to transitions

that occur aboveground, and the effect of an ecotone can be functionally negligible (resembling an average between adjacent plant communities).

Considering the protocol used to identify ecotone (the point at which two separately classified communities contributed to approximately half of the canopy and litter composition), it makes sense that C/N ratios in the soil (impacted by plant inputs) changed with the vegetation along the transects (Table 5.2). Woody material (common in forest settings; not common in grasslands) has higher C/N content than herbaceous litter (Cotrufo et al., 2013). While we did not measure C/N ratios of forest littler along the transects, it would have been interesting to compare C/N ratios of said organic horizons to those of the corresponding mineral soil. Furthermore, our findings of decreasing C/N content from the redwoods into the grasslands conform to the general understanding of ectomycorrhizal systems (e.g. temperate coniferous forests) being characterized by higher C/N ratios than in arbuscular mycorrhizal systems (e.g. temperate grasslands; Cotrufo et al., 2019). Broadleaf tree species (such as *Quercus* taxa in the mixed-evergreen forests) have the ability to associate with either ecto- or arbuscular mycorrhiza (Cotrufo et al., 2019), and in our study the mixed-evergreen forest had intermediary C/N ratios to redwood and grassland. Thus, the graded pattern we observed in soil C/N may be a reflection of both litter quality and microbial community. Due to the interconnectedness of plants and mycorrhiza, it is difficult to identify a causal relationship in either plant traits or mycorrhiza on soil C/N ratios (Cotrufo et al., 2019).

An exception to the general decreasing trends of POXC/SOC and pH values from the redwood forest into the grasslands, were higher values of POXC/SOC and pH in the grassland community when compared to the grassland-mixed evergreen ecotone (Figure

5.2 and Table 5.2); this phenomenon was accentuated in the pH values (Table 5.2). One reason for this occurrence is explained by higher standard errors across all response variables in the grassland and mixed-evergreen forest ecotone (Table 5.2). This ecotone (grassland and mixed-evergreen forest) had the fewest number of observations (n=9) included in the model (Table 5.2). Observations were excluded from the model in instances of gaps in the data (i.e. if slope, one of the explanatory variables in the model, was not recorded in the field). Another reason for fewer observations in this ecotone (mixed-evergreen forest and grassland) is because we described a coastal scrub community in between the mixed-evergreen forest and grassland (in 1 of the 5 transects; labeled "5849"), thus, in this case there was no ecotone between the grassland and mixed-evergreen forest communities. Furthermore, in consultation with a statistician, it was determined that another (more influential) reason for the higher standard error in this ecotone (grassland and mixed-evergreen forest) was due to the co-linearity between ecotone with slope and particularly the low variability of slope observed within the grassland and mixed-evergreen forest compared to other ecotones.

Some of the confidence intervals presented in Table 5.2 for the grassland and mixed-evergreen forest ecotone contain values that were abnormally high (e.g. 95% confidence interval for percent SOC was between 4.41 and 42.5%); large uncertainty on one end of the interval can attributed to the asymmetric distribution associated with the data in this ecotone. Recall that 95% confidence intervals were displayed instead of LSM, for response variables transformed during regression analysis (see "Multivariate regression design for transects" in Chapter 4 and Eq. 23, Appendix F).

In some ways, the *multiple comparisons* feature in JMP made data interpretations clearer (in terms of visualizing the co-occurring influence of depth through vegetative categories) but less clear, in terms of being able to comment on general tends (because of all the individual categories with fewer observations) which highlighted the importance of parsimony in regression analysis.

Least squares mean values for other soil properties (SOC, N, BD, CEC, and BS) were not significantly associated with vegetation category, and instead, slope, depth interval, and transect number were associated controls (if any) on these levels (Table 5.2).

The study of soil properties across vegetative transects has been limited (Marfo et al., 2019a; b); however, it is not a novel approach (Parker et al., 2015). We found that many of the soil properties across transects exhibited inconclusive results (or no trends across the gradients), however, there were relatively distinct trends exhibited in C/N ratios, POXC/SOC ratios, and pH (Table 5.2). Regardless of the aforementioned findings, the study design, alone, contributed to the limited exploration of soil properties across natural vegetation gradients. More novelty was imparted by these efforts, when the observations of this transect study are considered in conjunction with the independent comparison of profiles found in redwood and grassland communities of the same location (objective 1).

6.3 Objective 4: compare levels of basic cations between the forest floor and mineral horizons

Our mean elemental concentrations for Ca, K, Mg, and Na in the forest floor (Appendix N) closely resembled previously reported cation data in redwood litter (Enloe et al., 2006).

The presence of calcium is an important soil forming factor in the genesis of mollic epipedons as calcium binds to negatively charged organic matter and forms black and stabilized Ca-humates (Bockheim, 2014). Because calcium was the main contributor to total basic charge (average contributions of calcium to total extracted basic charge was above 58% for redwood and grasslands at LHBCR and SPR), and, if the significant relationship observed for forest floor and calcium in the mineral surface ($P<0.05$; Figure 5.3a) was the result of plant-soil cycling (Popenoe et al., 1992), it would make sense that redwood litter (relatively high in calcium compared to the other cations, Appendix N) was an important facilitator of high base saturation (and moreover mollic formation) in our soils. Redwood populations (at both locations) had higher calcium levels in the surface than in the grasslands, and both redwood populations decreased in calcium through depth ($P<0.05$; Figure 5.5),which suggested the main source of extractable calcium in redwood horizons may be from above and not from parent material below; similar observations in calcium levels were reported in a comparison of forests and grassland soils in northwestern California (Popenoe et al., 1992). A common garden experiment (Reich et al., 2005) supports this notion, and found that litter calcium (of varied tree species) was interconnected with exchangeable calcium in the soil. Another pathway for bases to enter the soil, that is pertinent to redwood systems, can be from fog

(Ewing et al., 2012). Weathering of minerals from parent material is another source of soil bases (Bockheim, 2014), that was not incorporated into this study.

Regardless, we can assert the relatively large role of calcium (in relation to the other cations) in contributing to the basic saturation values that qualified soils beneath the redwoods for mollic classification.

One consideration is that we were not able to discern what fraction of the extractable calcium measured was from exchangeable calcium and what fraction was from carbonates. We assumed any extractable basic charge above the cation exchange capacity was from carbonates, and this was particularly relevant at LHBCR where 17 of 56 horizons had a BS greater than 100% (Appendix B); these values were amended to be 100% as per U.S. taxonomic protocol (Soil Survey Staff, 2014). One way to avoid dissolution of carbonates is to raise the pH of the extraction matrix (cite), but this method does not match the criteria of mollic epipedon classification set forth in USDA soil taxonomy.

Despite evidence for significant positive relationships ($P<0.05$) in calcium, sodium, and magnesium levels between overlain and underlying horizons (Figure 5.3), low coefficients of determination (R2 values of 0.23, 0.17 and 0.44 for calcium, sodium, and magnesium respectively) suggested there were other factors left unexplained that contributed to the observed variance. We postulate that slope and horizon thickness may have had impacts on said cation relationships, these were variables we measured but did not include in the model due to small sample sizes. Regardless, we can assert the relatively large role of calcium (in relation to the other cations) in contributing to the basic saturation values that qualified soils beneath the redwoods for mollic classification.

One consideration is that we were not able to discern what fraction of the extractable calcium measured was from exchangeable calcium and what fraction was from carbonates. We assumed any extractable basic charge above the cation exchange capacity was from carbonates, and this was particularly relevant at LHBCR where 17 of 56 horizons had a BS greater than 100% (Appendix B); these values were amended to be 100% as per U.S. taxonomic protocol (Soil Survey Staff, 2014).

Despite evidence for significant positive relationships ($P<0.05$) in calcium, sodium, and magnesium levels between overlain and underlying horizons (Figure 5.3), low coefficients of determination (R^2 values of 0.23, 0.17 and 0.44 for calcium, sodium, and magnesium respectively) suggested there were other factors left unexplained that contributed to the observed variance. We postulate that slope and horizon thickness may have had impacts on said cation relationships, these were variables we measured but did not include in the model due to small sample sizes.

6.4 Objective 5: characterize the total C and active C pools within these ecosystems and to explore interpretations of these pools

6.4.1 POXC as a pool of SOC

POXC was positively and logarithmically associated with SOC ($R^2 > 0.83$ for each plant community at both locations; Figure 5.6); this finding conformed to previous studies (Tirol-Padre and Ladha, 2004a; Skjemstad et al., 2006a; USDA-NRCS, 2014; Romero et al., 2018). Because of the direct proportionality, we chose to investigate the fraction of SOC that was POXC in an effort to improve our understanding of how soil C pools differed across vegetation, slope, depth, etc. (Table 5.1; Appendix E). Depsite the number of studies that have investigated POXC, we only found two studies (Hurisso et

al., 2016; Romero et al., 2018) that have presented the fraction of SOC that was POXC; using this metric, mentioned studies provided limited investigation. Thus, the focus of POXC/SOC ratios in this study has made the efforts in this chapter unique amongst previous studies that have measured POXC. Our mean values for POXC/SOC ratios were slightly lower (but comparable) to Romero et al. (2018) who observed 2.0-5.8% POXC/SOC fractions in Mollisols from Montana.

At SPR, our least squares mean values for POXC/SOC were 1.5% ($\pm$0.1) and 2.5% ($\pm$0.1) in grassland and redwood horizons, respectively; said values were significantly different ($P < 0.05$; Table 5.1). This finding at SPR was corroborated in our transect study (under Objective 3), and we observed higher POXC/SOC values in the redwood forest (2.7% in the 0-10 cm depth range; Table 5.2) when compared to the preceding plant communities (2.1% and 1.6 % in the 0-10 cm depth range, for mixed-evergreen forest and grassland communities respectively; Table 5.2). In the soil profiles at LHBCR, there was no evidence of a difference between vegetation types; the POXC/SOC values of this population were within range of those reported above.

6.4.2 Differences in POXC/SOC across plant communities and localities

To explore the POXC/SOC fraction represented, we looked at the behaviors of other soil C pools in the literature and compared this to the behavior of POXC/SOC in our study. A compost application experiment (Gulde et al., 2008) and study of forest and rangeland soils (Cotrufo et al., 2019) showed accretion of mineral associated C exhibited a threshold at certain levels of SOC, after which, particulate organic matter (POM) was the only contributor to SOM accumulation. In contrast to the POM pool which does not interact (and bind) with soil minerals, mineral associated C represents a pool that has

been microbially degraded (<53 um). If a soil is undersaturated with respect to mineral associated C, there is potential for active mineral associated C to become inactivated (i.e. stabilized and relatively not sensitive to management). Alternatively, POM (even if stabilized within soil aggregates) could be released upon disturbance such as tillage. Due to the robust nature of inactive mineral associated C, raising levels of said pool to the SOC threshold is a promising objective for soil C sequestration. Likewise, because POM does not saturate, raising POM levels is a useful objective to sequester to soil C in areas where physical disturbance is minimized.

Using the depth interval of soil in Cotrufo et al. (2019), we compared POXC/SOC ratios across SOC values in the upper 20 cm of redwood and grassland profiles. Significant negative relationships were observed for redwood pits at both locations, and a negative relationship was observed in the grasslands of LHBCR ($P < 0.05$; Figure 5.7). There were no significant relationships between stoichiometries (C/N ratio) and SOC at this depth ($P > 0.05$; Figure 5.7). If a SOC threshold like the one observed in Cotrufo et al. (2019) was relevant to our study, our findings suggested that POXC did not discriminate between mineral associated C and POM. For instance, if POXC was selective for POM (Culman et al., 2012; Hurisso et al., 2016), we would have expected a non-restricted accumulation of POXC/SOC (or POM resembling SOM) across SOC values; furthermore, an increase in C/N ratio as a function of SOC would have strengthened this case of POXC as a measure of POM. These findings (decreased POXC with SOC) suggested POXC did not discriminate toward POM or MAOM exclusively, and instead, was a heterogenous pool of SOC. One reason we didn't see similar results to Cotrufo et al. (2019) in the top 20 cm may be because the 5% MAOM threshold the

authors reported, was observed across an expansive and diverse pool of soil types found in European forests and rangelands, whereas our data came from two unique populations of forests and rangelands on the CA Central coast.

Many efforts to study SOC have focused on the topsoil and fail to include observations of SOC at greater depths (Harrison et al., 2011; Jandl et al., 2014); under objective 1, we collected data to 1.5 m, weathered bedrock, or to the extent feasible (whichever was shallower). Using horizon data for all depths (as opposed to the 20 cm, alone), we examined the relationship between POXC/SOC and SOC again; our interpretations remained mostly the same (significantly negative relationships between POXC/SOC and SOC; $P < 0.05$; Figure 5.8a). One difference we observed was increased POXC/SOC ratios with SOC for grasslands at SPR when all depths were included ($P < 0.05$; Figure 5.8a), as opposed to no relationship in the top 20 cm ($P < 0.05$; Figure 5.7).

Because interpretations changed once all horizon depths were included, we decided to plot the POXC/SOC fractions against depth (Figure 5.8b). In these plots we observed increased POXC/SOC with depth for redwood horizons at LHBCR, and decreased POXC/SOC with depth for grassland horizons at SPR. At LHBCR, there was no significant relationship between POXC/SOC and depth for grasslands, and at SPR, there was no relationship between POXC/SOC and depth for redwoods. Overall, the plots showed redwoods had higher POXC/SOC values across depths at SPR, but at LHBCR, there was clear no difference between vegetation types across depths (Figure 5.8b); these descriptive observations of POXC/SOC in the linear regression plots (Figure 5.8b) conformed to the significant association from vegetation (or lack thereof) in the larger regression model used for objective 1 (Table 5.1). To explore why there were contrasting

trends across locations in POXC/SOC with depth, we considered ecological differences between the plant communities as well as differences in land management between the locations we sampled from.

6.4.2.1 Ecological differences in SOM

Fundamental ecological differences exist for the way SOM enters the soil in redwood forests and grasslands. Main inputs of SOM in redwood forests ecosystems are from woody residues and litter fall, that have higher C/N ratios, molecular weights, and carbon complexities when compared to grassland inputs (Cotrufo et al., 2015, 2019). Most plant biomass C in grasslands is found belowground where main inputs to SOM are from root secretions and exudates as well as from root decay (Follett et al., 2001). The life cycle of annual grasslands in California is one of fall germination, accelerated growth in the spring, and summer death and desiccation (Silver et al., 2010) . The temperate climate and absence of fall leaf cessation in redwoods forests serve to minimize seasonal impacts to SOM. In coniferous forests, ectomycorrhizal fungi dominate the soil microflora and have higher C/N stoichiometries when compared to arbuscular mycorrhizal fungi which dominate soil communities in grasslands (Orgiazzi et al., 2016a; Cotrufo et al., 2019).

In redwood arboreal soils, Enloe et al. (2010) suggested mechanisms of selective preservation and limited microbial processing of recalcitrant materials through soil depth. In contrast, we found that depth had a significant association ($P < 0.05$) on SOM in the redwoods, as we observed decreased C/N ratios with depth at LHBCR and SPR alike (Figure 5.9). Contrary findings were not surprising given that arboreal Histisols are a unique occurrence of soil suspended in redwood branches at least 50 m above the forest

floor, and they presumably experience different soil forming processes (e.g. biota, parent material, topography, etc.). Nonetheless, reported C/N ratios of redwood bark litter and leaf litter from Enloe et al. (2010) which ranged from 50-75, provided insights into the successional stage of SOM in our redwood soils. The highest C/N ratio in our mineral soil horizons was 24, this was from a C horizon with relatively low SOC (0.56%) and suggested organic material from redwood litter was not selectively preserved, but rather, there had been considerable decomposition in respect to original stoichiometry; this is under the assumption that redwood litter from our sites was comparable to the values reported by Enloe et al. (2010).

Using POXC as generally representing POM (Culman et al., 2012; Hurisso et al., 2016), higher POXC/SOC ratios at depth in the redwood horizons at LHBCR (Figure 5.8b) could have been a signature of increased microbial populations near the surface that were not present in the subsurface. Perhaps the impact of depth was accentuated in forest soils when compared to grasslands, as microbial communities fed off sustained organic inputs deposited near the surface that then translocated (e.g. via bioturbation) into the subsurface, and perhaps this impact was not observed in the grasslands because POM (e.g. from root tissues) was persistent across soil depth (Figure 5.8b). Lower C/N ratios at depth for both redwood locations (Figure 5.9) did not support this hypothesis. An understanding of the relationship between POXC and dissolved organic C (DOC) may aid interpretations of our data. A study of soil in redwood and grassland settings (Sanderman et al., 2008) found that total concentration of DOC was diminished, and the recalcitrant nature of DOC was enhanced with soil depth; this change occurred in both communities and was attributed to mechanisms of rapid microbial decomposition and

selective adsorption to soil exchange sites. Interestingly, this change in DOC chemistry was more was more rapid in the redwoods than in the grasslands and the authors attributed this to the differing SOM inputs between communities (Sanderman et al., 2008).

None the less, contrasting trends we observed in POXC/SOC and depth at LHBCR and SPR (Figure 5.8b) confound interpretations, and this highlights a challenge associated with interpreting POXC across vegetation and soil types (Skjemstad et al., 2006a)

6.4.2.2 Differences in land management

One key distinction to consider given differences observed in POXC fractionation within the two locations and between redwood and grassland soils is the differing land management. Swanton Pacific Ranch is a "living working ranch", and the California Polytechnic State University has continually (holistically) grazed the rangelands since the property was endowed to the school in 1993 (Swanton Pacific Ranch, 2020a). In contrast, the goal of the University of California is to maintain their Reserves as wild ecosystems limited to educational and research-use, and there here has been no grazing at LHBCR since 1984 (Bickford and Rich, 1984).

Research from one long-term grazing study (Gill, 2007) showed increased mineralizable C in the top 15 cm of grazed sites when compared to non-grazed sites, and no difference in total soil C or POM between grazed and non-grazed sites; mineralizable C is measured by the amount of CO_2 released from dried soil when water is added and indicates an active fraction of active C susceptible to loss (Hurisso et al., 2016). These observations were attributed to lower soil moisture in grazed sites that served to decrease

decomposition rates and offset the reduced SOM inputs when compared to non-grazed sites (Gill, 2007).

Hurisso et al. (2016) showed POXC and mineralizable C were positively and logarithmically proportional, but claimed the relationship between the two fractions was different across management strategies (grazing not included as one of the strategies). Our data showed increased POXC/SOC in the surface of grazed horizons at SPR, but no trend with depth at LHBCR (Figure 5.8b). If POXC were an appropriate predictor of mineralizable C under grazing, perhaps our findings at SPR suggested an impact from grazing at the surface of grasslands soils (Figure 5.8b). A better understanding of the relationship between POXC and grazing, as well as the impact of grazing on any carbon pools across soil depths is warranted to improve interpretations of this data. Additional information about the grazing history and strategies implemented above our grassland sites would aid the interpretations.

Another main difference between study locations is forest age. The Forest Management Plan for Swanton Pacific Ranch (1991) states first cuts of Little Creek occurred in 1907, and secondary harvests occurred in the 1960s (Big Creek Lumber Co., 1991). While scattered old growth trees exist, most redwood stands encountered at SPR were second and third generation. Since 1990, several units at SPR have been managed under a non-industrial timber harvest plan. In contrast to the Santa Cruz Mountains, redwoods along the Big Sur Coastline were protected from extensive logging due to the remote terrain; LHBCR is one locations where old growth redwood stands still exist (Bickford and Rich, 1984; Potter, 2012; Van Pelt et al., 2016). The extent to which historic logging at SPR and lack thereof at LHBCR impacted the redwood soils we

studied, is an important consideration but outside the scope of this project and we did not expect any noticeable impacts on the soil properties we measured.

6.4.3 Implications for management of soil C

Within the redwood forest ecosystem, there has been variation in reported C densities for aboveground biomass. A study of old-growth canopy structure (Van Pelt et al., 2016) found aboveground biomass C to be 1380 and 1043 tons C per hectare at Big Basin State Park and Landels-Hill Big Creek reserve respectively (these locations found in the southern redwoods and have less biomass when compared to northern forests, e.g. 2596 tons C per hectare at Jedidiah Smith Redwoods State Park which is the global maxima for aboveground C per unit area). These numbers confined to old-growth forests (Van Pelt et al., 2016), are much larger than estimates from statewide efforts to inventory forest C across the redwood range which reported 302 tons (Forest Climate Action Team, 2018) and approximately 270 tons (Christensen et al., 2018) of aboveground C per hectare, on average. Because trees found in old growth forests can be considerably taller when compared to trees in younger forests, it makes sense that old growth forests would be capable of harboring more aboveground C than in younger forests.

Regardless of tree height, our findings suggested that in contrast to the general understanding of the pedosphere as a larger terrestrial carbon pool than the aboveground pool (Lal, 2004a), redwood forest ecosystems are an exception, as we found 143 and 221 tons of organic C per hectare, on average, in the top meter of redwood soil at SPR and LHBCR respectively (Table 5.3). Most of the soil profiles we investigated beneath redwoods (21 of 24 at LHBCR and SPR; Figure 5.1) were classified as Mollisols, and our

C numbers are comparable to the globally averaged SOC density in the top meter of soil for the Mollisol order, 134 tons C per hectare (Lal, 2004b).

The soils beneath the redwood trees maintained SOC densities that were higher (LHBCR) or as high as (SPR) than the neighboring grassland communities (Table 5.3); this is a unique finding, as globally, temperate grassland soils are accepted as more capable of sequestering carbon per unit area than temperate forests (Lal, 2004b), presumably due to the contrasting the root structures and ecologies. Furthermore, until now, most efforts to the highlight ecosystem service of redwood forests as carbon sinks have focused on the trees (Van Pelt et al., 2016; Christensen et al., 2018; Forest Climate Action Team, 2018). Our findings have highlighted that soils beneath the redwoods are similarly as important to carbon sequestration as the redwood trees themselves.

Using Van Pelt et al. (2016) value for aboveground C at LHBCR (1043 tons C per hectare), SOC density (221 tons C per hectare) to 1 m depth was only 21% of the above ground density. Aboveground C densities in adjacent grasslands were presumably much less than in the redwoods, and in general, grasslands contain 90% of total ecosystem organic C belowground (Reeder and Schuman, 2002). Despite disparity in aboveground biomass C when compared to forests, the grasslands we studied were able to sequester a considerable amount at both locations (over 50% of the total SOC stored in redwoods; Table 5.7). In grassland profiles, C densities values were 126 ($\pm$24) tons C per hectare at LHBCR and 123 ($\pm$25) tons C per hectare at SPR and these compared well to that of Silver et al. (2010) who reported C density in non-woody California grasslands as 116 ($\pm$9) tons C per hectare.

No significant difference in SOC densities for grassland and redwood profiles at SPR suggested the evidently larger aboveground pool (in redwoods when compared to the grasslands) was not reflected belowground. While we were not able to conceptualize what the POXC pool represented in the soils we studied (see discussion section above titled "Differences in POXC/SOC across plant communities and localities"), interpretation of higher POXC/SOC ratios in the redwood horizons and transects at SPR in the context of previous efforts (Culman et al., 2012), suggested the pool of SOC in those redwoods was more active (sensitive to changes in management or disturbance) than in the grasslands. It should be noted that out of all of our soil samples, the highest fraction of SOC that was POXC observed was, 4.5%, which indicated a considerable amount (at least 95%) of SOC was not categorized in the POXC pool. In future soil C sequestration efforts to increase levels of a particular pool, consideration of a pool with a higher relative contribution than POXC to the total SOC pool, may direct better allocation of resources.

In order for SOC stocks for specific locations to acuate management guidance on a local level, it is not only necessary to have an understanding of impacts from management practices on the pool of SOC measured (e.g. no-till agriculture increases POXC; Hurisso et al., 2016), but also to have an understanding of the stabilization mechanism associated with said pool of SOC (e.g. POM is representative of SOM that can be preserved via spatial inaccessibility in soil aggregates and exhibits limitless accrual with additional C inputs; Cotrufo et al., 2019) as well as the residence time expected for that pool of SOC (e.g. physical preservation in aggregates operates on a

short-term residence time in comparison to organo-mineral interactions; Cotrufo et al., 2013).

Despite our recommendation to avoid future measurement of POXC due to lack of an associated stabilization mechanism, in keeping with the original motivation of objective 5, to "explore interpretations" of the soil C pools measured, the POXC measurements collected in this study were used to demonstrate the conversion of a stock for a particular pool of SOC into carbon metrics more relevant to governing bodies (e.g. CO_2-equivalents; Appendix P). The purpose of this approach was strictly an exercise, to provide an example of how quantities of soil C pools can be conveyed to land management in alternative perspectives, and not, to assert the usefulness of the POXC stocks themselves.

By connecting an active stock of SOC to CO_2-equivalent emissions (Intergovernmental Panel on Climate Change, 2014), we explored: 1) the monetary value of the POXC pool if land managers in California were compensated for sequestration of C at the same rate as C emitters (approximately $15 per ton of CO_2-equivalent emitted over the cap; California Air Resources Board, 2021) and 2) the number of California automobile drivers encapsulated in the POXC pool (based on average annual emissions, the CO_2 equivalent for one thousand tons of C represents approximate annual emissions of 788 California automobile drivers; Federal Highway Administration, 2017; California Air Resources Board, 2019; Appendix P). Comparisons such as these are not common in the literature, and when appropriately interpreted in the context of actions or disturbances that can diminish soil C levels, these types of metrics (based on CO_2-equivalent

emissions) may provide increased relevancy (e.g. money) and tangibility (e.g. auto-emissions) to land managers when compared to stand alone stocks (tons of C).

In California, land managers can receive compensation for costs associated with voluntary soil C sequestration projects but cannot collect direct payment for sequestration of soil C (P. Alvarez of California Carbon Cycle Institute, personal communication, 6 April 2020). Outside of the Chicago Climate Exchange (operational form 2003-2010; DiPerna, 2018) we are not aware of any governing agency or market-based project that has used an emissions cap framework to discourage release of soil C by direct compensation to land managers for reporting rates of C sequestered (P. Alvarez of California Carbon Cycle Institute, personal communication, 6 April 2020).

6.4.3.1 Looking into the future

Whereas most native grassland communities of California rangelands have been outcompeted by introduction of invasive Euro-Asian exotics (Ryals and Silver, 2013; Ryals et al., 2016), California forests appear as a less visually-adulterated ecosystem in relation (presumably due to the longer life span of trees compared to grass species). Despite this, climate-induced risks of fire and disease are pressing threats to relic forests ecosystems. Research in our study region suggested that Redwood trees (generally physiologically resistant to fire) are more vulnerable to fire due to *Phytophthora ramorum* and its impact on neighboring tree species *(e.g. Notholithocrpus densiflorus*; Metz et al., 2013); compounded fire-disease effects were responsible for increased losses of C in the topsoil (Cobb et al., 2016). Furthermore, summer fog is a crucial factor that drives redwood distribution; long term measurements showed a 33% reduction in summer fog frequency over the California coast in the last century, it was suggested that

redwoods (and other coastal species) have, and will continue to be increasingly drought-stressed in the future due to greater evaporative demand (Johnstone and Dawson, 2010). Despite aforementioned climatic vulnerabilities of redwood forests (Johnstone and Dawson, 2010; Metz et al., 2013); soil respiration under redwoods was well buffered from climactic extremes in comparison to nearby grasslands, attributed to the stable microclimate found beneath the canopy (Sanderman and Amundson, 2010).

Consideration of soil impacts from climate induced stresses is important to future management of the diverse ecosystems in California. Large-scale budgeting of C in forest ecosystems in response to climatic stress (Forest Climate Action Team, 2018) would be improved if impacts to soil C were included.

In keeping with our original intention under objective 5, to "explore interpretations" of SOC pools, we applied the POXC densities towards species extent projections found in the California Forest Carbon Plan (Forest Climate Action Team, 2018; Appendix P) for demonstrative purposes, exclusively. Values in this table necessarily assumed average POXC densities from our redwood populations were applicable across the entire redwood range. The purpose of this exercise was to provide an example of how soil data can be included in efforts to budget forest C (such as projected impacts under future climate scenarios) and was not meant to provide an authoritative estimate of expected changes to soil C in this ecosystem. In reiteration, our efforts to communicate information regarding active quantities of SOC in ways relevant to management would be more informative had we measured a pool of SOC with a particular stabilization mechanism attached.

6.5 Future research, considerations and improvements to the project

6.5.1 Methods and mensuration

One way these efforts would be improved is through a measurement of calcium carbonate (for determination of SOC from total C) that is non-approximated, as were our values (see "Soil Organic Carbon and Total Nitrogen" under "Description of Laboratory procedures" in Chapter 4; and Appendix F, Eq. 12-14). Calcium carbonate can be determined using the 3 *N* HCl and monometer method (Chapter 4E; Rebecca Burt and Soil Survey Staff, 2014).

As mentioned earlier, densities used for stocks were determined with bulk density values of each horizon (see "Stock calculation for SOC and POXC" in Chapter 4). The SOC and POXC stocks provided in this document (Table 5.3) would be more accurate with a more complete dataset of bulk density values. The collection of soil cores (used for bulk density determination) was compromised when a soil horizon had rock fragments ("Missing bulk density values" in Chapter 4); in these instances, an estimate of bulk density was created using data from adjacent horizons (Appendix J). A method of bulk density collection in the field that is less impacted by rock fragments would improve the accuracy of SOC and POXC stocks we provided.

Another recommendation is to measure a pool of SOC more clearly associated with a particular stabilization mechanism(s) than POXC, in this way, insights to differences in pools of SOC between communities (like the differences we observed in POXC/SOC between locations and ecologies; Table 5.1 and Figures 5.6-5.8) may be more easily explained. Given what's known about the origins of accumulation and mechanisms for stabilization of mineral associated organic C and particulate organic

matter (Cotrufo et al., 2015, 2019; Sokol and Bradford, 2019)- these two pools are promising measurements to those interested in monitoring changes to SOC in response to efforts to sequester soil C in the forests and rangelands we studied. Additionally, given proposed mechanisms of DOC dynamics with depth in redwood and grassland settings (Sanderman et al., 2008), an investigation of this pool could be helpful from a mechanistic perspective.

One thought to improve the study design, would be to have the number of observations more balanced between the locations we compared. At SPR, we dug 28 pits dug (102 horizons) and at LHCR, we dug 15 pits (56 horizons), this was due to time and budgetary constraints.

6.5.2 Aspect and its effect on the study regions

Aspect is an important factor influencing soil formation and was recorded at each site where soil was collected, however, it was not included in the regression models as an explanatory variable.

At a lager level, the positioning of redwood stands and grassland in the landscapes we studied is somewhat aspect driven. In San Vicente Creek (the overall basin where our soils were collected from in LHBCR) redwood positioning is in more of a broadcast pattern on the north-facing slopes when compared to the south; these north-facing slopes were across the valley from the incised, south-facing drainage where we investigated redwood soils. Contrastingly, in San Vicente Creek, and as a general trend in Big Sur, grasslands are found on south-facing slopes and often in association with yucca shrublands. At SPR, the topography is different than in Big Sur, and the effect of aspect on redwood and grassland distribution is less formulaic (Kenny, 2020).

Given the amount of micro-topographic variations we observed in the landscapes we collected soil from, and given that aspect was measured on a profile-level (i.e. “What was the aspect of the site within a few meters?”) and not on a landscape-level, we did not expect aspect to be important enough to include in the regression model.

6.5.3 Seasonal considerations

It is reasonable to assert that, across ecosystems, soils exhibit temporal changes as a reflection of environmental conditions, and these changes in the environment can occur on various time scales (e.g. isolated weather events, seasons, and long-term decadal changes). One phenomenon not incorporated into this study, was how sampling time may have influenced the results. We sampled in the spring of 2018 and 2019, as well as the summer of 2019 for the transect study.

Generally speaking, there are certain soil properties of which we can expect changes to as the result of a weather event (e.g. soil moisture content, soil temperature, soil respiration, and dissolved organic C levels). Similarly, it is reasonable to assume that there can be seasonal response and temporal changes in soil properties of a given ecosystem. Within the suite of soil properties measured in this study, we did not expect seasonality to play a powerful role on our observations, that is not to say we don’t acknowledge the fact that seasons could have impacted the observations made in the redwood forest and grasslands we studied. A study on seasonal fluctuations in SOC (Wuest, 2014) serves to remind and clarify-that our findings (particularly those related to SOM) are relevant only to the spring and summer seasons of the year we collected data in- and they are limited, in that they fail represent data collected from more than one season.

Nonetheless, the climate of redwood forest, when compared to other coniferous forests, is relatively stable. For example, there is no snow and the soil moisture and temperatures are not dramatically different in the coolest and driest months. The Mediterranean climate of the California coast generally produces most rainfall in the winter months, and this, in conjunction with the fog-belt influence on redwood distribution serves to maintain localized moisture year-long, while adjacent inland habitats experience drying conditions in the summertime. As the climate in the redwood canopy is not particularly seasonal, so can be said about the soil organic matter inputs. Being that redwood stands and the adjacent canopies are predominantly evergreen (*Umbellularia californica*, *Notholithocarpos densiflorus, Pseudotsuga menziesii*) with occasional deciduous buckeye (*Aesculus californica)* and big leaf maple *(Acer macrophyllum*), it is reasonable to expect that pools of soil carbon representative of litterfall (e.g. POM) are relatively unimpacted by the seasons in this ecosystem.

In the grasslands we studied, flora was dominated by Euro-Asian exotics that die in the summer. Since SOM inputs in grasslands are dominated by roots (as opposed to litterfall), seasonal trends of organic matter in the grasslands would be most influenced by seasonal behavior of the rhizophore (Sanderman et al., 2008). The extent to which the rhizosphere had seasonal impacts on the soil properties we studied is outside the scope of this project. In sum, we expect any seasonal impacts on our soils to be more identifiable in the grasslands than in the redwood forest because of the plant life-cycles in those ecosystems.

6.5.4 Disturbances

Sudden oak death and pine pitch canker are two diseases that threaten forests on the Central Coast of California and with impacts to Tan Oak and Monterey Pine species, respectively (Meentemeyer et al., 2008; Loe, 2010). These tree species were not components of the redwood or grassland communities we studied but were present in the mixed evergreen forest (and adjacent ecotones) in the transect study (objective 3) at SPR (Appendix A). We did not consider the effect of forest disease in our study; future efforts to study forest soil on the Central Coast of California should consider the impact of disease.

Grazing is a disturbance relevant to the grasslands at SPR. Outside of a holistic management approach, we were not clear on specific historical management (e.g. grazing densities) implemented on the pastures we collected soil from. Such knowledge of grazing history for each pasture (and a better understanding of grassland resilience to grazing disturbance) may have benefitted insights to our belowground observations; it will certainly serve to improve future research in these grassland soils.

6.5.5 Wildfires of 2020

Prior to August 2020, the most recent fire in our study sites was the 2009 Lockheed fire that burned 90% of the Little Creek watershed within SPR (the next most recent fire in our study areas was the 1999 Kirk Complex fire in Big Sur). The impact of fire history was not incorporated into the design of this study, but it is reasonable to assert that the soil we collected in 2018 from sites burned in 2009, may have had exhibited lingering effects from the fire (e.g. increased charcoal content).

More recently, since the writing stage of this project began (after the design and empirical implementation of this project were completed), an unprecedented episode of heat and dry lighting swept the North American West in August 2020. Aptly named the "August Siege of 2020", this surge incurred over 900 individual fires in a month's span (Hansen, 2020). Of these fires, the CZU Lightning Complex (86,500 acres in the Santa Cruz Mountains) burned almost the entirety of SPR (save for limited areas of the coastal terraces and lower Scotts Creek), and the Dolan fire (125,000 acres in the Santa Lucia Mountains, caused by arson) burned almost the entirety of LHBCR (CalFire, 2021; InciWeb, 2021). The wildfires of 2020 will unquestionably impact efforts to understand these ecosystems in the immediate future; any efforts to incorporate the findings of this study (such as our C stocks) will be complicated by these recent fires. While there is potential to utilize the information gathered in this study (for example, to estimate losses of SOC form fire), perhaps 2020 marks more of blank slate, for a new baseline, as these landscapes respond and reestablish their ecologies.

6.5.6 Soil flora and fauna

Considering the floristic diversity in the regions we collected soil from, a look at the diversity of soil organisms in these regions would be interesting. The scale of such research could range from efforts to study the microbial communities, up in size, to mammalian interactions with the soil ecosystem, for example.

6.5.7 Ultisols of the redwoods

Last, just north of SPR (near the Santa Cruz-San Mateo county line), soil map units beneath redwoods shift from predominantly Mollisols to Utilsols, an investigation of said soils could provide an interesting comparison to the soils in this study. In

particular, it would be interesting to look at base cation levels in the mineral soil and forest litter beneath these redwoods, as to investigate said geographic shift in soil map unit classification.

CHAPTER 7

Conclusion

As greenhouse gas emissions continue to rise at an unprecedented rate, the sequestration of C in the soil is of increasing concern to the global community. Because soils offer a range of ecosystem services, efforts to restore and increase soil C should consider soils intrinsically capable at C retention. Undisturbed old growth coast redwood forests in California contain the highest aboveground biomass per acre of any ecosystem in the world (Van Pelt et al., 2016), but the extent to which C is retained in the soil of these same systems is not well understood. The presence of mollic epipedons in the southern coast redwoods provided an opportunity to compare C pools in adjacent yet contrasting communities: one community generally understood as conducive to mollic formation (grasslands) with the other community (coniferous forest) representing more of an exception to the distribution of mollic epipedons.

This study aimed to collect baseline data for a relatively unexplored soil community (soil beneath the coast redwood forest of Central California) in an effort to provide insights into soil properties and implications for C management. The objectives of this study were fivefold: (i) to gather baseline data for mollic soils in the redwood forest and compare this with adjacent grassland communities, (ii) to identify the taxonomic classifications of said soils, (iii) to investigate the influence of localized vegetative gradation on soil properties, (iv) to investigate the relationship of basic cation levels in the forest floor and those in the mineral soil, and (v) to characterize total SOC and active soil C pools in redwood forest and grassland ecosystems, and to explore the interpretations of these pools.

Under objective 1, we used samples of horizons collected from randomized profiles (up to 1.5 m in depth) in redwood forest and grassland communities on the Central Coast of California, and when potential influences of soil formation (depth, vegetation, slope, and horizon type) and associated interactions (depth*slope, veg*slope, veg*depth) were included in a multivariate regression model-we found higher values of pH, C/N, and CEC in redwood soils than in grasslands, and lower values of bulk density in redwoods than in grasslands; these trends were ubiquitous across both locations.

Of all the profiles we classified for objective 2, none failed to meet mollic requirements because of low SOC. In general, we found that redwood profiles were conducive to mollic formation and maintained base saturation above 50% through soil depth. At Swanton Pacific Ranch, we classified more Mollisols in the redwoods (15 of 16 profiles as Mollisols) than in the grasslands (3 of 12 profiles as Mollisols). At Landels-Hill Big Creek Reserve, the spread was more even, with 6 of 8 profiles as Mollisols in the redwoods and all of the 7 profiles as Mollisols in the grasslands.

Under objective 3, univariate regression models provided evidence for a significant relationship between cation levels in the organic material of redwood litter and cation levels in the mineral surface for Ca, Mg, and Na. Calcium was generally the largest cation contributor to total basic charge on soil exchange sites (at least 58%, of the contribution to basic charge, on average, for redwood and grassland horizons at both study locations).

Under objective 4, a multivariate regression model to investigate soil properties along five transects at SPR returned generally consistent and graded patterns for C/N ratios, POXC/SOC ratios, and pH; these variables were generally highest in the redwood

forest and decreased sequentially across the vegetative gradients through mixed-evergreen forest and into the grassland; this was consistent across the three depth-intervals. Said patterns observed in the transects also conformed to our comparisons of C/N, POXC/SOC, and pH from redwood and grassland profiles at SPR.

Observations made under objective 5 provided the main discussion. Permanganate oxidizable C has been labeled as a pool of SOC that is sensitive to release from changes in management, and has been used commonly in recent studies (Culman et al., 2012; USDA-NRCS, 2014; Hurisso et al., 2016). One novelty imparted in this study was focused investigation towards the fraction of SOC that was POXC, as opposed to evaluation of the POXC pool alone. The POXC pool increases with total SOC (Tirol-Padre and Ladha, 2004a; Skjemstad et al., 2006a; USDA-NRCS, 2014; Romero et al., 2018), thus, comparisons of POXC to SOC ratios provided an opportunity to evaluate grassland and redwood populations with deeper insight.

Across two locations, dissimilar trends were observed between redwood and grassland communities for the POXC fractions of the SOC pools. At LHBCR, the regression model provided no evidence for a difference in POXC/SOC ratios between redwood and grassland horizons, however, at SPR, redwood horizons had significantly higher fractions of POXC than in the grasslands. Data from the transect study at SPR corroborated these findings and indicated POXC/SOC ratios generally decreased across a redwood forest to grassland vegetative gradient. Furthermore, in the profiles, we found that the way in which depth impacted POXC/SOC fractions was influenced by plant community.

Observed differences in POXC fractions were postulated as the result of contrasting SOM inputs between plant communities, and differences in locations may have been influenced by different management strategies or disturbance, however, the data collected in this study does not provide clear mechanisms to explain these discrepancies, and further research is needed.

Disharmonious interpretations of POXC across the literature (Tirol-Padre and Ladha, 2004b; Culman et al., 2012; Hurisso et al., 2016; Romero et al., 2018) suggested that the replacement of operationally defined C fractions (e.g. POXC) with fractions tied to a particular stabilization mechanism (e.g. particulate organic carbon; mineral associated organic matter) would provide clearer insights across ecosystems to land managers. Our findings maintained this lack of clarity associated with the POXC pool, and after attempting to describe the observations of POXC/SOC in our study, we recommend future avoidance of POXC measurement, and instead, to focus on other pools of SOC with a particular stabilization mechanism attached.

Nonetheless, outside of one large-scale, poorly constrained effort to estimate C stocks for each forest type in California (Christensen et al., 2018; Forest Climate Action Team, 2018), we are unaware of another peer-reviewed study that has quantified fractionated pools of SOC beneath the redwood forest, let alone, one that has provided stocks of SOC for specific localities. While we did not test any management strategies, we are curious to see how the data we collected on the California Central Coast can inform future studies that may one day impact decisions for soil management. The carbon densities provided in this study can be used as a baseline to measure changes in SOC and POXC pools in response to any future activities to sequester C in our study regions (e.g.

application of compost and green waste amendments over wildlands, changes to grazing strategies or no grazing at all, application of mulch over wildlands from fuels reduction projects, native spore dispersal and integration of commercial mushroom foraging in wildlands, etc.); the "living laboratory" atmosphere at SPR provides an excellent platform to experiment with innovative and interdisciplinary land management activities. This data can also be used to assess losses of soil C released from the recent 2020 wildfires in the ecosystems we studied.

In the United States (as for many signatory to the United Nations Framework Convention on Climate Change), SOC inventories have been generated and reported through model predictions that use estimated values from state-wide databases. These values represent averages over large land areas (map units) and are not expected to provide accurate estimates of SOC for specific locations (Domke et al., 2017). Better accounting of soil C pools within the diverse ecosystems of California will be important for potential integration of soil management with state policies or cap and trade markets.

The most successful example of a system that, amongst incentivizing emissions reductions, provided direct compensation to land managers for each ton of CO_2 equivalent sequestered in the soil (i.e. C farming) was the Chicago Climate Exchange (operational from 2003-2010; Lal et al., 2007; Lal, 2008; DiPerna, 2018). Unfortunately, members of the Chicago Climate Exchange decided to discontinue operations with the failed passage of the American Clean Energy and Security Act in 2010 (DiPerna, 2018).

As the atmosphere becomes increasingly C abundant, the message to land managers to sequester C in the soil will need to reach beyond those currently involved. As of now, California provides sponsorship over startup costs to those willing to engage,

voluntarily, in practices shown to increase soil C drawdown. This incentive has only reached landowners who were already educated and/or concerned about the state of the atmosphere. The challenge of budgeting and understanding C pools is apparent at the governmental level: the California Forest Carbon Plan (Forest Climate Action Team, 2018) failed to provide convincing belowground C stocks- given the intricacy of soil C and given the lack of soils detail provided in the document and its focus on trees. Perhaps one day, stringent policy measures or monetary motivations to promote C drawdown in soils will become more relevant and cost-effective enough to reach greater swaths of land. At the forefront of all of this, soils data needs to be collected on the diverse ecosystems we, as a society, look to manage into the future.

While redwood forests are commonly associated with their ability to provide habitat and grow (i.e. retain biomass C) to unparalleled heights, we demonstrated that this forest type is also capable of harboring considerable amounts of C in the soil-so much so, that in our study region, most of the profiles beneath the redwoods were classified as mollic, which is a unique taxonomic finding. Our estimates of SOC in the top 1 m of soil showed redwood soils stored as much or more C than soils in the neighboring grasslands, at SPR, 144 (± 21) and 123 (± 25) tons SOC per ha in the top 1 m of redwoods and grasslands, respectively, and at LHBCR, 221 (± 23) and 126 (± 24) tons SOC per ha in the top 1 m of redwoods and grasslands, respectively. The breadth of information gathered in this study serves as a testament to the little we still know about the soils comprising the land we manage, and how each set of questions that are investigated provide refinement for following questions that will hopefully one day, direct considerate and conscientious management in response to the environmental challenges ahead.

REFERENCES

Appel, C., and C. Stubler. 2018. SS 423 Soil and Water Chemistry Laboratory Manual. 11th ed. California State Polytechnic University of San Luis Obispo.

Auten, S.R. 2012. Mortality assessment of redwood and mixed conifer forest types in Santa Cruz County following wildfire. doi: 10.15368/theses.2012.200.

Bakeman, M.E. 1983. Genesis of Mollisols under Douglas-fir. Univeristy Mont. Grad. Student Theses, Diss. Prof. Pap. http://scholarworks.umt.edu/etd.

Bickford, C., and P. Rich. 1984. Vegetation and flora of the Landels-Hill Big Creek Reserve, California. (M Brown, Ed.). 2nd ed. Univerity of California, Santa Cruz: Environmental Field Program.

Big Creek Lumber Co. 1991. Forest Managment Plan for the Swanton Pacific Ranch.

Birdsey, R.A. 1992. Carbon storage and accumulation in United States forest ecosystems.

Bockheim, J.G. 2014. Mollic Epipedon. p. 29–46. *In* Soil Geography of the USA. Springer International Publishing, Cham.

Brabb, E.E. 1989. Geologic Map of Santa Cruz County, California.

Brian C. Dietterck, A. Thulin, L. Leetham, and C. Villa. 2020. Swanton Pacifc Ranch Managment Plan.

Burgess, S.S.O., and T.E. Dawson. 2004. The contribution of fog to the water relations of Sequoia sempervirens (D. Don): Foliar uptake and prevention of dehydration. Plant, Cell Environ. 27(8): 1023–1034. doi: 10.1111/j.1365-3040.2004.01207.x.

CalFire. 2021. Cal Fire CZU Fire Damage Information. https://www.arcgis.com/apps/webappviewer/index.html?id=5461c7f372e24ab68ca386e73d58e35a (accessed 2 February 2021).

California Air Resources Board. 2019. California greenhouse gas 2000 to 2017 emissions, trends, and indicators report.

California Air Resources Board. 2021. Auction Notices and Reports. https://ww2.arb.ca.gov/our-work/programs/cap-and-trade-program/auction-information/auction-notices-and-reports (accessed 10 March 2021).

Capital Public Radio. 2019. A History of California Wildfires. https://projects.capradio.org/california-fire-history/#5.6/37.314/-122.645.

Christensen, G.A., A.N. Gray, O. Kuegler, N.A. Tase, M. Rosenberg, D. Loeffler, N. Anderson, K. Stockmann, and T.. Morgan. 2018. AB 1504 California Forest Ecosystem and Harvested Wood Product Carbon Inventory: 2017 Reporting Period. Final Report. Sacramento, California.

Climate Policy Initiative. 2019. California Carbon Dashboard: Carbon Prices, the Latest News, and California Policy. http://calcarbondash.org/ (accessed 24 February 2019).

Cobb, R.C., R.K. Meentemeyer, and D.M. Rizzo. 2016. Wildfire and forest disease

interaction lead to greater loss of soil nutrients and carbon. Oecologia 182(1): 265–276. doi: 10.1007/s00442-016-3649-7.

Cotrufo, M.F., M.G. Ranalli, M.L. Haddix, J. Six, and E. Lugato. 2019. Soil carbon storage informed by particulate and mineral-associated organic matter. Nat. Geosci. 12(12): 989–994. doi: 10.1038/s41561-019-0484-6.

Cotrufo, M.F., J.L. Soong, A.J. Horton, E.E. Campbell, M.L. Haddix, D.H. Wall, and W.J. Parton. 2015. Formation of soil organic matter via biochemical and physical pathways of litter mass loss. Nat. Geosci. 8(10): 776–779. doi: 10.1038/ngeo2520.

Cotrufo, M.F., M.D. Wallenstein, C.M. Boot, K. Denef, and E. Paul. 2013. The Microbial Efficiency-Matrix Stabilization (MEMS) framework integrates plant litter decomposition with soil organic matter stabilization: do labile plant inputs form stable soil organic matter? Glob. Chang. Biol. 19(4): 988–995. doi: 10.1111/gcb.12113.

Culman, S., M. Freeman, and S. Snapp. 2014. Procedure for the Determination of Permanganate Oxidizable Carbon. Hickory Corners, MI.

Culman, S.W., S.S. Snapp, M.A. Freeman, M.E. Schipanski, J. Beniston, R. Lal, L.E. Drinkwater, A.J. Franzluebbers, J.D. Glover, A.S. Grandy, J. Lee, J. Six, J.E. Maul, S.B. Mirksy, J.T. Spargo, and M.M. Wander. 2012. Permanganate oxidizable carbon reflects a processed soil fraction that is sensitive to management. Soil Sci. Soc. Am. J. 77(2): 494–504. doi: 10.2136/sssaj2011.0286.

DeLonge, M.S., R. Ryals, and W.L. Silver. 2013. A Lifecycle Model to Evaluate Carbon Sequestration Potential and Greenhouse Gas Dynamics of Managed Grasslands. Ecosystems 16(6): 962–979. doi: 10.1007/s10021-013-9660-5.

DiPerna, P. 2018. Pricing Carbon: Integrating Promise, Practice and Lessons Learned from the Chicago Climate Exchange. p. 115–148. *In* Designing a Sustainable Financial System. Springer International Publishing.

Domke, G.M., C.H. Perry, B.F. Walters, L.E. Nave, C.W. Woodall, and C.W. Swanston. 2017. Toward inventory-based estimates of soil organic carbon in forests of the United States. Ecol. Appl. 27(4): 1223–1235. doi: 10.1002/eap.1516.

Earth Systems Research Lab. 2019. Trends in atmospheric carbon dioxide. https://www.esrl.noaa.gov/gmd/ccgg/trends/global.html (accessed 5 February 2019).

Enloe, H.A., R.C. Graham, and S.C. Sillett. 2006. Arboreal Histosols in Old-Growth Redwood Forest Canopies, Northern California. Soil Sci. Soc. Am. J. 70(2): 408–418. doi: 10.2136/sssaj2004.0229.

Enloe, H.A., S.A. Quideau, R.C. Graham, S.C. Sillett, S.-W. Oh, and R.E. Wasylishen. 2010. Soil Organic Matter Processes in Old-Growth Redwood Forest Canopies. Soil Sci. Soc. Am. J. 74(1): 161–171. doi: 10.2136/sssaj2009.0031.

Ewing, H., K. Weathers, A.M. Lindsey, P. Templer, T. Dawson, D.C. Bradbury, M. Firestone, and V. Boukili. 2012. Fog and soil weathering as sources of nutrients in a California redwood forest. p. 265–272. *In* Proceedings of coast redwood forests in a

changing California: A symposium for scientists and managers. Pacific Southwest Research Station, Forest Service, U.S. Department of Agriculture, Albany, CA.

Federal Highway Administration. 2017. Licensed Drivers By Sex And Ratio To Population - 2015. Highw. Stat. Ser. https://www.fhwa.dot.gov/policyinformation/statistics/2015/dl1c.cfm (accessed 21 January 2021).

Follett, R.F. (Ronald F.., J.M. (John M.. Kimble, and R. Lal. 2001. The potential of U.S. grazing lands to sequester carbon and mitigate the greenhouse effect. Lewis Publishers.

Forest Climate Action Team. 2018. California Forest Carbon Plan: Managing Our Forest Landscapes in a Changing Climate. Sacramento, CA.

Georgette, S.E. 1981. In the Rough Land to the South: An Oral History of the Lives and Events at Big Creek, Big Sur, California. Univerity of California, Santa Cruz: Environmental Field Program.

Gill, R.A. 2007. Influence of 90 years of protection from grazing on plant and soil processes in the subalpine of the Wasatch Plateau, USA. Rangel. Ecol. Manag. 60(1): 88–98. doi: 10.2111/05-236R2.1.

Graven, H., C.E. Allison, D.M. Etheridge, S. Hammer, R.F. Keeling, I. Levin, H.A.J. Meijer, M. Rubino, P.P. Tans, C.M. Trudinger, B.H. Vaughn, and J.W.C. White. 2017. Compiled records of carbon isotopes in atmospheric CO 2 for historical simulations in CMIP6. Geosci. Model Dev 10: 4405–4417. doi: 10.5194/gmd-10-4405-2017.

Gulde, S., H. Chung, W. Amelung, C. Chang, and J. Six. 2008. Soil carbon saturation controls labile and stable carbon pool dynamics. Soil Sci. Soc. Am. J. 72(3): 605–612. doi: 10.2136/sssaj2007.0251.

Hansen, K. 2020. California Continues to Burn. Nasa Earth Obs. https://earthobservatory.nasa.gov/images/147215/california-continues-to-burn (accessed 2 February 2021).

Harrison, R.B., P.W. Footen, and B.D. Strahm. 2011. Deep soil horizons: Contribution and importance to soil carbon pools and in assessing whole-ecosystem response to management and global change. For. Sci. 57(1): 67–76. doi: 10.1093/forestscience/57.1.67.

Henson, P., and D.J. Usner. 1993. The Natural History of Big Sur. University of California Press.

Hublin, J.J., A. Ben-Ncer, S.E. Bailey, S.E. Freidline, S. Neubauer, M.M. Skinner, I. Bergmann, A. Le Cabec, S. Benazzi, K. Harvati, and P. Gunz. 2017. New fossils from Jebel Irhoud, Morocco and the pan-African origin of Homo sapiens. Nature 546(7657): 289–292. doi: 10.1038/nature22336.

Hurisso, T.T., S.W. Culman, W.R. Horwath, J. Wade, D. Cass, J.W. Beniston, T.M. Bowles, A.S. Grandy, A.J. Franzluebbers, M.E. Schipanski, S.T. Lucas, and C.M.

Ugarte. 2016. Comparison of permanganate-oxidizable carbon and mineralizable carbon for assessment of organic matter stabilization and mineralization. Soil Sci. Soc. Am. J. 80(5): 1352–1364. doi: 10.2136/sssaj2016.04.0106.

Huston, M.A., and G. Marland. 2003. Carbon management and biodiversity. J. Environ. Manage. 67(1): 77–86. doi: 10.1016/S0301-4797(02)00190-1.

InciWeb. 2021. Dolan Fire Information. https://inciweb.nwcg.gov/incident/7018/ (accessed 2 February 2021).

Intergovernmental Panel on Climate Change. 2013. Annex III: glossary. p. 1447–1565. *In* Planton, S. (ed.), Climate change 2013: the physical science basis. contribution of working group I to the fifth assessment report of the intergovernmental panel on climate change. Intergovernmental Panel on Climate Change, Cambridge University Press, Cambridge, United Kingdom and New York, NY, USA.

Intergovernmental Panel on Climate Change. 2014. Climate change 2014 synthesis report. Contribution of working groups I, II and III to the fifth assessment report of the intergovernmental panel on climate change (Core Writing Team; R.K. Pachauri and L.A. Meyer, Ed.). Geneva, Switzerland.

Jandl, R., M. Rodeghiero, C. Martinez, M.F. Cotrufo, F. Bampa, B. van Wesemael, R.B. Harrison, I.A. Guerrini, D. de B. Richter, L. Rustad, K. Lorenz, A. Chabbi, and F. Miglietta. 2014. Current status, uncertainty and future needs in soil organic carbon monitoring. Sci. Total Environ. 468–469: 376–383. doi: 10.1016/j.scitotenv.2013.08.026.

John Hardy. 2017. Spatiotemporal variability in the macroinvertebrate community of a small coastal California stream, Little Creek, Davenport, California.

Johnstone, J.A., and T.E. Dawson. 2010. Climatic context and ecological implications of summer fog decline in the coast redwood region. Proc. Natl. Acad. Sci. U. S. A. 107(10): 4533–4538. doi: 10.1073/pnas.0915062107.

Keeley, J.E. 2002. Native American impacts on fire regimes of the California coastal ranges. J. Biogeogr. 29(3): 303–320. doi: 10.1046/j.1365-2699.2002.00676.x.

Kelleher, B.P., and A.J. Simpson. 2006. Humic substances in soils: Are they really chemically distinct? Environ. Sci. Technol. 40(15): 4605–4611. doi: 10.1021/es0608085.

Kenny, R. 2020. A Floristic Study of the Cal Poly Swanton Pacific Ranch and a New Combination in Sanicula crassicaulis (Apiaceae), Sanicula crassicaulis var. nudicaulis.

Lal, R. 2004a. Soil carbon sequestration impacts on global climate change and food security. Science 304(5677): 1623–1627. doi: 10.1126/science.1097396.

Lal, R. 2004b. Soil carbon sequestration to mitigate climate change. Geoderma 123: 1–22. doi: 10.1016/j.geoderma.2004.01.032.

Lal, R. 2005. Forest soils and carbon sequestration. For. Ecol. Manage. 220(1–3): 242–

258. doi: 10.1016/J.FORECO.2005.08.015.

Lal, R. 2007. Carbon management in agricultural soils. Mitig. Adapt. Strateg. Glob. Chang. 12(2): 303–322. doi: 10.1007/s11027-006-9036-7.

Lal, R. 2008. Soils and sustainable agriculture. A review. Agron. Sustain. Dev. 28(1): 57–64. doi: 10.1051/agro:2007025.

Lal, R., R.F. Follett, B.A. Stewart, and J.M. Kimble. 2007. Soil carbon sequestration to mitigate climate change and advance food security. Soil Sci. 172(12): 943–956. doi: 10.1097/ss.0b013e31815cc498.

Lehmann, J., and M. Kleber. 2015. The contentious nature of soil organic matter. Nature 528(7580): 60–68. doi: 10.1038/nature16069.

Lehmann, J., D. Solomon, J. Kinyangi, L. Dathe, S. Wirick, and C. Jacobsen. 2008. Spatial complexity of soil organic matter forms at nanometre scales. Nat. Geosci. 1(4): 238–242. doi: 10.1038/ngeo155.

Liu, X., C. Lee Burras, Y.S. Kravchenko, A. Duran, T. Huffman, H. Morras, G. Studdert, X. Zhang, R.M. Cruse, and X. Yuan. 2012. Overview of Mollisols in the world: Distribution, land use and management. Can. J. Soil Sci. 92(3): 383–402. doi: 10.4141/cjss2010-058.

Loe, V.A. 2010. Management Strategies for Pitch Canker Infected Año Nuevo Stands of Monterey Pine.

Loganbill, A.W. 2013. Post-fire Response of Little Creek Watershed: Evaluation of Change in Sediment Production and Suspended Sediment Transport. Master's Theses. doi: 10.15368/theses.2013.68.

Lorenz, K., and R. Lal. 2018. Soil carbon stock. p. 39–136. *In* Carbon sequestration in Agricultural Ecosystems. Springer International Publishing, Cham.

Lützow, M. V., I. Kögel-Knabner, K. Ekschmitt, E. Matzner, G. Guggenberger, B. Marschner, and H. Flessa. 2006. Stabilization of organic matter in temperate soils: Mechanisms and their relevance under different soil conditions - A review. Eur. J. Soil Sci. 57(4): 426–445. doi: 10.1111/j.1365-2389.2006.00809.x.

Marfo, T., R. Datta, S. Pathan, and V. Vranová. 2019a. Ecotone Dynamics and Stability from Soil Scientific Point of View. Diversity 11(4): 53. doi: 10.3390/d11040053.

Marfo, T.D., R. Datta, V. Vranová, and A. Ekielski. 2019b. Ecotone Dynamics and Stability from Soil Perspective: Forest-Agriculture Land Transition. Agriculture 9(10): 228. doi: 10.3390/agriculture9100228.

Margolin, M. 1978. The Ohlone Way. Heyday, Berkeley, California.

Meentemeyer, R.K., N.E. Rank, D.A. Shoemaker, C.B. Oneal, A.C. Wickland, K.M. Frangioso, and D.M. Rizzo. 2008. Impact of sudden oak death on tree mortality in the Big Sur ecoregion of California. Biol. Invasions 10(8): 1243–1255. doi: 10.1007/s10530-007-9199-5.

Metz, M.R., J.M. Varner, K.M. Frangioso, R.K. Meentemeyer, and D.M. Rizzo. 2013.

Unexpected redwood mortality from synergies between wildfire and an emerging infectious disease. Ecology 94(10): 2152–2159. doi: 10.1890/13-0915.1.

Miller, R.O., R. Gavlak, and D. Horneck. 2013. Soil, Plant, and Water Reference Methods for the Western Region, 4th Ed.

Mooney, S., J. Antle, S. Capalbo, and K. Paustian. 2004. Influence of project scale and carbon variability on the costs of measuring soil carbon credits. Environ. Manage. 33(1): S252–S263. doi: 10.1007/s00267-003-9135-0.

National Interagency Fire Center. 2020. Historically Significant Wildland Fires. https://www.nifc.gov/fireInfo/fireInfo_stats_histSigFires.html (accessed 8 February 2021).

Natural Resource Conservation Service. 2020. Henry Mount Soil Temperature and Water Database. http://soilmap2-1.lawr.ucdavis.edu/henry/ (accessed 26 July 2020).

Niebrugge, L.K. 2012. Assessment of Site and Soil Characteristics of Rill Erosion Following the Lockheed Fire in the Little Creek Watershed, Swanton Pacific Ranch. doi: 10.15368/theses.2012.108.

NOAA: ESRL-Global Monitoring Division Laboratory. 2020. Stable and Radiocarbon Isotopes of Carbon Dioxide. https://www.esrl.noaa.gov/gmd/outreach/isotopes/c14tracer.html (accessed 11 February 2020).

Norris, R. 1985. Geology of the Landels-Hill Big Creek Reserve.

Noss, R.F. 2000a. Chapter 3. Characteristics of Redwood Forests. p. 39–81. *In* The Redwood Forest: History, Ecology, and Conservation of the Coast Redwoods. Island Press, Washington, D.C. and Covelo, CA.

Noss, R.F. 2000b. Chapter 4. Redwood Trees, Communities, and Ecosystems. p. 81–119. *In* The Redwood Forest: History, Ecology, and Conservation of the Coast Redwoods. Washington, D.C. and Covelo, CA.

Noss, R.F. 2000c. No Title. p. xii–xxiii. *In* The Redwood Forest: History, Ecology, and Conservation of the Coast Redwoods.

Orgiazzi, A., R.D. Bardgett, E. Barrios, V. Behan-Pelletier, M.J.I. Briones, J.-L. Chotte, G.B. De Deyn, P. Eggleton, N. Fierer, T. Fraser, K. Hedlund, S. Jeffery, N.C. Johnson, and A. Jones. 2016a. Geographic and temporal distribution. *In* Global Soil Biodidveristy Atlas. European Commission Joint Research Centre and the Global Soil Biodiversity Initiative.

Orgiazzi, A., R.D. Bardgett, E. Barrios, V. Behan-Pelletier, M.J.I. Briones, J.-L. Chotte, G.B. De Deyn, P. Eggleton, N. Fierer, T. Fraser, K. Hedlund, S. Jeffery, N.C. Johnson, and A. Jones. 2016b. Global Soil Biodidveristy Atlas.

Owen, J.J., W.J. Parton, and W.L. Silver. 2015. Long-term impacts of manure amendments on carbon and greenhouse gas dynamics of rangelands. Glob. Chang. Biol. 21(12): 4533–4547. doi: 10.1111/gcb.13044.

Parker, T.C., J. Subke, and P.A. Wookey. 2015. Rapid carbon turnover beneath shrub and tree vegetation is associated with low soil carbon stocks at a subarctic treeline. Glob. Chang. Biol. 21(5): 2070–2081. doi: 10.1111/gcb.12793.

Parolari, A.J., and A. Porporato. 2016. Forest soil carbon and nitrogen cycles under biomass harvest: Stability, transient response, and feedback. Ecol. Modell. 329: 64–76. doi: 10.1016/j.ecolmodel.2016.03.003.

Patterson, C. 1956. Age of meteorites and the earth. Geochim. Cosmochim. Acta 10(4): 230–237. doi: 10.1016/0016-7037(56)90036-9.

Pearson, T., S. Brown, and R. Birdsey. 2007. United States Department of Agriculture Measurement Guidelines for the Sequestration of Forest Carbon. Newtown Square, PA.

Van Pelt, R., S.C. Sillett, W.A. Kruse, J.A. Freund, and R.D. Kramer. 2016. Emergent crowns and light-use complementarity lead to global maximum biomass and leaf area in Sequoia sempervirens forests. For. Ecol. Manage. 375: 279–308. doi: 10.1016/j.foreco.2016.05.018.

Pillers, M.D., and J.D. Stuart. 1993. Leaf-litter accretion and decomposition in interior and coastal old-growth redwood stands. Can. J. For. Res. 23(3): 552–557. doi: 10.1139/x93-073.

Popenoe, J.H., K.A. Bevis, B.R. Gordon, N.K. Sturhan, and D.L. Hauxwell. 1992. Soil-Vegetation Relationships in Franciscan Terrain of Northwestern California. Soil Sci. Soc. Am. J. 56(6): 1951. doi: 10.2136/sssaj1992.03615995005600060050x.

Potter, C. 2012. Net primary production and carbon cycling in coast redwood forests of central California. Open J. Ecol. 02(03): 147–153. doi: 10.4236/oje.2012.23018.

Prentice, I.C., G.D. Farquhar, M.J.R. Fasham, M.L. Goulden, M. Heimann, V.J. Jaramillo, H.S. Kheshgi, C. Le Quéré, R.J. Scholes, D.W.R. Wallace, D. Archer, M.R. Ashmore, O. Aumont, D. Baker, M. Battle, M. Bender, L.P. Bopp, P. Bousquet, K. Caldeira, P. Ciais, P.M. Cox, W. Cramer, F. Dentener, I.G. Enting, C.B. Field, P. Friedlingstein, E.A. Holland, R.A. Houghton, J.I. House, A. Ishida, A.K. Jain, I.A. Janssens, F. Joos, T. Kaminski, C.D. Keeling, R.F. Keeling, D.W. Kicklighter, K.E. Kohfeld, W. Knorr, R. Law, T. Lenton, K. Lindsay, E. Maier-Reimer, A.C. Manning, R.J. Matear, A.D. Mcguire, J.M. Melillo, R. Meyer, M. Mund, J.C. Orr, S. Piper, K. Plattner, P.J. Rayner, S. Sitch, R. Slater, S. Taguchi, P.P. Tans, H.Q. Tian, M.F. Weirig, T. Whorf, and A. Yool. 2001. The carbon cycle and atmospheric carbon dioxide. p. 183–239. *In* Pitelka, L., Rojas, A.R. (eds.), Climate Change 2001: The Scientific Basis. Cambridge, United Kingdom.

Prescott, C.E. 2010. Litter decomposition: what controls it and how can we alter it to sequester more carbon in forest soils? Biogeochemistry 101(1–3): 133–149. doi: 10.1007/s10533-010-9439-0.

Raynaud, D., J. Jouzel, J.M. Barnola, J. Chappellaz, R.J. Delmas, and C. Lorius. 1993. The ice record of greenhouse gases. Science (80-.). 259(5097): 926–934. doi: 10.1126/science.259.5097.926.

Rebecca Burt and Soil Survey Staff. 2014. Kellogg Soil Survey Laboratory Methods Manual. Lincoln, Nebraska.

Reeder, J.D., and G.E. Schuman. 2002. Influence of livestock grazing on C sequestration in semi-arid mixed-grass and short-grass rangelands. p. 457–463. *In* Environmental Pollution. Elsevier.

Retallack, G.J. 2009. Greenhouse crises of the past 300 million years. Bull. Geol. Soc. Am. 121(9–10): 1441–1455. doi: 10.1130/B26341.1.

Retallack, G.J. 2013. Global Cooling by Grassland Soils of the Geological Past and Near Future. Annu. Rev. Earth Planet. Sci. 41(1): 69–86. doi: 10.1146/annurev-earth-050212-124001.

Riebeek, H. 2011. The carbon cycle. NASA-Earth Obs. https://earthobservatory.nasa.gov/features/CarbonCycle/page1.php (accessed 2 July 2019).

Romero, C.M., R.E. Engel, J. D'Andrilli, C. Chen, C. Zabinski, P.R. Miller, and R. Wallander. 2018. Patterns of change in permanganate oxidizable soil organic matter from semiarid drylands reflected by absorbance spectroscopy and Fourier transform ion cyclotron resonance mass spectrometry. Org. Geochem. 120: 19–30. doi: 10.1016/j.orggeochem.2018.03.005.

Rosenberg, L., and C.J. Wills. 2016. Preliminary Geologic Map of the Point Sur 30' x 60' Quadrangle, California.

Ryals, R., V.T. Eviner, C. Stein, K.N. Suding, and W.L. Silver. 2016. Grassland compost amendments increase plant production without changing plant communities (DPC Peters, Ed.). Ecosphere 7(3). doi: 10.1002/ecs2.1270.

Ryals, R., and W.L. Silver. 2013. Effects of organic matter amendments on net primary productivity and greenhouse gas emissions in annual grasslands. Ecol. Appl. 23(1): 46–59. doi: 10.1890/12-0620.1.

Sanderman, J., and R. Amundson. 2008. A comparative study of dissolved organic carbon transport and stabilization in California forest and grassland soils. Biogeochemistry 89(3): 309–327. doi: 10.1007/s10533-008-9221-8.

Sanderman, J., and R. Amundson. 2010. Soil Carbon Dioxide Production and Climatic Sensitivity in Contrasting California Ecosystems. Soil Sci. Soc. Am. J. 74(4): 1356–1366. doi: 10.2136/sssaj2009.0290.

Sanderman, J., J.A. Baldock, and R. Amundson. 2008. Dissolved organic carbon chemistry and dynamics in contrasting forest and grassland soils. Biogeochemistry 89(2): 181–198. doi: 10.1007/s10533-008-9211-x.

SAS Institute Inc. 2018. JMP 14 Fitting Linear Models. Cary, NC.

Save the Redwoods League. 2020. Coast Redwoods. https://www.savetheredwoods.org/redwoods/coast-redwoods/ (accessed 4 May 2020).

Scaramozzino, J.M. 2015. Una Legua Cuadrada: Exploring the History of Swanton Pacific Ranch and Environs. doi: 10.15368/theses.2015.170.

Schleussner, C.-F., J. Rogelj, M. Schaeffer, T. Lissner, R. Licker, E.M. Fischer, R. Knutti, A. Levermann, K. Frieler, and W. Hare. 2016. Science and policy characteristics of the Paris Agreement temperature goal. Nat. Publ. Gr. 6: 827–835. doi: 10.1038/NCLIMATE3096.

Schmidt, M.W.I., M.S. Torn, S. Abiven, T. Dittmar, G. Guggenberger, I.A. Janssens, M. Kleber, I. Kögel-Knabner, J. Lehmann, D.A.C. Manning, P. Nannipieri, D.P. Rasse, S. Weiner, and S.E. Trumbore. 2011. Persistence of soil organic matter as an ecosystem property. Nature 478(7367): 49–56. doi: 10.1038/nature10386.

Schoeneberger, P.J., D.A. Wysocki, E.C. Benham, and Soil Survey Staff. 2012. Field Book for Describing and Sampling Soils. 3.0. National Soil Survey Center, Lincoln, NE.

Schrag, D.P. 2007. Preparing to capture carbon. Science 315(5813): 812–813. doi: 10.1126/science.1137632.

Sequeira, C.H., S.A. Wills, C.A. Seybold, and L.T. West. 2014. Predicting soil bulk density for incomplete databases. Geoderma 213: 64–73. doi: 10.1016/j.geoderma.2013.07.013.

Silver, W.L., R. Ryals, and V. Eviner. 2010. Soil Carbon Pools in California's Annual Grassland Ecosystems. Rangel. Ecol. Manag. 63(1): 128–136. doi: 10.2111/REM-D-09-00106.1.

Skjemstad, J.O., R.S. Swift, and J.A. McGowan. 2006a. Comparison of the particulate organic carbon and permanganate oxidation methods for estimating labile soil organic carbon. Soil Res. 44(3): 255. doi: 10.1071/SR05124.

Skjemstad, J.O., R.S. Swift, and J.A. McGowan. 2006b. Comparison of the particulate organic carbon and permanganate oxidation methods for estimating labile soil organic carbon. Soil Res. 44(3): 255. doi: 10.1071/SR05124.

Smith, A. 1990. The History of Swanton - As told by Al Smith, July, 1990. https://spranch.calpoly.edu/mission (accessed 17 May 2020).

Soil Science Division Staff. 2017. Soil survey manual (C Ditzler, K Scheffe, and HC Monger, Eds.). USDA, Washington D.C.

Soil Survey Staff. 2014. Keys to soil taxonomy. 12th ed. USDA-NRCS, Washington, D.C.

Sokol, N.W., and M.A. Bradford. 2019. Microbial formation of stable soil carbon is more efficient from belowground than aboveground input. Nat. Geosci. 12(1): 46–53. doi: 10.1038/s41561-018-0258-6.

Srivastava, P., A. Kumar, S.K. Behera, Y.K. Sharma, and N. Singh. 2012. Soil carbon sequestration: an innovative strategy for reducing atmospheric carbon dioxide concentration. Biodivers. Conserv. 21(5): 1343–1358. doi: 10.1007/s10531-012-

0229-y.

State of California. 2019. Background-California Climate Investments. http://www.caclimateinvestments.ca.gov/about-cci (accessed 24 February 2019).

Stephenson, J.R., and G.M. Calcarone. 1999. Mountains and foothill ecosytems. p. 15–60. *In* Southern California mountains and foothills assessment: habitat and species conservation issues. Pacific Southwest Research Station, Albany, California.

Swanton Pacific Ranch. 2020a. About the Ranch. https://spranch.calpoly.edu/about (accessed 17 May 2020).

Swanton Pacific Ranch. 2020b. Ranch Operations: Livestock. https://spranch.calpoly.edu/livestock (accessed 17 May 2020).

Theobald, D. 2014. Evaluation of Red Alder Mortality in the Little Creek Watershed Following the 2009 Lockheed fire.

Tirol-Padre, A., and J.K. Ladha. 2004a. Assessing the reliability of permanganate-oxidizable carbon as an index of soil labile carbon. Soil Sci. Soc. Am. J. 68(3): 969–978. doi: 10.2136/sssaj2004.9690.

Tirol-Padre, A., and J.K. Ladha. 2004b. Assessing the Reliability of Permanganate-Oxidizable Carbon as an Index of Soil Labile Carbon_aaaaaaaaaa. Soil Sci. Soc. Am. J. 68(3): 969–978. doi: 10.2136/sssaj2004.9690.

UC Davis California Soil Resource Lab. 2018. SoilWeb: An Online Soil Survey Browser. https://casoilresource.lawr.ucdavis.edu/gmap/ (accessed 10 January 2019).

United States E.P.A. 2020. Greenhouse as Emissions: Understanding Global Warming Potentials. https://www.epa.gov/ghgemissions/understanding-global-warming-potentials (accessed 20 February 2020).

University of California at Santa Cruz. 2020. Landels-Hill Big Creek Natural Reserve. https://naturalreserves.ucsc.edu/our-reserves-infopages/big-creek-infopage/index.html (accessed 1 June 2020).

USDA-NRCS. 2014. Soil Quality Indicator Sheets: Reactive Carbon.

Waters, C.N., J. Zalasiewicz, C. Summerhayes, A.D. Barnosky, C. Poirier, A. Ga uszka, A. Cearreta, M. Edgeworth, E.C. Ellis, M. Ellis, C. Jeandel, R. Leinfelder, J.R. McNeill, D. d. Richter, W. Steffen, J. Syvitski, D. Vidas, M. Wagreich, M. Williams, A. Zhisheng, J. Grinevald, E. Odada, N. Oreskes, and A.P. Wolfe. 2016. The Anthropocene is functionally and stratigraphically distinct from the Holocene. Science (80-.). 351(6269): aad2622–aad2622. doi: 10.1126/science.aad2622.

West, J.A. 2016. Traversing Swanton Road.

Wolff, E.W. 2011. Greenhouse gases in the Earth system: a palaeoclimate perspective. Philos. Trans. R. Soc. A Math. Phys. Eng. Sci. 369(1943): 2133–2147. doi: 10.1098/rsta.2010.0225.

Wuest, S. 2014. Seasonal Variation in Soil Organic Carbon. Soil Sci. Soc. Am. J. 78(4): 1442–1447. doi: 10.2136/sssaj2013.10.0447.

APPENDICES

Appendix A: Plant community physiognomy of study areas

Redwood and grassland communities

Grasslands communities at both locations were dominated by annual exotic grasses and herbs, perennial species were less common.

There were limited recordings of sp. at LHBCR, but field notes and photos highlighted the presence of *Bromus deandrus, Stipa pulcra, Trifolium angustifoliam, Calystegia* sp., *Lupinus* sp. and *Eschosholzia californica* as common components of the community.

At SPR, the grasslands were more diverse in composition because they covered a larger land area. In the transect study we made detailed observations of grassland components in the upper rangeland zone, "Zone 3" which can be broadly be applied as an example of grasslands at SPR. Here, the community was primarily composed of annual invasive but some native perennials like *Junucus patens* occurred in areas near with a shallow water table. Throughout these grasslands there was tall woody patches of *Bacharis pilularis* in association with *Toxicodendron diversolum, Rubus ursinus, Conium maculatum* and mixed thistle species (e.g. *Carduous pycnocephalus, Silybum marianum*), however, for grassland sites we only sampled soils in open non-woody areas. Dominant exotics grass species (*Cynosurus echinatus, Bromus deandrus, Festuca perrenis, Bromus rubens, Hordeum murinum,* and *Avena* sp.,) formed an overstory up to several feet above the lower herbaceous flora (*Plantago lanceolata, Eurpapus lindelyii, Lysmachia aervensis, Trifolium* sp.*).*

Plant cover in forest floor of redwood understories varied across sites and ranged from sparse coverage to dense. Dominant species in redwood understories were similar across locations and included: *Polystichum munitum, Dryopteris arguta, Toxicondendron diversilobum, Oreganna oxalis, Rubus ursinus, Rubus parviflorus,* and *Ribes* sp. At the edge of the redwood canopy, the vigor of understory increased and *Aesculus californica* and *Umbellularia californica* were usually the first tree species to occur and created a continuous ladder into the taller canopy of *Pseudotsuga menziesii* in the mixed evergreen forest.

Communities along the transects

The transition of plant communities from discontinuous stands of *Sequoia sempervirens* into the coastal grasslands of SPR was longer in distance than we had anticipated.

From the gently sloped grasslands below Cooke's Peak on the upper rangelands of SPR, we positioned ourselves along the canopy edge (at ecotone of the mixed evergreen or coastal scrub communities). Here, *Baccharis pilularis* and *Toxicodendron diversilobum* were co-dominant species that formed boundaries, and sometimes trail networks to the outer edges of the range where the landscape began to bend downward and often coincided with a barbed wired fence. From these locations, we descended steep terrain into east-facing tributaries that drained down the western slopes of Scotts Creek At these locations we began to travel through brambles of *Toxicodendron diversilobum*

and *Rubus ursinus* that formed a vertically complex and horizontally continuous understory beneath mature *Pinus radiata* and *Pseudotsuga menziesii* mixed overstories. Under the canopy, masses of *Ramalina menziesii* were scattered about in drapery. In areas where the overstory was more sparse, there was more of a coastal scrub influence (*Toxicondendron diversilobum,* dominant, with *Artemesia californica, Frangula californica,* and *Pseudognaphalium* sp.*,* to name a few). On some transects, a patchy midstory of hardwoods (*Quercus agrifolia, Umbellularia californica, Notholithocarpus desniflorus*) occurred separately or concurrently below the conifers. Beneath the mixed forest, a thin organic horizon covered the mineral surface, and species composition of the canopy was reflected in the litter. On one transect we observed a chaparral community (*Arctostaphylos crustacea)* beneath *Pinus radiata*. In this location, the forest floor was dominated by pine needles and the soils were extremely rocky. As we moved further downslope, *Pseudotsuga menziesii* would begin to dominate towards the redwoods. When we found *Sequoia sempervirens,* they were located on the side slopes of canyons within a hundred feet of the watercourse. At the edge of the *Sequoia sempervirens* stands, *Umbellularia californica* and hugged the branch line and created arching ladders into the mixed evergreen forest. Beneath the redwoods, mineral soil was buried beneath a thick mat of redwood leaves and *Polystichum munitum, Dryopteris arguta, Toxicondendron diversilobum,* and *Rubus ursinus* were main understory constituents.

Appendix B: Data sheets for classification and regression modeling (see supplemental data in excel workbook)

Profiles

Soil classification sheet for 28 profiles at Swanton Pacific Ranch:

Sample ID	Pit	Slope (%)	Subgroup	Particle Size Control section	Texture	Coarse fragments (%)	Particle size class	CEC/Clay	Activity Class	Depth Class	Top Depth (cm)	Bottom Depth (cm)	Thickness (cm)	Clay %	Sand %	1.2X caly (%)	clay films	Argillic?	Moist Hue	Moist Value	Moist Chroma	Dry Hue	Dry Value	Dry Chroma	SOC (%)	CEC (cmolc per kg soil)	BS(%)	Redoxomporphic features
1_ A		29			L	1		1.83			0	19	19	20	34	24	n		10yr	2	1	10yr	4	2	6.44	36.1	0.75	
1_ Bw1	1_	29	Pachic Ultic Haploxeroll	25-RRL	L	1	Fine-loamy	0.93	Superactive		19	55	36	22	34	26	n	n	10yr	2	2	10yr	4	2	2.31	20.3	0.77	
1_ BW2		29			L	10		0.77			55	93+	38	26	31	31	n		10yr	2	2	10yr	4	2	2.33	19.9	0.62	
1_1 A	1_1	7	Lithic Haploxerept	0-RRL	SCL	15	Loamy	1.24	Superactive	Shallow	0	14	14	21	47	26	N	n	10yr	4	2	10yr	4	2	6.17	26.5	0.46	
1_12 A1		29			L	1		1.75			0	14	14	26	38	32	n		10yr	2	1	10yr	4	1	5.85	46.1	0.94	
1_12 A2	1_12	26	Pachic Haploxerolls	25-RRL	CL	1	Fine-loamy	1.05	Superactive		14	31	17	29	34	35	n	n	10yr	2	1	10yr	4	1	3.88	30.8	1.00	
1_12 AB		26			L	1		1.19			31	49	18	25	41	30	n		10yr	2	1	10yr	4	1	2.40	29.9	0.91	
1_12 BW		26			L	1		1.19			49	89	40	26	40	32	n		10yr	2	1	10yr	4	1	1.97	31.4	0.75	
1_2 A		13			CL	1		0.77			0	12	12	29	31	34	N		10yr	3	2	10yr	5	2	3.27	22.0	0.48	
1_2 Bt1	1_2	13	Fluventic Humixerept	25-RRL	SICL	1	Fine-loamy	0.56	Active		12	42	30	39	19	46	N	n	10yr	3	2	10yr	5	2	1.61	21.8	0.40	Few redox conc
1_2 Bt2		13			CL	20		0.58			42	53	11	33	31	40	N		10yr	3	2	10yr	6	3	4.10	19.0	0.44	common redox conc
1_20 A		27			L	40		1.73			0	31	31	23	46	28	n		10yr	2	1	10yr	4	2	5.25	39.8	0.76	
1_20 Ab	1_20	27	Pachic Ultic Haploxeroll	25-100	L	10	Fine-loamy	1.23	Superactive		31	62	31	27	41	32	n	n	10yr	2	1	10yr	4	1	3.63	32.7	0.77	
1_20 C1		27			SCL	30		1.20			62	99	37	21	58	25	n		10yr	3	1	10yr	5	2	1.48	25.3	0.72	
1_20 C2		27			L	50		1.21			99	104+	5	25	47	30	n		10yr	4	2	10yr	5	2	2.24	30.3	0.69	
1_3 A		29			CL	2		0.92			0	13	13	33	26	39	n		10yr	3	2	10yr	5	2	3.08	30.4	0.54	
1_3 Bt1	1_3	29	Pachic Humixerept	25-RRL	CL	2	Fine-loamy	1.14	Superactive		13	27	14	28	36	33	Y	n	10yr	3	2	10yr	5	2	2.19	31.6	0.46	
1_3 Bt2		29			CL	4		1.00			27	44	17	32	37	38	y		10yr	3	2	10yr	5	2	1.82	31.6	0.41	
1_3 Bt3		29			CL	25		1.08			44	69	25	37	38	36	y		10yr	3	2	10yr	5	2	1.66	32.9	0.37	
1_4 BW A		21			L	1		1.30			0	29	29	24	32	28	n		10yr	3	1.5	10yr	4	2	4.32	30.5	0.79	
1_4 RW AB1	1_4	21	Cumulic humixerept	25-100	L	1	Fine-loamy	1.16	Superactive		29	81	52	23	35	27	n	n	10yr	3	2	10yr	5	1	2.16	26.3	0.67	
1_4 RW AB2		21			CL	1		0.95			81	110	29	22	37	26	n		10yr	3	2	10yr	6	2	1.39	20.9	0.40	
1_4 RW Bt		21			L	5		1.18			110	139	29	20	45	23	y		10yr	4	4	10yr	7	2	0.76	23.1	0.39	
1_5 A1	1_5	17	Lithic Humixerept	0-RRL	L	1	Fine-loamy	1.00	Superactive	Shallow	0	15	15	21	44	25	n	n	10yr	3	2	10yr	4	2	4.34	20.7	0.39	
1_5 A2		17			L	40		1.60			15	25	10	21	46	25	n		10yr	2	2	10yr	4	2	3.94	33.1	0.20	
1_5 RW A		28			L	1		1.55			0	28	28	24	30	29	n		10yr	2	1	10yr	3	2	4.13	37.4	0.80	
1_5 RW AB	1_5	28	Pachic Haploxerolls	25-100	CL	1	Fine-loamy	1.04	Superactive		28	46	18	28	27	33	n	n	10yr	2	1	10yr	4	1	2.32	28.9	0.76	
1_5 RW BW1		28			CL	1		0.83			46	73	27	29	28	35	n		10yr	2	1	10yr	4	2	2.21	24.5	0.83	
1_5 RW BW2		28			L	10		0.75			73	120	47	20	36	29	n		10yr	2	2	10yr	4	1	1.93	22.6	0.82	
1_6 RW A		13			CL	15		0.98			0	22	22	28	28	34	n		10yr	2	1	10yr	4	2	3.21	27.7	0.96	
1_6 RW BA	1_6	13	Pachic Ultic Haploxerolls	25-100	CL	15	Fine-loamy	0.89	Superactive		22	57	35	31	29	37	n	n	10yr	3	2	10yr	5	2	2.00	27.2	0.82	
1_6 RW BW		13			CL	10or 10 cb		0.90			57	110	53	33	27	40	n		10yr	4	3	10yr	6	3	0.86	30.1	0.68	
2_1 G A		21			CL	1		0.63			10	24	14	29	40	35	n		10yr	3	2	10yr	5	3	1.51	18.1	0.55	
2_1 G AB		21			CL	1		0.63			24	36	12	30	39	36	y		10yr	3	2	10yr	4	2	1.48	18.9	0.56	
2_1 G Ap		21			L	1		0.81			0	30	10	26	40	32	n		10yr	4	3	10yr	5	3	2.95	21.2	0.58	
2_1 G Bt1	2_1 G	21	Ultic Palexeralf	36-86 (Upper 50 cm of Argillic)	C	1	Fine	0.28	Semiactive		36	77	41	54	-13	65	y	yes (36-138+)	10yr	2	2	10yr	5	3	1.29	15.3	0.65	
2_1 G Bt2		21			CL	2		0.57			77	99	22	31	41	38	y		10yr	4	2	10yr	5	3	0.92	17.7	0.43	common redox conc and depl
2_1 g Btg		21			CL	7		0.63			99	138+	39	32	42	38	y		10yr	4	1	10yr	6	2	0.76	19.8	0.36	Common redox conc and gleyed matrix
2_1 RW A		23			SL	45		1.70			0	21	21	27	39	33	n		10yr	3	1	10yr	4	2	7.63	46.5	0.81	
2_1 RW B		23			L	80	Loamy-skeletal	1.26	Superactive		21	64	43	17	#DIV/0!	#DIV/0!	n		10yr	4	3	10yr	6	3	1.10	21.5	0.93	
2_1 RW C	2_1 RW	23	Typic Haploxeroll	25-100	SL	70		1.16			64	84	20	17	68	20	n	n	10yr	4	4	10yr	6	3	0.58	19.5	0.81	
2_1 RW C2		23			SL	70		0.97			84	104	20	19	65	23	n		10yr	4	3	10yr	5	3	0.72	18.7	0.81	
2_1 RW C3		23			SL	70		1.26			104	115	11	15	#DIV/0!	#DIV/0!	n		10yr	4	3	10yr	5	3	0.76	18.9	0.82	
2_2 G AB		20			CL	1		0.63			30	38	8	34	39	41	n		10yr	2	2	10yr	4	2	2.32	21.4	0.63	
2_2 G Ap		20			CL	13		0.71			0	30	30	29	43	35	n		10yr	4	4	10yr	4	3	3.82	20.7	0.70	
2_2 G Bt1	2_2 G	20	Cumulic Ultic Haploxerolls	25-100	CL	1	Fine-loamy	0.58	Active		38	96	58	34	39	41	y	n	10yr	2	2	10yr	4	3	1.72	19.7	0.62	
2_2 G Bt2		20			CL	5		0.56			96	133	37	34	39	41	y		10yr	2	2	10yr	5	3	1.35	19.1	0.55	
2_2 G Bt3		20			CL	15		0.54			133	147+	14	34	40	41	y		10yr	2	2	10yr	5	2	1.59	18.4	0.61	
2_2 RW A		14			SCL	75	Loamy-skeletal over sandy	0.77	Superactive		0	28	28	21	60	26	n	n	10yr	3	1	10yr	5	2	2.12	16.4	0.61	
2_2 RW B		14			SCL	35		1.04			28	51	23	14	76	17	n		10yr	4	2	10yr	5	3	0.94	14.4	0.91	
2_2 RW C	2_2 RW	14	Ultic Haploxeroll	25-100	LS	35		1.09	Superactive		51	66	15	9	84	11	n	n	10yr	4	4	10yr	5	4	0.57	10.2	1.00	
2_2 RW C2		14			LS	95	skeletal	0.74			66	104	38	8	91	10	n		10yr	4	4	10yr	5	3	0.26	5.9	1.00	
2_3 G A	2_3 G	29	Lithic Humixerept	25-RRL	CL	5	Fine	0.86	Active		0	15	15	38	28	45	n	n	10yr	3	2	10yr	4	4	3.76	32.5	0.37	
2_3 G Bt		29			C	30		0.57			15	46	31	43	29	50	y		10yr	4	4	10yr	4	4	1.88	23.8	0.37	
2_4 G A	2_4 G	21	Lithic Ultic Haploxeroll	0-RRL	CL	62	Loamy-skeletal	0.70	Superactive	Shallow	0	10	10	31	39	37	n	n	10yr	3	2	10yr	4	4	4.48	21.4	0.55	
2_7 RW A		6			SCL	5	Fine loamy over sandy	1.09	Superactive		0	27	27	23	61	28	n	n	10yr	2	1	10yr	3	2	4.60	25.0	0.72	
2_7 RW B	2_7 RW	6	Fluventic Haploxeroll	25-100	SL	5		0.78			27	71	44	14	84	17	n		10yr	4	3	10yr	4	2	0.77	10.7	0.81	
2_7 RW C		6			LS	50		0.67			71	135+	64	12	84	14	n		10yr	4	3	10yr	6	3	0.49	8.0	0.90	
2_8 RW A		18			CL	5		0.90			0	14	14	31	21	37	n		10yr	2	2	10yr	5	2	5.51	27.5	0.89	
2_8 RW AB	2_8 RW	18	Lithic Haploxeroll	25-RRL	CL	5	Loamy	0.57	Active	Shallow	14	24	10	33	24	39	y	n	10yr	2	2	10yr	4	2	2.40	18.8	0.83	
2_8 RW B		18			CL	30		0.47			24	34	10	34	34	41	y		10yr	4	4	10yr	5	2	1.10	15.9	0.92	
2_8 RW BC		18			CL	1		0.59			34	39	5	36	35	43	y		10yr	4	4	10yr	5	2	1.17	21.3	0.81	
3_1 G A		10			CL	10		0.61			0	20	20	33	25	43	n		10yr	2	1	10yr	4	2	5.12	32.8	0.57	
3_1 G AB1		10			CL	3		0.75			20	46	26	37	27	45	n		10yr	2	1	10yr	3	2	3.14	27.9	0.60	
3_1 G AB2	3_1 G	10	Cumulic Humixerept	25-100	CL	5	Fine	0.64	Superactive		46	80	34	37	29	44	n	n	10yr	2	1	10yr	5	2	2.34	23.6	0.46	
3_1 G Bt1		10			CL	5		0.46			80	113	33	31	32	37	y		10yr	4	3	10yr	6	2	0.64	14.2	0.37	
3_1 G Bt2		10			CL	5		0.46			113	150+	37	20	38	37	y		10yr	4	3	10yr	7	2	0.68	14.1	0.34	
3_10 RW A		9			CL	5		0.80			0	12	12	28	24	33	n		10yr	2	1	10yr	5	2	4.93	22.1	0.90	
3_10 RW BC	3_10 RW	9	Ultic Haploxeroll	25-RRL	L	30	Fine-loamy	0.35	Active		47	79	35	25	35	29	n	n	7.5yr	4	4	10yr	6	3	2.15	8.5	0.57	
3_10 RW Bt		9			CL	5		0.60			12	47	32	27	26	33	y		7.5yr	2.5	2	10yr	5	2	1.82	16.4	0.61	
3_2 G A1		4		39 RF (upper 50cm of Argillic) not mollic bc not one-third of argillic with	SL	0	Fine-loamy	0.36	Semiactive		0	17	17	19	68	23	n	Yes (39-119+)	10yr	3	2	10yr	4	2	1.82	7.1	0.53	
3_2 G A2		4			SCL	0		0.36			17	39	22	20	68	24	n		10yr	3	2	10yr	5	2	0.83	7.1	0.49	common redox conc
3_2 G Bt1		4			SCL	0		0.31			39	68	29	29	61	35	y		10yr	4	3	10yr	5	4	0.38	9.1	0.51	common redox conc
3_2 G Bt2	3_2 G	4	Aquic Palexeralf		SCL	0		0.43			68	95	27	32	48	38	y		10yr	5	2	10yr	6	3	0.27	13.7	0.59	common redox conc and dep
3_2 G Btg		4			SCL	0		0.42			95	119+	24	31	51	38	y		10yr	4	1	10yr	6	2	0.19	13.3	0.59	common redox conc and dep
3_2 RW A		27			CL	30	Loamy-skeletal	1.35	Superactive		0	11	11	39	28	46	n	n	10yr	2	1	10yr	3	2	11.45	52.3	1.00	
3_2 RW AB	3_2 RW	27	Typic Haploxeroll	25-RRL	CL	35		1.19	Superactive		11	34	23	39	30	47	n	n	10yr	2	1	10yr	3	2	7.76	46.7	1.00	
3_2 RW B		27			CL	75		0.92			34	88	55	32	40	39	n		10yr	4	2	10yr	6	2	1.65	29.8	1.00	
3_3 G A		5			SICL	1		0.95			0	19	19	34	16	41	n		10yr	2	1	10yr	3	2	5.55	32.5	0.71	
3_3 G AB	3_3 G	5	Cumulic Ultic Haploxerolls	25-100	SICL	1	Fine loamy	0.80	Superactive		19	47	28	34	16	41	n	n	10yr	2	1	10yr	3	2	8.79	27.2	0.78	
3_3 G BA1		5			SICL	4		0.71			47	66	19	34	17	41	y		10yr	2	1	10yr	4	2	2.60	23.9	0.67	
3_3 G Bt1		5			CL	10		0.60			66	92	26	31	21	37	y		10yr	2	1	10yr	5	2	1.56	18.7	0.57	
3_3 G Bt2		5			CL	15		0.57			92	150+	58	28	24	34	y		10yr	3	2	10yr	6	3	0.98	16.2	0.52	
3_3 RW A	3_3 RW	21	Lithic Ultic Haploxeroll	0-RRL	CL	20	Loamy-skeletal	1.28	Superactive	Shallow	0	11	11	30	30	36	n	n	10yr	2	1	10yr	4	2	5.39	38.7	0.78	
3_3 RW AB		21			CL	40		1.23			11	34	23	30	35	36	n		10yr	3	2	10yr	4	2	2.75	36.5	0.72	
3_5 RW A1	3_5 RW	11	Lithic Ultic Haploxeroll	0-RRL	CL	10	Loamy-skeletal	1.07	Superactive	Shallow	0	7	7	31	29	37	n	n	10yr	2	2	10yr	4	2	6.80	33.1	0.88	
3_5 RW A2		11			CL	50		1.15			7	21	14	31	32	37	n		10yr	2	1	10yr	3	2	5.13	35.4	0.72	
3_6 G A1		9			SCL	1		0.69			0	16	16	23	50	28	n		10yr	2	1	10yr	4	2	2.14	11.4	0.59	
3_6 G A2		9			SCL	1		0.43			16	33	17	23	51	27	n		10yr	2	2	10yr	4	2	1.04	9.7	0.59	
3_6 G Bt1	3_6 G	9	Typic humixerept	25-100	SCL	1	Fine-loamy	0.37	Semiactive		33	53	20	24	56	29	y	n	10yr	4	4	10yr	5	4	0.42	9.1	0.48	common redox conc
3_6 G Bt2		9			SCL	1		0.27			53	91	38	20	60	24	y		10yr	4	6	10yr	6	4	0.21	5.5	0.58	common redox conc
3_6 G Bt3		9			SCL	1		0.34			91	111	20	22	60	26	y		10yr	4	6	10yr	6	4	0.29	7.4	0.38	common redox conc
3_6 G Bt4		9			SL	5		0.28			111	115+	4	19	53	23	y		10yr	3	3	10yr	6	3	0.07	5.4	0.35	common redox conc
3_7 RW A1		21			CL	20		1.25			0	33	33	30	31	36	n		10yr	2	1	10yr	5	2	3.87	37.0	0.90	
3_7 RW A2	3_7 RW	21	Cumulic Haploxeroll	25-100	CL	10	Fine-loamy	1.43	Superactive		33	61	28	30	33	36	n	n	10yr	2	1	10yr	3	1	5.97	42.9	0.91	
3_7 RW AB		21			CL	4		1.08			61	117	56	29	31	35	y		10yr	2	1	10yr	3	2	3.77	32.0	0.93	
3_7 RW BA		21			CL	7		1.03			117	124+	7	30	33	36	y		10yr	2	1	10yr	4	2	2.33	30.8	0.81	
3_9 RW A		17			L	5		1.09			0	15	15	24	41	29	n		10yr	2	1	10yr	4	2	3.14	26.0	0.65	
3_9 RW Ab		17		48-98 (Upper 50 Argillic)	CL	5	Fine-loamy	0.64	Superactive		15	48	33	35	30	42	y	Yes (48-119+)	10yr	2	1	10yr	4	2	3.00	22.0	1.00	
3_9 RW B1	3_9 RW	17	Pachic Ultic Argixeroll		L	5		1.19			48	78	30	21	51	24	n		10yr	4	2	10yr	6	3	1.25	23.6	0.73	
3_9 RW B2		17			L	20		0.86			78	113	35	26	43	32	y		10yr	4	2	10yr	6	2	1.07	22.6	0.79	
3_9 RW B3		17			L	40		1.08			113	119	6	24	40	29	y		10yr	3	2	10yr	6	2	0.92	26.5	0.65	

Data sheet for regression model on 102 horizons at Swanton Pacific Ranch:

No	Sample ID	Pit	Field Horizon	Horizon Simple	Zone	Zone Cat.	Veg	Slope (%)	Upper depth (cm)	Lower depth (cm)	Center Depth (cm)	Thickness (cm)	Air-dry moisture content	SON (%)	SOC (%)	C/N	BD (g per cm3 soil)	pH water	pH CaCl2	POXC (mg POXC per g soil)	POXC/SOC	Ca (cmolc per kg soil)	K (cmolc per kg soil)	Mg (cmolc per kg soil)	Na (cmolc per kg soil)	Sum of basic charge (cmolc per kg soil)	CEC (cmolc per kg soil)	BS
1	1,- A	1,-	A	A	1	A	RW	29	0	19	9.5	19	0.0481	0.360	6.44	17.90	0.81	6.87	6.33	1.263	0.020	21.861	2.260	3.021	0.077	27.22	36.08	0.75
2	1,- Bw1	1,-	Bw1	B	1	A	RW	29	19	55	37	36	0.0340	0.189	2.31	12.18	0.94	7.06	6.36	0.498	0.022	10.893	2.291	2.357	0.059	15.60	20.33	0.77
3	1,- BW2	1,-	BW2	B	1	A	RW	29	55	93	74	38	0.0414	0.173	2.33	13.44	1.03	6.41	5.52	0.461	0.020	7.341	1.979	2.814	0.112	12.25	19.89	0.62
4	1,1 A	1,1	A	A	1	A	G	7	0	14	7	14	0.0682	0.587	6.17	10.51	0.46	5.08	4.64	0.980	0.016	9.317	1.176	1.467	0.149	12.11	26.50	0.46
5	1,12 A1	1,12	A1	A	1	A	RW	26	0	14	7	14	0.0809	0.342	5.85	17.14	0.71	7.83	7.53	1.080	0.018	37.489	2.983	2.740	0.139	43.35	46.14	0.94
6	1,12 A2	1,12	A2	A	1	A	RW	26	14	31	22.5	17	0.1179	0.255	3.88	15.25	0.76	8.01	7.6	0.884	0.023	31.014	2.882	2.637	0.138	36.67	30.76	1.00
7	1,12 AB	1,12	AB	AB	1	A	RW	26	31	49	40	18	0.0560	0.189	2.40	12.72	0.86	7.59	7.04	0.627	0.026	21.879	2.668	2.461	0.158	27.17	29.89	0.91
8	1,12 BW	1,12	BW	B	1	A	RW	26	49	89	69	40	0.0573	0.159	1.97	12.39	0.68	7.26	6.61	0.493	0.025	18.500	2.392	2.476	0.204	23.57	31.45	0.75
9	1,2 A	1,2	A	A	1	A	G	13	0	12	6	12	0.0424	0.303	3.27	10.77	0.98	5.69	5.18	0.653	0.020	7.178	1.036	2.280	0.138	10.63	22.01	0.48
10	1,2 Bt1	1,2	Bt1	B	1	A	G	13	12	42	27	30	0.0321	0.164	1.61	9.81	1.18	5.9	4.93	0.185	0.012	5.257	0.857	2.367	0.153	8.63	21.79	0.40
11	1,2 Bt2	1,2	Bt2	B	1	A	G	13	42	53	47.5	11	0.0533	0.448	4.10	9.16	1.17	5.57	4.57	0.054	0.001	4.077	0.694	3.283	0.233	8.29	18.99	0.44
12	1,20 A	1,20	A	A	1	A	RW	27	0	31	15.5	31	0.0831	0.248	5.25	21.20		6.93	6.4	1.217	0.023	24.204	2.052	3.897	0.142	30.29	39.79	0.76
13	1,20 Ab	1,20	Ab	A	1	A	RW	27	99	104	101.5	5	0.0606	0.235	3.63	15.40		6.96	6.37	0.935	0.026	17.656	2.059	5.358	0.216	25.29	32.68	0.77
14	1,20 C1	1,20	C1	C	1	A	RW	27	31	62	46.5	31	0.0585	0.114	1.48	12.99		7.06	6.4	0.441	0.030	13.403	1.268	3.454	0.140	18.26	25.34	0.72
15	1,20 C2	1,20	C2	C	1	A	RW	27	62	99	80.5	37	0.0911	0.156	2.24	14.32		7.13	6.38	0.582	0.026	14.270	1.663	4.875	0.183	20.99	30.33	0.69
16	1,3 A	1,3	A	A	1	A	G	29	0	13	6.5	13	0.0523	0.309	3.08	9.97	0.82	5.92	5.29	0.679	0.022	11.146	1.638	3.350	0.128	16.26	30.38	0.54
17	1,3 Bt1	1,3	Bt1	B	1	A	G	29	13	27	20	14	0.0589	0.250	2.19	8.78	0.93	5.73	4.91	0.358	0.016	10.630	1.022	2.831	0.146	14.63	31.62	0.46
18	1,3 Bt2	1,3	Bt2	B	1	A	G	29	27	44	35.5	17	0.0496	0.213	1.82	8.53	0.87	5.65	4.67	0.342	0.019	9.046	0.638	3.030	0.173	12.89	31.64	0.41
19	1,3 Bt3	1,3	Bt3	B	1	A	G	29	44	69	56.5	25	0.0544	0.201	1.66	8.24	0.88	5.62	4.69	0.257	0.016	8.112	0.443	3.461	0.228	12.24	32.86	0.37
20	1,4 RW A	1,4 RW	A	A	1	A	RW	21	0	29	14.5	29	0.0406	0.299	4.32	14.45	0.80	6.86	6.37	1.152	0.027	19.999	1.713	2.177	0.106	23.99	30.55	0.79
21	1,4 RW AB1	1,4 RW	AB1	AB	1	A	RW	21	29	81	55	52	0.0944	0.177	2.16	12.21	0.95	6.85	6.14	0.557	0.026	13.824	1.519	2.142	0.150	17.64	26.25	0.67
22	1,4 RW AB2	1,4 RW	AB2	AB	1	A	RW	21	81	110	95.5	29	0.0369	0.122	1.39	11.37	0.79	5.57	4.71	0.241	0.017	4.391	1.158	2.611	0.160	8.32	20.88	0.40
23	1,4 RW Bt	1,4 RW	Bt	B	1	A	RW	21	110	139	124.5	29	0.0429	0.084	0.76	9.10	0.91	5.54	4.62	0.157	0.021	3.756	0.882	4.064	0.348	9.05	23.08	0.39
24	1,5 A1	1,5	A1	A	1	A	G	17	0	15	7.5	15	0.1076	0.414	4.34	10.47	0.51	4.93	4.38	0.736	0.017	5.479	1.219	1.243	0.108	8.05	20.69	0.39
25	1,5 A2	1,5	A2	A	1	A	G	17	15	25	20	10	0.0643	0.391	3.94	10.08		4.8	4.23	0.626	0.016	4.518	1.112	0.946	0.092	6.67	33.09	0.20
26	1,5 RW A	1,5 RW	A	A	1	A	RW	28	0	28	14	28	0.0691	0.309	4.13	13.40	0.80	7.55	7.09	0.799	0.019	24.852	2.576	2.456	0.090	29.97	37.38	0.80
27	1,5 RW AB	1,5 RW	AB	AB	1	A	RW	28	28	46	37	18	0.0476	0.188	2.32	12.33	0.98	7.6	6.94	0.442	0.019	17.276	2.620	2.127	0.096	22.12	28.94	0.76
28	1,5 RW BW1	1,5 RW	BW1	B	1	A	RW	28	46	73	59.5	27	0.0511	0.180	2.21	12.27	1.00	7.47	6.73	0.385	0.017	15.193	2.526	2.576	0.106	20.40	24.49	0.83
29	1,5 RW BW2	1,5 RW	BW2	B	1	A	RW	28	73	120	96.5	47	0.0638	0.166	1.93	11.63	1.10	7.34	6.52	0.334	0.017	13.068	2.366	2.776	0.148	18.36	22.39	0.82
30	1,6 RW A	1,6 RW	A	A	1	A	RW	13	0	22	11	22	0.0582	0.225	3.21	14.25	0.85	7.08	6.65	0.856	0.027	21.364	1.548	3.355	0.147	26.41	27.66	0.96
31	1,6 RW BA	1,6 RW	BA	AB	1	A	RW	13	22	57	39.5	35	0.0727	0.144	2.00	13.90	0.89	6.93	6.22	0.679	0.034	16.484	1.173	4.482	0.229	22.37	27.25	0.82
32	1,6 RW BW	1,6 RW	BW	B	1	A	RW	13	57	110	83.5	53	0.1009	0.084	0.86	10.21		7.13	6.33	0.217	0.025	13.718	1.189	5.506	0.219	20.63	30.12	0.68
33	2,1 G A	2,1 G	A	A	2	B	G	21	10	24	17	14	0.0332	0.121	1.51	12.51	1.08	5.84	5.11	0.291	0.019	7.826	0.511	1.532	0.050	9.92	18.08	0.55
34	2,1 G AB	2,1 G	AB	A	2	B	G	21	24	36	30	12	0.0290	0.104	1.48	14.23	1.22	6.28	5.35	0.243	0.016	8.394	0.330	1.743	0.055	10.52	18.88	0.56
35	2,1 G Ap	2,1 G	Ap	A	2	B	G	21	0	10	5	10	0.0329	0.236	2.95	12.46	0.93	5.86	5.51	0.768	0.026	9.156	1.120	1.972	0.063	12.31	21.16	0.58
36	2,1 G Bt1	2,1 G	Bt1	B	2	B	G	21	36	77	56.5	41	0.0291	0.093	1.29	13.87	1.16	6.32	5.36	0.225	0.017	7.701	0.279	1.830	0.059	9.87	15.29	0.65
37	2,1 G Bt2	2,1 G	Bt2	B	2	B	G	21	77	99	88	22	0.0312	0.068	0.92	13.41	1.25	6.06	4.91	0.080	0.009	4.748	0.113	2.574	0.184	7.62	17.74	0.43
38	2,1 g Btg	2,1 G	Btg	B	2	B	G	21	99	138	118.5	39	0.0375	0.065	0.76	11.65	1.21	5.93	4.71	0.025	0.003	3.908	0.119	2.832	0.368	7.23	19.83	0.36
39	2,1 RW A	2,1 RW	A	A	2	B	RW	23	0	21	10.5	21	0.0735	0.461	7.63	16.56	0.62	6.78	6.5	1.464	0.019	33.203	1.896	2.718	0.089	37.91	46.51	0.81
40	2,1 RW B	2,1 RW	B	B	2	B	RW	23	21	64	42.5	43	0.0471	0.121	1.10	9.10		7.12	6.53	0.286	0.026	16.485	1.348	2.023	0.133	19.99	21.47	0.93
41	2,1 RW C	2,1 RW	C	C	2	B	RW	23	64	84	74	20	0.0861	0.086	0.58	6.68		7.33	6.64	0.133	0.023	12.429	1.371	1.759	0.133	15.69	19.48	0.81
42	2,1 RW C2	2,1 RW	C2	C	2	B	RW	23	84	104	94	20	0.0391	0.088	0.72	8.15		7.45	6.85	0.168	0.023	12.189	1.111	1.775	0.108	15.18	18.74	0.81
43	2,1 RW C3	2,1 RW	C3	C	2	B	RW	23	104	115	109.5	11	0.0412	0.084	0.76	9.10		7.31	6.67	0.244	0.032	12.398	1.021	1.929	0.113	15.46	18.92	0.82
44	2,2 G AB	2,2 G	AB	A	2	B	G	20	30	38	34	8	0.0374	0.157	2.32	14.80	1.01	6.25	5.35	0.419	0.018	10.839	0.425	2.134	0.073	13.47	21.44	0.63
45	2,2 G Ap	2,2 G	Ap	A	2	B	G	20	0	30	15	30	0.0453	0.210	3.82	18.16	1.07	5.95	5.35	0.884	0.023	11.819	0.643	2.058	0.061	14.58	20.70	0.70
46	2,2 G Bt1	2,2 G	Bt1	B	2	B	G	20	38	96	67	58	0.0385	0.111	1.72	15.51	1.11	6.28	5.29	0.261	0.015	9.247	0.214	2.711	0.108	12.28	19.68	0.62
47	2,2 G Bt2	2,2 G	Bt2	B	2	B	G	20	96	133	114.5	37	0.0429	0.089	1.35	15.15	1.29	6.3	4.96	0.186	0.014	6.996	0.123	3.167	0.274	10.56	19.13	0.55
48	2,2 G Bt3	2,2 G	Bt3	B	2	B	G	20	133	147	140	14	0.0423	0.102	1.59	15.53	0.99	6.2	5.06	0.269	0.017	7.699	0.174	2.995	0.276	11.14	18.40	0.61
49	2,2 RW A	2,2 RW	A	A	2	B	RW	14	0	28	14	28	0.0452	0.142	2.12	14.90		5.39	4.79	0.385	0.018	8.054	0.630	1.241	0.033	9.96	16.43	0.61
50	2,2 RW B	2,2 RW	B	B	2	B	RW	14	28	51	39.5	23	0.0293	0.052	0.94	18.11		6.24	5.62	0.346	0.037	11.329	0.265	1.458	0.020	13.07	14.43	0.91
51	2,2 RW C	2,2 RW	C	C	2	B	RW	14	51	66	58.5	15	0.0252	0.023	0.57	24.59		6.55	5.83	0.138	0.024	8.988	0.197	1.348	0.019	10.55	10.20	1.00
52	2,2 RW C2	2,2 RW	C2	C	2	B	RW	14	66	104	85	38	0.0152	0.012	0.26	21.13		6.92	6.34	0.067	0.026	5.695	0.141	0.879	0.017	6.73	5.92	1.00
53	2,3 G A	2,3 G	A	A	2	B	G	29	0	15	7.5	15	0.0699	0.340	3.76	11.06	0.73	5.27	4.58	0.787	0.021	8.886	0.748	2.327	0.169	12.13	32.50	0.37
54	2,3 G Bt	2,3 G	Bt	B	2	B	G	29	15	48	31.5	33	0.0575	0.189	1.88	9.95	0.71	5.34	4.45	0.239	0.013	5.481	0.827	2.389	0.158	8.86	23.77	0.37
55	2,4 G A	2,4 G	A	A	2	B	G	21	0	10	5	10	0.0487	0.366	4.48	12.24		5.33	4.71	0.940	0.021	8.737	0.915	2.053	0.131	11.84	21.39	0.55
56	2,7 RW A	2,7 RW	A	A	2	B	RW	6	0	27	13.5	27	0.1269	0.237	4.60	19.42	0.73	5.49	5.08	1.036	0.023	15.170	0.622	2.233	0.074	18.10	25.00	0.72
57	2,7 RW B	2,7 RW	B	B	2	B	RW	6	27	71	49	44	0.0202	0.039	0.77	19.56	1.12	6.48	5.84	0.283	0.037	7.203	0.216	1.178	0.041	8.64	10.73	0.81
58	2,7 RW C	2,7 RW	C	C	2	B	RW	6	71	135	103	64	0.0183	0.031	0.49	15.92		6.7	5.94	0.162	0.033	5.830	0.174	1.165	0.068	7.24	8.00	0.90
59	2,8 RW A	2,8 RW	A	A	2	B	RW	18	0	14	7	14	0.0469	0.321	5.51	17.16	0.75	6.62	6.2	1.335	0.024	19.975	1.552	2.985	0.086	24.60	27.53	0.89
60	2,8 RW AB	2,8 RW	AB	AB	2	B	RW	18	14	24	19	10	0.0392	0.165	2.40	14.59	0.90	6.88	6.25	0.675	0.028	13.051	1.375	1.180	0.072	15.68	18.78	0.83
61	2,8 RW B	2,8 RW	B	B	2	B	RW	18	24	34	29	10	0.0337	0.080	1.10	13.78	1.05	6.45	5.78	0.321	0.029	12.293	0.954	1.234	0.095	14.58	15.85	0.92
62	2,8 RW BC	2,8 RW	BC	C	2	B	RW	18	34	39	36.5	5	0.0511	0.075	1.17	15.51		6.32	5.66	0.327	0.028	14.302	1.021	1.717	0.118	17.16	21.28	0.81
63	3,1 G A	3,1 G	A	A	3	C	G	10	0	20	10	20	0.0547	0.383	5.12	13.37		5.81	5.38	0.899	0.018	14.267	1.707	2.569	0.101	18.64	32.82	0.57
64	3,1 G AB1	3,1 G	AB1	AB	3	C	G	10	20	46	33	26	0.0875	0.234	3.14	13.45	0.78	6.18	5.42	0.513	0.016	12.526	1.245	2.807	0.131	16.71	27.91	0.60
65	3,1 G AB2	3,1 G	AB2	AB	3	C	G	10	46	80	63	34	0.0355	0.179	2.34	13.12	0.90	5.9	4.98	0.365	0.016	6.498	0.801	3.275	0.147	10.72	23.55	0.46
66	3,1 G Bt1	3,1 G	Bt1	B	3	C	G	10	80	113	96.5	33	0.0274	0.078	0.64	8.23	1.38	5.52	4.37	0.073	0.011	2.789	0.301	1.920	0.203	5.21	14.20	0.37
67	3,1 G Bt2	3,1 G	Bt2	B	3	C	G	10	113	150	131.5	37	0.0466	0.073	0.68	9.25	1.14	5.36	4.22	0.050	0.007	2.425	0.205	1.904	0.223	4.76	14.07	0.34
68	3,10 RW A	*3,10 RW*	A	A	2	B	RW	9	0	12	6	12	0.0382	0.308	4.93	16.01	1.04	6.66	6.18	1.232	0.025	15.668	1.514	2.593	0.168	19.94	22.10	0.90
69	3,10 RW BC	*3,10 RW*	BC	C	2	B	RW	9	47	79	63	32	0.0162	0.145	2.15	14.86		5.69	4.63	0.145	0.007	3.570	0.476	0.719	0.111	4.88	8.50	0.57
70	3,10 RW Bt	*3,10 RW*	Bt	B	2	B	RW	9	12	47	29.5	35	0.0225	0.166	1.82	10.98	1.01	6.34	5.53	0.462	0.025	7.479	1.058	1.234	0.154	9.92	16.40	0.61
71	3,2 G A1	3,2 G	A1	A	3	C	G	4	0	17	8.5	17	0.0160	0.166	1.82	10.98	0.97	5.25	4.77	0.392	0.022	2.696	0.313	0.689	0.052	3.75	7.11	0.53
72	3,2 G A2	3,2 G	A2	A	3	C	G	4	17	39	28	22	0.0132	0.084	0.83	9.94	1.32	5.92	5	0.143	0.017	2.614	0.325	0.476	0.074	3.49	7.13	0.49
73	3,2 G Bt1	3,2 G	Bt1	B	3	C	G	4	39	68	53.5	29	0.0218	0.057	0.38	6.79	1.42	6.46	5.38	0.042	0.011	2.685	0.242	1.524	0.154	4.61	9.06	0.51
74	3,2 G Bt2	3,2 G	Bt2	B	3	C	G	4	68	95	81.5	27	0.0447	0.041	0.27	6.63	1.43	5.67	4.86	0.036	0.013	3.603	0.112	3.896	0.513	8.12	13.72	0.59
75	3,2 G Btg	3,2 G	Btg	B	3	C	G	4	95	119	107	24	0.0440	0.034	0.19	5.65	1.46	5.24	4.68	0.017	0.009	3.328	0.110	3.816	0.578	7.83	13.25	0.59
76	3,2 RW A	3,2 RW	A	A	3	C	RW	27	0	11	5.5	11	0.1318	0.676	11.45	16.93	0.59	7.14	6.9	1.592	0.014	60.243	1.693	2.793	0.172	64.90	52.32	1.00
77	3,2 RW AB	3,2 RW	AB	AB	3	C	RW	27	11	34	22.5	23	0.1104	0.526	7.76	14.74	0.86	7.41	7.06	1.451	0.019	50.139	1.687	1.936	0.179	53.94	46.73	1.00
78	3,2 RW B	3,2 RW	B	B	3	C	RW	27	34	89	61.5	55	0.1026	0.128	1.65	12.91		7.22	6.68	0.504	0.030	29.373	1.251	2.039	0.281	32.94	29.79	1.00
79	3,3 G A	3,3 G	A	A	3	C	G	5	0	19	9.5	19	0.0502	0.402	5.55	13.79	0.90	5.95	5.44	0.956	0.017	20.455	0.669	1.859	0.105	23.09	32.55	0.71
80	3,3 G AB	3,3 G	AB	AB	3	C	G	5	19	47	33	28	0.0466	0.265	3.79	14.29	0.83	6.47	5.78	0.594	0.016	18.975	0.338	1.768	0.116	21.20	27.18	0.78

Continued data sheet for regression model on 102 horizons at Swanton Pacific Ranch:

No	Sample ID	Pit	Field Horizon	Horizon Simple	Zone	Zone Cat.	Veg	Slope (%)	Upper depth (cm)	Lower depth (cm)	Center Depth (cm)	Thickness (cm)	Air-dry moisture content	SON (%)	SOC (%)	C/N	BD (g per cm3 soil)	pH water	pH CaCl2	POXC (mg POXC per g soil)	POXC/SOC	Ca (cmolc per kg soil)	K (cmolc per kg soil)	Mg (cmolc per kg soil)	Na (cmolc per kg soil)	Sum of basic charge (cmolc per kg soil)	CEC (cmolc per kg soil)	BS
81	3,3 G BAt	3,3 G	BAt	AB	3	C	G	5	47	66	56.5	19	0.0381	0.191	2.60	13.61	0.90	6.52	5.62	0.463	0.018	11.977	0.426	3.433	0.064	15.90	23.90	0.67
82	3,3 G Bt1	3,3 G	Bt1	B	3	C	G	5	66	92	79	26	0.0305	0.125	1.56	12.43	1.09	6.38	5.23	0.231	0.015	6.950	0.176	3.419	0.117	10.66	18.65	0.57
83	3,3 G Bt2	3,3 G	Bt2	B	3	C	G	5	92	150	121	58	0.0318	0.092	0.98	10.67	1.21	6.28	5.12	0.111	0.011	4.770	0.114	3.413	0.169	8.47	16.22	0.52
84	3,3 RW A	3,3 RW	A	A	3	C	RW	21	0	11	5.5	11	0.0984	0.316	5.39	17.06	0.79	5.92	5.49	1.377	0.026	23.489	2.248	4.064	0.187	29.99	38.66	0.78
85	3,3 RW AB	3,3 RW	AB	AB	3	C	RW	21	11	34	22.5	23	0.0765	0.203	2.75	13.54		6.27	5.69	0.882	0.032	20.576	2.183	3.422	0.168	26.35	36.54	0.72
86	3,5 RW A1	3,5 RW	A1	A	3	C	RW	11	0	7	3.5	7	0.1238	0.395	6.80	17.19	0.63	5.41	5.14	1.309	0.019	22.489	1.979	4.405	0.194	29.07	33.09	0.88
87	3,5 RW A2	3,5 RW	A2	A	3	C	RW	11	7	21	14	14	0.0743	0.341	5.13	15.04		5.51	5.16	1.232	0.024	19.833	1.685	3.808	0.190	25.52	35.43	0.72
88	3,6 G A1	3,6 G	A1	A	3	C	G	9	0	16	8	16	0.0278	0.184	2.14	11.65	1.27	5.72	5.02	0.459	0.021	4.796	0.691	1.206	0.058	6.75	11.42	0.59
89	3,6 G A2	3,6 G	A2	A	3	C	G	9	16	33	24.5	17	0.0179	0.101	1.04	10.26	1.20	6.04	5.12	0.198	0.019	4.229	0.463	1.006	0.060	5.76	9.74	0.59
90	3,6 G Bt1	3,6 G	Bt1	B	3	C	G	9	33	53	43	20	0.0203	0.056	0.42	7.53	1.43	6.16	5.09	0.045	0.011	2.700	0.318	1.225	0.065	4.31	9.06	0.48
91	3,6 G Bt2	3,6 G	Bt2	B	3	C	G	9	53	91	72	38	0.0151	0.034	0.21	6.16	1.66	6.25	5.1	0.013	0.006	1.779	0.141	1.176	0.078	3.17	5.50	0.58
92	3,6 G Bt3	3,6 G	Bt3	B	3	C	G	9	91	111	101	20	0.0153	0.040	0.29	7.15	1.22	5.36	4.45	0.030	0.011	1.322	0.103	1.223	0.137	2.78	7.36	0.38
93	3,6 G Bt4	3,6 G	Bt4	B	3	C	G	9	111	115	113	4	0.0137	0.020	0.07	3.69	1.26	5.05	4.3	0.000	0.000	0.731	0.065	0.933	0.138	1.87	5.36	0.35
94	3,7 RW A1	3,7 RW	A1	A	3	C	RW	21	0	33	16.5	33	0.0788	0.271	3.87	14.30		6.83	6.42	1.072	0.028	26.929	2.050	3.960	0.206	33.15	37.01	0.90
95	3,7 RW A2	3,7 RW	A2	A	3	C	RW	21	33	61	47	28	0.0889	0.348	5.97	17.14	0.73	6.9	6.47	1.178	0.020	32.575	2.201	4.192	0.209	39.18	42.92	0.91
96	3,7 RW AB	3,7 RW	AB	AB	3	C	RW	21	61	117	89	56	0.0722	0.262	3.77	14.39	0.74	7.13	6.59	0.820	0.022	23.418	2.046	3.906	0.215	29.59	31.95	0.93
97	3,7 RW BA	3,7 RW	BA	AB	3	C	RW	21	117	124	120.5	7	0.0832	0.183	2.33	12.70	0.82	7.25	6.65	0.565	0.024	18.198	1.786	4.693	0.243	24.92	30.77	0.81
98	3,9 RW A	3,9 RW	A	A	3	C	RW	17	0	15	7.5	15	0.0566	0.220	3.14	14.25	0.89	5.97	5.53	0.908	0.029	13.237	1.135	2.487	0.075	16.93	25.99	0.65
99	3,9 RW Ab	3,9 RW	Ab	A	3	C	RW	17	48	78	63	30	0.0661	0.214	3.00	14.02	0.77	6.45	5.86	0.625	0.021	17.025	1.925	4.670	0.108	23.73	22.04	1.00
100	3,9 RW B1	3,9 RW	B1	B	3	C	RW	17	15	48	31.5	33	0.0558	0.104	1.25	12.11	0.91	6.52	5.81	0.337	0.027	12.120	1.610	3.452	0.100	17.28	23.56	0.73
101	3,9 RW B2	3,9 RW	B2	B	3	C	RW	17	78	113	95.5	35	0.0573	0.101	1.07	10.60	1.08	6.63	5.83	0.205	0.019	12.171	1.221	4.269	0.153	17.82	22.61	0.79
102	3,9 RW B3	3,9 RW	B3	B	3	C	RW	17	113	119	116	6	0.0599	0.091	0.92	10.10		6.6	5.72	0.240	0.026	11.655	0.919	4.304	0.228	17.11	26.52	0.65

Soil classification sheet for 15 profiles at Landels-Hill Big Creek Reserve:

No	Sample ID	Pit	Slope (%)	Sub group	Particle size control section	Particle size class	Text class	Coarse fragments	CEC/Clay	Activity Class	Depth Class	Upper depth (cm)	Lower depth (cm)	Thickness (cm)	Clay %	1.2X clay (%)	Clay films	Argillic?	M Hue	M Value	M Chroma	D Hue	D Value	D Chroma	SOC (%)	CEC (cmolc per kg soil)	BS(%)
1	85 RW A	85	84	Mollic Palexeralf	Upper 50cm of Argillic	Fine	L	40% coarse gravel	1.94	Subactive		0	16	16	18	22	N	Yes (57-107)	10YR	3	1	10YR	5	2	4.48	34.9	0.80
2	85 RW Bw	85	84				L	50% coarse gravel	0.55			16	57	41	20	24	N		10YR	4	2	10YR	5	2	3.03	11.1	1.00
3	85 RW 2Bt	85	84				CL	20% medium gravel	0.20			57	107	50	38	46	Y		2.5YR	5	3	10YR	7	3	0.33	7.7	1.00
4	85 RW 2Btg	85	84				CL	0.4	0.27			107	137+	30	39	47	-		2.5YR	6	1	Gley 1	6	2	1.02	10.5	1.00
5	58 RW A	58	19	Fluventic haploxerept	25-100	Loamy-skeletal	L	20% MGR	2.76	Superactive		0	15	15	17	20	N	No	10YR	2	1	10YR	3	2	10.14	46.9	0.86
6	58 RW Bw	58	19				SL	40% CoGR 10% cobble	1.13			15	50	35	19	23	N		10YR	3	1	10YR	4	2	2.92	21.5	1.00
7	58 RW C	58	19				SL	60% cobbles	0.90			50	90+?	40	16	19	N		10YR	4	2	10YR	6	3	0.91	14.3	1.00
8	328 RW A	328	13	Cumulic Haploxeroll	25-100	Loamy-skeletal	L	35% M GR	3.48	Superactive		0	12	12	17	20	N	No	10YR	2	1	10YR	3	2	12.45	59.1	0.72
9	328 RW Bw	328	13				SL	30% MGR 30% cobble	1.06			12	56.5	44.5	17	20	N		10YR	2	1	10YR	4	2	3.96	17.9	1.00
10	328 RW C	328	13				SL	20% stones 45% gravel	0.65			56.5	90+	33.5	24	29	N		10YR	4	1	10YR	5	2	1.70	15.5	0.90
11	290 A	290	38	Pachic Haploxeroll	25-100	Loamy-skeletal over sandy-skeletal	L	50% cobbles	5.74	Superactive		0	20	20	13	16	-	No	10YR	2	1	10YR	3	2	14.08	74.6	0.70
12	290 Bw1	290	38				L	45% GR	2.84			20	43	23	15	18	N		10YR	3	1	10YR	3	2	7.03	42.6	0.76
13	290 Bw2	290	38				SL	60% cobbles	1.77			43	84	41	11	13	-		10YR	3	2	10YR	6	2	2.13	19.5	1.00
14	290 2C	290	38				LS	60% cobbles	3.96			84	96+	12	5	6	-		10YR	3	2	10YR	4	2	1.99	19.8	0.84
15	165 A	165	46	Pachic Haploxeroll	25-RRL	Loamy-skeletal	L	0.1	3.43	Superactive		0	24	24	14	17	-	No	10YR	2	1	10YR	4	2	8.43	48.0	0.70
16	165 Bw	165	46				L	40% medium GR	0.77			24	74	50	23	28	-		10YR	3	1	10YR	5	2	2.78	17.6	1.00
17	165 C	165	46				SL	60% coarse GR	1.15			74	99	25	12	14	-		10YR	3	2	10YR	5	2	1.47	13.8	1.00
18	442g A	442g	27	Humic Lithic Haploxeroll	0-RRL	Loamy-skeletal	L	40% fine GR	0.89	Superactive	Shallow	0	7	7	18	22	-	No	10YR	3	2	10YR	5	3	2.69	16.0	1.00
19	8490g A1	8490g	51	Typic Haploxeroll	25-100	Loamy-skeletal	L	30% fine GR	0.72	Active		0	15	15	21	25	N	No	10YR	3	2	10YR	5	3	2.68	15.1	0.92
20	8490g A2	8490g	51				L	35% med GR	0.61			15	30	15	23	28	N		10YR	3	2	2.5Y	5	2	1.38	13.9	1.00
21	8490g Bw	8490g	51				L	75% cobble	0.66			30	84	54	23	28	N		10YR	4	2	10YR	5	2	1.23	15.2	1.00
22	8490g C	8490g	51				SCL	60% coarse GR	0.35			84	127+	43	34	41	N		10YR	4	3	10YR	6	3	0.34	12.0	1.00
23	7029g A2-A	7029g	44	Typic Argixeroll	Entire Argillic (60-73)	Loamy-skeletal	GRL	15	0.99	Active		0	8	8	18	22	-	Yes (60-73)	10YR	3	3				3.05	17.8	1.00
24	7029g A2-B	7029g	44				GRL	20	0.81			8	26	18	20	24	-		10YR	3	2	10YR	5	3	1.14	16.2	1.00
25	7029g A3	7029g	44				L	10	0.80			26	60	34	22	26	-		10YR	4	3	10YR	5	3	0.79	17.5	1.00
26	7029g 2Bt	7029g	44				XCR CL	70	0.51			60	73	13	28	34	Y		10YR	4	6	10YR	6	4	0.38	14.2	1.00
27	532 RW A1	532	50	Pachic Haploxeroll	25-RRL	Fine-loamy	L	7 GR	2.21	Superactive		0	15	15	18	22	-	No	10YR	2	1	10YR	4	2	8.39	39.9	0.93
28	532 RW A2	532	50				L	12 GR	1.09			15	51	36	20	24	-		10YR	2	2	10YR	5	2	2.33	21.9	0.92
29	532 RW Bt	532	50				VGR L	60 GR	0.52			51	57	6	24	29	Y		10YR	4	4	10YR	6	3	0.75	12.4	1.00
30	322 RW A1	322	24	Cumulic Haploxeroll	25-100	Coarse-loamy	GR L	30% GR	3.01	Superactive		0	14	14	15	18	-	No	10YR	2	1	10YR	3	2	8.53	45.1	0.66
31	322 RW A2	322	24				GRS L	30% GR	1.38			14	52	38	12	14	-		10YR	2	1	10YR	4	2	2.05	16.6	0.89
32	322 RW Bw1	322	24				CB SL	20% CB 10% GR	0.88			52	87	35	14	17	-		10YR	3	3	10YR	5	2	1.19	12.3	1.00
33	322 RW Bw2	322	24				VGR SL	35% GR 10 CB	0.92			87	138	51	14	17	-		10YR	3	4				0.66	12.9	1.00
34	129 RW A1	129	10	Fluventic Haploxeroll	25-100	Loamy-skeletal over sandy-skeletal (over loamy skeletal?)	GR L	20 GR	4.46	Superactive		0	16	16	12	14	-	No	10YR	2	1	10YR	3	2	11.90	53.5	0.71
35	129 RW A2	129	10				VGR L	30% 10 CB GR	2.72			16	42	26	12	14	-		10YR	2	1	10YR	3	2	5.73	32.6	0.71
36	129 RW C1	129	10				VCB LS	55% CB	1.24			42	67	25	7	8	-		10YR	4	3	10YR	6	3	0.51	8.7	1.00
37	129 RW C2	129	10				XCB SL	55% CB 25% GR	0.62			67	89+	22	20	24	-		10YR	4	4	10YR	7	3	0.66	12.3	1.00
38	1425g A1	1425g	18	Cumulic Haploxeroll	25-100	Fine-loamy	L	10% GR	1.02	Superactive		0	10	10	23	28	-	No	10YR	2	2	10YR	4	2	4.23	23.4	0.99
39	1425g A2	1425g	18				L	5% GR	1.14			10	30	20	24	29	-		10YR	2	2	10YR	4	2	2.40	27.5	0.92
40	1425g A3	1425g	18				L	5% GR	1.02			30	75	45	24	29	-		10YR	2	2	10YR	4	2	1.65	24.5	1.00
41	1425g Bw1	1425g	18				GR CL	15% GR	0.70			75	111	36	28	34	-		10YR	3	2	10YR	4	2	1.32	19.6	1.00
42	1425g Bw2	1425g	18				CR CL	25% GR	0.62			111	150+	39	28	34	-		10YR	3	2	10YR	5	3	0.85	17.5	1.00
43	5820g A1	5820g	61	Pachic Argixeroll	Enitre Argillic (84-110)	Fine	GR L	15% GR	0.80	Active		0	14	14	19	23	-	Yes (84-110)	10YR	3	2	10YR	5	2	2.57	15.2	1.00
44	5820g A2	5820g	61				L	5% GR	0.72			14	40	26	20	24	-		10YR	3	2	10YR	5	2	1.30	14.4	1.00
45	5820g A3	5820g	61				L	5% GR	0.82			40	84	44	22	26	-		10YR	3	2	10YR	6	3	1.02	17.9	1.00
46	5820g 2Bt	5820g	61				GR C	15% GR	0.46			84	110	26	43	52	Y		10YR	4	6	10YR	6	6	0.36	19.6	1.00
47	8012g A1	8012g	25	Typic Haploxeroll	25-100	Coarse-loamy	GR L	25% GR	1.53	Superactive		0	19	19	12	14	-	No	10YR	3	2	10YR	5	3	2.64	18.3	0.94
48	8012g A2	8012g	25				L	10% GR	1.20			19	45	26	14	17	-		10YR	3	3	10YR	5	3	1.48	16.8	1.00
49	8012g AB	8012g	25				L	5% GR	1.10			45	73	28	16	19	-		10YR	4	3	10YR	5	3	1.29	17.7	1.00
50	8012g Bt1	8012g	25				GR L	20% GR	0.93			73	92	19	16	19	Y		10YR	4	4	10YR	6	4	0.42	14.8	1.00
51	8012g Bt2	8012g	25				VGR SL	45% GR	0.82			92	150+	58	18	22	Y		10YR	4	4	10YR	6	4	0.32	14.8	1.00
52	3277g A1	3277g	18	Cumulic Ultic Haploxeroll	25-100	Fine-loamy	GR L	20 GR	1.78	Superactive		0	23	23	12	14	-	No	10YR	3	2	10YR	4	2	3.12	21.3	0.63
53	3277g A2	3277g	18				GR L	20 GR	0.91			23	60	37	20	24	-		10YR	3	2	10YR	5	2	1.56	18.2	0.66
54	3277g Bw1	3277g	18				VGR L	35 GR	0.61			60	90	30	25	30	-		10YR	3	2	10YR	6	2	1.24	15.2	0.84
55	3277g Bw2	3277g	18				VGR L	40 GR	0.61			90	127	37	25	30	-		10YR	3	2	10YR	6	2	1.11	15.1	0.77
56	3277g Bw3	3277g	18				VGR CL	50 GR	0.47			127	150+	23	30	36	-		10YR	4	3	10YR	6	3	0.94	14.0	0.53

Data sheet for regression model on 56 horizons at Landels-Hill Big Creek Reserve:

No	Sample ID	Pit	Field Horizon	Horizon_Simple	Veg	veg+horizon	Slope (%)	Aspect (deg)	Upper depth (cm)	Lower depth (cm)	Center Depth (cm)	Thickness (cm)	Air-dry moisture content	SON (%)	SOC (%)	C/N	BD (g per cm3 soil)	pH water	pH CaCl2	POXC (mg POXC per g soil)	POXC/SOC	Ca (cmolc per kg soil)	K (cmolc per kg soil)	Mg (cmolc per kg soil)	Na (cmolc per kg soil)	Sum of basic charge (cmolc per kg soil)	CEC (cmolc per kg soil)	BS
1	85 RW A	85	A	A	RW	RW A	84	130	0	16	8	16	0.0435	0.223	4.48	20.10	1.27	7	6.55	1.352	0.0302	22.713	0.655	4.703		28.07	34.91	0.80
2	85 RW Bw	85	Bw	B	RW	RW B	84	130	16	57	36.5	41	0.0332	0.191	3.03	15.86		7.12	6.69	0.940	0.0310	18.089	0.510	3.334		21.93	11.07	1.00
3	85 RW 2Bt	85	2Bt	B	RW	RW B	84	130	57	107	82	50	0.0213	0.034	0.33	9.70	1.54	7.84	7.08	0.146	0.0444	10.788	0.296	1.509		12.59	7.74	1.00
4	85 RW 2Btg	85	2Btg	B	RW	RW B	84	130	107	137	122	30	0.0214	0.057	1.02	17.84		8.02	7.69	0.299	0.0294	19.507	0.302	1.994		21.80	10.47	1.00
5	58 RW A	58	A	A	RW	RW A	19	110	0	15	7.5	15	0.0726	0.504	10.14	20.12	0.97	6.7	6.35	1.506	0.0149	30.319	0.365	9.013	0.824	40.52	46.89	0.86
6	58 RW Bw	58	Bw	B	RW	RW B	19	110	15	50	32.5	35	0.0381	0.196	2.92	14.88		6.8	6.27	0.854	0.0293	17.307	0.178	4.588		22.07	21.53	1.00
7	58 RW C	58	C	C	RW	RW C	19	110	50	90	70	40	0.0273	0.064	0.91	14.14		7	6.29	0.268	0.0296	12.635	0.212	3.346		16.19	14.33	1.00
8	328 RW A	328	A	A	RW	RW A	13	195	0	12	6	12	0.0989	0.681	12.45	18.28	0.80	6.53	6.21	1.498	0.0120	33.923	0.830	6.828	0.891	42.47	59.11	0.72
9	328 RW Bw	328	Bw	B	RW	RW B	13	195	12	56.5	34.25	44.5	0.0332	0.246	3.96	16.09		6.66	6.07	0.883	0.0223	15.654	0.423	2.998		19.07	17.94	1.00
10	328 RW C	328	C	C	RW	RW C	13	195	56.5	90	73.25	33.5	0.0244	0.114	1.70	14.94		6.63	5.88	0.558	0.0328	10.981	0.332	2.752		14.06	15.55	0.90
11	290 A	290	A	A	RW	RW A	38	164	0	20	10	20	0.0859	0.698	14.08	20.17	0.90	6.84	6.6	1.544	0.0110	39.653	1.498	10.346	0.749	52.25	74.57	0.70
12	290 Bw1	290	Bw1	B	RW	RW B	38	164	20	43	31.5	23	0.0429	0.386	7.03	18.20		6.89	6.47	1.294	0.0184	23.775	1.077	6.966	0.601	32.42	42.60	0.76
13	290 Bw2	290	Bw2	B	RW	RW B	38	164	43	84	63.5	41	0.0311	0.107	2.13	19.92		7.13	6.45	0.649	0.0304	15.149	0.787	4.237	0.596	20.77	19.51	1.00
14	290 2C	290	2C	C	RW	RW C	38	164	84	96	90	12	0.0302	0.096	1.99	20.72		6.81	6.22	0.565	0.0284	12.064	0.703	3.362	0.557	16.69	19.82	0.84
15	165 A	165	A	A	RW	RW A	46	77	0	24	12	24	0.0586	0.4	8.43	21.07	0.78	6.91	6.57	1.413	0.0168	26.217	0.925	5.680	0.721	33.54	48.04	0.70
16	165 Bw	165	Bw	B	RW	RW B	46	77	24	74	49	50	0.0311	0.159	2.78	17.46		7.48	6.93	0.780	0.0281	13.914	0.717	3.016	0.813	18.46	17.63	1.00
17	165 C	165	C	C	RW	RW C	46	77	74	99	86.5	25	0.0255	0.081	1.47	18.12		7.42	6.75	0.424	0.0289	10.690	0.334	2.929	0.708	14.66	13.76	1.00
18	442g A	442g	A	A	G	G A	27	-	0	7	3.5	7	0.0298	0.239	2.69	11.25	0.96	6.25	5.6	0.573	0.0213	10.929	0.606	5.765	0.663	17.96	16.02	1.00
19	8490g A1	8490g	A1	A	G	G A	51	211	0	15	7.5	15	0.0261	0.243	2.68	11.05	1.45	6.3	5.72	0.631	0.0235	8.746	0.433	4.092	0.589	13.86	15.14	0.92
20	8490g A2	8490g	A2	A	G	G A	51	211	15	30	22.5	15	0.0267	0.127	1.38	10.83		6.4	5.6	0.341	0.0248	9.195	0.257	4.707		14.16	13.94	1.00
21	8490g Bw	8490g	Bw	B	G	G B	51	211	30	84	57	54	0.0286	0.121	1.23	10.12		6.59	5.53	0.233	0.0190	10.551	0.208	5.533	0.600	16.89	15.21	1.00
22	8490g C	8490g	C	C	G	G C	51	211	84	127	105.5	43	0.0265	0.053	0.34	6.36		7.01	5.79	0.078	0.0232	9.577	0.160	7.797		17.53	12.02	1.00
23	7029g A2-A	7029g	A2-A	A	G	G A	44	164	0	8	4	8	0.0307	0.27	3.05	11.29	1.06	6.91	6.01	0.645	0.0212	10.427	0.640	7.930		19.00	17.78	1.00
24	7029g A2-B	7029g	A2-B	A	G	G A	44	164	8	26	17	18	0.0343	0.104	1.14	10.95	1.29	6.22	5.68	0.318	0.0279	9.852	0.202	9.120		19.17	16.21	1.00
25	7029g A3	7029g	A3	A	G	G A	44	164	26	60	43	34	0.0300	0.085	0.79	9.30	1.52	7.16	6.21	0.247	0.0312	11.499	0.159	11.377		23.03	17.49	1.00
26	7029g 2Bt	7029g	2Bt	B	G	G B	44	164	60	73	66.5	13	0.0416	0.075	0.38	5.02		7.06	6.14	0.121	0.0322	14.121	0.133	16.655	0.679	31.59	14.15	1.00
27	532 RW A1	532	A1	A	RW	RW A	50	38	0	15	7.5	15	0.0657	0.559	8.39	15.00	0.98	6.62	6.33	1.334	0.0159	24.704	0.848	10.564	0.803	36.92	39.86	0.93
28	532 RW A2	532	A2	A	RW	RW A	50	38	15	51	33	36	0.0356	0.172	2.33	13.56	1.29	7.21	6.48	0.484	0.0208	12.400	0.415	6.612	0.709	20.14	21.89	0.92
29	532 RW Bt	532	Bt	B	RW	RW B	50	38	51	57	54	6	0.0321	0.075	0.75	10.04		7.4	6.45	0.243	0.0323	11.602	0.264	6.844	0.656	19.37	12.39	1.00
30	322 RW A1	322	A1	A	RW	RW A	24	72	0	14	7	14	0.0615	0.539	8.53	15.83	0.85	6.45	6.1	1.191	0.0140	22.027	1.100	6.449		29.58	45.09	0.66
31	322 RW A2	322	A2	A	RW	RW A	24	72	14	52	33	38	0.0296	0.145	2.05	14.13	1.21	6.79	6.1	0.444	0.0217	10.597	0.285	3.853		14.73	16.58	0.89
32	322 RW Bw1	322	Bw1	B	RW	RW B	24	72	52	87	69.5	35	0.0234	0.083	1.19	14.36	1.56	6.94	5.98	0.252	0.0211	9.859	0.275	2.895		13.03	12.29	1.00
33	322 RW Bw2	322	Bw2	B	RW	RW B	24	72	87	138	112.5	51	0.0276	0.054	0.66	12.24		7.15	6.07	0.198	0.0299	12.762	0.193	3.319	0.637	16.91	12.87	1.00
34	129 RW A1	129	A1	A	RW	RW A	10	190	0	16	8	16	0.0740	0.631	11.90	18.86	0.86	6.44	6.17	1.353	0.0114	30.569	0.980	6.655		38.20	53.54	0.71
35	129 RW A2	129	A2	A	RW	RW A	10	190	16	42	29	26	0.0503	0.346	5.73	16.57	1.25	6.63	6.14	0.877	0.0153	18.222	0.803	3.988		23.01	32.61	0.71
36	129 RW C1	129	C1	C	RW	RW C	10	190	42	67	54.5	25	0.0188	0.037	0.51	13.81		6.89	6.02	0.127	0.0248	7.862	0.249	2.299		10.41	8.71	1.00
37	129 RW C2	129	C2	C	RW	RW C	10	190	67	89	78	22	0.0299	0.056	0.66	11.79		6.78	6.08	0.179	0.0270	13.361	0.351	3.914		17.63	12.31	1.00
38	1425g A1	1425g	A1	A	G	G A	18	220	0	10	5	10	0.0421	0.35	4.23	12.08	1.14	6.07	5.57	0.751	0.0178	14.227	0.575	8.335		23.14	23.38	0.99
39	1425g A2	1425g	A2	A	G	G A	18	220	10	30	20	20	0.0401	0.202	2.40	11.87	1.12	6	5.37	0.452	0.0188	16.340	0.450	8.482		25.27	27.48	0.92
40	1425g A3	1425g	A3	A	G	G A	18	220	30	75	52.5	45	0.0692	0.131	1.65	12.60	1.35	6.64	5.66	0.347	0.0210	18.337	0.182	10.410		28.93	24.47	1.00
41	1425g Bw1	1425g	Bw1	B	G	G B	18	220	75	111	93	36	0.0410	0.102	1.32	12.93	1.63	6.75	5.82	0.347	0.0263	14.985	0.122	9.367	0.636	25.11	19.61	1.00
42	1425g Bw2	1425g	Bw2	B	G	G B	18	220	111	150	130.5	39	0.0358	0.072	0.85	11.76	1.58	7.21	6.05	0.218	0.0258	16.277	0.107	9.773	0.586	26.74	17.49	1.00
43	5820g A1	5820g	A1	A	G	G A	61	212	0	14	7	14	0.0284	0.229	2.57	11.22	1.36	6.47	5.84	0.661	0.0257	10.328	0.536	7.088		17.95	15.16	1.00
44	5820g A2	5820g	A2	A	G	G A	61	212	14	40	27	26	0.0297	0.128	1.30	10.17	1.49	6.78	5.97	0.376	0.0289	10.069	0.315	7.947		18.33	14.39	1.00
45	5820g A3	5820g	A3	A	G	G A	61	212	40	84	62	44	0.0292	0.093	1.02	10.95	1.41	7.1	6.03	0.314	0.0308	11.912	0.199	9.130		21.24	17.94	1.00
46	5820g 2Bt	5820g	2Bt	B	G	G B	61	212	84	110	97	26	0.0486	0.062	0.36	5.87	1.78	7.23	6.34	0.118	0.0324	14.140	0.183	15.022	0.598	29.94	19.61	1.00
47	8012g A1	8012g	A1	A	G	G A	25	193	0	19	9.5	19	0.0295	0.243	2.64	10.88	1.00	6.15	5.55	0.518	0.0196	10.562	0.709	6.003		17.27	18.30	0.94
48	8012g A2	8012g	A2	A	G	G A	25	193	19	45	32	26	0.0287	0.148	1.48	10.02	0.97	6.25	5.55	0.307	0.0207	11.046	0.466	5.518		17.03	16.79	1.00
49	8012g AB	8012g	AB	B	G	G B	25	193	45	73	59	28	0.0312	0.123	1.29	10.50	1.20	6.85	5.94	0.250	0.0193	12.650	0.381	5.178	0.773	19.98	17.67	1.00
50	8012g Bt1	8012g	Bt1	B	G	G B	25	193	73	92	82.5	19	0.0309	0.056	0.42	7.41	1.52	6.91	5.98	0.121	0.0291	11.338	0.181	8.622		20.14	14.81	1.00
51	8012g Bt2	8012g	Bt2	B	G	G B	25	193	92	150	121	58	0.0287	0.052	0.32	6.18		7.09	6.17	0.079	0.0245	11.664	0.313	7.831		19.81	14.83	1.00
52	3277g A1	3277g	A1	A	G	G A	18	148	0	23	11.5	23	0.0266	0.303	3.12	10.30	1.32	5.85	5.44	0.576	0.0185	8.147	0.968	4.225		13.34	21.34	0.63
53	3277g A2	3277g	A2	A	G	G A	18	148	23	60	41.5	37	0.0269	0.156	1.56	9.99	1.54	5.91	5.06	0.349	0.0224	7.508	0.589	3.857		11.95	18.25	0.66
54	3277g Bw1	3277g	Bw1	B	G	G B	18	148	60	90	75	30	0.0244	0.111	1.24	11.13	1.39	6.17	5.26	0.304	0.0247	7.733	0.346	4.654		12.73	15.20	0.84
55	3277g Bw2	3277g	Bw2	B	G	G B	18	148	90	127	108.5	37	0.0228	0.107	1.11	10.33	1.55	6.18	5.22	0.234	0.0212	6.639	0.313	4.636		11.59	15.15	0.77
56	3277g Bw3	3277g	Bw3	B	G	G B	18	148	127	150	138.5	23	0.0221	0.092	0.94	10.18		6.25	5.09	0.001	0.0147	3.524	0.113	3.821		7.46	13.99	0.53

Mass of SOC and POXC per acre in top meter of soil (densities) for 28 profiles at Swanton Pacific Ranch, used to generate LSM for density values in regression model:

Pit	Veg	Zone	Zone Cat	Slope	tonsCperha_1m	tonsPOXCperha_1m
1,-	RW	1	A	29	256.748776	5.20091669
1,1	G	1	A	7	34.1291979	0.54244196
1,12	RW	1	A	26	196.996376	4.4784305
1,2	G	1	A	13	136.601663	1.46047494
1,20	RW	1	A	27	143.936728	3.63783552
1,3	G	1	A	29	113.23185	2.07404377
1,4 RW	RW	1	A	21	224.90027	5.71403401
1,5	G	1	A	17	50.6383846	0.84002719
1,5 RW	RW	1	A	28	243.058749	4.4671704
1,6 RW	RW	1	A	13	124.64176	3.68732927
2,1 G	G	2	B	21	157.631884	2.77288151
2,1 RW	RW	2	B	23	66.8510484	1.34724635
2,2 G	G	2	B	20	241.464219	4.55735277
2,2 RW	RW	2	B	14	31.0883575	0.85925575
2,3 G	G	2	B	29	70.2272071	1.21590583
2,4 G	G	2	B	21	16.4365159	0.34461463
2,7 RW	RW	2	B	6	129.547929	3.505985
2,8 RW	RW	2	B	18	89.1305123	2.30233139
3,1 G	G	3	C	10	226.511554	3.66575451
3,10 RW	RW	2	B	9	169.018208	3.34326959
3,2 G	G	3	C	4	81.825659	1.38250607
3,2 RW	RW	3	C	27	176.187447	3.34220954
3,3 G	G	3	C	5	271.526075	4.42603107
3,3 RW	RW	3	C	21	66.1419321	1.87575264
3,5 RW	RW	3	C	11	52.2389149	1.12553205
3,6 G	G	3	C	9	92.3199352	1.56153593
3,7 RW	RW	3	C	21	291.518445	6.5740699
3,9 RW	RW	3	C	17	161.504583	3.86891657

Mass of SOC and POXC per acre in top meter of soil (densities) for 15 profiles at Landels-Hill Big Creek Reserve, used to generate LSM for density values in regression model:

Pit	Slope	Veg	tonsPOXCperha_1m	tonsCperha_1m
85	84	RW	5.123513788	159.1222063
58	19	RW	4.232389637	202.4855024
328	13	RW	3.670441853	187.6021823
290	38	RW	5.294906399	299.324385
165	46	RW	5.6793597	258.8217156
442g	27	G	0.231698013	10.86895387
8490g	51	G	1.934539729	85.88050645
7029g	44	G	2.276868083	82.17744521
532	50	RW	3.882615019	212.3910151
322	24	RW	3.599093799	189.7181228
129	10	RW	3.512504128	254.9942738
1425g	18	G	4.928815105	234.9720099
5820g	61	G	4.589839794	158.3584015
8012g	25	G	2.563429734	124.2791449
3277g	18	G	4.027627301	190.3714198

Transects

Data sheet for regression model on 75 transect samples at Swanton Pacific Ranch

No	Sample ID	Transect No.	Ecotone	Depth	Depth_new	Ecotone and Depth	Slope (%)	Air-dry moisture content	SON (%)	SOC (%)	C/N	pH water	pH cacl2	POXC (mg POXC per g soil)	POXC/SOC	Ca (cmolc per kg soil)	K (cmolc per kg soil)	Mg (cmolc per kg soil)	Na (cmolc per kg soil)	Sum of basic charge (cmolc per kg soil)	CEC (cmolc per kg soil)	BS
1	114 RW A	114	RW	A	X	RW A	60	0.2058	0.356	4.86	13.65	6.15	5.77	1.418	0.029	23.126	2.829	7.446	0.850	34.25	48.38	0.71
2	114 RW B	114	RW	B	Y	RW B	60	0.1539	0.303	3.63	11.99	6.62	5.86	1.175	0.032	19.948	2.546	6.843	0.869	30.21	37.53	0.80
3	114 RW C	114	RW	C	Z	RW C	60	0.1260	0.21	2.71	12.91	6.73	5.77	0.814	0.030	16.428	2.350	8.793	0.810	28.38	35.03	0.81
4	114 RW/ME A	114	RW/ME	A	X	RW/ME A	61	0.1536	0.392	5.15	13.13	5.75	4.95	1.236	0.024	16.165	2.210	7.020	0.695	26.09	41.23	0.63
5	114 RW/ME B	114	RW/ME	B	Y	RW/ME B	61	0.1621	0.254	3.12	12.28	5.77	4.9	0.868	0.028	12.270	1.970	6.619	0.728	21.59	33.83	0.64
6	114 RW/ME C	114	RW/ME	C	Z	RW/ME C	61	0.1352	0.229	2.30	10.05	5.58	4.92	0.607	0.026	10.303	1.902	7.619	0.801	20.62	31.12	0.66
7	114 ME A	114	ME	A	X	ME A	24	0.0889	0.284	4.09	14.38	5.85	4.97	0.955	0.023	16.452	1.366	7.841		25.66	33.24	0.77
8	114 ME B	114	ME	B	Y	ME B	24	0.1145	0.236	2.43	10.30	6.06	5.08	0.594	0.024	13.787	1.153	7.741		22.68	30.62	0.74
9	114 ME C	114	ME	C	Z	ME C	24	0.0687	0.184	1.98	10.77	6.02	5.02	0.466	0.024	11.615	1.118	7.501	0.680	20.91	30.73	0.68
10	114 ME/G A	114	ME/G	A	X	ME/G A		0.0547	0.346	3.92	11.33	6.01	5.1	0.791	0.020	12.336	0.901	4.170	0.787	18.19	23.23	0.78
11	114 ME/G B	114	ME/G	B	Y	ME/G B		0.0480	0.275	3.08	11.18	6.03	5.06	0.547	0.018	10.694	0.674	3.908		15.28	25.66	0.60
12	114 ME/G C	114	ME/G	C	Z	ME/G C		0.0492	0.121	1.24	10.21	6.24	4.87	0.231	0.019	4.893	0.292	3.358		8.54	13.90	0.61
13	114 G A	114	G	A	X	G A	21	0.0415	0.338	3.79	11.22	5.64	4.67	0.589	0.016	9.475	0.804	3.671	0.601	14.55	24.14	0.60
14	114 G B	114	G	B	Y	G B	21	0.0522	0.246	2.69	10.91	5.94	4.72	0.401	0.015	8.481	0.642	3.547		12.67	22.38	0.57
15	114 G C	114	G	C	Z	G C	21	0.0458	0.187	1.99	10.64	6.15	4.71	0.287	0.014	7.533	0.500	4.605		12.64	20.16	0.63
16	6092 RW A	6092	RW	A	X	RW A	76	0.1209	0.307	4.87	15.87	6.17	5.51	1.237	0.025	19.320	2.349	7.820	0.895	30.38	45.32	0.67
17	6092 RW B	6092	RW	B	Y	RW B	76	0.1169	0.202	2.74	13.55	6.6	5.68	0.847	0.031	19.543	2.282	8.176	0.704	30.70	17.16	1.00
18	6092 RW C	6092	RW	C	Z	RW C	76	0.1046	0.18	2.28	12.69	6.63	5.67	0.678	0.030	17.869	2.168	8.624	0.724	29.39	36.87	0.80
19	6092 RW/ME A	6092	RW/ME	A	X	RW/ME A		0.2330	0.388	5.85	15.07	6.73	6.05	1.554	0.027	45.157	3.220	12.493	0.790	61.66	63.15	0.98
20	6092 RW/ME B	6092	RW/ME	B	Y	RW/ME B		0.1869				7.29	6.5	1.022		32.248	2.818	9.592		44.66	46.59	0.96
21	6092 RW/ME C	6092	RW/ME	C	Z	RW/ME C		0.2072				7.05	6.39	1.381		31.540	2.652	8.917		43.11	46.76	0.92
22	6092 ME A	6092	ME	A	X	ME A	68	0.1416	0.223	4.31	19.33	6.27	5.37	1.009	0.023	25.995	2.341	9.355	0.962	38.65	50.91	0.76
23	6092 ME B	6092	ME	B	Y	ME B	68	0.1530	0.187	3.28	17.53	6.1	5.16	0.626	0.019	23.843	1.900	7.363	0.811	33.92	58.67	0.58
24	6092 ME C	6092	ME	C	Z	ME C	68	0.1359	0.151	2.08	13.80	5.17	4.19	0.438	0.021	16.828	1.714	7.033	0.994	26.57	46.29	0.57
25	6092 ME/G A	6092	ME/G	A	X	ME/G A	25	0.0921	0.306	4.13	13.49	5.85	4.95	0.714	0.017	12.939	1.631	8.507		23.08	32.59	0.71
26	6092 ME/G B	6092	ME/G	B	Y	ME/G B	25	0.1222	0.236	3.01	12.75	5.92	4.81	0.547	0.018	10.860	1.424	9.163	0.739	22.19	25.49	0.87
27	6092 ME/G C	6092	ME/G	C	Z	ME/G C	25	0.1210	0.168	2.25	13.39	5.68	4.42	0.411	0.018	8.217	1.317	7.400	0.876	17.81	21.93	0.81
28	6092 G A	6092	G	A	X	G A	19	0.0876	0.345	4.24	12.29	5.67	4.9	0.870	0.021	16.425	2.294	10.502	0.660	29.88	43.00	0.69
29	6092 G B	6092	G	B	Y	G B	19	0.1443	0.227	2.76	12.16	5.74	4.74	0.492	0.018	14.243	1.799	12.429		28.47	50.01	0.57
30	2156 RW A	2156	RW	A	X	RW A	50	0.0847	0.304	6.16	20.25	6.31	5.57	1.529	0.025	17.685	1.131	4.463		23.28	38.96	0.60
31	2156 RW B	2156	RW	B	Y	RW B	50	0.0588	0.184	3.08	16.74	6.6	5.78	0.989	0.032	14.055	1.123	3.447		18.63	21.35	0.87
32	2156 RW C	2156	RW	C	Z	RW C	50	0.0465	0.084	1.63	19.36	6.44	5.42	0.488	0.030	8.338	0.795	3.028		12.16	13.61	0.89
33	2156 RW/ME A	2156	RW/ME	A	X	RW/ME A	35	0.2816	0.481	8.66	18.00	6.02	5.39	1.758	0.020	28.276	3.624	8.611	0.910	41.42	54.20	0.76
34	2156 RW/ME B	2156	RW/ME	B	Y	RW/ME B	35	0.1528	0.392	6.73	17.17	6.21	5.51	1.535	0.023	28.221	2.454	9.109	0.874	40.66	57.64	0.71
35	2156 ME A	2156	ME	A	X	ME A	1	0.0359	0.183	2.79	15.23	5.28	4.43	0.684	0.025	7.918	0.686	2.816	1.028	12.45	14.35	0.87
36	2156 ME B	2156	ME	B	Y	ME B	1	0.0255	0.103	1.50	14.60	5.52	4.59	0.431	0.029	5.401	0.561	2.320	0.693	8.97	12.77	0.70
37	2156 ME C	2156	ME	C	Z	ME C	1	0.0608	0.072	0.89	12.38	5.13	4.24	0.216	0.024	6.348	0.272	5.199	0.915	12.73	25.30	0.50
38	2156 ME/G A	2156	ME/G	A	X	ME/G A	13	0.0368	0.218	2.99	13.72	5.76	4.79	0.687	0.023	5.996	0.917	2.285	0.915	10.11	14.73	0.69
39	2156 ME/G B	2156	ME/G	B	Y	ME/G B	13	0.0318	0.178	1.96	11.00	5.86	4.85	0.407	0.021	7.622	0.721	1.887	0.793	11.02	14.50	0.76
40	2156 ME/G C	2156	ME/G	C	Z	ME/G C	13	0.0319	0.088	0.92	10.43	5.92	4.66	0.148	0.016	4.733	0.325	2.710		7.77	14.12	0.55
41	2156 G A	2156	G	A	X	G A	34	0.0467	0.44	5.08	11.54	5.63	4.94	0.825	0.016	12.715	1.455	3.706	0.748	18.62	23.87	0.78
42	2156 G B	2156	G	B	Y	G B	34	0.0611	0.31	3.61	11.65	5.8	4.85	0.601	0.017	13.621	1.186	2.374	0.643	17.82	25.18	0.71
43	3339 RW A	3339	RW	A	X	RW A	56	0.1303	0.375	5.56	14.83	7.21	6.5	1.197	0.022	24.363	2.570	5.167	1.183	33.28	44.57	0.75
44	3339 RW B	3339	RW	B	Y	RW B	56	0.0876	0.285	4.21	14.77	6.92	6.17	1.071	0.025	21.226	2.662	5.124	0.765	29.78	40.05	0.74
45	3339 RW C	3339	RW	C	Z	RW C	56	0.0750	0.206	2.67	12.94	6.33	5.54	0.716	0.027	15.853	2.641	5.204	0.970	24.67	24.33	1.00
46	3339 RW/ME A	3339	RW/ME	A	X	RW/ME A	10	0.1425	0.368	5.77	15.68	5.98	5.45	1.353	0.023	21.083	2.229	6.211	1.109	30.63	52.52	0.58
47	3339 RW/ME B	3339	RW/ME	B	Y	RW/ME B	10	0.1501	0.228	2.87	12.59	5.92	4.9	0.719	0.025	15.117	2.055	7.682	0.750	25.60	26.12	0.98
48	3339 RW/ME C	3339	RW/ME	C	Z	RW/ME C	10	0.1558	0.12	1.56	13.01	5.91	4.81	0.409	0.026	9.099	1.618	8.923	1.119	20.76	26.15	0.79
49	3339 ME A	3339	ME	A	X	ME A	67	0.0740	0.361	4.73	13.10	5.83	5.05	0.818	0.017	15.773	1.504	4.548		21.83	21.69	1.00
50	3339 ME B	3339	ME	B	Y	ME B	67	0.0587	0.222	2.86	12.88	5.24	4.38	0.585	0.020	8.211	1.078	3.599		12.89	20.76	0.62
51	3339 ME C	3339	ME	C	Z	ME C	67	0.0542	0.168	1.84	10.96	5.49	4.46	0.381	0.021	7.270	1.167	5.456	0.825	14.72	18.46	0.80
52	3339 ME/G A	3339	ME/G	A	X	ME/G A	19	0.0421	0.29	4.07	14.04	5.95	5.09	0.829	0.020	13.455	0.919	2.539		16.91	19.39	0.87
53	3339 ME/G B	3339	ME/G	B	Y	ME/G B	19	0.0575	0.251	3.50	13.96	6.07	5.12	0.687	0.020	16.691	0.793	3.240		20.72	30.29	0.68
54	3339 ME/G C	3339	ME/G	C	Z	ME/G C	19	0.0612	0.198	2.81	14.18	5.95	4.69	0.458	0.016	10.457	0.435	5.230	0.694	16.82	24.23	0.69
55	3339 G A	3339	G	A	X	G A		0.0549	0.346	4.62	13.35	5.86	5.1	0.750	0.016	13.842	1.471	4.382		19.69	28.54	0.69
56	3339 G B	3339	G	B	Y	G B		0.0653	0.254	3.18	12.53	6.01	4.99	0.579	0.018	13.168	1.334	5.306	0.701	20.51	22.83	0.90
57	3339 G C	3339	G	C	Z	G C		0.0772	0.16	2.06	12.90	6	4.75	0.361	0.018	8.591	0.868	6.491	0.750	16.70	23.26	0.72
58	5849 RW A	5849	RW	A	X	RW A	66	0.1118	0.478	7.24	15.15	7.21	6.72	1.515	0.021	32.137	2.114	8.085	0.689	43.03	53.00	0.81
59	5849 RW B	5849	RW	B	Y	RW B	66	0.0955	0.404	5.86	14.51	7.02	6.4	1.378	0.024	29.286	2.674	6.427	0.804	39.19	54.03	0.73
60	5849 RW C	5849	RW	C	Z	RW C	66	0.0810	0.293	4.08	13.94	7.07	6.46	1.100	0.027	19.839	2.540	6.081	0.893	29.35	42.19	0.70
61	5849 RW/ME A	5849	RW/ME	A	X	RW/ME A	60	0.0991	0.336	5.38	16.02	6.8	6.19	1.370	0.025	22.655	2.716	7.867	0.684	33.92	48.50	0.70
62	5849 RW/ME B	5849	RW/ME	B	Y	RW/ME B	60	0.1534	0.212	3.10	14.62	6.92	6.16	0.971	0.031	21.974	2.176	7.038	1.028	32.22	29.68	1.00
63	5849 RW/ME C	5849	RW/ME	C	Z	RW/ME C	60	0.1458	0.149	2.27	15.26	6.49	5.67	0.787	0.035	16.008	2.008	7.468	1.032	26.52	41.62	0.64
64	5849 ME A	5849	ME	A	X	ME A	31	0.2065	0.592	10.15	17.14	6.1	5.54	1.741	0.017	29.797	3.442	6.795		40.03	75.00	0.53
65	5849 ME B	5849	ME	B	Y	ME B	31	0.1556	0.423	6.57	15.54	6.27	5.67	1.571	0.024	24.055	3.676	5.894	0.703	34.33	58.38	0.59
66	5849 ME C	5849	ME	C	Z	ME C	31	0.1573	0.24	3.52	14.68	6.24	5.5	0.958	0.027	17.899	2.524	6.468	1.027	27.92	38.29	0.73
67	5849 ME/CS A	5849	ME/CS	A	X	ME/CS A	45	0.0450	0.341	4.60	13.48	6.7	5.85	1.013	0.022	16.276	4.290	5.975	0.617	27.16	44.56	0.61
68	5849 ME/CS B	5849	ME/CS	B	Y	ME/CS B	45	0.1383	0.284	3.57	12.55	6.36	5.44	0.854	0.024	13.994	3.775	5.813	0.956	24.54	42.11	0.58
69	5849 ME/CS C	5849	ME/CS	C	Z	ME/CS C	45	0.1352	0.221	2.79	12.64	6.03	5.09	0.658	0.024	11.428	2.133	8.783		22.34	36.54	0.61
70	5849 CS/G A	5849	CS/G	A	X	CS/G A	28	0.0867	0.46	5.03	10.94	5.42	4.6	0.801	0.016	13.440	1.612	5.688	0.854	21.59	42.96	0.50
71	5849 CS/G B	5849	CS/G	B	Y	CS/G B	28	0.1501	0.368	3.79	10.30	5.27	4.23	0.636	0.017	8.133	1.048	5.068	0.695	14.94	28.30	0.53
72	5849 CS/G C	5849	CS/G	C	Z	CS/G C	28	0.1116	0.205	1.79	8.75	5.25	3.97	0.314	0.018	6.075	0.891	5.718		12.68	31.72	0.40
73	5849 G A	5849	G	A	X	G A	4	0.0878	0.475	5.81	12.23	6.15	5.44	1.186	0.020	15.836	2.276	5.386	0.627	24.12	43.77	0.55
74	5849 G B	5849	G	B	Y	G B	4	0.0749	0.424	5.31	12.53	6.09	5.33	0.981	0.018	16.560	1.646	4.571		22.78	29.64	0.77
75	5849 G C	5849	G	C	Z	G C	4	0.0802	0.343	4.29	12.51	6.28	5.43	0.774	0.018	17.118	0.854	3.882	0.630	22.48	26.14	0.86

Forest floor analysis

Data sheet for forest floor analysis:

No	Location	A horiozn ID	Pit	Field Horizon	Horizon_Simple	A horizon No	Zone	Zone_Cat	Veg	veg+horizon	Slope (%)	Top Depth (cm)	Bottom Depth (cm)	Center Depth (cm)	Thickness (cm)	Ca (cmolc per kg soil)	K (cmolc per kg soil)	Mg (cmolc per kg soil)	Na (cmolc per kg soil)	Sum of basic charge (cmolc per kg soil)	Pit_2	O horizon ID	percentCa	percentK	percentMg	percentNA	SUM_ percent basic cations	O horizon thickness (cm)
1	SPR	1,- A	1,-	A	A	1	1	A	RW	RW A	29	0	19	9.5	19	21.861	2.260	3.021	0.077	27.219	1,-	1,- Oi	1.000	0.086	0.164	0.011	1.262	9
2	SPR	1,12 A1	1,12	A1	A	1	1	A	RW	RW A	26	0	14	7	14	37.489	2.983	2.740	0.139	43.351	1,12	1,12 Oi	1.297	0.119	0.114	0.014	1.544	8
3	SPR	1,12 A2	1,12	A2	A	2	1	A	RW	RW A	26	14	31	22.5	17	31.014	2.882	2.637	0.138	36.671	1,12							
4	SPR	1,20 A	1,20	A	A	1	1	A	RW	RW A	27	0	31	15.5	31	24.204	2.052	3.897	0.142	30.295	1,20	1,20 Oi	1.840	0.070	0.239	0.010	2.158	6
5	SPR	1,20 Ab	1,20	Ab	A	2	1	A	RW	RW A	27	99	104	101.5	5	17.656	2.059	5.358	0.216	25.289	1,20							
6	SPR	1,4 RW A	1,4 RW	A	A	1	1	A	RW	RW A	21	0	29	14.5	29	19.997	1.713	2.177	0.106	23.993	1,4 RW	1,4 RW O	1.634	0.076	0.164	0.009	1.883	13
7	SPR	1,5 RW A	1,5 RW	A	A	1	1	A	RW	RW A	28	0	28	14	28	24.852	2.576	2.456	0.090	29.975	1,5 RW	1,5 RW O	2.734	0.057	0.296	0.016	3.103	10
8	SPR	1,6 RW A	1,6 RW	A	A	1	1	A	RW	RW A	13	0	22	11	22	21.364	1.548	3.355	0.147	26.414	1,6 RW	1,6 RW Oi	1.926	0.064	0.198	0.009	2.197	10
9	SPR	2,1 RW A	2,1 RW	A	A	1	2	B	RW	RW A	23	0	21	10.5	21	33.203	1.896	2.718	0.089	37.906	2,1 RW	2,1 RW O	1.930	0.090	0.129	0.009	2.157	8
10	SPR	2,2 RW A	2,2 RW	A	A	1	2	B	RW	RW A	14	0	28	14	28	8.054	0.630	1.241	0.033	9.958	2,2 RW	2,2 RW O	1.165	0.052	0.134	0.006	1.356	6
11	SPR	2,7 RW A	2,7 RW	A	A	1	2	B	RW	RW A	6	0	27	13.5	27	15.170	0.622	2.233	0.074	18.099	2,7 RW	2,7 RW Oi	1.047	0.035	0.160	0.007	1.250	8
12	SPR	2,8 RW A	2,8 RW	A	A	1	2	B	RW	RW A	18	0	14	7	14	19.975	1.552	2.985	0.086	24.597	2,8 RW	2, 8RW Oi	1.833	0.089	0.331	0.014	2.267	15
13	SPR	3,10 RW A	*3,10 RW*	A	A	1	2	B	RW	RW A	9	0	12	6	12	15.668	1.514	2.593	0.168	19.942	*3,10 RW*	2,10 RW O	1.003	0.108	0.162	0.025	1.298	6
14	SPR	3,2 RW A	3,2 RW	A	A	1	3	C	RW	RW A	27	0	11	5.5	11	60.243	1.693	2.793	0.172	64.900	3,2 RW	3,2 RW O	2.638	0.061	0.204	0.010	2.912	16
15	SPR	3,3 RW A	3,3 RW	A	A	1	3	C	RW	RW A	21	0	11	5.5	11	23.489	2.248	4.064	0.187	29.987	3,3 RW	3,3 RW Oi	1.109	0.117	0.216	0.015	1.458	8
16	SPR	3,5 RW A1	3,5 RW	A1	A	1	3	C	RW	RW A	11	0	7	3.5	7	22.489	1.979	4.405	0.194	29.067	3,5 RW	3,5 RW Oi	0.657	0.111	0.129	0.011	0.907	3
17	SPR	3,5 RW A2	3,5 RW	A2	A	2	3	C	RW	RW A	11	7	21	14	14	19.833	1.685	3.808	0.190	25.517	3,5 RW							
18	SPR	3,7 RW A1	3,7 RW	A1	A	1	3	C	RW	RW A	21	0	33	16.5	33	26.929	2.050	3.960	0.206	33.146	3,7 RW	3,7 RW O	1.314	0.073	0.234	0.013	1.634	15
19	SPR	3,7 RW A2	3,7 RW	A2	A	2	3	C	RW	RW A	21	33	61	47	28	32.575	2.201	4.192	0.209	39.178	3,7 RW							
20	SPR	3,9 RW A	3,9 RW	A	A	1	3	C	RW	RW A	17	0	15	7.5	15	13.237	1.135	2.487	0.075	16.933	3,9 RW	3,9 RW O	0.951	0.061	0.145	0.006	1.163	3
21	SPR	3,9 RW Ab	3,9 RW	Ab	A	2	3	C	RW	RW A	17	48	78	63	30	17.025	1.925	4.670	0.108	23.728	3,9 RW							
22	BC	85 RW A	85	A	A	1			RW	RW A	84	0	16	8	16	22.713	0.655	4.703		28.071		85 RW O	3.074	0.114	0.254	0.015	3.457	8
23	BC	58 RW A	58	A	A	1			RW	RW A	19	0	15	7.5	15	30.319	0.365	9.013	0.824	40.522		58 RW Oi	2.189	0.070	0.207	0.025	2.492	4
24	BC	328 RW A	328	A	A	1			RW	RW A	13	0	12	6	12	33.923	0.830	6.828	0.891	42.471		328 RW Oi	1.743	0.043	0.260	0.016	2.062	6
25	BC	290 A	290	A	A	1			RW	RW A	38	0	20	10	20	39.653	1.498	10.346	0.749	52.246		290 O	1.989	0.089	0.376	0.027	2.481	18
26	BC	165 A	165	A	A	1			RW	RW A	46	0	24	12	24	26.217	0.925	5.680	0.721	33.543		165 Oi	2.037	0.077	0.220	0.035	2.369	8
27	BC	532 RW A1	532	A1	A	1			RW	RW A	50	0	15	7.5	15	24.704	0.848	10.564	0.803	36.919		532 RW Oi	1.505	0.080	0.567	0.018	2.170	14
28	BC	532 RW A2	532	A2	A	2			RW	RW A	50	15	51	33	36	12.400	0.415	6.612	0.709	20.137								
29	BC	322 RW A1	322	A1	A	1			RW	RW A	24	0	14	7	14	22.027	1.100	6.449		29.576		322 RW Oi	1.955	0.065	0.248	0.018	2.286	12
30	BC	322 RW A2	322	A2	A	2			RW	RW A	24	14	52	33	38	10.597	0.285	3.853		14.734								
31	BC	129 RW A1	129	A1	A	1			RW	RW A	10	0	16	8	16	30.569	0.980	6.655		38.204								
32	BC	129 RW A2	129	A2	A	2			RW	RW A	10	16	42	29	26	18.222	0.803	3.988		23.013								
33	Transect	114 RW A					114		RW	RW A	60			5	10	23.126	2.829	7.446	0.850	34.251		114 RW O	2.125	0.053	0.295	0.010	2.483	10
34	Transect	6092 RW A					6092		RW	RW A	76			5	10	19.320	2.349	7.820	0.895	30.384		6092 RW O	1.093	0.086	0.162	0.016	1.357	4
35	Transect	2156 RW A					2156		RW	RW A	50			5	10	17.685	1.131	4.463		23.280		2156 RW O	1.454	0.084	0.218	0.026	1.781	
36	Transect	3339 RW A					3339		RW	RW A	56			5	10	24.363	2.570	5.167	1.183	33.283		3339 RW1 O	1.525	0.066	0.237	0.027	1.854	11
37	Transect	5849 RW A					5849		RW	RW A	66			5	10	32.137	2.114	8.085	0.689	43.026		5849 RW O	2.022	0.063	0.292	0.012	2.390	15

Appendix C: Data sheet for 20 cm fixed-depth horizon averages, for Cotrufo comparison

Swanton Pacific Ranch: data sheets for average C/N, SOC, and POXC/SOC in top 20 cm of each profile

										POXC/SOC								%SOC							C/N							
No	Sample ID	Pit	Zone	Horizon _Simple	Veg	New Top Depth (cm)	New Bottom Depth (cm)	Thickness (cm)		POXC/SOC	If and 1 (cm)	If and 2 (cm)	POXC/C	POXC/C per 20 cm	POXC/C top 20	If under 20	Final POXC/C top 20	Pit	POXC/SOC	% SOC	If and 1 (cm)	If and 2 (cm)	%C *20 cm	%C per 20 cm	%C top 20	If under 20	%C avg top 20	Pit	% SOC	C/N	If and 1 (cm)	If and 2 (cm)	C/N
1	1,- A	1,-	1	A	RW	0	19	19		0.0196	19	0	0.372339	0.01861693	0.019698		0.019698	1,-	0.0197	6.44	19	0	122.4429083	6.12214541	6.23344775		6.23744775	1,-	6.24	17.9	19	0	340.109744
2	1,- Bw1	1,-	1	B	RW	19	55	36		0.0216	0	1	0.021613	0.00310863				1,1	0.0159	2.31	0	1	2.306040724	0.11530234				1,1	6.17	12.2	0	1	12.17797613
3	1,- BW2	1,-	1	B	RW	55	93	38		0.0268	0	0	0	0				1,12	0.0207	2.33	0	0	0	0				1,12	5.26	13.4	0	0	0
4	1,1 A	1,1	1	A	G	0	14	14		0.0159	14	0	0.222513	0.01113565	0.011126	0.0159	0.015894	1,2	0.0166	6.17	14	0	86.35495377	4.31774769	4.31774769	6.168213	6.16821098	1,2	2.60	10.5	14	0	147.122722
5	1,12 A1	1,12	1	A	RW	0	14	14		0.0184	14	0	0.258298	0.01291492	0.019744		0.019744	1,20	0.0232	5.85	14	0	81.95624828	4.09781241	5.26289277		5.26289277	1,20	5.25	17.1	14	0	239.932574
6	1,12 A2	1,12	1	A	RW	14	31	17		0.0228	0	6	0.136575	0.00682873				1,3	0.0200	3.88	0	0	23.30160713	1.16508036				1,3	2.77	15.2	0	6	91.47890576
7	1,12 AB	1,12	1	AB	RW	31	49	18		0.0261	0	0	0	0				1,4 RW	0.0266	2.40	0	0	0	0				1,4 RW	4.32	12.7	0	0	0
8	1,12 BW	1,12	1	B	RW	49	89	40		0.0250	0	0	0	0				1,5	0.0167	1.97	0	0	0	0				1,5	4.24	12.4	0	0	0
9	1,2 A	1,2	1	A	G	0	12	12		0.0200	12	0	0.239633	0.01198165	0.016583		0.016583	1,5 RW	0.0193	3.27	12	0	39.21113491	1.96055675	2.60358343		2.60358343	1,5 RW	4.13	10.8	12	0	129.254978
10	1,2 Bt1	1,2	1	B	G	12	42	30		0.0115	0	8	0.092029	0.00460147				1,6 RW	0.0267	1.61	0	8	12.86053371	0.64302669				1,6 RW	3.21	9.8	0	8	78.51136
11	1,2 Bt2	1,2	1	B	G	42	53	11		0.0013	0	0	0	0				2,1 G	0.0227	4.10	0	0	0	0				2,1 G	2.23	9.2	0	0	0
12	1,20 A	1,20	1	A	RW	0	31	31		0.0232	0	20	0.463257	0.02316283	0.023163		0.023163	2,1 RW	0.0192	5.25	0	20	105.0806618	5.25403309	5.25403309		5.25403309	2,1 RW	7.63	21.2	0	20	423.96475
13	1,20 Ab	1,20	1	Ab	RW	99	104	5		0.0258	0	0	0	0				2,2 G	0.0232	3.63	0	0	0	0				2,2 G	3.82	15.6	0	0	0
14	1,20 C1	1,20	1	C	RW	31	62	31		0.0298	0	0	0	0				2,2 RW	0.0181	1.48	0	0	0	0				2,2 RW	2.12	13.0	0	0	0
15	1,20 C2	1,20	1	C	RW	62	99	37		0.0260	0	0	0	0				2,3 G	0.0189	2.24	0	0	0	0				2,3 G	3.29	14.3	0	0	0
16	1,3 A	1,3	1	A	G	0	13	13		0.0220	13	0	0.28659	0.01432949	0.020044		0.020044	2,4 G	0.0210	3.08	13	0	40.01345849	2.00067292	2.76791812		2.76791812	2,4 G	4.48	10.0	13	0	129.557176
17	1,3 Bt1	1,3	1	B	G	13	27	14		0.0163	0	7	0.114298	0.00571491				2,7 RW	0.0225	2.19	0	7	15.34460395	0.7672452				2,7 RW	4.60	8.8	0	7	61.47272179
18	1,3 Bt2	1,3	1	B	G	27	44	17		0.0188	0	0	0	0				2,8 RW	0.0254	1.82	0	0	0	0				2,8 RW	4.58	8.5	0	0	0
19	1,3 Bt3	1,3	1	B	G	44	69	25		0.0155	0	0	0	0				3,1 G	0.0176	1.66	0	0	0	0				3,1 G	5.12	8.2	0	0	0
20	1,4 RW A	1,4 RW	1	A	RW	0	29	29		0.0266	0	20	0.53292	0.02664602	0.026646		0.026646	*3,10 RW	0.0251	4.32	0	20	86.45963669	4.32298183	4.32298183		4.32298183	*3,10 RW	3.69	14.5	0	20	289.08346
21	1,4 RW AB1	1,4 RW	1	AB	RW	29	81	52		0.0258	0	0	0	0				3,2 G	0.0208	2.16	0	0	0	0				3,2 G	1.68	12.2	0	0	0
22	1,4 RW AB2	1,4 RW	1	AB	RW	81	110	29		0.0174	0	0	0	0				3,2 RW	0.0161	1.39	0	0	0	0				3,2 RW	9.79	11.4	0	0	0
23	1,4 RW Bt	1,4 RW	1	B	RW	110	139	29		0.0206	0	0	0	0				3,3 G	0.0172	0.76	0	0	0	0				3,3 G	5.46	9.1	0	0	0
24	1,5 A1	1,5	1	A	G	0	15	15		0.0170	15	0	0.254393	0.01272966	0.016691		0.016691	3,3 RW	0.0285	4.34	15	0	65.06489038	3.25324452	4.2392996		4.2392996	3,3 RW	4.20	10.5	15	0	157.109734
25	1,5 A2	1,5	1	A	G	15	25	10		0.0159	0	5	0.079438	0.00397092				3,5 RW	0.0223	3.94	0	5	19.72110152	0.98605508				3,5 RW	5.71	10.1	0	5	50.41175
26	1,5 RW A	1,5 RW	1	A	RW	0	28	28		0.0193	0	20	0.386624	0.01932121	0.019331		0.019331	3,6 G	0.0210	4.13	0	20	82.68351555	4.13417578	4.13417578		4.13417578	3,6 G	1.92	13.4	0	20	267.986405
27	1,5 RW AB	1,5 RW	1	AB	RW	28	46	18		0.0191	0	0	0	0				3,7 RW	0.0277	2.32	0	0	0	0				3,7 RW	3.87	12.3	0	0	0
28	1,5 RW BW1	1,5 RW	1	B	RW	46	73	27		0.0174	0	0	0	0				3,9 RW	0.0284	2.21	0	0	0	0				3,9 RW	2.67	12.3	0	0	0
29	1,5 RW BW2	1,5 RW	1	B	RW	73	120	47		0.0173	0	0	0	0						1.93	0	0	0	0						11.6	0	0	0
30	1,6 RW A	1,6 RW	1	A	RW	0	22	22		0.0267	0	20	0.534033	0.02670163	0.026702		0.026702	3,21	0	3.21	0	20	64.12098885	3.20604944	3.20604944		3.20604944	3,21	0	14.2	0	20	284.978953
31	1,6 RW BA	1,6 RW	1	AB	RW	22	57	35		0.0340	0	0	0	0				2,00	0	2.00	0	0	0	0				3,9	0	13.9	0	0	0
32	1,6 RW BW	1,6 RW	1	B	RW	57	110	53		0.0254	0	0	0	0				0,86	0	0.86	0	0	0	0						10.2	0	0	0
33	2,1 G A	2,1 G	2	A	G	10	34	14		0.0193	0	10	0.193036	0.00965031	0.022683		0.022683	1,51	0	1.51	0	10	15.08219719	0.75410986	2.22780728		2.22780728	1,51	0	12.5	0	10	125.13708
34	2,1 G AB	2,1 G	2	A	G	24	36	12		0.0164	0	0	0	0				1,48	0	1.48	0	0	0	0						14.2	0	0	0
35	2,1 G Ap	2,1 G	2	A	G	0	10	10		0.0261	10	0	0.260655	0.01303276				2,95	10	2.95	0	0	29.47394848	1.47369742						12.5	10	0	134.642989
36	2,1 G Bt1	2,1 G	2	B	G	36	77	41		0.0174	0	0	0	0				1,29	0	1.29	0	0	0	0						13.9	0	0	0
37	2,1 G Bt2	2,1 G	2	B	G	77	99	22		0.0087	0	0	0	0				0,92	0	0.92	0	0	0	0						13.4	0	0	0
38	2,1 BTg	2,1 G	2	B	G	99	138	39		0.0033	0	0	0	0				0,76	0	0.76	0	0	0	0						13.6	0	0	0
39	2,1 RW A	2,1 RW	2	A	RW	0	21	21		0.0192	0	20	0.383729	0.01918643	0.019186		0.019186	7,63	0	7.63	0	20	152.6275539	7.6313777	7.6313777		7.6313777	7,63	0	16.6	0	20	331.219826
40	2,1 RW B	2,1 RW	2	B	RW	21	64	43		0.0260	0	0	0	0				1,30	0	1.30	0	0	0	0						9.1	0	0	0
41	2,1 RW C	2,1 RW	2	C	RW	64	84	20		0.0230	0	0	0	0				0,58	0	0.58	0	0	0	0						6.7	0	0	0
42	2,1 RW C2	2,1 RW	2	C	RW	84	104	20		0.0225	0	0	0	0				0,72	0	0.72	0	0	0	0						8.1	0	0	0
43	2,1 RW C3	2,1 RW	2	C	RW	104	115	11		0.0320	0	0	0	0				0,76	0	0.76	0	0	0	0						9.1	0	0	0
44	2,2 G AB	2,2 G	2	A	G	30	38	8		0.0181	0	0	0	0	0.023162		0.023162	2,32	0	2.32	0	0	0	0	1.81680584		1.81680584	2,32	0	14.8	0	0	0
45	2,2 G Ap	2,2 G	2	A	G	0	30	30		0.0222	0	20	0.443242	0.02216209				3,82	0	3.82	0	20	76.33616579	3.81680584	3.81680584		3.81680584	3,82	0	14.2	0	20	363.25162
46	2,2 G Bt1	2,2 G	2	B	G	38	96	58		0.0151	0	0	0	0				1,72	0	1.72	0	0	0	0						15.5	0	0	0
47	2,2 G Bt2	2,2 G	2	B	G	96	133	37		0.0138	0	0	0	0				1,35	0	1.35	0	0	0	0						15.1	0	0	0
48	2,2 G Bt3	2,2 G	2	B	G	133	147	14		0.0169	0	0	0	0				1,59	0	1.59	0	0	0	0						15.5	0	0	0
49	2,2 RW A	2,2 RW	2	A	RW	0	28	28		0.0181	0	20	0.362836	0.01814182	0.018142		0.018142	2,12	0	2.12	0	20	42.42671013	2.12133551	2.12133551		2.12133551	2,12	0	14.9	0	20	297.940574
50	2,2 RW B	2,2 RW	2	B	RW	28	51	23		0.0369	0	0	0	0				0,94	0	0.94	0	0	0	0						18.1	0	0	0
51	2,2 RW C	2,2 RW	2	C	RW	51	66	15		0.0242	0	0	0	0				0,57	0	0.57	0	0	0	0						24.6	0	0	0
52	2,2 RW C2	2,2 RW	2	C	RW	66	104	38		0.0259	0	0	0	0				0,26	0	0.26	0	0	0	0						23.1	0	0	0
53	2,3 G A	2,3 G	2	A	G	0	15	15		0.0209	15	0	0.314231	0.01571153	0.018892		0.018892	3,76	15	3.76	0	0	56.34639859	2.81731993	3.28780803		3.28780803	3,76	0	11.1	15	0	165.895416
54	2,3 G Bt	2,3 G	2	B	G	15	46	33		0.0127	0	5	0.063616	0.00318081				1,86	0	1.86	0	5	9.407926205	0.4704681				1,86	0	9.9	0	5	49.74288351
55	2,4 G A	2,4 G	2	A	G	0	10	10		0.0210	10	0	0.209664	0.0104832	0.010483	0.021	0.020966	4,48	10	4.48	0	10	44.8265038	2.24132514	2.24132514	4.48265	4.48265038	4,48	0	12.2	10	0	122.444232
56	2,7 RW A	2,7 RW	2	A	RW	0	27	27		0.0225	0	20	0.450303	0.02251513	0.022515		0.022515	4,60	0	4.60	0	20	92.03510284	4.60175514	4.60175514		4.60175514	4,60	0	19.4	0	20	388.323727
57	2,7 RW B	2,7 RW	2	B	RW	27	71	44		0.0368	0	0	0	0				0,77	0	0.77	0	0	0	0						19.6	0	0	0
58	2,7 RW C	2,7 RW	2	C	RW	71	135	64		0.0327	0	0	0	0				0,49	0	0.49	0	0	0	0						15.9	0	0	0
59	2,8 RW A	2,8 RW	2	A	RW	0	14	14		0.0242	14	0	0.339468	0.01697342	0.025412		0.025412	5,51	14	5.51	0	14	77.10794558	3.85539728	4.57557738		4.57557738	5,51	14	17.2	14	0	240.190235
60	2,8 RW AB	2,8 RW	2	AB	RW	14	24	10		0.0281	0	6	0.168781	0.00843903				2,40	0	2.40	0	6	14.40420198	0.7202101				2,40	0	14.6	0	6	87.5546261
61	2,8 RW B	2,8 RW	2	B	RW	24	34	10		0.0201	0	0	0	0				1,10	0	1.10	0	0	0	0						13.8	0	0	0
62	2,8 RW BC	2,8 RW	2	BC	RW	34	39	5		0.0281	0	0	0	0				1,17	0	1.17	0	0	0	0						15.5	0	0	0
63	3,1 G A	3,1 G	3	A	G	0	20	20		0.0176	20	0	0.352277	0.01756387	0.017564		0.017564	5,12	20	5.12	0	0	102.3512554	5.11756277	5.11756277		5.11756277	5,12	0	13.4	20	0	267.399188
64	3,1 G AB1	3,1 G	3	AB	G	20	46	26		0.0163	0	0	0	0				3,14	0	3.14	0	0	0	0						13.4	0	0	0
65	3,1 G AB2	3,1 G	3	AB	G	46	80	34		0.0156	0	0	0	0				2,34	0	2.34	0	0	0	0						13.1	0	0	0
66	3,1 G Bt1	3,1 G	3	B	G	80	113	33		0.0114	0	0	0	0				0,64	0	0.64	0	0	0	0						8.2	0	0	0
67	3,1 G Bt2	3,1 G	3	B	G	113	150	37		0.0074	0	0	0	0				0,68	0	0.68	0	0	0	0						9.2	0	0	0
68	3,10 RW A	*3,10 RW	2	A	RW	0	12	12		0.0250	12	0	0.299781	0.01498905	0.025122		0.025122	4,93	12	4.93	0	12	59.1722	2.95861	3.68849106		3.68849106	4,93	12	16.0	12	0	192.116883
69	3,10 RW BC	*3,10 RW	2	BC	RW	47	79	32		0.0068	0	0	0	0				2,35	0	2.35	0	0	0	0						14.9	0	0	0
70	3,10 RW Bt	*3,10 RW	2	B	RW	12	47	35		0.0253	0	8	0.202662	0.01013311				1,82	0	1.82	0	8	14.59782124	0.72989106				1,82	0	11.0	0	8	87.8125956
71	3,2 G A1	3,2 G	3	A	G	0	17	17		0.0215	17	0	0.365612	0.0182806	0.020849		0.020849	1,82	17	1.82	0	17	31.02037013	1.55101851	1.67587057		1.67587057	1,82	0	11.0	17	0	186.607667
72	3,2 G A2	3,2 G	3	A	G	17	39	22		0.0171	0	3	0.051374	0.00256869				0,83	0	0.83	0	3	2.497041285	0.12485206				0,83	0	9.9	0	3	29.81033111
73	3,2 G Bt1	3,2 G	3	B	G	39	68	29		0.0110	0	0	0	0				0,38	0	0.38	0	0	0	0						6.8	0	0	0
74	3,2 G Bt2	3,2 G	3	B	G	68	95	27		0.0132	0	0	0	0				0,27	0	0.27	0	0	0	0						6.6	0	0	0
75	3,2 G Bt3	3,2 G	3	B	G	95	119	24		0.0088	0	0	0	0				0,19	0	0.19	0	0	0	0						5.7	0	0	0
76	3,2 RW A	3,2 RW	3	A	RW	0	11	11		0.0139	11	0	0.152918	0.00764592	0.016064		0.016064	11,45	11	11.45	0	0	125.9608117	6.29804059	9.78858895		9.78858895	11,45	0	16.9	11	0	188.222172
77	3,2 RW AB	3,2 RW	3	AB	RW	11	34	23		0.0187	0	9	0.168367	0.00841835				7,76	0	7.76	0	9	69.81116724	3.49055836				7,76	0	14.7	0	9	132.659363
78	3,2 RW B	3,2 RW	3	B	RW	34	89	55		0.0305	0	0	0	0				1,65	0	1.65	0	0	0	0						12.9	0	0	0
79	3,3 G A	3,3 G	3	A	G	0	19	19		0.0172	19	0	0.327312	0.01636562	0.01715		0.01715	5,55	19	5.55	0	19	105.4168534	5.27084267	5.46019775		5.46019775	5,55	19	13.8	19	0	261.939805
80	3,3 G AB	3,3 G	3	AB	G	19	47	28		0.0157	0	1	0.0158	0.00079852				3,79	0	3.79	0	1	3.787101507	0.18935508				3,79	0	14.3	0	1	14.2931681
81	3,3 G BA1	3,3 G	3	AB	G	47	66	19		0.0178	0	0	0	0				2,60	0	2.60	0	0	0	0						13.6	0	0	0
82	3,3 G BA2	3,3 G	3	B	G	66	92	26		0.0149	0	0	0	0				1,56	0	1.56	0	0	0	0						12.4	0	0	0
83	3,3 G Bt2	3,3 G	3	B	G	92	150	58		0.0113	0	0	0	0				0,96	0	0.96	0	0	0	0						10.7	0	0	0
84	3,3 RW A	3,3 RW	3	A	RW	0	11	11		0.0255	11	0	0.280798	0.01403994	0.028456		0.028456	5,39	11	5.39	0	0	59.31671762	2.96583588	4.20473428		4.20473428	5,39	11	17.1	11	0	187.038869
85	3,3 RW AB	3,3 RW	3	AB	RW	11	34	23		0.0320	0	9	0.288323	0.01441613				2,75	0	2.75	0	9	24.77796793	1.2388984				2,75	0	13.5	0	9	121.894553
86	3,5 RW A1	3,5 RW	3	A	RW	0	7	7		0.0193	7	0	0.134815	0.00674073	0.02235		0.02235	6,80	7	6.80	0	7	47.59155989	2.37957799	5.7148926		5.7148926	6,80	7	17.2	7	0	120.356094
87	3,5 RW A2	3,5 RW	3	A	RW	7	21	14		0.0240	0	13	0.312126	0.0156388				5,13	14	5.13	0	13	66.70623215	3.33531461				5,13	14	19.5	0	13	195.519336
88	3,6 G A1	3,6 G	3	A	G	0	16	16		0.0214	16	0	0.342792	0.0171396	0.020962		0.020962	2,14	16	2.14	0	0	34.28432465	1.71421623	1.92143686		1.92143686	2,14	0	11.7	16	0	186.426529
89	3,6 G A2	3,6 G	3	A	G	16	33	17		0.0191	0	4	0.076439	0.00382194				1,04	0	1.04	0	4	4.164412518	0.20722063				1,04	0	10.3	0	4	41.05211044
90	3,6 G Bt1	3,6 G	3	B	G	33	53	20		0.0106	0	0	0	0				0,42	0	0.42	0	0	0	0						7.5	0	0	0
91	3,6 G Bt2	3,6 G	3	B	G	53	91	38		0.0060	0	0	0	0				0,21	0	0.21	0	0	0	0						6.2	0	0	0
92	3,6 G Bt3	3,6 G	3	B	G	91	111	20		0.0105	0	0	0	0				0,29	0	0.29	0	0	0	0						7.2	0	0	0
93	3,6 G Bt4	3,6 G	3	B	G	111	115	4		0.0000	0	0	0	0				0,07	0	0.07	0	0	0	0						3.7	0	0	0
94	3,7 RW A1	3,7 RW	3	A	RW	0	33	33		0.0277	0	20	0.553553	0.02767765	0.027678		0.027678	3,87	0	3.87	0	20	77.46534824	3.87326741	3.87326741		3.87326741	3,87	0	14.3	0	20	285.924108
95	3,7 RW A2	3,7 RW	3	A	RW	33	61	28		0.0197	0	0	0	0				5,97	0	5.97	0	0	0	0						17.1	0	0	0
96	3,7 RW AB	3,7 RW	3	AB	RW	61	117	56		0.0218	0	0	0	0				3,77	0	3.77	0	0	0	0						14.4	0	0	0
97	3,7 RW BA	3,7 RW	3	AB	RW	117	124	7		0.0243	0	0	0	0				2,33	0	2.33	0	0	0	0						12.7	0	0	0
98	3,9 RW A	3,9 RW	3	A	RW	0	15	15		0.0289	15	0	0.43415	0.02170749	0.028425		0.028425	3,14	15	3.14	0	0	47.07082729	2.35384136	2.66749331		2.66749331	3,14	0	14.2	15	0	213.678116
99	3,9 RW Ab	3,9 RW	3	Ab	RW	48	76	28		0.0208	0	0	0	0				3,00	0	3.00	0	0	0	0						14.0	0	0	0
100	3,9 RW B1	3,9 RW	3	B	RW	15	48	33		0.0269	0	5	0.134356	0.00671778				1,25	0	1.25	0	5	8.273038983	0.41365195				1,25	0	12.1	0	5	60.55120938
101	3,9 RW B2	3,9 RW	3	B	RW	76	113	35		0.0192	0	0	0	0				1,07	0	1.07	0	0	0	0						10.6	0	0	0
102	3,9 RW B3	3,9 RW	3	B	RW	113	119	6		0.0260	0	0	0	0				0,92	0	0.92	0	0	0	0						10.1	0	0	0

Landels-Hill Big Creek Reserve: data sheets for average C/N, SOC, and POXC/SOC in top 20 cm of each profile

										POXC/SOC										% SOC										C/N									
No	Sample ID	Pit	Field Horizon	Horizon_ Simple	Veg	New upper	New lower	Thickness		POXC/SOC	If and 1 (cm)	If and 2 (cm)	POXC/C *20 cm	POXC/C per 20 cm	POXC/C top 20	if under 20	POXC/C avg top 20		Pit	POXC/SOC	% SOC	If and 1 (cm)	If and 2 (cm)	%C *20 cm	%C per 20 cm	%C top 20	if under 20	%C avg top 20		Pit	% SOC	C/N_053 12020	If and 1 (cm)	If and 2 (cm)	C/N per *cm	C/Na per 20 cm	C/N Top 20	if under 20	C/N avg top 20		Pit	C/N
1	85 RW A	85	A	A	RW	0	16	16		0.03016	16	0	0.482632	0.024132	0.030339		0.030339		85	0.0303	4.48	16	0	71.712	3.5856	4.19157014		4.1915701		85	4.19	20.1	16	0	321.578475	16.0789238	19.2515423		19.2515423		85	19.3
2	85 RW Bw	85	Bw	B	RW	16	57	41		0.03104	0	4	0.124144	0.006207					58	0.0185	3.03	0	4	12.1194028	0.60597014					58	8.33	15.9	0	4	63.4523705	3.17261852					58	18.8
3	85 RW 2Bt	85	2Bt	B	RW	57	107	50		0.04438	0	0	0.000000	0.000000					328	0.0161	0.33	0	0	0	0					328	9.05	9.7	0	0	0	0					328	17.4
4	85 RW 2Btg	85	2Btg	B	RW	107	137	30		0.02935	0	0	0.000000	0.000000					290	0.0110	1.02	0	0	0	0					290	14.08	17.8	0	0	0	0					290	20.2
5	58 RW A	58	A	A	RW	0	15	15		0.01485	15	0	0.222811	0.011141	0.018460		0.018460		165	0.0168	10.14	15	0	152.115	7.60575	8.33475		8.33475		165	8.43	20.1	15	0	301.815476	15.0907738	18.8101616		18.8101616		165	21.1
6	58 RW Bw	58	Bw	B	RW	15	50	35		0.02928	0	5	0.146398	0.007320					442g	0.0213	2.92	0	5	14.58	0.729					442g	2.69	14.9	0	5	74.3877551	3.71938776					442g	11.3
7	58 RW C	58	C	C	RW	50	90	40		0.02956	0	0	0.000000	0.000000					8490g	0.0238	0.91	0	0	0	0					8490g	2.36	14.1	0	0	0	0					8490g	11.0
8	328 RW A	328	A	A	RW	0	12	12		0.01203	12	0	0.144388	0.007219	0.016142		0.016142		7029g	0.0252	12.45	12	0	149.352	7.4676	9.0508		9.0508		7029g	1.90	18.3	12	0	219.312775	10.9656388	17.4014111		17.4014111		7029g	11.1
9	328 RW Bw	328	Bw	B	RW	12	56.5	44.5		0.02231	0	8	0.178444	0.008922					532	0.0171	3.96	0	8	31.664	1.5832					532	6.87	16.1	0	8	128.715447	6.43577236					532	14.6
10	328 RW C	328	C	C	RW	56.5	90	33.5		0.03279	0	0	0.000000	0.000000					322	0.0163	1.70	0	0	0	0					322	6.59	14.9	0	0	0	0					322	15.3
11	290 A	290	A	A	RW	0	20	20		0.01097	20	0	0.219389	0.010969	0.010969		0.010969		129	0.0122	14.08	20	0	281.6	14.08	14.08		14.08		129	10.67	20.2	20	0	403.438395	20.1719198	20.1719198		20.1719198		129	18.4
12	290 Bw1	290	Bw1	B	RW	20	43	23		0.01842	0	0	0.000000	0.000000					1425g	0.0183	7.03	0	0	0	0					1425g	3.31	18.2	0	0	0	0					1425g	12.0
13	290 Bw2	290	Bw2	B	RW	43	84	41		0.03044	0	0	0.000000	0.000000					5820g	0.0267	2.13	0	0	0	0					5820g	2.19	19.9	0	0	0	0					5820g	10.9
14	290 2C	290	2C	C	RW	84	96	12		0.02843	0	0	0.000000	0.000000					8012g	0.0196	1.99	0	0	0	0					8012g	2.59	20.7	0	0	0	0					8012g	10.8
15	165 A	165	A	A	RW	0	24	24		0.01676	0	20	0.335262	0.016763	0.016763		0.016763		3277g	0.0185	8.43	0	20	168.54	8.427	8.427		8.427		3277g	3.12	21.1	0	20	421.35	21.0675	21.0675		21.0675		3277g	10.3
16	165 Bw	165	Bw	B	RW	24	74	50		0.02811	0	0	0.000000	0.000000							2.78	0	0	0	0							17.5	0	0	0	0						
17	165 C	165	C	C	RW	74	99	25		0.02890	0	0	0.000000	0.000000							1.47	0	0	0	0							18.1	0	0	0	0						
18	442g A	442g	A	A	G	0	7	7		0.02132	7	0	0.149222	0.007461	0.007461	0.021317	0.021317				2.69	7	0	18.823	0.94115	0.94115	2.689	2.689				11.3	7	0	78.7573222	3.93786611	3.93786611	11.251046	11.251046			
19	8490g A1	8490g	A1	A	G	0	15	15		0.02351	15	0	0.352604	0.017630	0.023827		0.023827				2.68	15	0	40.26	2.013	2.35675		2.35675				11.0	15	0	165.679012	8.28395062	10.9906435		10.9906435			
20	8490g A2	8490g	A2	A	G	15	30	15		0.02479	0	5	0.123931	0.006197							1.38	0	5	6.875	0.34375							10.8	0	5	54.1338583	2.70669291						
21	8490g Bw	8490g	Bw	B	G	30	84	54		0.01904	0	0	0.000000	0.000000							1.23	0	0	0	0							10.1	0	0	0	0						
22	8490g C	8490g	C	C	G	84	127	43		0.02315	0	0	0.000000	0.000000							0.34	0	0	0	0							6.4	0	0	0	0						
23	7029g A2-A	7029g	A2-A	A	G	0	8	8		0.02118	8	0	0.169404	0.008470	0.025210		0.025210				3.05	8	0	24.384	1.2192	1.9026		1.9026				11.3	8	0	90.3111111	4.51555556	11.0867094		11.0867094			
24	7029g A2-B	7029g	A2-B	A	G	8	26	18		0.02790	0	12	0.334804	0.016740							1.14	0	12	13.668	0.6834							11.0	0	12	131.423077	6.57115385						
25	7029g A3	7029g	A3	A	G	26	60	34		0.03124	0	0	0.000000	0.000000							0.79	0	0	0	0							9.3	0	0	0	0						
26	7029g 2Bt	7029g	2Bt	B	G	60	73	13		0.03225	0	0	0.000000	0.000000							0.38	0	0	0	0							5.0	0	0	0	0						
27	532 RW A1	532	A1	A	RW	0	15	15		0.01591	15	0	0.238628	0.011931	0.017120		0.017120				8.39	15	0	125.775	6.28875	6.872		6.872				15.0	15	0	225	11.25	14.6409884		14.6409884			
28	532 RW A2	532	A2	A	RW	15	51	36		0.02075	0	5	0.103767	0.005188							2.33	0	5	11.665	0.58325							13.6	0	5	67.8197674	3.39098837						
29	532 RW Bt	532	Bt	B	RW	51	57	6		0.03227	0	0	0.000000	0.000000							0.75	0	0	0	0							10.0	0	0	0	0						
30	322 RW A1	322	A1	A	RW	0	14	14		0.01396	14	0	0.195474	0.009774	0.016278		0.016278				8.53	14	0	119.448	5.9724	6.5871		6.5871				15.8	14	0	221.61039	11.0805195	15.3198298		15.3198298			
31	322 RW A2	322	A2	A	RW	14	52	38		0.02168	0	6	0.130094	0.006505							2.05	0	6	12.294	0.6147							14.1	0	6	84.7862069	4.23931034						
32	322 RW Bw1	322	Bw1	B	RW	52	87	35		0.02112	0	0	0.000000	0.000000							1.19	0	0	0	0							14.4	0	0	0	0						
33	322 RW Bw2	322	Bw2	B	RW	87	138	51		0.02989	0	0	0.000000	0.000000							0.66	0	0	0	0							12.2	0	0	0	0						
34	129 RW A1	129	A1	A	RW	0	16	16		0.01137	16	0	0.181938	0.009097	0.012155		0.012155				11.90	16	0	190.432	9.5216	10.6684		10.6684				18.9	16	0	301.793978	15.0896989	18.4041498		18.4041498			
35	129 RW A2	129	A2	A	RW	16	42	26		0.01529	0	4	0.061157	0.003058							5.73	0	4	22.936	1.1468							16.6	0	4	66.2890173	3.31445087						
36	129 RW C1	129	C1	C	RW	42	67	25		0.02482	0	0	0.000000	0.000000							0.51	0	0	0	0							13.8	0	0	0	0						
37	129 RW C2	129	C2	C	RW	67	89	22		0.02705	0	0	0.000000	0.000000							0.66	0	0	0	0							11.8	0	0	0	0						
38	1425g A1	1425g	A1	A	G	0	10	10		0.01775	10	0	0.177521	0.008876	0.018299		0.018299				4.23	10	0	42.29	2.1145	3.3135		3.3135				12.1	10	0	120.828571	6.04142857	11.9770721		11.9770721			
39	1425g A2	1425g	A2	A	G	10	30	20		0.01885	0	10	0.188457	0.009423							2.40	0	10	23.98	1.199							11.9	0	10	118.712871	5.93564356						
40	1425g A3	1425g	A3	A	G	30	75	45		0.02102	0	0	0.000000	0.000000							1.65	0	0	0	0							12.6	0	0	0	0						
41	1425g Bw1	1425g	Bw1	B	G	75	111	36		0.02631	0	0	0.000000	0.000000							1.32	0	0	0	0							12.9	0	0	0	0						
42	1425g Bw2	1425g	Bw2	B	G	111	150	39		0.02579	0	0	0.000000	0.000000							0.85	0	0	0	0							11.8	0	0	0	0						
43	5820g A1	5820g	A1	A	G	0	14	14		0.02574	14	0	0.360349	0.018017	0.026681		0.026681				2.57	14	0	35.966	1.7983	2.18870178		2.1887018				11.2	14	0	157.056769	7.85283843	10.9028523		10.9028523			
44	5820g A2	5820g	A2	A	G	14	40	26		0.02888	0	6	0.173275	0.008664							1.30	0	6	7.80803554	0.39040178							10.2	0	6	61.0002776	3.05001388						
45	5820g A3	5820g	A3	A	G	40	84	44		0.03082	0	0	0.000000	0.000000							1.02	0	0	0	0							10.9	0	0	0	0						
46	5820g 2Bt	5820g	2Bt	B	G	84	110	26		0.03239	0	0	0.000000	0.000000							0.36	0	0	0	0							5.9	0	0	0	0						
47	8012g A1	8012g	A1	A	G	0	19	19		0.01959	19	0	0.372182	0.018609	0.019645		0.019645				2.64	19	0	50.236	2.5118	2.58595		2.58595				10.9	19	0	206.72251	10.3366255	10.837639		10.837639			
48	8012g A2	8012g	A2	A	G	19	45	26		0.02073	0	1	0.020727	0.001036							1.48	0	1	1.483	0.07415							10.0	0	1	10.2022703	0.50101351						
49	8012g AB	8012g	AB	AB	G	45	73	28		0.01932	0	0	0.000000	0.000000							1.29	0	0	0	0							10.5	0	0	0	0						
50	8012g Bt1	8012g	Bt1	B	G	73	92	19		0.02908	0	0	0.000000	0.000000							0.42	0	0	0	0							7.4	0	0	0	0						
51	8012g Bt2	8012g	Bt2	B	G	92	150	58		0.02452	0	0	0.000000	0.000000							0.32	0	0	0	0							6.2	0	0	0	0						
52	3277g A1	3277g	A1	A	G	0	23	23		0.01846	0	20	0.369272	0.018464	0.018464		0.018464				3.12	0	20	62.44	3.122	3.122		3.122				10.3	0	20	206.072607	10.3036304	10.3036304		10.3036304			
53	3277g A2	3277g	A2	A	G	23	60	37		0.02237	0	0	0.000000	0.000000							1.56	0	0	0	0							10.0	0	0	0	0						
54	3277g Bw1	3277g	Bw1	B	G	60	90	30		0.02465	0	0	0.000000	0.000000							1.24	0	0	0	0							11.1	0	0	0	0						
55	3277g Bw2	3277g	Bw2	B	G	90	127	37		0.02121	0	0	0.000000	0.000000							1.11	0	0	0	0							10.3	0	0	0	0						
56	3277g Bw3	3277g	Bw3	B	G	127	150	23		0.01474	0	0	0.000000	0.000000							0.94	0	0	0	0							10.2	0	0	0	0						

Appendix D: Interaction charts for regression models

Profile study at Swanton Pacific Ranch

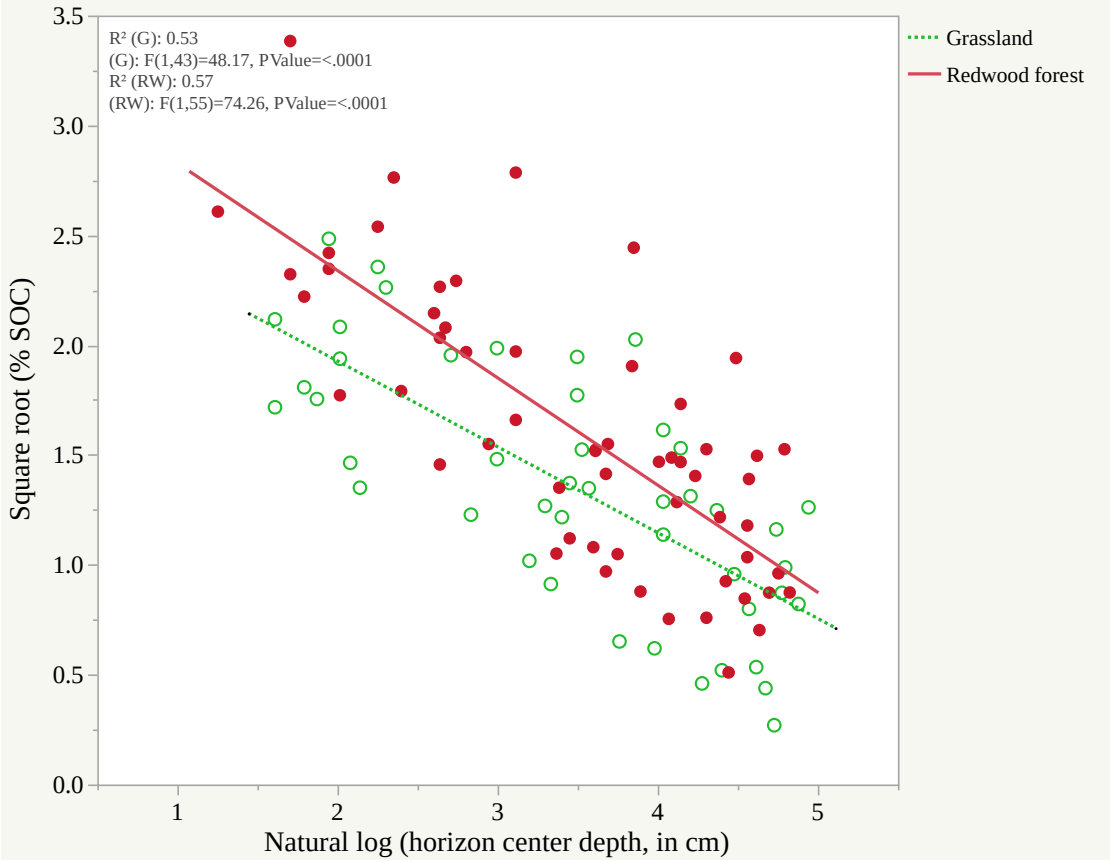

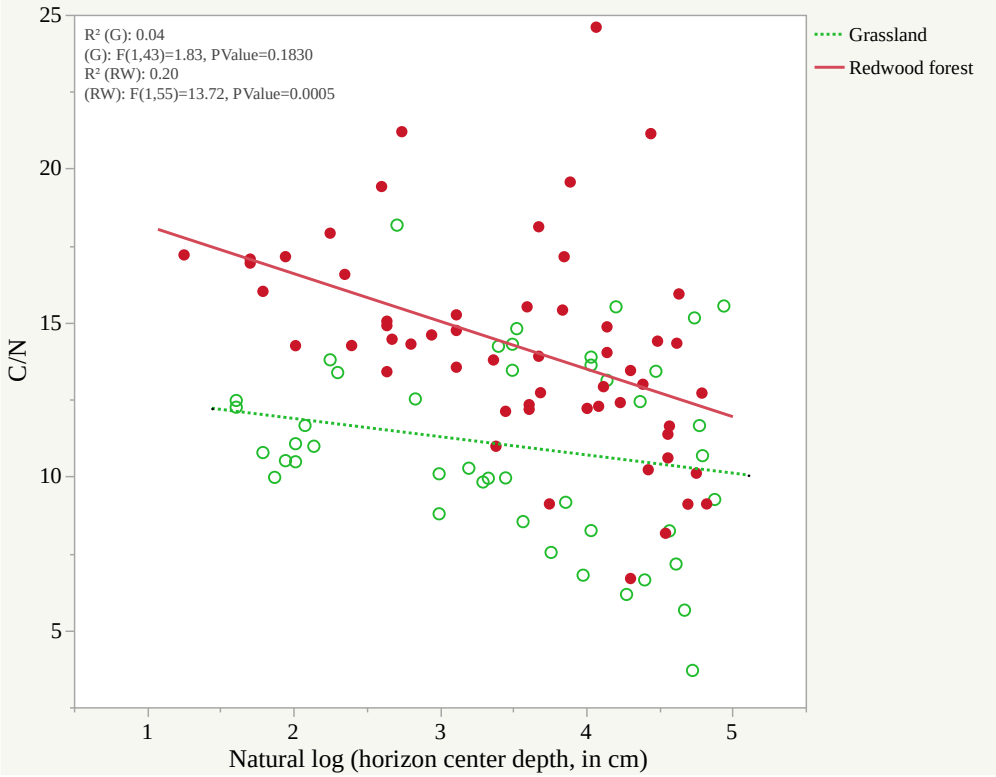
R² (G): 0.04
(G): F(1,43)=1.83, PValue=0.1830
R² (RW): 0.20
(RW): F(1,55)=13.72, PValue=0.0005
Grassland
Redwood forest
C/N
Natural log (horizon center depth, in cm)

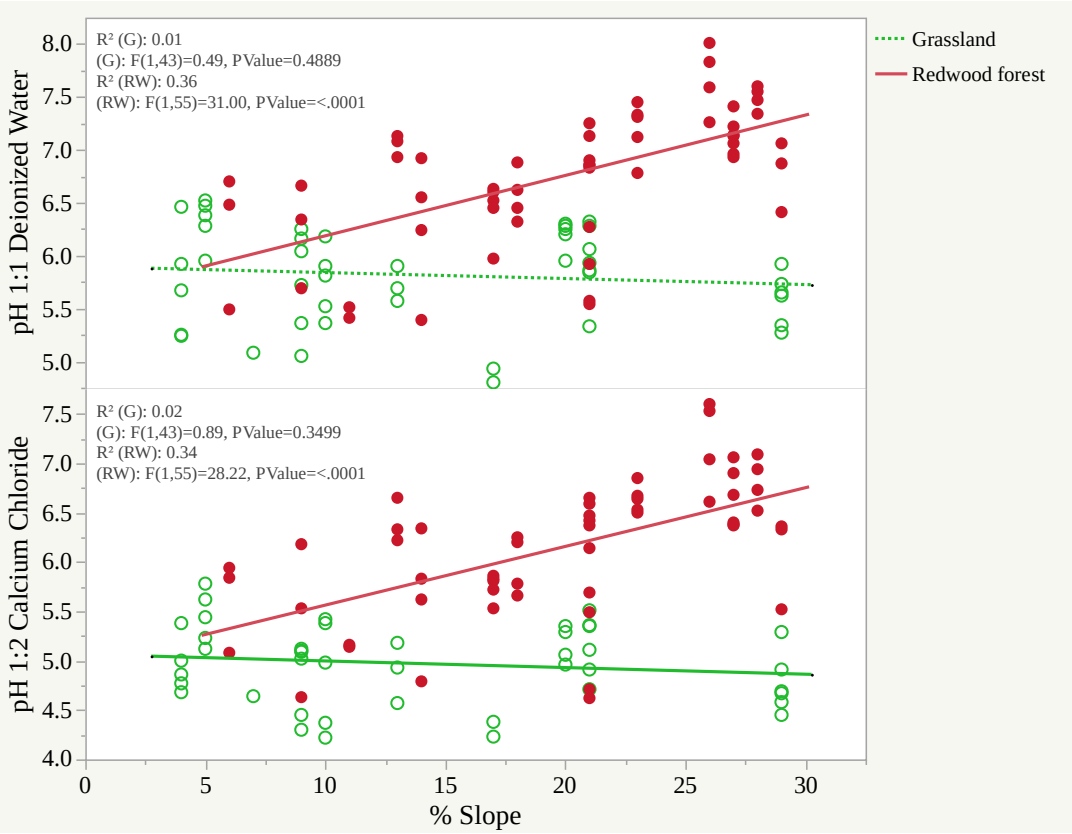
R² (G): 0.01
(G): F(1,43)=0.49, PValue=0.4889
R² (RW): 0.36
(RW): F(1,55)=31.00, PValue=<.0001
R² (G): 0.02
(G): F(1,43)=0.89, PValue=0.3499
R² (RW): 0.34
(RW): F(1,55)=28.22, PValue=<.0001
Grassland
Redwood forest
pH 1:1 Deionized Water
pH 1:2 Calcium Chloride
% Slope

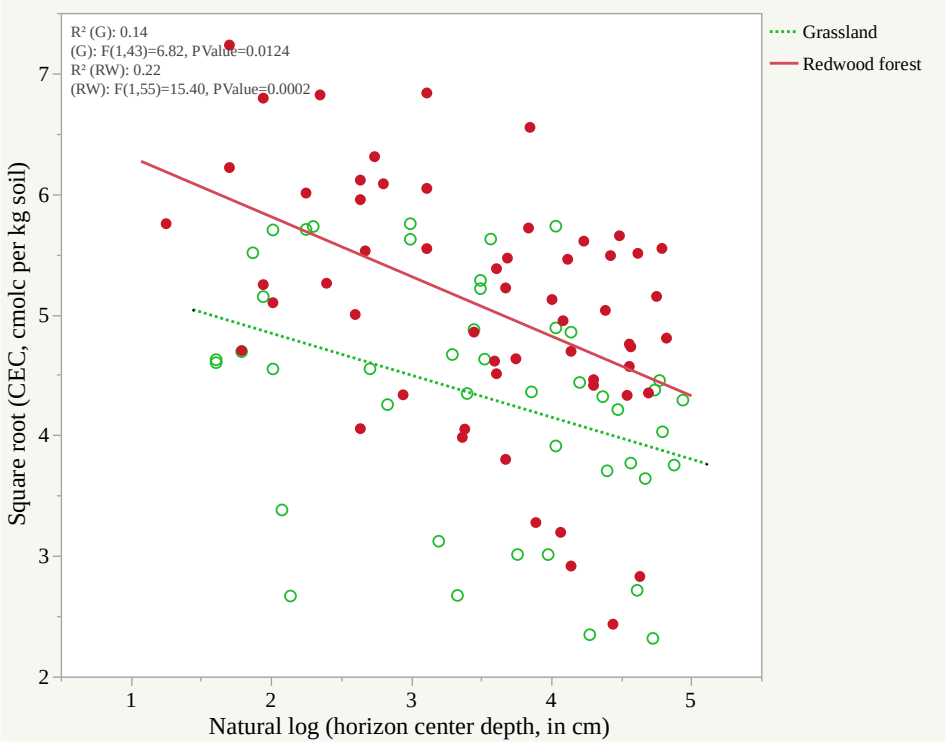
R² (G): 0.14
(G): F(1,43)=6.82, PValue=0.0124
R² (RW): 0.22
(RW): F(1,55)=15.40, PValue=0.0002
Grassland
Redwood forest
Square root (CEC, cmolc per kg soil)
Natural log (horizon center depth, in cm)
2
3
4
5
6
7
1
2
3
4
5

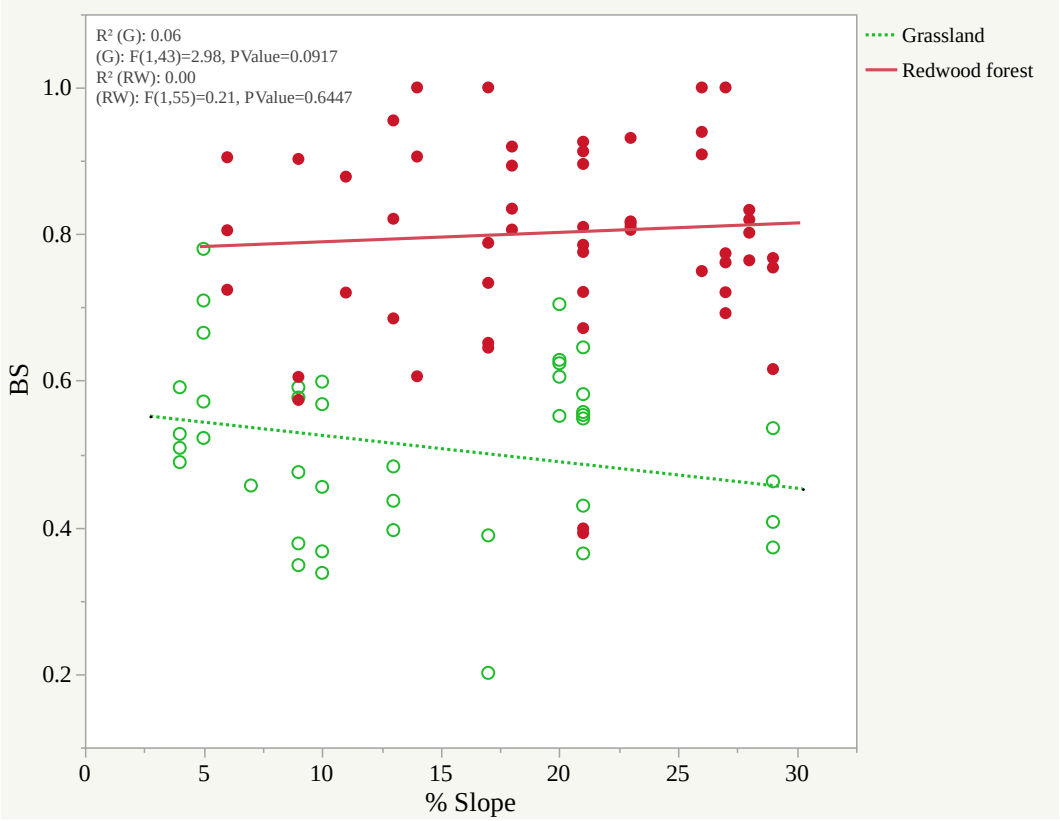
R² (G): 0.06
(G): F(1,43)=2.98, PValue=0.0917
R² (RW): 0.00
(RW): F(1,55)=0.21, PValue=0.6447
Grassland
Redwood forest
BS
% Slope
0.2
0.4
0.6
0.8
1.0
0
5
10
15
20
25
30

Transects study at Swanton Pacific Ranch

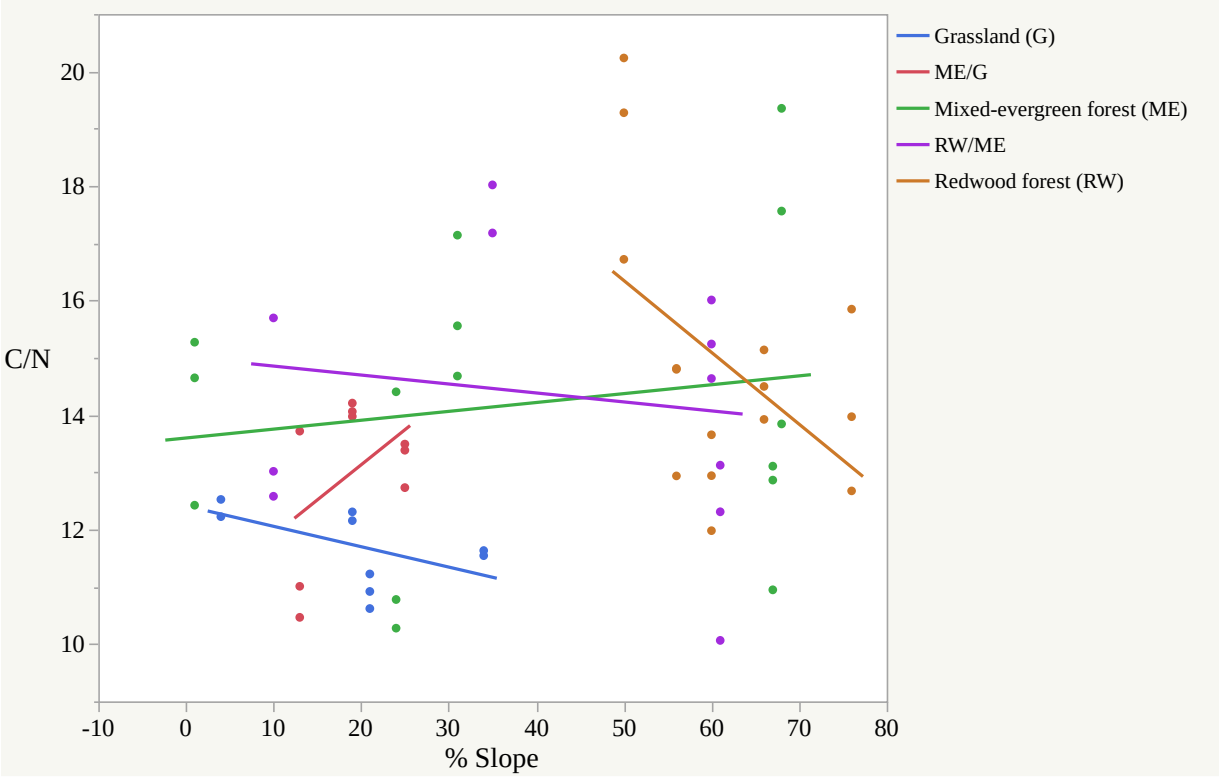

Profile study at Landels-Hill Big Creek Reserve

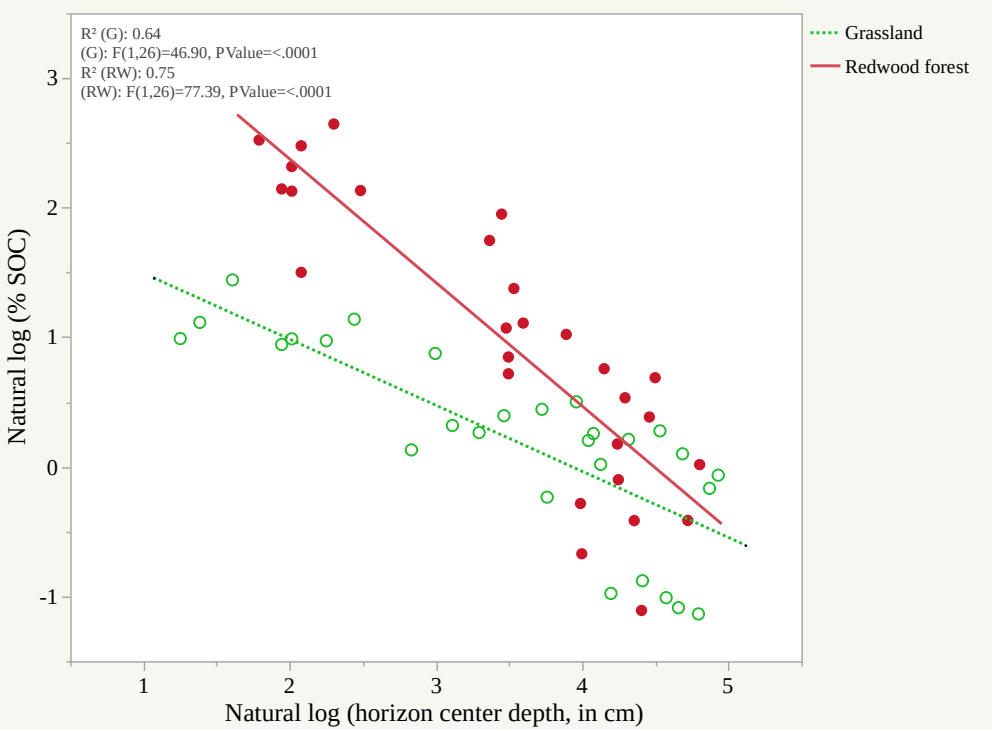

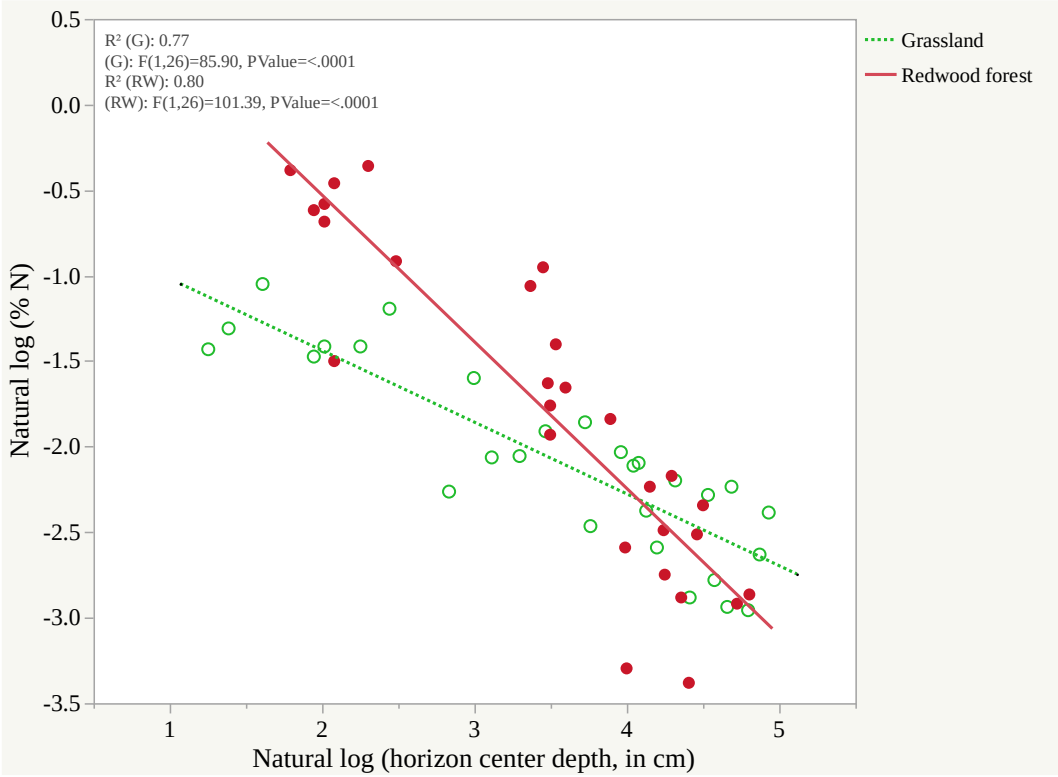

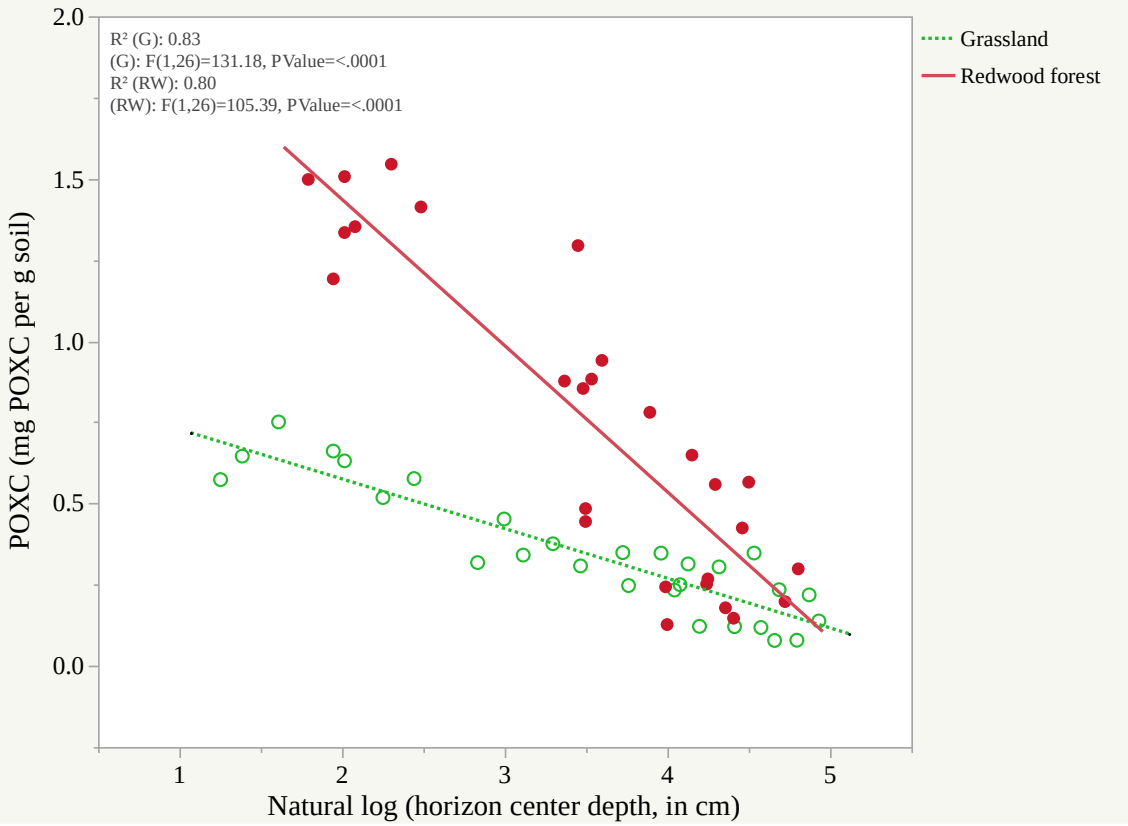
R² (G): 0.83
(G): F(1,26)=131.18, PValue=<.0001
R² (RW): 0.80
(RW): F(1,26)=105.39, PValue=<.0001
Grassland
Redwood forest
POXC (mg POXC per g soil)
2.0
1.5
1.0
0.5
0.0
1
2
3
4
5
Natural log (horizon center depth, in cm)

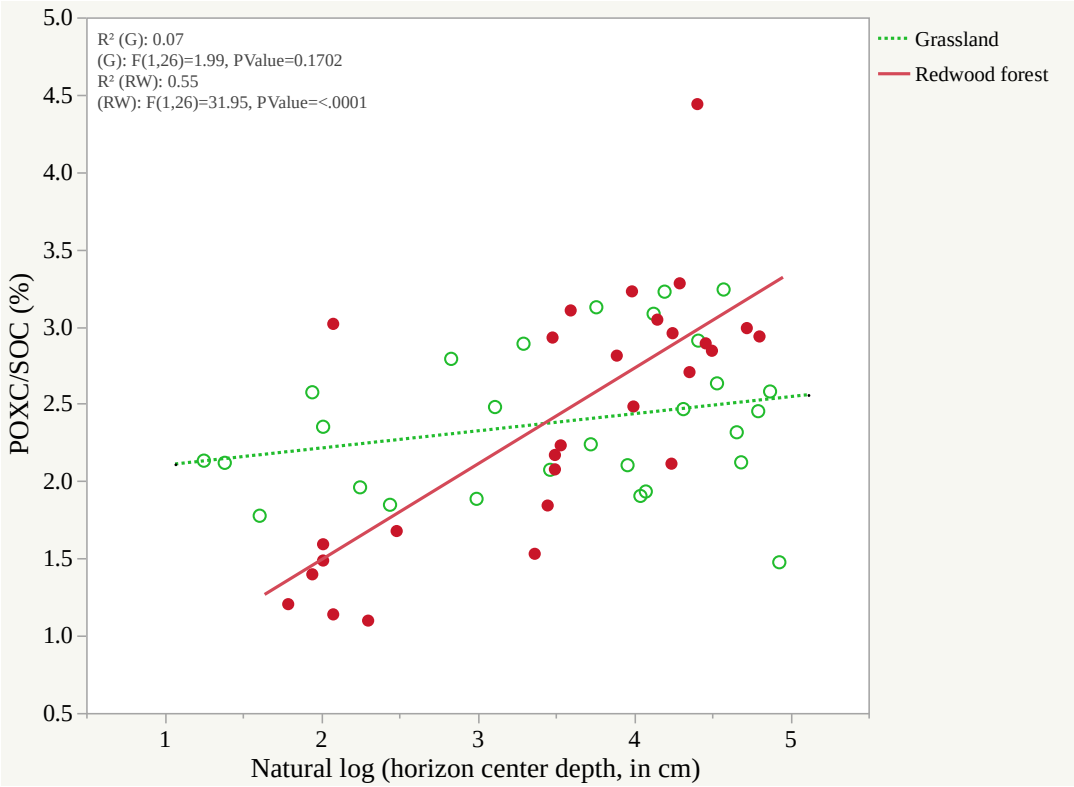
R² (G): 0.07
(G): F(1,26)=1.99, PValue=0.1702
R² (RW): 0.55
(RW): F(1,26)=31.95, PValue=<.0001
Grassland
Redwood forest
POXC/SOC (%)
5.0
4.5
4.0
3.5
3.0
2.5
2.0
1.5
1.0
0.5
1
2
3
4
5
Natural log (horizon center depth, in cm)

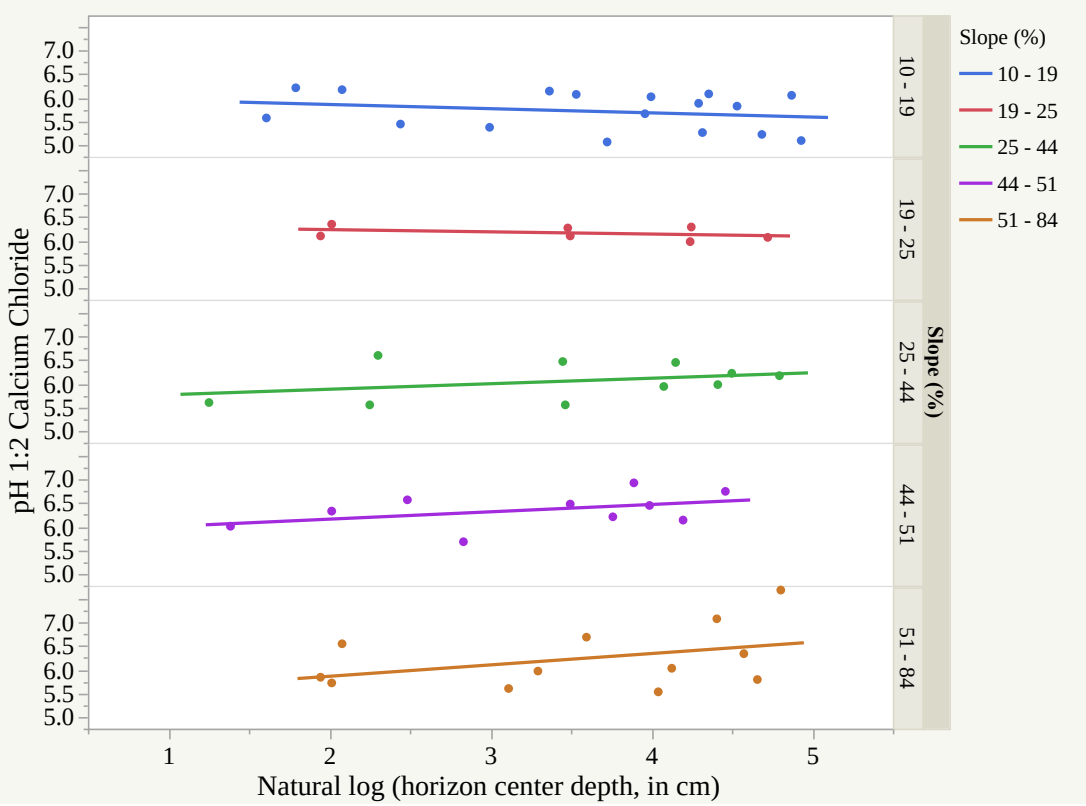
pH 1:2 Calcium Chloride
7.0
6.5
6.0
5.5
5.0
1
2
3
4
5
Natural log (horizon center depth, in cm)
10 - 19
19 - 25
25 - 44
44 - 51
51 - 84
Slope (%)
Slope (%)
10 - 19
19 - 25
25 - 44
44 - 51
51 - 84

Appendix E: Original results section (with more detailed information)

Profiles

Table E.1. Summary of regression analysis on soil properties from 102 horizons collected at Swanton Pacific Ranch, Santa Cruz Co., CA in 2018. Values reported as least square's means (LSM) and standard error (SE) of the regression model in JMP (SAS Institute, Carey, North Carolina) and presented as a function of vegetation type (redwood forest versus mixed annual-perennial grassland). Each response variable was analyzed under the same model, significant effects and interactions (P<0.05) are reported for each response variable. If a transformation was preformed, the 95% confidence interval is reported in back-tranformed units for each vegetation type in parentheses.

Response variable	**R^2**	**Interaction (P<0.05)**	**Sig. Model Predictor (P<0.05)**	**Redwood forest (n=57)**		**Grassland (n=45)**	
				LSM	SE	LSM	SE
√ (SOC)†	0.71	veg*logdepth	slope, horiz, log depth	1.53	0.05	1.40	0.07
				(2.046, 2.687)		(1.573, 2.398)	
√ (N)‡	0.69		zone, slope, horiz, log depth	0.410	0.013	0.421	0.018
				(0.147, 0.19)		(0.147, 0.209)	
C/N§	0.48	veg*logdepth	zone, veg, horiz	14.3*	0.4	11.4	0.6
√ (POXC)¶	0.83		veg, slope, horiz, log depth	0.739*	0.020	0.551	0.028
				(0.490, 0.607)		(0.245, 0.368)	
POXC/C#	0.60	veg*logdepth	veg, log depth	0.025*	0.001	0.015	0.001
log (air-dry θg) ††	0.48		slope, veg, zone	-2.93	0.06	-3.16	0.09
				(0.047, 0.06)		(0.036, 0.051)	
ρ_b‡‡	0.58		veg, slope, horiz, log depth	0.881*	0.032	0.986	0.031
pH 1:1 H_2O	0.62	veg*slope	slope, veg	6.624*	0.072	5.843	0.101
pH 1:2 $CaCl_2$	0.68	veg*slope	slope, veg	6.013*	0.074	4.984	0.104
√ (CEC)§§	0.66	veg*logdepth	slope, horiz, zone, veg	4.928*	0.100	4.599	0.141
				(22.353, 26.3)		(18.632, 23.827)	
BS¶¶	0.66	veg*slope	veg, zone	0.79*	0.02	0.50	0.03

*Significant model association with plant community on response, P <0.05

† Square root of soil organic carbon (%)

‡ Soil total nitrogen (%)

§Soil organic carbon to nitrogen ratio

¶ Square root of permanganate oxidizable carbon (mg POXC g $soil^{-1}$)

Fraction of soil carbon that is permanganate oxidizable carbon

†† Natural log of air-dry soil moisture content

‡‡ Soil bulk density (g soil cm^3 $soil^{-1}$)

§§Square root of soil cation exchange capacity (cmol charge kg $soil^{-1}$)

¶¶ Basic saturation of soil cations

Table E.2. Summary of model predictors on soil properties for 102 soil horizons collected at Swanton Pacific Ranch, Santa Cruz Co., CA in 2018. Model effects are reported for

quantitative explanatory variables and vegetation, if the association was significant (P<0.05). Effects from interactions are not displayed, but can be found in Appendix D.

		Quantitative (P<0.05)		Categorical (P<0.05)			
Response variable	**R^2**		**effect**	**veg**	**effect**	**horizon**	**effect**	**zone**	**effect**
		slope	0.019			A	0.242		
√ (SOC)†	0.71	log depth	-0.265			AB	0.227		
						B	-0.216		
						C	-0.253		
		slope	0.005			A	0.034	1	0.026
√ (N)‡	0.69	log depth	-0.077			AB	0.052	2	-0.044
						B	-0.036	3	0.018
						C	-0.050		
				G	-1.417	A	1.459	1	-0.591
C/N§	0.48			RW	1.417	AB	0.797	2	1.496
						B	-1.782	3	-0.904
						C	-0.474		
		slope	0.009	G	-0.094	A	0.126		
√ (POXC)¶	0.83	log depth	-0.129	RW	0.094	AB	0.125		
						B	-0.105		
						C	-0.145		
POXC/SOC#	0.60	log depth	-0.002	G	-0.005				
				RW	0.005				
		slope	0.030	G	-0.113			1	0.067
log (air-dry θg)††	0.48			RW	0.113			2	-0.254
								3	0.187
		slope	-0.007	G	0.053	A	-0.015		
ρ_b	0.58	log depth	0.065	RW	-0.053	AB	-0.091		
						B	0.106		
						C	n/a		
pH 1:1 H_2O	0.62	slope	0.025	G	-0.391				
				RW	0.391				
pH 1:2 $CaCl_2$	0.68	slope	0.026	G	-0.515				
				RW	0.515				
		slope	0.075	G	-0.165	A	0.208	1	0.147
√ (CEC)§§	0.66			RW	0.165	AB	0.460	2	-0.456
						B	-0.266	3	0.310
						C	-0.402		
				G	-0.149			1	-0.078
BS¶¶	0.66			RW	0.149			2	0.057
								3	0.021

† Square root of soil organic carbon (%)

‡ Soil total nitrogen (%)

§Soil organic carbon to nitrogen ratio

¶ Square root of permanganate oxidizable carbon (mg POXC g soil^{-1})

Fraction of soil carbon that is permanganate oxidizable carbon
†† Natural log of air-dry soil moisture content
‡‡ Soil bulk density (g soil cm^3 $soil^{-1}$)
§§Square root of soil cation exchange capacity (cmol charge kg $soil^{-1}$)
¶¶ Basic saturation of soil cations

Table E.3. Summary of regression analysis on soil properties from 56 horizons collected at Landels-Hill Big Creek Reserve, Monterrey Co., CA in 2019. Values reported as least square's means (LSM) and standard error (SE) of the regression model in JMP (SAS Institute, Carey, North Carolina) and presented as a function of vegetation type (redwood forest versus mixed annual-perennial grassland). Each response variable was analyzed under the same model (see above), significant effects and interactions (P<0.05) are reported for each response variable. If a transformation was preformed, the 95% confidence interval is reported in back-transformed units for each vegetation type in parentheses.

Response variable	R^2	Interaction	sig. alpha	Redwood forest (n=28)		Grassland (n=28)	
				LSM	SE	LSM	SE
log (SOC)†	0.80	veg*log depth	veg, slope, log depth	0.92*	0.09	0.08	0.13
				(2.066, 3.018)		(0.842, 1.394)	
log (N)‡	0.84	veg*log depth	veg, slope, log depth	-1.85*	0.07	-2.17	0.09
				(0.138, 0.181)		(0.095, 0.136)	
log (C/N)§	0.68		veg	2.76*	0.04	2.25	0.05
				(14.6, 17.139)		(8.548, 10.58)	
POXC¶	0.87	veg*log depth	veg, log depth	0.762*	0.034	0.352	0.045
POXC/SOC#	0.65	veg*log depth	slope, log depth	0.024	0.001	0.024	0.001
log(air-dry θg)††	0.70	veg*log depth	veg, log depth	-3.31*	0.04	-3.49	0.06
				(0.034, 0.04)		(0.027, 0.034)	
BD‡‡	0.78		veg, slope, log depth	1.21*	0.05	1.34	0.04
pH 1:1 H_2O	0.72		veg, slope, log depth	6.95*	0.05	6.57	0.07
pH 1:2 $CaCl_2$	0.78	slope*log depth	veg, slope	6.37*	0.05	5.74	0.07
log (CEC)§§	0.77	veg*log depth	veg, slope, log depth	3.05*	0.05	2.77	0.07
				(19.1, 23.278)		(13.945, 18.141)	
BS¶¶	0.42	veg*log depth	slope	0.90	0.02	0.95	0.03

*Significant model association with plant community on response, P <0.05
† Natural log of soil organic carbon (%)
‡ Natural log of total nitrogen (%)
§Natural log of soil organic carbon to nitrogen ratio
¶ Permanganate oxidizable carbon (mg POXC g $soil^{-1}$)
# Fraction of soil organic carbon that is permanganate oxidizable carbon
†† Natural log of air-dry soil moisture content
‡‡ Soil bulk density (g soil $cm^3 soil^{-1}$)
§§Natural log of soil cation exchange capacity (cmol charge kg $soil^{-1}$),
¶¶ Basic saturation of soil cations

Table E.4. Summary of model predictors on soil properties for 56 soil horizons collected at Landels-Hill Big Creek Reserve, Monterrey Co., CA in 2019. Model effects are reported for quantitative explanatory variables and vegetation, if the association was significant (P<0.05). Pedogenic horizon had no significant effect across response variables and is not shown. Effects from interactions are not displayed, but can be found in Appendix D.

		Quantitative. (P<0.05)		**Vegetation (P<0.05)**	
Response variable	**R^2**		**Effect**	**Veg. type**	**Effect**
log (SOC)†	0.80	slope	-0.009	G	-0.418
		log depth	-0.644	RW	0.418
log (N)‡	0.83	slope	-0.007	G	-0.163
		log depth	-0.593	RW	0.163
log (C/N)§	0.68			G	-0.254
				RW	0.254
POXC¶	0.87	log depth	-0.335	G	-0.205
				RW	0.205
POXC/SOC#	0.65	slope	0.000		
		log depth	0.003		
log (air-dry θg)††	0.70	log depth	-0.173	G	-0.092
				RW	0.092
ρ_b‡‡	0.78	slope	0.004	G	0.067
		log depth	0.172	RW	-0.067
pH 1:1 H_2O	0.72	slope	0.012	G	-0.188
		log depth	0.177	RW	0.188
pH 1:2 $CaCl_2$	0.78	slope	0.012	G	-0.312
				RW	0.312
log (CEC)§§	0.77	slope	-0.005	G	-0.141
		log depth	-0.230	RW	0.141
BS¶¶	0.42	slope	0.002		

† Natural log of soil organic carbon (%)
‡ Natural log of total nitrogen (%)
§Natural log of soil organic carbon to nitrogen ratio
¶ Permanganate oxidizable carbon (mg POXC g $soil^{-1}$)
# Fraction of soil organic carbon that is permanganate oxidizable carbon
†† Natural log of air-dry soil moisture content
‡‡ Soil bulk density (g soil $cm^3 soil^{-1}$)
§§Natural log of soil cation exchange capacity (cmol charge kg $soil^{-1}$),
¶¶ Basic saturation of soil cations

Transects

Table E.5. Summary of regression analysis on soil properties from 60 samples collected along 5 transects in 2019 at Swanton Pacific Ranch, Santa Cruz Co., CA. Values reported as the least square's means (LSM) and standard error (SE) of multiple comparisons between depth (X,Y,Z, or 0-10, 10-25 cm, and 25-50 cm respectively) and plant community in the regression model made in JMP (SAS Institute, Carey, North Carolina). Each response variable was analyzed under the same model (see above), significant associations and interactions ($P<0.05$) are reported for each response variable. If a transformation was preformed, the 95% confidence interval is reported in back-transformed in parentheses.

Response variable				Plant Community									
			Depth	G		ME/G		ME		ME/RW		RW	
	R^2	Sig		LSM	SE	LSM	SE	LSM	SE	LSM	SE	LSM	SE
log (SOC)	0.80	Depth Slope	X	1.56 (2.83, 7.92)	0.26	2.62 (4.41, 42.5)	0.57	1.56 (3.64, 6.16)	0.13	1.77 (4.32, 7.92)	0.15	1.71 (2.99, 10.22)	0.31
		Transect No.	Y	1.29 (2.18, 6.09)	0.26	2.36 (3.41, 32.86)	0.57	1.09 (2.28, 3.86)	0.13	1.26 (2.6, 4.77)	0.15	1.25 (1.9, 6.47)	0.31
			Z	1.08 (1.43, 6.02)	0.36	2.02 (2.42, 23.29)	0.57	0.64 (1.46, 2.47)	0.13	0.60 (1.29, 2.6)	0.18	0.77 (1.17, 4)	0.31
√(N)	0.78	Depth Slope	X	0.63 (0.27, 0.56)	0.06	0.83 (0.33, 1.18)	0.13	0.56 (0.25, 0.39)	0.03	0.61 (0.29, 0.46)	0.03	0.51 (0.14, 0.43)	0.07
		Transect No	Y	0.54 (0.18, 0.44)	0.06	0.78 (0.27, 1.07)	0.13	0.47 (0.17, 0.28)	0.03	0.50 (0.18, 0.32)	0.03	0.43 (0.09, 0.33)	0.07
			Z	0.48 (0.1, 0.42)	0.08	0.71 (0.21, 0.94)	0.13	0.40 (0.11, 0.21)	0.03	0.37 (0.09, 0.2)	0.04	0.32 (0.03, 0.21)	0.07
C/N	0.75	Ecotone	X	11.4	1.3	15.0	2.9	15.8	0.7	16.1	0.8	20.4	1.6
		Depth	Y	11.7	1.3	14.2	2.9	14.2	0.7	14.5	0.8	18.3	1.6
		Ecotone*Slope Transect No.	Z	11.7	1.9	13.8	2.9	12.5	0.7	13.6	0.9	18.9	1.6
√(POXC)	0.83	Ecotone Depth	X	0.881 (0.45, 1.18)	0.103	1.194 (0.55, 2.72)	0.228	1.007 (0.81, 1.24)	0.053	1.182 (1.12, 1.7)	0.061	1.211 (0.93, 2.12)	0.123
		Transect No.	Y	0.742 (0.29, 0.9)	0.103	1.078 (0.39, 2.35)	0.228	0.848 (0.55, 0.91)	0.053	0.989 (0.75, 1.23)	0.061	1.067 (0.67, 1.72)	0.123
			Z	0.643 (0.13, 0.87)	0.145	0.944 (0.24, 1.96)	0.227	0.682 (0.33, 0.62)	0.053	0.738 (0.36, 0.77)	0.071	0.849 (0.36, 1.2)	0.123
POXC/C	0.82	Ecotone	X	0.016	0.002	0.012	0.005	0.021	0.001	0.024	0.001	0.027	0.003

		Slope	Y	0.015	0.002	0.011	0.005	0.023	0.001	0.027	0.001	0.032	0.003
			Z	0.014	0.003	0.009	0.005	0.023	0.001	0.029	0.002	0.031	0.003
	0.71	Ecotone	X	0.25	0.05	0.30	0.11	0.32	0.03	0.43	0.03	0.42	0.06
		Transect No.		(0.02, 0.12)		(0.01, 0.27)		(0.07, 0.14)		(0.13, 0.23)		(0.09, 0.29)	
√(air-dry θg)			Y	0.29	0.05	0.34	0.11	0.31	0.03	0.41	0.03	0.36	0.06
				(0.04, 0.15)		(0.02, 0.31)		(0.06, 0.13)		(0.13, 0.22)		(0.06, 0.23)	
			Z	0.23	0.07	0.33	0.11	0.30	0.03	0.39	0.03	0.36	0.06
				(0.01, 0.13)		(0.01, 0.3)		(0.06, 0.12)		(0.11, 0.21)		(0.06, 0.23)	
	0.81	Ecotone	X	6.15	0.24	5.39	0.53	5.87	0.12	6.14	0.14	6.93	0.29
pH 1:1 H_2O		Transect No.	Y	6.19	0.24	5.41	0.53	5.84	0.12	6.22	0.14	7.17	0.29
			Z	6.40	0.34	5.28	0.53	5.61	0.12	5.90	0.17	7.09	0.29
	0.88	Ecotone	X	5.33	0.24	4.64	0.52	5.07	0.12	5.47	0.14	6.29	0.28
pH 1:2 $CaCl_2$		Depth	Y	5.19	0.24	4.56	0.52	4.98	0.12	5.36	0.14	6.33	0.28
		Transect No.	Z	5.18	0.33	4.20	0.52	4.68	0.12	5.01	0.16	6.15	0.28
	0.63	Depth	X	6.20	0.84	3.70	1.86	6.00	0.43	7.32	0.50	8.31	1.01
		Transect No.		(20.39, 62.25)		(0, 54.98)		(26.4, 47.13)		(39.99, 69.08)		(39.69, 106.6)	
√(CEC)			Y	6.21	0.84	4.03	1.86	5.80	0.43	6.28	0.50	7.03	1.01
				(20.45, 62.36)		(0.1, 59.91)		(24.33, 44.35)		(27.97, 52.94)		(25.14, 81.7)	
			Z	5.34	1.18	3.65	1.86	5.57	0.43	5.74	0.58	6.78	1.01
				(8.9, 59.33)		(0, 54.22)		(22.19, 41.45)		(21.05, 47.49)		(22.77, 77.3)	
	0.47		X	0.68	0.10	1.11	0.23	0.79	0.05	0.65	0.06	0.57	0.12
BS			Y	0.61	0.10	1.07	0.23	0.65	0.05	0.82	0.06	0.77	0.12
			Z	0.73	0.15	1.01	0.23	0.66	0.05	0.70	0.07	0.75	0.12

† Natural log of soil organic carbon (%)
‡ Natural log of total nitrogen (%)
§Natural log of SOC to N ratio
¶ Permanganate oxidizable carbon (mg POXC g $soil^{-1}$)
# Fraction of SOC that is permanganate oxidizable carbon
†† Natural log of air-dry soil moisture content
‡‡ Soil bulk density (g soil cm^3 $soil^{-1}$)
§§Natural log of soil cation exchange capacity (cmol charge kg $soil^{-1}$)
¶¶ Basic saturation of soil cations

Table E.6. Summary of model predictors on soil properties for 60 soil samples collected along 5 transects at Swanton Pacific Ranch, Santa Cruz Co., CA in 2019. Model effects are reported for explanatory variables, if the association was significant (P<0.05). Interactions are not shown and can be found in Appendix D.

Response variable	**Quantitative Predictor (P<0.05)**			**Categorical Predictor(P<0.05)**					
	R^2		**Effect**	**Depth**	**Effect**	**Depth**	**Effect**	**Transect No**	**Effect**
log (SOC)	0.8	Slope	0.015			X	0.403	114	-0.028
						Y	0.013	2156	-0.058
						Z	-0.416	3339	-0.095
								5849	0.441
								6092	-0.261
√(N)	0.78	Slope	0.004			X	0.085	114	0.022
						Y	0.002	2156	-0.010
						Z	-0.086	3339	-0.014
								5849	0.094
								6092	-0.093
C/N	0.75			G	-3.221	X	0.930	114	-1.910
				ME/G	-0.477	Y	-0.231	2156	0.760
				ME	-0.625	Z	-0.699	3339	-1.068
				RW/ME	-0.078			5849	0.975
				RW	4.401			6092	1.244
√(POXC)	0.83			G	-0.182	X	0.158	114	-0.018
				ME/G	0.135	Y	0.008	2156	-0.025
				ME	-0.091	Z	-0.166	3339	-0.076
				RW/ME	0.033			5849	0.198
				RW	0.105			6092	-0.079
POXC/C	0.82	Slope	-0.0001	G	-0.006				
				ME/G	-0.010				
				ME	0.002				
				RW/ME	0.006				
				RW	0.009				
√(air-dry θg)	0.71			G	-0.081			114	0.019
				ME/G	-0.011			2156	-0.059
				ME	-0.028			3339	-0.058
				RW/ME	0.074			5849	0.041
				RW	0.045			6092	0.057
pH 1:1 H_2O	0.81			G	0.144				
				ME/G	-0.745				
				ME	-0.334				
				RW/ME	-0.019				
				RW	0.955				
pH 1:2 $CaCl_2$	0.88			G	0.002	X	0.132	114	-0.149
				ME/G	-0.761	Y	0.053	2156	-0.362
				ME	-0.318	Z	-0.185	3339	-0.126
				RW/ME	0.050			5849	0.709
				RW	1.027			6092	-0.071
√(CEC)	0.63					X	0.443	114	-0.060
						Y	0.004	2156	-1.201
						Z	-0.446	3339	-0.803

	5849	1.176
	6092	0.887

*Significant difference between plant communities at $P < 0.05$
† Natural log of soil organic carbon (%)
‡ Natural log of total nitrogen (%)
§Natural log of SOC to SON ratio
¶ Permanganate oxidizable carbon (mg POXC g $soil^{-1}$)
# Fraction of SOC that is permanganate oxidizable carbon
†† Natural log of air-dry soil moisture content
‡‡ Soil bulk density (g soil cm^3 $soil^{-1}$)
§§Natural log of soil cation exchange capacity (cmol charge kg $soil^{-1}$),
¶¶ Basic saturation of soil cations

Appendix F: List of equations

F.1 Laboratory methods

F.1.1 Air-dry gravimetric water content and oven dried mass calculation:

$$\theta_g = \frac{m_{water\ lost}}{m_{air-dry}} \quad \text{Eq. 1}$$

$$m_b = \frac{m_{air-dry}}{1 + \theta_g} \quad \text{Eq. 2}$$

F.1.2 Bulk density:

$$\rho_b = \frac{m_b}{V_b} \quad \text{Eq. 3}$$

F.1.3 Cation exchange capacity (CEC) and extraction of soil basic cations:

Conversion of extractable basic cation levels to cmolc per kg of soil:

$$\frac{\text{cmolc Ca}}{\text{kg soil}} = \frac{\text{mg Ca}}{\text{L Am Ac.}} \frac{\text{0.035 L Am Ac.}}{\sim\text{2500 mg soil}} \frac{\text{1 mol Ca}}{\text{40.08 g Ca}} \frac{\text{100 cmolc}}{\text{1 mol}} \frac{\text{2 protons}}{\text{1 ion Ca}} \quad \text{Eq. 4}$$

$$\frac{\text{cmolc K}}{\text{kg soil}} = \frac{\text{mg Ca}}{\text{L Am Ac.}} \frac{\text{0.035 L Am Ac.}}{\sim\text{2500 mg soil}} \frac{\text{1 mol K}}{\text{39.10 g K}} \frac{\text{100 cmolc}}{\text{1 mol}} \frac{\text{1 proton}}{\text{ion K}} \quad \text{Eq. 5}$$

$$\frac{\text{cmolc Mg}}{\text{kg soil}} = \frac{\text{mg Ca}}{\text{L Am Ac.}} \frac{\text{0.035 L Am Ac.}}{\sim\text{2500 mg soil}} \frac{\text{1 mol Mg}}{\text{24.31 g Mg}} \frac{\text{100 cmolc}}{\text{1 mol}} \frac{\text{2 protons}}{\text{1 ion Mg}} \quad \text{Eq. 6}$$

$$\frac{\text{cmolc Na}}{\text{kg soil}} = \frac{\text{mg Ca}}{\text{L Am Ac.}} \frac{\text{0.035 L Am Ac.}}{\sim\text{2500 mg soil}} \frac{\text{1 mol Na}}{\text{22.99 g Na}} \frac{\text{100 cmolc}}{\text{1 mol}} \frac{\text{1 proton}}{\text{1 ion Na}} \quad \text{Eq. 7}$$

Sum of extractable basic charge:

Eq. 8

$$\Sigma \text{ basic chage } \left(\frac{\text{cmolc}}{\text{kg soil}}\right) = \frac{\text{cmolc Ca}}{\text{kg soil}} + \frac{\text{cmolc K}}{\text{kg soil}} + \frac{\text{cmolc Mg}}{\text{kg soil}} + \frac{\text{cmolc Na}}{\text{kg soil}}$$

Determination of ammonium concentration from colorimetric analysis:

$$\frac{\text{mg NH4}}{\text{L KCl}} = \frac{\text{(Yintercept, standard curve) – Absorbance value}}{\text{slope, standard curve}} \qquad \text{Eq. 9}$$

Conversion of ammonium concentration to cation exchange capacity:

$$\text{CEC } \left(\frac{\text{cmolc NH4}}{\text{kg soil}}\right) = \frac{\text{mg NH4}}{\text{L KCl}} \frac{\text{0.035 L KCL.}}{\sim\text{2500 mg soil}} \frac{\text{1 mol NH4}}{\text{180 g NH4}} \frac{\text{100 cmolc}}{\text{1 mol}} \frac{\text{1 proton}}{\text{1 ion NH4}} \frac{\text{450 mL KCl dilution}}{\text{10 mL sample}} \qquad \text{Eq. 10}$$

Determination of basic saturation:

$$\text{Basic saturation} = \frac{\Sigma \text{ basic charge}}{\text{CEC Ammonium Replacment}} \qquad \text{Eq. 11}$$

F.1.4 Soil organic carbon correction:

$$\begin{gathered}\text{Non exchangeable, extracted basic charge} \\ = \text{charge from calcium associated with carbonate } \left(\frac{\text{cmolc}}{\text{kg soil}}\right) \\ = \text{cation exchange capacity } \left(\frac{\text{cmolc}}{\text{kg soil}}\right) \\ \times \text{ (measured saturation of extractable bases -100\% extraction of exchangeable bases)}\end{gathered} \qquad \text{Eq. 12}$$

$$\%\text{C inorganic from CaCO3} = \text{Charge from calcium (associated with cabronate; } \frac{\text{cmolc}}{\text{kg soil}}) \times \frac{\text{1 cmol Ca}}{\text{2 cmolc charge}} \frac{\text{1 mol}}{\text{100 cmol}} \frac{\text{1 mol CaCO3}}{\text{1 mol Ca}} \frac{\text{1 mol C}}{\text{1 mol CaCO3}} \frac{\text{12 g C}}{\text{1 mol C}} \frac{\text{1kg}}{\text{1000g}} \times 100\% \qquad \text{Eq. 13}$$

$$\%\text{ soil organic C} = \text{ total soil C (\%)} - \%\text{ inorganic from CaCO3} \qquad \text{Eq. 14}$$

F.1.5 Permanganate oxidizable carbon:

$$\frac{\text{mg POXC}}{\text{g soil}} = \left(\frac{0.02 \text{ mol KMnO4}}{\text{L stock solution}} \text{-(Y intercept(std. curve)+slope (std. curve)} \times \text{ Absorbance value)}\right) \times \frac{9000\text{mg C oxidized}}{1 \text{ mol KMnO4}} \times \frac{.02 \text{ L of 0 .2} M \text{ KMnO4 stock solution}}{\sim 2.5 \text{ g of soil}} \quad \text{Eq. 15}$$

F.2 Regression model expressions

Expression for soil profiles:

$$\begin{aligned}\text{Response variable} = {} & \beta_0 + (\beta_1 \times \text{slope}) + (\beta_2 \times \text{log center depth}) \\ & + \text{match veg.} \begin{cases} \beta_3, \text{Redwood} \\ \beta_3, \text{Grassland} \end{cases} \\ & + \text{match horizon} \begin{cases} \beta_4, \text{A} \\ \beta_4, \text{AB} \\ \beta_4, \text{B} \\ \beta_4, \text{C} \end{cases} \\ & + \text{match zone, *SPR only} \begin{cases} \beta_5, \text{Zone 1} \\ \beta_5, \text{Zone 2} \\ \beta_5, \text{Zone 3} \end{cases} \\ & + \text{Interactions: veg*slope+ veg*log center depth+ log center depth*slope}\end{aligned} \quad \text{Eq. 16}$$

Expression for transects:

$$\begin{aligned}\text{Response variable} = {} & \beta_0 + (\beta_1 \times \text{slope}) \\ & + \text{match ecotone} \begin{cases} \beta_2, \text{RW} \\ \beta_2, \text{RW/ME} \\ \beta_2, \text{ME} \\ \beta_2, \text{ME/G} \\ \beta_2, \text{G} \end{cases} + \text{match depth} \begin{cases} \beta_3 \text{X} \\ \beta_3, \text{Y} \\ \beta_3, \text{Z} \end{cases} + \text{match transect no.} + \begin{cases} \beta_4, 1145 \\ \beta_4, 2156 \\ \beta_4, 3339 \\ \beta_4, 5849 \\ \beta_4, 6092 \end{cases} \\ & + \text{Interactions: veg*slope+ veg*depth+ depth*slope}\end{aligned} \quad \text{Eq. 17}$$

Expression for determination of average POXC and SOC densities in top m of soil:

$$\begin{aligned}&\text{Response variable (SOC or POXC Density)}=\\&\beta_0+(\beta_1\times\text{slope})\\&+\text{match veg.}\begin{cases}\beta_2,\text{ Redwood}\\\beta_2,\text{Grassland}\end{cases}\\&+\text{match zone, *SPR only}\begin{cases}\beta_3,\text{ Zone 1}\\\beta_3,\text{Zone 2}\\\beta_3,\text{Zone 3}\end{cases}\\&+\text{Interaction: veg*slope}\end{aligned}\qquad\text{Eq. 18}$$

F.3 Quality control

$$\begin{aligned}&\text{Criteria for inclusion of observation}=\\&<\text{Median of group}\pm(3\times\text{ Amended "method error"})\end{aligned}\qquad\text{Eq. 19}$$

$$\begin{aligned}&\text{Amended "method error"}=\\&\text{Average of standard deviations for of triplicate groups}\\&\text{(clip top and bottom 10\% of observations)}\end{aligned}\qquad\text{Eq. 20}$$

$$\begin{aligned}&\text{Method detection limit}=\\&\text{Average concentration of blanks}+\\&\left(\begin{array}{c}\text{Standard deviations of blanks}\times\\\text{Student's t-test critical value, for (n-1) degrees of freedom}\end{array}\right)\end{aligned}\qquad\text{Eq. 21}$$

F.4 Depth-weighted averages of POXC/SOC and C/N ratios in the upper 20 cm of profiles

Given the following categories of horizon depth-intervals we collected in the field:

#1, horizon with depth interval between 0 and 20 cm
#2, horizon with depth interval that begins within 20 cm and ends deeper than 20 cm
#3, horizon with depth interval that begins deeper than 20 cm (not included)

$$\text{POXC/SOC in upper 20 cm of profile} = \frac{\frac{POXC_{horizon\ 1}}{SOC_{horizon\ 1}} * Total\ depth_{horizon\ 1}}{20\ cm} + \frac{\frac{POXC_{horizon\ 2}}{SOC_{horizon\ 2}} * (20\ cm - Top\ Depth_{horizon\ 2})}{20\ cm} \quad \text{Eq. 22}$$

*note the same procedure was performed for C/N values to obtain C/N ratio in upper 20 cm of each profile

Example of depth weighted average POXC/SOC value in top 20 cm for pit "1,12 RW" as determined in Excel tabular format:

Horizon	Top depth (cm)	Bottom depth (cm)	Thickness (cm)	POXC/SOC	Depth of horizon applied (if both below 20 cm)	Depth of horizon applied (if top below 20 cm)	POXC/SOC value multiplied by applied horizon depth	Horizon weighted average in top 20 cm (following value divided by 20)	Pit average for top 20 cm (sum of horizon averages)
1,12 A1	0	14	14	0.108	14	0	1.512	0.076	0.103
1,12 A2	14	31	17	0.088	0	6	0.530	0.027	
1,12 AB	31	49	18	0.063	0	0	0	0	
1,12 BW	49	89	40	0.049	0	0	0	0	

F.5 Back-calculation of transformed response variables into normal units in 95% confidence interval

For LSM (1.53) and SE (±0.05), of square-root of SOC in model prediction for redwoods horizons from profile study at SPR: Eq. 23

95% confidence interval= $LSM \pm (2 \times \text{SE}) = 1.53 - (2 \times 0.05), 1.53 + (2 \times 0.05) = (1.43, 1.64)$
Back-transform (square-root units to normal units) = $(1.43^2, 1.64^2) = (2.05, 2.69)$ % SOC

*note: (2.05,2.69) is the confidence interval found in Table 5.1

Appendix G: Quality control

Refer to "Lab schedule and batches" under the "Description of laboratory procedures" section of Chapter 4, for information about batch number.

G.1 Instrument level quality control

G.1.1 Measurement of basic cations

For analyses on the Horiba Scientific-Ultima 2 ICP Emission Spectrometer, working standards were prepared in the matrix of the respective extract using Ca, K, Mg, and Na stock standards. The standard concentrations were designed to capture the spectrum of expected unknown analyte values on a five-point curve. For each batch of analysis, a curve was established (for each cation) and the minimum accepted value for coefficient of determination was 0.999 on each curve. Additionally, for each day of analysis, an initial calibration verification of the curve was performed with external standards (i.e. separate from the standards used to create the curve) and the minimum percent recovery accepted foreach analyte was 90-110%. Throughout the analysis, a continuing calibration verification occurred (for each cation) for every 11 unknown samples analyzed and these values are reported by batch in Tables G.1-G.3.

G.1.2 Measurement of ammonium for cation exchange determination

For determination of ammonium concentration (for of cation exchange capacity) on the Thermo-Scientific 201 UV-visible spectrometer, a 5-point calibration curve of known ammonium concentrations (0, 1, 2.5,5, 10 ppm) was prepared for the start of analysis and for every 24 unknown samples thereafter. The absorbance of each repeated ammonium standard (0, 1, 2.5, 5, 10 ppm) was averaged, and these averaged values were used to create a line with desired slope and intercept to convert unknown absorbance readings into ammonium concentrations (Eq. 9-10, Appendix F). The ranges of averaged coefficients of determinations, by batch, are reported in tables G.1 and G.2.

G.1.3 Measurement of pH

For determination of soil pH, a new Accumet AB 150 Potentiometer with Accumet Combination Glass Electrode was used. Before analysis, the instrument was calibrated with 3 buffer solutions (acid, base, and neutral solutions). A continuing calibration verification check with neutral buffer solution occurred once for every 10 unknown samples analyzed. The range of continuing calibration verification recoveries, by batch, are reported in Tables G.1 and G.2. Additional 3-point calibration events were not documented. When not in use, the electrode was kept in storage solution and the instrument was only used for the purpose of this study between all measurements that occurred in the Jun-Aug. 2019 timeframe.

G.1.4 Measurement of POXC

For POXC determination, a 4-point initial calibration curve was prepared with standards of KMnO4 (0.05, 0.01, 0.015, and 0.02 *M*) and diluted in the same fashion as

the unknown samples (see Chapter 4 for POXC procedure). The range of R^2 values for initial calibration can be found by batch, in tables G.1 and G.2. For every 10 samples, we measured the absorbance of the 10^{th} sample again and measured the absorbance of one KMnO4 standard (in rotating order; for continuing calibration verification). In batch 1 of analysis, 6 of 27 continuing verification samples had poor recoveries and it was assumed another standard than the one labeled was used. In these cases, recovery was calculated with the assumed true standard concentration according to the relative absorbance signature.

G.1.5 Carbon and nitrogen analysis

Before each day of analysis on the Elemantar Vario MAX Cube, a standard reference material was measured three consecutive times for C and N concentrations. The average C and N values were compared to the internal calibration system of the instrument to create "daily factors" that were applied to all readings thereafter (data not shown).

Table G.1. Summary of instrument quality control for 102 mineral soil samples (Batch 1-SPR pits) collected form forest and range sites on the California Coast in 2018 and analyzed from June-August 2019.

Analyte	Instrument	Dates extracted/analyzed	$R^{2\dagger}$	$\%R_{ICV}$	$\%R_{CCV}$ ‡	%RD§
$KMnO_4$;POXC¶	Milton Roy Co. 20D Spectronic	Jul.-Aug. 2019	>0.999	-	94-102	0-18.18
Ca	Horiba Scientific-Ultima 2 ICP Emission Spectrometer	Jul.-Aug. 2019	*	*	93-108	-
K			*	*	93-101	-
Mg			*	*	92-104	-
Na			*	*	90-101	-
NH_4 (for CEC)	Thermo-Scientific 201 UV-visible spectrometer	Jul-Aug. 2019	>0.999	***	***	-
pH	Accumet AB 150 Potentiometer Accumet Combination Glass Electrode	Jun. 2019	n/a	-	100.00-100.57	-

* Minimum acceptable coefficients of determinations for cation standard calibrations curves was R^2= 0.999. For each day of analysis on ICP, an initial calibration verification was performed with an external standard, minimum accepted recovery was 90-110%.
****5-point calibrations curves were analyzed at the start and end of analysis, and once per every 24 samples. Coefficient of determination for one analysis day was the average readings across curves.
† Range of coefficients of determinations for standard calibration curves (if range boundaries are within 0.999, range is expressed > 0.999)
‡ Range of percent recoveries for continuing calibration verifications of standards, measured once per 10-11 unknowns
§Range of percent relative differences in sequential duplicated measurements, measured once per 10 unknowns
¶ R^2 and $\%R_{CCV}$ value pertains to $KMnO_4$ concentrations whereas %RD pertains to POXC concentration

Table G.2. Summary of instrument level quality control for 131 mineral soil samples (Batch 2- LHBCR pits and SPR transects) collected from forest and range sites on the California Coast in 2019 and analyzed from December 2019-Jan 2020.

Analyte	Instrument	Dates extracted/analyzed	$R^{2\dagger}$	$\%R_{ICV}$	$\%R_{CCV}$ ‡	%RD§
$KMnO_4$;POXC¶	Milton Roy Co. 20D Spectronic	Aug 2019	>0.999	-	90-103	0-3.09
Ca	Horiba Scientific-Ultima 2 ICP Emission Spectrometer	Nov. 2019.-Jan 2020	*	*	77-113	-
K			*	*	91-104	-
Mg			*	*	94-111**	-
Na			*	*	85-102**	-
NH_4 (for CEC)	Thermo-Scientific 201 UV-visible spectrometer	Nov. 2019.-Jan 2020	0.997-0.999	***	***	-
pH	Accumet AB 150 Potentiometer Accumet Combination Glass Electrode	Jun-Aug. 2019	n/a	-	99.86-100.57	-

* Minimum acceptable coefficients of determinations for cation standard calibrations curves was R^2= 0.999. For each day of analysis on ICP, an initial calibration verification was performed with an external standard, minimum accepted recovery was 90-110%.
** Two blunders removed from recovery range (two CCV samples analyzed with unknown concentrations)
****5-point calibrations curves were analyzed at the start and end of analysis, and once per every 24 samples. Coefficient of determination for one analysis day was the average readings across curves.
† Range of coefficients of determinations for standard calibration curves (if range boundaries are within 0.999, range is expressed > 0.999)
‡ Range of percent recoveries for continuing calibration verifications of standards, measured once per 10-11 unknowns
§Range of percent relative differences in sequential duplicated measurements, measured once per 10 unknowns
¶ R^2 and $\%R_{CCV}$ value pertains to $KMnO_4$ concentrations, whereas %RD pertains to POXC concentration

Table G.3. Instrument quality control for 41 organic horizons collected from forest sites along the California Central Coast from 2018-2019. Samples analyzed on Horiba-Ultima Inductively Coupled Plasma (ICP) Emission Spectrometer in 2020. Minimum expectable percent recovery from initial calibration verification was 90-110% for each cation. Minimum acceptable coefficient of determination for standard curve was 0.99.

Analyte	Instrument	Dates extracted/analyzed	%R_{CCV}†
Ca	Horiba Scientific-Ultima 2 ICP Emission Spectrometer	Nov. 2019.-Jan 2020	88-97
K			93-104
Mg			94-106
Na			85-102

† Range recoveries for continuing calibration calibrations measured once per 11 unknowns

G.2 Method Quality Control

Standard reference soils were included in every method to generate recoveries from assumed known values (provided by performance lab reports) as method quality control checks for accuracy. Blank samples were included in extraction methods to provide background concentrations associated with the method (method detection limit). Triplicate and duplicate replications of sample extractions and analyses were performed to ensure precision.

G.2.1 Analysis of Analytical Triplicates

Triplicate extractions and analyses of each soil sample were implemented to generate mean values for POXC, CEC, and base cation data. We estimated the average error associated with each method, but first removed the influence of outliers with the *trimmean* tool in Excel (Microsoft, Redman, WA). Using *trimmean*, we calculated the average standard deviation for the middle 80% of the data (i.e. the top and bottom 10% of the data values were not included in the mean calculation). This "method average standard deviation" was multiplied by 3 and used to generate an upper and lower limit from the median triplicate observation so that no observation was included for analysis that was outside of three "average method standard deviations" from the group median (see equation). If a replicate had a value above or below these bounds, the sample was reported as a duplicate or individual value (depending on whether there were one or two replicates that fell outside of these limits). Expressions for the screening process are found in Appendix F, Eq. 19-20.

The goal of this screening process was to eliminate experimental observations (without bias) that were abnormally far from the triplicate median on the basis that those

deviations were greater than the calculated error associated with the method. This protocol was determined consultation with a statistician. Table G.4 (below) highlights the number of observations excluded for each measurement of interest.

Table G.4. Summary of laboratory observations that were identified as outliers and excluded from statistical analyses (in units of % of samples excluded). Observations were excluded on the basis of being more than three method-standard deviations away from the triplicate group median. Each sample was analyzed in triplicate, "n" represents groups of triplicates. The values in this table reflect the percent of samples excluded after non-detects (measurements below the method detection limit, Table G.9) were already removed from the dataset.

Analysis		% of samples excluded from analyses by batch		
		SPR 2018 Lab batch 1; (n=102)	**Transects and LHBCR 2019; Lab batch 2 (n=131)**	**Organic horizons (n=41)**
POXC		3.6	5.3	-
CEC-NH4 replacement		6.2	9.7	-
Ammonium Acetate Extraction	Ca	6.2	7.9	-
	K	47.1 (17.3)*	15.0†	-
	Mg	6.2	7.1	-
	Na	7.5	1.8	-
HCl Digestion	Ca	-	-	5.7
	K	-	-	6.5
	Mg	-	-	7.3
	Na	-	-	4.9

* Number in parentheses is percent of samples excluded when endpoint criteria was changed from: (group median $\pm$ 3 $\times$ method σ) to [group median $\pm$ 3 $\times$ method σ]. Parentheses indicate exclusion of criteria endpoints and brackets indicate inclusion of endpoints. Potassium levels in lab batch 1 were the only data that exhibited sensitivity to endpoint exclusion. Because some triplicate groups had total exclusion of observations when criteria endpoints were excluded, the number in parentheses (endpoints included) is the percent of samples excluded for statistical analysis. The average percent-change among group potassium levels was 0.9% when endpoint criteria was changed.
†For this value, mean standard deviation of groups or "method error" was calculated from middle 20% of group standard deviations due to potassium contamination (as opposed to middle 80% in all other variables listed).

G.2.2 Potassium chloride contamination

In an effort to minimize the use of plastic, several hundred falcon tubes and scintillation vials were washed and re-used for subsequent analyses. Despite adherence to a thorough and standardized washing procedure, many of the scintillation vials had residual salt crystals after washing. After initial reuse of washed vials in batch 2, we returned to using new vials again, and it was noted when in the chronology of the samples this switch was made (approximately halfway through batch 2). This presumed contamination was corroborated by non-systematic spiked potassium levels in the ICP data for the second bath of extractions, and these elevated levels dropped from the data after we began to use new vials again (data not shown).

Sources of potassium contamination were considered, and it was determined that the contamination could be attributed to the potassium chloride solution used in the ammonium replacement extraction and stored in the vials to determine CEC.

In an effort to exclude contaminated extractable potassium levels (for samples collected in the transect study and in pits at LHBCR, i.e. batch 2) in a non-biased manner, we created the triplicate screening process for outliers mentioned above (Eq. 19 and 20 in Appendix F). However, for potassium in this batch, we changed the mean standard deviation for extractable K to only be representative of only the middle 20% of the triplicate standard deviations (instead of the middle 80%). This process removed all standard deviations higher than 1 cmolc per kg^{-1} soil (see Figure G.1) After exclusion, the average standard deviation across groups was lowered to 0.0401 cmolc per kg^{-1} soil (this value was close to the median standard deviation of the original data). We used this value to create upper and lower bounds for exclusion of potassium observations in the batch 2 data set.

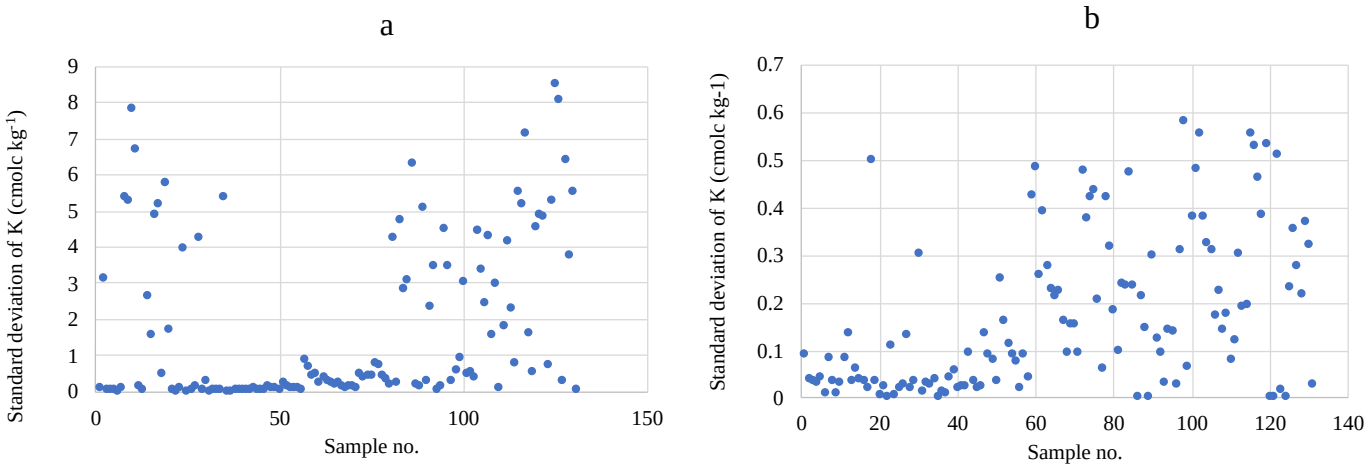

Figure G.1. Standard deviation of extractable potassium levels for "Batch 2", 131 triplicate groups of mineral soil samples that were analyzed and extracted between Dec. 2019-Jan. 2020. Chart (a) shows original triplicate standard deviations and chart (b) shows standard deviation of amended groups.

G.2.3 Quality control challenges

We had a total of 233 mineral soil samples (from SPR and LHBR) that were analyzed in the laboratory in triplicates (699 analytical samples in total). This is a conservative estimate and did not include standard reference soils, blanks, organic horizons, and sample re-runs. We kept tabs on which sample was extracted on which day, and furthermore, which extract was analyzed on which day- this made for considerable organizational efforts.

We have created tables of method-level quality control results that reflect our efforts to collet precise and accurate observations (see Table G.5-G.9)

Overall, the observations in the second batch (Dec. 2019-Jan 2020) of base cation extractions and CEC determinations had lower accuracy and precision than in the first batch (July-August 2019). The reason why percent recoveries of known reference materials were poor in the second batch is a convoluted inquiry and were not able to feasibly answer this question given the scope of the project. The following discussion is what we have to explain about our observations in the quality control samples.

G.2.4 Poor recoveries in ICP data

As mentioned previously, we discovered that some of our soil samples were contaminated with potassium (Figure G.1). One extract of standard refence material (not displayed) had 2,000-3,000% recoveries of potassium across analysis days. For the sake of clarity, we manually excluded all quality control samples (standard reference materials) that had possibility of potassium contamination (i.e. any extracts that were not placed in new vials) from Table G.6.

Despite this effort, some extracted reference materials still had poor recoveries in the other cations (up to 542 and 177 % for sodium magnesium respectively, Table G.6). This suggested that there were other paths of contamination outside of the reused extract vials. We postulated another source of contamination could have be from cations bound to washed, falcon tubes where the extractions took place.

Shifting towards sodium in particular, we noticed poor recoveries occurred in reference materials that were intrinsically low in sodium. The known concentration of sodium in reference materials SRS 1506 and SRS 1607 was 0.8 mg L^{-1} for both, and the each had recovery values outside of a desirable range (Table G.5 and G.6). Conversely, recovery values for sodium improved in soils 1606 and 1608 which had higher sodium levels (Table G.6; sodium concentrations were 3.5 and 52.5 mg L^{-1}, respectively). This trend was consistent across extraction days and analysis days (data not shown) and suggested that the ICP instrument was not measuring extracts low in sodium with desirable resolution. The average sodium concentrations across replicate group means in our raw data sheets (before method detection limit and other quality control measures were considered) was and 3.95 and 8.13 mg L^{-1}, in batch 1 and 2, respectively. Because our samples had higher sodium levels, on average, than SRS 1506 and SRS 1607, we assumed the resolution of sodium was better, on average.

Furthermore, because the contribution of sodium to the total basic charge was relatively non-impactful compared to the other cations (approximately and 1.3 and 3.5% contribution to total charge in batch 1 and 2, respectively)-we were comfortable with the accuracy of the sodium values given the effort expended in quality control monitoring and considering our time and monetary constraints with the project.

In the acid-ash digestion extractions, sodium recovery was also not optimal (Table G.8), despite having a known concentration of 63 mg L^{-1}.The reason why the trend we observed in our soil samples (increased accuracy at higher sodium levels) was not maintained in the pine needle refence material, SRM 1575a, may be because: 1) the material is not a soil, 2) the extract is in hydrochloric acid solution (as opposed to ammonium acetate) and 3) because the instrument was calibrated differently.

Another confounding factor in the interpretation of the second batch of ICP data (Table G.6), was the effect of analysis day on the instrument (Table G.7). This effect can be described as a general spike in all cation levels (up to 33% higher than the replicate group mean, on average) on the second day of ICP analysis for batch 2. This effect on the samples was corroborated in the reference soils as we observed slightly higher recoveries on day 2 of analysis (see range of recoveries in Table G.6, individual values not shown). Given the scope of the project and intricacy of the ICP instrument, it was not feasible to thoroughly investigate this phenomenon.

Despite the inadequacies in base cation accuracy (Table G.6), we used the screening procedure (already mentioned and found in Eq. 19 and 20 in Appendix F) as a final quality control check before any interpretations of our data were performed. The number of observations excluded as a result of the screening procedure (Table G.4) served as an indicator of method precision.

When there was a question of accuracy (e.g. potassium contamination), we were confident in our data because (1) at least one of the triplicates was extracted in new labware, (2) we explored the average error associated with the method (after clipping for outliers, and in the case of potassium, only looked at the error associated with the middle 20% of observations), and (3) we used the group median as compared to the mean (less subject to skew from outliers) to create upper and lower bounds of exclusion.

Table G.5. Summary of method quality control for 102 mineral soil samples (Batch 1-SPR pits) collected from forest and range sites on the California Coast in 2018 and analyzed from June-August 2019 in the NRES soil laboratories of the California Polytechnic University of San Luis Obispo.

			----------Method Quality Control Check------				
Analyte	**Method**	**Dates extracted/analyzed**	**Mean-σ** [§]	**Trimmed mean-σ** [¶]	**MDL**[#]	**%RD**[††]	**%R SRS 1506**[‡‡]
N	Combustion	Dec. 2018	-	-	-	1-11	91-100
SOC			-	-	-	0-11	95-108
POXC[†]	Basic cation extraction in Ammonium acetate	Jul.-Aug. 2019	0.026	0.023	-	-	-
Ca[‡]			0.499	0.431	-1.74	-	106-122
K[‡]			0.021	0.019	0.81	-	123-134
Mg[‡]			0.092	0.087	0.08	-	98-113
Na[‡]			0.003	0.003	0.05	-	45-54
CEC[‡]	Ammonium displacemnt via 2M KCl	July-Aug. 2019	3.05	2.74	-	-	81-131
pH 1:1 H_2O		Jun. 2019	-	-	-	0-2.65	99.19-99.51
pH 1:2 $CaCl_2$			-	-	-	0-0.75	101.59

† mg POXC kg soil $^{-1}$

‡ cmolc kg soil $^{-1}$

§ Average of all triplicates group standard deviations

¶ Average of middle 80% of triplicates group standard deviations, this is value used for screening criteria

Method detection limit of method blanks in units, mg L^{-1}. MDL= avg. concertation of blanks + (std. dev. of blanks x student's t-test critical value, for (n-1) degrees of freedom)

†† Range of percent relative differences of duplicates (10% of sample size)

‡‡ Range of percent recoveries of known values from standard reference soils

Table G.6. Summary of method quality control for 131 mineral soil samples (Batch 2- LHBCR pits and SPR transects) collected from forest and range sites on the California Coast in 2019 and analyzed from December 2019-Jan 2020 in the NRES soil laboratories of the California Polytechnic University of San Luis Obispo.

			----------Method Quality Control Check----------								
Analyte	**Method**	**Dates Analyzed**	**Mean-σ** [§]	**Trimmed mean-σ** [¶]	**MDL**[#]	**%RD**[††]	**%R_{SRS}**[‡‡]				
							B2182	**1506**	**1606**	**1607**	**1608**
N	Combustion	Dec. 2019	-	-	-	1-49 (1-13)	93-106	-	-	-	-
SOC			-	-	-	1-49 (1-13)	100-103	-	-	-	-
POXC†		Aug 2019	0.027	0.026	-	-	-	-	-	-	-
Ca‡	Basic cation extraction in Ammonium acetate	Nov. 2019.-Jan 2020	2.996	2.612	23.73	-	-	-	95-176	93-146	84-102
K‡			1.705	0.389	3.54	-	-	-	92-149	103-153	90-108
Mg‡			1.577	1.462	0.59	-	-	-	97-170	98-177	94-123
Na‡			0.263	0.259	8.83	-	-	-	143-212	356-542	90-107
CEC‡	Ammonium displacement via 2M KCl	Nov. 2019.-Jan 2020	3.25	2.75	-	-	-	-	78-133	81-159	67-137
pH 1:1 H_2O		Jun-Aug. 2019	-	-	-	-	-	98.87-100.16	-	-	-
pH 1:2 $CaCl_2$			-	-	-	-	-	98.66-101.94	-	-	-

† mg POXC kg soil $^{-1}$

‡ cmolc kg soil $^{-1}$

§ Average of all triplicates group standard deviations

¶ Average of middle 80% of triplicates group standard deviations, this is value used for screening criteria

Method detection limit of method blanks in units, mg L^{-1}. MDL= avg. concertation of blanks + (std. dev. Of blanks x student's t-test critical value, for (n-1) degrees of freedom)

†† Range of percent relative differences of duplicates (10% of sample size); parenthesis indicates range when one duplicate was removed as a blunder

‡‡ Range of percent recoveries of known values from standard reference soils

Table G.7. Average percent-difference in replicates from group mean by day-analyzed for exchangeable soil basic cations. This data represents "Batch 2", an extraction batch of 131 soil samples collected in 2019 from forest and rangeland sites on the California Central Coast. Each sample was extracted (in triplicate) for exchangeable basis cations (Ca, K, Mg, Na) via Ammonium Acetate and analyzed on the Horiba-Ultima Inductively Coupled Plasma (ICP) Emission Spectrometer. Each day of analysis represented one replication cycle of analytical triplicates. If replicates of the same group were analyzed on the same day, one replicate was removed from this analysis for the purpose of quality control investigation. In the same vein, observations that were removed as outliers were not displayed.

	Average percent difference in replicates from group mean			
Day of ICP analysis	**Ca**	**K**	**Mg**	**Na**
1	-6	-6	-14	-20
2	24	19	33	25
3	-9	-11	-6	3

Table G.8. Method quality control for acid-ash extracts collected from forest sites along the California Central Coast from 2018-2019. Samples extracted in the NRES soil laboratories of the California Polytechnic University of San Luis Obispo and analyzed on Horiba-Ultima Inductively Coupled Plasma (ICP) Emission Spectrometer in 2020.

Analyte	**Method**	**Dates Analyzed**	**Mean-σ** †	**Trimmed mean-σ** ‡	**MDL**§	**Recov. SRM 1575a**¶
Ca	Acid-ash digestion	Jan. 2020	451.53	390.81	8.613	89-93
P			40.54	38.69	3.085	84-88
Mg			63.38	55.50	5.338	81-84
Na			7.73	7.28	0.540	51-71

† Average standard deviation of triplicates groups expressed in units of mg kg soil $^{-1}$
‡ Average standard deviation of middle 80% of triplicates group standard deviations expressed in units of mg kg soil $^{-1}$, this is value used for screening criteria
§Method detection limit of method blanks in units, mg L^{-1}. MDL= avg. concertation of blanks + (std. dev. Of blanks x student's t-test critical value, for (n-1) degrees of freedom)
¶ Range of recoveries of known value from standard reference material (in %)

G.2.5 Method detection limit

We calculated method detection limits (MDLs) for base cation levels in extraction solutions of blank quality-control samples, that were treated the same as soil samples throughout the entire method (Table G.9). For each day of extractions (regardless of batch number) a blank was included in the method. For each batch, a MDL calculation was performed for each cation (Eq. 21, Appendix F).

The only analyte with measurements below the MDL occurred for sodium in the second batch of ICP analyses; the non-detection rate for sodium was 73% of all samples included the analysis (this percentage accounts for each induvial triplicate of the 131 soil soils analyzed, i.e. the 393 total samples; Table G.9). Each sample with a concentration below the MDL was not included in the statistical analysis, and the value was made blank in Excel (Microsoft, Redman, WA) before the data screening protocol was implemented. All samples were extracted and analyzed in triplicate; if/when all triplicates within the triplicate group had values that measured below the MDL, then the mean value associated with that sample was treated as blank and effectively served as zero charge towards the total basic charge.

The large number of samples below the MDL for sodium in batch 2 (Table G.9) suggested the calibration of the ICP instrument for sodium, was not as resolute as it was for sodium in the first batch, or when compared to the other cation levels that were measured in batch 2. The general trend of higher MDL values across cations for batch 2 to in respect to batch 1 suggested that there was more contamination in the second round when compared to the first. One possible cause of contamination is from multiple reuse and washing cycles of reaction tubes (50 mL plastic falcon tubes). We did not document which samples were extracted in new tubes and which samples were extracted in washed (reused) tubes during the extraction processes. The use of both new and reused falcon tubes represents a flaw in the protocol, as ideally, any-one sample in the procedure should not have been treated any different than another.

Despite the large number of sodium measurements below the MDL, we mentioned earlier that the contribution of sodium to the total basic charge was relatively small. The motivation to measure cation levels was not to provide the published sodium levels in our soils, but rather to determine basic saturation for taxonomic inquiries. Given the goals associated with extractions and given the time and monetary constraints associated with the project- we were comfortable to move forward with our ICP data despite the challenges to digest the quality control measures that are mentioned above.

Table G.9. Summary of method detection limit (MDL) for base cation concentrations in ammonium acetate and hydrochloric extracts. Base cation occurred from 2019-2020 in the NRES soil laboratories of the California Polytechnic State University of San Luis Obispo and analyzed on the Horiba-Ultima Inductively Coupled Plasma (ICP) Emission Spectrometer in 2020. MDLs for each cation are separated by batch of ICP analysis.

	----Mineral Batch 1--- (2019)				------Mineral Batch 2------ (2019-2020)				------Organic samples------ (2019-2020)			
Blank No.	**Ca**	**K**	**Mg**	**Na**	**Ca**	**K**	**Mg**	**Na**	**Ca**	**K**	**Mg**	**Na**
1	-2.59	0.51	-0.04	-0.02	21.66*	201.04*	1.71*	3.09*	3.45	-2.43	0.75	-0.28
2	-2.68	0.49	-0.05	-0.02	6.81	0.61	0.25	0.09	3.75	-3.63	0.74	-0.52
3	-2.22	0.56	-0.01	-0.02	8.12	0.29	-0.20	0.32	4.97	-1.65	-0.81	-0.23
4	-2.20	0.36	-0.01	-0.01	6.26	1.24	0.13	4.18				
5	-2.57	0.60	0.03	0.02	25.24*	233.97*	0.06*	3.33*				
6	-2.73	0.46	0.03	-0.01	1.12	0.64	-0.15	3.50				
7					16.19	0.56	0.08	3.92				
μ‡	-2.46	0.50	0.01	-0.01	7.70	0.67	0.02	2.40	4.05	-2.57	0.23	-0.35
σ§	0.21	0.09	0.02	0.02	4.87	0.31	0.17	1.81	0.65	0.81	0.73	0.13
MDL¶	-1.74	0.81	0.08	0.05	25.94	1.84	0.67	9.18	4.05	-2.57	0.23	-0.35
No. of non-detects#	0	0	0	0	0	0	0	287 (73%)	0	0	0	0

* Identified as contaminated, removed from MDL calculation

† Concentrations in mg L^{-1} of ammonium acetate

‡ Average concentration of blanks by cation

§ Standard deviation of blank by cation

¶ Method detection limit for each cation. MDL= avg. concentration of blanks + (std. dev. of blanks x student's t-test critical value, for (n-1) degrees of freedom)

Number of replicates with concentrations below MDL, in parenthesis expressed as % of replicates below

Appendix H: Photographs

Figure H.1. Photographs of (a) profile-description in soil pit and (b) auger sampling in transect study (photos by author).

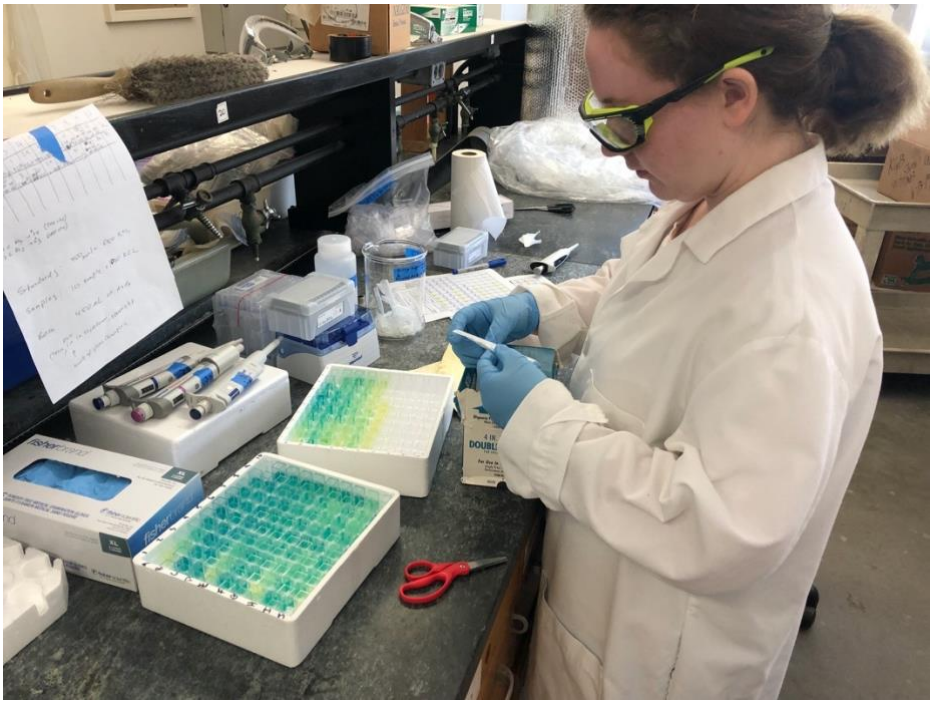

Figure H.2. Photograph of sample preparation for ammonium colorimetric analysis in summer of 2019 at the NRES Dept soil science laboratories at the California State Polytechnic University of San Luis Obispo (photo by author).

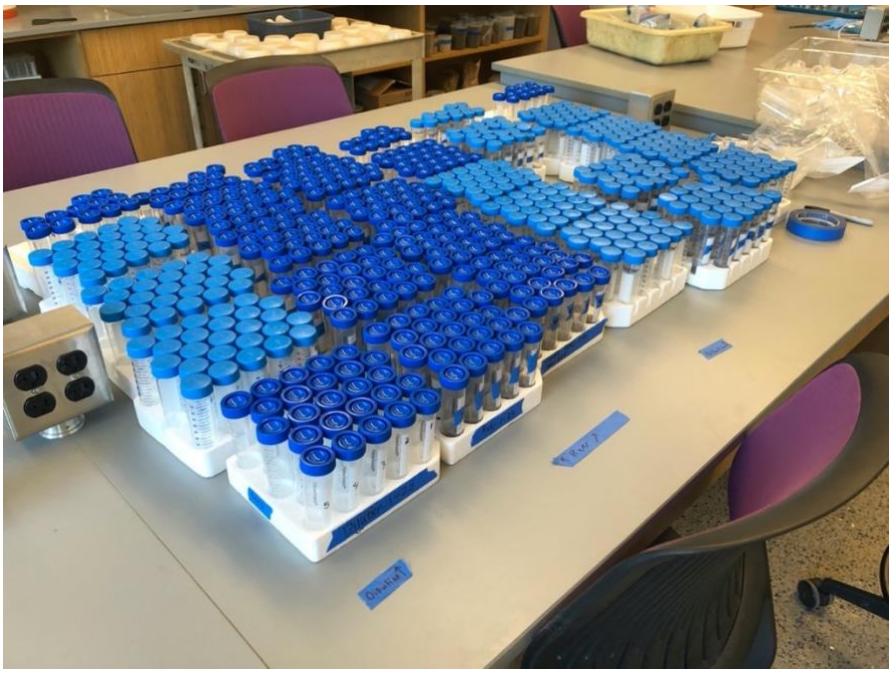

Figure H.3. Photograph of POXC sample preparation (batch 1) in summer of 2019 at the NRES Dept soil science laboratories at the California State Polytechnic University of San Luis Obispo (photo by author).

Figure H.4. Photographs of author in the field, spring 2019 at LHBCR (photo by Braden Povah).

Appendix I: Family name classifications of soil profiles

Table I.1. Summary of soil classification using *Keys to Soil Taxonomy* (2014) from lab and field data collected from soil pits sampled at Swanton Pacific Ranch (2018). While weather station data (see "Climate" under Swanton Pacific Ranch section of Chapter 3) suggested some regions of Swanton Pacific Ranch were in an isomesic temperature regime (which disqualifies xeric moisture regime classification), it was assumed that all profiles were in a xeric moisture regime.

Pit	Veg	Order	Family name
1,-	RW	Mollisol	Fine-loamy superactive thermic Pachic Ultic Haploxeroll
1,12	RW	Mollisol	Fine-loamy superactive thermic Pachic Haploxeroll
1,20	RW	Mollisol	Fine-loamy superactive thermic Pachic Ultic Haploxeroll
1,4 RW	RW	Inceptisol	Fine-loamy superactive thermic Cumulic Humixerept*
1,5 RW	RW	Mollisol	Fine-loamy superactive thermic Pachic Haploxeroll
1,6 RW	RW	Mollisol	Fine-loamy superactive thermic Pachic Ultic Haploxeroll
2,1 RW	RW	Mollisol	Loamy-skeletal superactive thermic Typic Haploxeroll
2,2 RW	RW	Mollisol	Loamy-skeletal over sandy-skeletal superactive thermic Ultic Haploxeroll
2,7 RW	RW	Mollisol	Fine loamy over sandy superactive thermic Fluventic Haploxeroll
2,8 RW	RW	Mollisol	Loamy active thermic shallow Lithic Haploxeroll
3,10 RW	RW	Mollisol	Fine-loamy active thermic Ultic Haploxeroll
3,2 RW	RW	Mollisol	Loamy-skeletal superactive thermic Typic Haploxeroll
3,3 RW	RW	Mollisol	Loamy-skeletal superactive thermic shallow Lithic Ultic Haploxeroll
3,5 RW	RW	Mollisol	Loamy-skeletal superactive thermic shallow Lithic Ultic Haploxeroll
3,7 RW	RW	Mollisol	Fine-loamy superactive thermic Cumulic Haploxeroll
3,9 RW	RW	Mollisol	Fine-loamy superactive thermic Pachic Ultic Argixeroll
1,1	G	Inceptisol	Loamy superactive thermic shallow Lithic Haploxerept
1,2	G	Inceptisol	Fine-loamy activethermic Fluventic Humixerept
1,3	G	Inceptisol	Fine-loamy superactive thermic Pachic Humixerept
1,5	G	Inceptisol	Fine-loamy superactive thermic shallow Lithic Humixerept
2,1 G	G	Alfisol	Fine semiactive thermic Ultic Palexeralf
2,2 G	G	Mollisol	Fine-loamy active thermic Cumulic Ultic Haploxeroll
2,3 G	G	Inceptisol	Fine active thermic Lithic Humixerept
2,4 G	G	Mollisol	Loamy-skeletal superactive thermic shallow Lithic Ultic Haploxeroll
3,1 G	G	Inceptisol	Fine superactive thermic Cumulic Humixerept*
3,2 G	G	Alfisol	Fine-loamy semiactive thermic Aquic Palexeralf
3,3 G	G	Mollisol	Fine-loamy superactive thermic Cumulic Ultic Haploxeroll
3,6 G	G	Inceptisol	Fine-loamy semiactive thermic Typic Humixerept*

*Inceptisol with mollic epipedon

Table I.2. Summary of soil classification using *Keys to Soil Taxonomy* (2014) from lab and field data collected from soil pits sampled at Landels-Hill Big Creek reserve (2019). All soil profiles were assumed to be in a xeric moisture regime.

Pit	Veg	Order	Family name
85	RW	Alfisol	Fine subactive thermic Mollic Palexeralf*
58	RW	Inceptisol	Loamy-skeletal superactive thermic Fluventic Haploexerept
328	RW	Mollisol	Loamy-skeletal superactive thermic Cumulic Haploxeroll
290	RW	Mollisol	Loamy-skeletal over sandy-skeletal superactive thermic Pachic Haploxeroll
165	RW	Mollisol	Loamy-skeletal superactive thermic Pachic Haploxeroll
532	RW	Mollisol	Fine-loamy superactive thermic Pachic Haploxeroll
322	RW	Mollisol	Coarse-loamy superactive thermic Cumulic Haploxeroll
129	RW	Mollisol	Loamy-skeletal over sandy-skeletal superactive thermic Fluventic Haploxeroll†
442g	G	Mollisol	Loamy-skeletal superactive thermic shallow Humic Lithic Haploxeroll
8490g	G	Mollisol	Loamy-skeletal active thermic Typic Haploxeroll
7029g	G	Mollisol	Loamy-skeletal active thermic Typic Argixeroll
1425g	G	Mollisol	Fine-loamy superactive thermic Cumulic Haploxeroll
5820g	G	Mollisol	Fine active thermic Pachic Argixeroll
8012g	G	Mollisol	Coarse-loamy superactive thermic Typic Haploxeroll
3277g	G	Mollisol	Fine-loamy superactive thermic CumulicUltic Haploxeroll

*Alfisol with mollic epipedon

† We did not perform particle size analysis on any soils from LHBCR. At this soil pit (129) we assume the "loamy materials" have less than 50%, by weight, fine sand or coarser sand. If this is not the case, the particle size class would be sandy skeletal.

Appendix J: Bulk density values used when data was missing

Table J.1 Average bulk density values (separated by location, horizon, and vegetation) used for SOC density calculations. C-horizon data is not available due to infeasibility of extraction in the field. Horizons designated as C horizons were assigned hypothetical bulk density values from adjacent horizons (in the same pit) or from the average of B horizons (by pit and location). See methodology for more details.

Location	Plant Community	Horizon†	n	BD	SE
Landels-Hill Big Creek Reserve	Grassland	A	15	1.26	0.05
		B	7	1.52	0.07
	Redwood forest	A	11	1.01	0.06
		B	2	1.55	0.14
Swanton Pacific Ranch	Grassland	A	15	0.96	0.05
		AB	4	0.85	0.09
		B	23	1.19	0.04
	Redwood forest	A	16	0.77	0.05
		AB	9	0.87	0.06
		B	11	0.98	0.05

†Simplified field horizon (similar to that used in the regression models) and based on availability of bulk density samples collected in the field

Appendix K: Clay settling times for particle size analysis

Table K.1. Temperature adjustments for clay settling times during particle size analysis, excerpted from (Miller et al., 2013)

Temperature °C	Settling time for clay hours and minutes
18	8:09
19	7:57
20	7:45
21	7:35
22	7:24
23	7:13
24	7:03
25	6:53
26	6:44
27	6:35
28	6:27

Gee and Bauder (1986).

Appendix L: Measurement of exchanged NH_4^+ via NH_3 gas electrode (a check method for validation of colorimetric analysis of ammonium for CEC determination)

1. Obtain soil extracts in 2 *M* KCl matrix (prepare standards of known ammonium concentrations)
2. Transfer exactly 20 mL of filtered extracts into appropriate glassware (30 mL beaker)
3. Prepare NH_3 gas electrode by rinsing it with deionized water and drying with a chemwipe
4. Gently drop stir rod into 30 mL beaker with sample and place beaker onto a stir-plate at medium setting
5. With clock available and using a calibrated pipette, transfer 1 mL of 1 *M* NaOH.
6. Immediately begin track of time (reading on electrode will be recorded after exactly one minute has passed since the NaOH was transferred into the sample)
7. Place electrode in beaker at 20-degree angle to ensure there are no air bubbles on or around the electrode tip and take recording (mV NH_3) after one minute has passed.
8. Repeat steps for all samples
9. Use Microsoft Excel to create a standard curve. Using readings from standards with known ammonium concentrations, plot relative mV NH_3 given by instrument (on y-axis) and ppm ammonium (on x-axis). Generate a linear regression to fit the curve and use this equation to solve for unknown ammonium values (x) using instrument readings (y; in relative mV) from soil extracts. Note: NH_4^+ is proportional to the amount of NH_3 measured by the electrode and this relationship is captured in the curve.
10. Convert ppm $NH_4^+$to cmolc NH_4^+ per kg of soil (because of our extraction procedure, this represented the CEC of the soil)

We compared CEC values obtained using colorimetric analysis on the photospectrometer to the values obtained using the ion-selective electrode procedure that is described above. We found that both methods of analysis provided the same values (data not shown), thus, we continued using the colorimetric analysis for sake of ease.

Appendix M: Average annual driver emissions for California

Source	Metric	Value
California Air Resources Board (2019)	Total annual GHG emissions in California (tons CO_2 equivalent emissions)	424,100,000.00
	Passenger car contribution to total state emissions	28%
	Annual emissions by passenger cars (tons CO_2 equivalent emissions)	118,748,000.00
Federal Highway Administration (2017)	Licensed drivers in California	25,532,920.00
	Average annual emission per driver (tons CO_2 equivalent emissions)	4.65

Sample Calculation:

$$1\ thousand\ tons\ POXC \times \frac{44\ tons\ CO_2}{12\ tons\ C} \times \frac{1\ CA\ driver}{4.65\ tons\ CO_2\ equiv.} = 788\ drivers$$

Appendix N: Summary of cation levels in forest litter

Average values and standard deviations for basic cation concentrations (mg g^{-1} organic soil) in 31 redwood forest floor horizons collected at along the CA Central Coast from 2018-2019.

	Cation levels (mg of cation g $litter^{-1}$)			
	Ca	**K**	**Mg**	**Na**
μ†	16.83	0.760	2.36	0.161
σ‡	5.48	0.210	0.92	0.080

† Mean concentration of cation, expressed in mg cation g forest $litter^{-1}$

‡ Standard deviation of cation concentration, expressed in mg cation

Appendix O: Geographic information (coordinates) of study sites

Coordinates for soil profiles at Landels-Hill Big Creek Reserve:

No	Pit	Y	X	Veg.
1	85	36.0479765	-121.5729529	Redwood forest
2	58	36.0479348	-121.5732312	Redwood forest
3	328	36.0485226	-121.5733871	Redwood forest
4	290	36.0484278	-121.5730003	Redwood forest
5	165	36.0481607	-121.5732826	Redwood forest
6	532	36.0493026	-121.5745387	Redwood forest
7	322	36.0485266	-121.5737201	Redwood forest
8	129	36.0480673	-121.5730068	Redwood forest
9	442	36.0492553	-121.5781474	Grassland
10	8490	36.0527006	-121.5798062	Grassland
11	7029	36.0517941	-121.5793784	Grassland
12	1425	36.0496628	-121.5783066	Grassland
13	5820	36.0511487	-121.5781689	Grassland
14	8012	36.0523799	-121.5793679	Grassland
15	3277	36.0503503	-121.5830678	Grassland

Coordinates for soil profiles at Swanton Pacific Ranch:

No	Pit	Zone	Veg.	Y	X
1	1,1	1	Grassland	37.0799955	-122.2453443
2	1,2	1	Grassland	37.0844377	-122.2421905
3	1,3	1	Grassland	37.0789683	-122.2451490
4	1,5	1	Grassland	37.0798671	-122.2447413
5	1,4 RW	1	Redwood forest	37.0836500	-122.2489438
6	1,5 RW	1	Redwood forest	37.0882565	-122.2439937
7	1,6 RW	1	Redwood forest	37.0879807	-122.2440730
8	1,20	1	Redwood forest	37.0867091	-122.2464435
9	1,12	1	Redwood forest	37.0874668	-122.2462897
10	1,-	1	Redwood forest	37.0905207	-122.2441321
11	2,1 G	2	Grassland	37.0629035	-122.2189918
12	2,2 G	2	Grassland	37.0628285	-122.2194186
13	2,3 G	2	Grassland	37.0629493	-122.2111949
14	2,4 G	2	Grassland	37.0634475	-122.2100066
15	2,1 RW	2	Redwood forest	37.0666906	-122.2183074
16	2,2 RW	2	Redwood forest	37.0685100	-122.2113218
17	2,7 RW	2	Redwood forest	37.0657489	-122.2216279
18	2,8 RW	2	Redwood forest	37.0643557	-122.2229670
19	2,10 RW	2	Redwood forest	37.0653176	-122.2182759
20	3,1 G	3	Grassland	37.0685858	-122.2387810
21	3,2 G	3	Grassland	37.0744350	-122.2517725
22	3,3 G	3	Grassland	37.0670921	-122.2376323
23	3,6 G	3	Grassland	37.0689347	-122.2476161
24	3,2 RW	3	Redwood forest	37.0693971	-122.2350290
25	3,3 RW	3	Redwood forest	37.0707675	-122.2352321
26	3,5 RW	3	Redwood forest	37.0708362	-122.2352337
27	3,7 RW	3	Redwood forest	37.0684182	-122.2315784
28	3,9 RW	3	Redwood forest	37.0744463	-122.2418309

Geographic information for transect lines:

No.	Transect point no. (ft along line forest-grass boundary)	Y	X	Tangential Az	Perpendicular Azimuth	Minus 45 deg	Plus 45 deg	Random Az in b/w
1	114	37.0766338028	-122.2503282976	331	241	196	286	219
2	2156	37.0711405552	-122.2446011074	331	241	196	286	204
3	3339	37.0701591526	-122.2392212274	265	175	130	220	198
4	5849	37.0648384988	-122.2342929377	359	269	224	314	313
5	6092	37.0640419334	-122.2355003507	53	-37	-82	8	-41

Appendix P: Exercise with quantities of active SOC

Table P.1 Management insights from POXC stocks in top 1 m of soil profiles in redwood forest and grassland sites along the California Central Coast. Stocks were calculated from LSM values determined via regression model, Eq. 18 in Appendix F. These stocks are approximate and confounded by estimated bulk density values used to fill data gaps when bulk density collection was infeasible in the field (Appendix J).

Location	Vegetation	Area† (ha)	POXC stock (thousand tons POXC in top m)‡	CO_2 equivalent (thousand tons CO_2 eq. in top m)	U.S. dollars ($15 per ton of CO_2 eq.)	Number of CA drivers in POXC pool§
Big Sur Ecoregion	Grassland	8,542	25.1 ± 4.3	91.9 ± 15.9	$1,378,019 ± $238,648	19,753 ± 3,421
	Redwood Forest	13,386	58.5 ± 6.4	214.2 ± 23.3	$3,213,695 ± $349,779	46,067 ± 5,014
Swanton Pacific Ranch	Grassland	508	1.1 ± 0.2	3.9 ± 0.9	$58,239 ± $13,618	835 ± 195
	Redwood Forest	372	1.2 ± 0.2	4.6 ± 0.6	$68,378 ± $8,496	980 ± 122

† Area calculated using data from Stephenson and Calcarone (1999) and Meentemeyer et al. (2008)

‡ Permanganate oxidizable carbon (POXC) stock determined using least squares means POXC density (mass POXC per acre in top meter of soil) from regression model of soil profiles, see Appendix B

§Data collected from California Air Resrources Board (2019) and Federal Highway Administration (2017), refer to Appendix M

Table P.2 Impacts to active SOC pool from projections in redwood forest distribution under four climate scenarios in the 2040-2069 time frame.

	Current status (thousand ha)	Climate and emissions scenario			
		Reduced Emissions (RCP 4.5)		Business as Usual (RCP 8.5)	
		Hot dry	Warm wet	Hot dry	Warm wet
Projected change in extent of redwood forest (thousand ha)†	2,860	-1,370	15	-1,245	-1,252
Possible change in active SOC pool (thousand tons POXC in top 1 m of soil) ‡		-5,279	59	-4,798	-4,826
Percent change (%)		-48	1	-44	-44

† Areas excerpted from Forest Climate Action Team (2018) in Appendix 1 (of that document): Changes in Extent for Individual Tree Species

‡ Calculated using 3.85 tons POXC hectare^{-1} in top 1 m of redwood soil (this is combined average of regression model POXC densities in top 1 m of redwood forest soil profiles between two locations, SPR and LHB; see Table 5.3 for further details)